

Durham E-Theses

Studies on the cardiomyocytic potential of dermal stem cells”

Cormack, Suzanne Marie

How to cite:

Cormack, Suzanne Marie (2008) *Studies on the cardiomyocytic potential of dermal stem cells”*, Durham theses, Durham University. Available at Durham E-Theses Online: <http://etheses.dur.ac.uk/2220/>

Use policy

The full-text may be used and/or reproduced, and given to third parties in any format or medium, without prior permission or charge, for personal research or study, educational, or not-for-profit purposes provided that:

- a full bibliographic reference is made to the original source
- a [link](#) is made to the metadata record in Durham E-Theses
- the full-text is not changed in any way

The full-text must not be sold in any format or medium without the formal permission of the copyright holders.

Please consult the [full Durham E-Theses policy](#) for further details.

“Studies on the Cardiomyocytic Potential of Dermal Stem Cells”

The copyright of this thesis rests with the author or the university to which it was submitted. No quotation from it, or information derived from it may be published without the prior written consent of the author or university, and any information derived from it should be acknowledged.

Suzanne Marie Cormack

(BSc (Hons) University of Durham)

0 6 OCT 2008

Thesis submitted for the degree of Doctor of Philosophy

University of Durham, Department of Biological Sciences

August 2008



This thesis is entirely the result of my own work. It has not been accepted for any other degree and is not being submitted for any other degree,

S. Cormack

Suzanne Marie Cormack

21st August 2008



Acknowledgements

To my supervisors, Nick, Andrew and Colin: for all the advice and time you have so graciously given. It has been a wonderful three years.

A big thank you to David Breault and Diana Carlone: for all your ideas and support, not to mention encouragement when the days were long!

Personal thanks to my lovely family. Especially Mum, Dad and Christine: I certainly wouldn't have made it to this day without your patience, guidance and support. Also to my extended family, the Breaults, for allowing me into your lives when I needed friends the most. Thank you David, Kate, Harry and Sam.

A final thank you to my dear lab friends, most especially Andy and Bridie: what would I do without you! Thank you, Andy, for such a good friendship over these last few years.

DP and DS clonal cell lines were a kind gift from Professor Colin Jahoda. Thanks to Ian Dimmick, for assistance and guidance with flow cytometry, and to my funding bodies, the NHS and One NorthEast.

Abstract

In Europe, diseases of the heart and circulatory system are the main cause of death; 48% of all deaths are from coronary heart disease, accounting for over 4.30 million deaths each year (European cardiovascular disease statistics 2008). Identifying stem cell types that can potentially contribute to the regeneration of cardiac tissue is one route to addressing this global problem.

The follicular dermis has been proposed as a tissue containing cells with adult stem cell properties that could be used for regenerative medicine. This study showed that follicular dermal structures demonstrated spontaneous synchronised contractions *in vitro*, indicative of cardiomyocytic commitment. In contrast, isolated populations of follicular dermis, the dermal papilla and sheath, did not demonstrate spontaneous cardiomyocytic commitment *in vitro*. Co-culture of isolated follicular dermal populations with embryonic cardiomyocytes, a cell type previously reported to support cardiomyocytic commitment of mesenchymal stem cell types, induced expression of a panel of gene products indicative of cardiomyocytic commitment, but only when the inducing cell and the target cell were of the same species. The level of gene induction indicated that the number of cells affected were likely to be very modest. In order to better identify the stem cell types in the follicular dermis, this study used a novel mTert-GFP transgenic mouse to identify candidate stem cells on the basis of their expression of the stem cell phenotypic marker, telomerase. A small population of GFP-expressing non-haematopoietic cells present in the dermis (0.17-0.49%) were identified and found associated with the follicular dermis and bulge region. This minor sub-population of GFP-expressing dermal cells contained all the detectable gene expression of four key markers of stem cells: Tert; Oct4; Nanog and Sox2, both at time of isolation and after 2 weeks *in vitro* culture. Intriguingly, non-haematopoietic, GFP-expressing cells were also detectable in the adult heart at low levels (0.08%). After cryo-induced infarct, these non-haematopoietic GFP-expressing cells were associated with the epicardium, concentrated close to the infarct site, in a fashion consistent with other reports of candidate cardiac stem cells. This study indicates that the population of stem cells within the follicular dermis may be very modest. Further, it shows that phenotypic markers of stem cells from different organs may be a suitable approach for the investigation of the stem cell phenotype.

Contents Page

Chapter 1: Dermal Follicular Cells as a model for investigation of Somatic Cell Differentiation

1.1 Stem Cell Identification	1
1.2 Significance of heart disease.....	3
1.3 Development and maintenance of the heart.....	7
1.3.1 Cardiac development	7
1.3.2 The evidence for the cardiac stem cell.....	13
1.4 A source of stem cells for cardiomyocyte differentiation.....	23
1.4.1 Satellite Cells	24
1.4.2 Embryonic Stem Cells	26
1.4.3 Haematopoietic stem cells	27
1.4.4 Mesenchymal stem cells	28
1.4.5 Clinical Trials	30
1.5 The skin and its appendages	34
1.5.1 Hair cycling.....	37
1.5.2 Stem cells of the skin	38
1.5.2.1 Epidermal stem cells.....	38
1.5.2.2 Bulge region stem cells.....	40
1.5.2.3 Dermal follicular cells – a novel source of donor cells	41
1.6 Thesis objectives	43

Chapter 2: Materials and Methods

2.1 Materials	45
2.1.1 Animals	45
2.2 Microscopy and centrifugation	45
2.3 Isolation of primary tissues	45
2.3.1 Isolation of vibrissae DP and DS from mouse/rat mystacial pad	45
2.3.2 Isolation of neonatal skin dermal cells	49
2.3.3 Removal of mouse/rat embryos	49
2.3.4 Isolation of cardiomyocytes from embryonic hearts	49
2.4 Tissue culture	50
2.4.1 Primary culture of isolated DS and DP.....	50
2.4.2 Primary culture of isolated embryonic cardiomyocytes	51
2.4.3 Culture of ES cells	51

2.4.4 Hanging drop culture of ES cells	52
2.4.5 Co-culture of DP and DS with ES cells in aggregates	52
2.4.6 Co-culture of rat DP and DS with mouse embryonic cardiomyocytes	54
2.4.7 Co-culture of DP and DS with matching species cardiomyocytes	54
2.4.8 Flow cytometry of CFSE labelled cells	56
2.5 RNA isolation	56
2.5.1 Harvesting cells for RNA	56
2.5.2 Harvesting tissues for RNA	56
2.5.3 RNA extraction	58
2.5.4 Agarose gel electrophoresis	58
2.5.5 RNA quantification	59
2.6 cDNA synthesis	59
2.6.1 cDNA synthesis for reverse transcriptase PCR (RT-PCR)	59
2.6.2 cDNA synthesis for real time quantitative PCR (Q-PCR)	59
2.7 Primer Design	60
2.7.1 Primers designed for RT-PCR	60
2.7.2 Primers for Q-PCR	60
2.8 Polymerase Chain Reaction	61
2.8.1 RT-PCR	61
2.8.2 Q-PCR	61
2.9 Induced myocardial cryo-injury	62
2.10 Immunohistology	63
2.10.1 Preparing tissue	63
2.10.2 Slide preparation	63
2.11 Immunohistochemistry antibody labelling	63
2.12 Immunofluorescence antibody labelling	65
2.12.1 Single labelling methods	65
2.12.2 Dual labelling method	66
2.13 Cell preparation for flow cytometry immunofluorescence analysis	67
2.13.1 Adult heart	67
2.13.2 Neonatal skin	67
2.14 Flow cytometry	68
2.15 Statistical analysis	68

Chapter 3: Characterisation of dermal follicular cells

3.1 Morphological characteristics of the dermal follicular cells in adherent culture	69
3.2 Expression of dermal follicular genes in DP and DS primary cultures	71

3.3 Dermal follicular cell population doubling time as determined by cell counts	74
3.4 Pulse chase proliferation assay to examine cell division	75
3.5 Investigation of hypoxic culture on population doubling time	81
3.5.1 Outgrowth from primary explant: day 1-14	81
3.5.2 DP and DS primary culture: day 14-30	81
3.5.3 DP and DS primary culture: day 30-46	82
3.6 Spontaneous appearance in DP and DS culture cardiomyocyte-like cells	85
3.6.1 Spontaneous appearance of myocyte-like cells	86
3.6.2 Spontaneous appearance of myotube-like cells	86
3.6.3 Synchronised contractions	89
3.7 Directed cardiomyocytic differentiation potential of DP and DS cultures by gene expression analysis	91
3.8 Chapter 3 Discussion	96

Chapter 4: In vitro cardiomyogenic differentiation potential of the dermal follicular cells

4.1 Inducing the dermal follicular cells to differentiate to cardiomyocytes by hanging drop co-culture with ES cells	105
4.1.1 Morphological comparison of ES cell embryoid bodies with DP and DS co-culture cell aggregates	106
4.1.2 Expression of cardiomyocyte associated genes in DP and DS primary cells after ES cell co-culture	109
4.2 Inducing the dermal follicular cells to differentiate to cardiomyocytes by co-culture with embryonic cardiomyocytes	115
4.2.1 Establishing embryonic cardiomyocytes in adherent culture for co-culture with DP and DS primary cells	115
4.2.2 Co-culture of rat dermal follicular cells with mouse embryonic cardiomyocytes	119
4.2.3 Expression of cardiomyocyte associated genes in DP and DS primary cells after embryonic cardiomyocyte co-culture	121
4.3 Inducing the dermal follicular cells to differentiate to cardiomyocytes by co-culture with embryonic cardiomyocytes of matching species	121
4.3.1 Identifying cells of dermal origin in same species co-culture	123
4.3.2 Expression of cardiomyocyte associated genes in DP and DS primary cells after same species embryonic cardiomyocyte co-culture	130
4.3.3 RT-PCR analysis	132
4.3.4 Q-PCR analysis	135
4.4 Chapter 4 Discussion	139

Chapter 5: The mTERT-GFP mouse model

5.1 Characterisation of the hair follicle and dermis of the mTERT-GFP mouse	150
5.1.1 Histological investigation of the mTERT-GFP vibrissae follicles	151
5.1.1.1 GFP epifluorescence of adult vibrissae follicles	153
5.1.1.2 Antibody labelling of adult vibrissae follicles	153
5.1.1.3 Antibody labelling of adult face pad	154
5.1.1.4 Antibody labelling of embryonic vibrissae	158
5.1.1.5 Antibody labelling of neonatal dermis	158
5.1.2 Isolation and characterisation of the mTERT-GFP neonatal dermis	166
5.1.2.1 Flow cytometric analysis of the dermis	166
5.1.2.2 Culture of FACS isolated GFP+ve and GFP-ve cells of the dermis	173
5.1.2.3 PCR analysis of FACS isolated dermal populations	174
5.2 Characterisation of GFP expression of the heart in the mTERT-GFP mouse	179
5.2.1 Histological investigation of the mTERT-GFP heart	180
5.2.2 Flow cytometric analysis of the heart	180
5.2.3 Investigation of GFP+ve cells of the myocardium in response to cryo-infarct....	182
5.2.3.1 Size of probe and placing of injury	182
5.2.3.2 Cryo-probe application time	182
5.2.3.3 Diaphragm damage	184
5.2.3.4 Survival Rate	184
5.2.3.5 Cardiac cryo-injury	184
5.2.3.6 Time course of the appearance of the cryo-injury site	184
5.2.3.7 GFP antibody labelling of the cryo-injured heart	191
5.3 Chapter 5 Discussion	196

Chapter 6: Discussion

Discussion	206
6.1 Future Studies	210

Appendix

1 Abbreviations	213
2 Chemicals and Reagents	215
3 Buffers	216
4 Kits	216
5 Cell lines and culture media	217
6 Primer Design	218

6.1 RT-PCR Primer Sequences.....	218
6.2 Q-PCR probes and primer sets.....	221
7 Antibodies and Fluorochromes	221
7.1 Immunohistochemistry	221
7.2 Flow cytometry	222
8 Equipment	222
References.....	224

Table of Figures

Chapter 1

Figure 1.1: Morphogenesis of the mammalian heart	10
Figure 1.2: Table of markers associated with putative stem cell populations	21
Figure 1.3: The hair follicle	36

Chapter 2

Figure 2.1: Location of the DP and DS and the end bulb in the hair follicle	47
Figure 2.2: Mystacial pad excision for hair follicle exposure and vibrissae isolation ...	48
Figure 2.3: Illustration of co-culture of DP and DS with ES cells in aggregates	53
Figure 2.4: Illustration of co-culture of rat DP and DS with mouse cardiomyocytes	55
Figure 2.5: Illustration of species matched co-culture of DP and DS with cardiomyocytes....	57

Chapter 3

Figure 3.1: Morphology of DP and DS <i>in vitro</i> culture	70
Figure 3.2: Gene expression profile of DP and DS primary cultures and clones	73
Figure 3.3: Cell population doubling time and passage cell density	76
Figure 3.4: Illustration of method of CFSE labelling	77
Figure 3.5: Pulse chase CFSE labelling of DP and DS in culture: control CFSE labelling of DP and DS primary cells	78
Figure 3.6: Pulse chase CFSE labelling of DP and DS in culture: CFSE proliferation assay of DP and DS primary culture cells	80
Figure 3.7: Morphology of DP and DS primary cells in normoxic and hypoxic <i>in vitro</i> culture	83
Figure 3.8: DP and DS primary culture population doubling time changes from passage 2 to passage 3 in normoxic and hypoxic <i>in vitro</i> culture	84
Figure 3.9: Morphology of cells similar to cardiomyocytes spontaneously appearing in mixed DP and DS primary cultures <i>in vitro</i>	87
Figure 3.10: Morphology of cells indicative of myotubules, spontaneously appearing in mixed DP and DS primary cultures <i>in vitro</i>	88
Figure 3.11: Morphology of spontaneous appearance of contractile cells in mixed DP and DS primary culture <i>in vitro</i>	90
Figure 3.12: Cardiac transcription factor-associated gene expression profile of DP and DS primary cultures and clones	93
Figure 3.13: Cardiac function-associated gene expression profile of DP and DS primary cultures and clones	94
Figure 3.14: Gene expression profile of DP and DS primary cultures and clones for genes associated with stem cells; sca-1 and TERT and vessel-associated gene tropoelastin	95

Chapter 4

Figure 4.1: Morphology of the ES cell embryoid bodies compared to the ES: dermal cell aggregates	108
Figure 4.2: Expression of genes characteristic of cardiomyocyte lineage during ES cell differentiation in the mouse EB and dermal cell aggregates	110

Figure 4.3: Expression of rat genes characteristic of cardiomyocyte lineage, during potential dermal cell differentiation in the presence of differentiating ES cells.....	112
Figure 4.4: Expression of mouse genes characteristic of cardiomyocyte lineage, during ES cell differentiation in the presence of dermal cells.....	114
Figure 4.5: Morphology of embryonic cardiomyocytes between day 3 to day 16 in adherent primary culture.....	117
Figure 4.6: Identification of individual embryonic cardiomyocytes at day 25 in adherent primary culture by cardiac actin labelling.....	118
Figure 4.7: 2D Co-culture of mouse embryonic cardiomyocytes with rat dermal cells.....	120
Figure 4.8: Expression of cardiomyocyte lineage genes in primary dermal follicular cells after embryonic cardiomyocyte co-culture.....	122
Figure 4.9: Analysis of the effect of CFSE labelling on dermal follicular cell viability.....	124
Figure 4.10: Flow cytometry analysis of CFSE labelled dermal follicular cells after 7 days culture.....	127
Figure 4.11: Comparative analysis of recovery of CFSE labelled dermal follicular cells from mixed labelled populations.....	128
Figure 4.12: Flow cytometry analysis of percentage recovery of CFSE labelled cells at immediate sorting and after 7 days culture.....	129
Figure 4.13: FACS identification of cells of dermal origin in co-culture with embryonic cardiomyocytes of matching species.....	131
Figure 4.14: RT-PCR Gene expression profile of CFSE +ive rat dermal follicular cells after co-culture with rat embryonic cardiomyocytes.....	133
Figure 4.15: RT-PCR Gene expression profile of CFSE +ive mouse dermal follicular cells after co-culture with mouse embryonic cardiomyocytes.....	134
Figure 4.16: Q-PCR Gene expression profile of CFSE +ive mouse dermal follicular cells after co-culture with mouse embryonic cardiomyocytes.....	136

Chapter 5

Figure 5.1: Immunohistochemical labelling for GFP+ve cells in mTERT-GFP testes	155
Figure 5.2: Immunohistochemical labelling for GFP+ve cells in the hair follicles of the mTERT-GFP vibrissae.....	156
Figure 5.3: Immunohistochemical labelling for GFP+ve cells in mTERT-GFP vibrissae....	157
Figure 5.4: Immunofluorescence labelling of neonatal skin of the WT mouse showing epidermal autofluorescence.....	159
Figure 5.5: Immunofluorescent labelling for GFP and CD45 cells in the neonatal skin of the WT mouse.....	160
Figure 5.6: Immunofluorescent labelling for GFP and CD45 cells in the neonatal skin of the mTERT-GFP mouse.....	161
Figure 5.7: Immunofluorescent labelling for GFP and CD34 cells in the neonatal skin of the WT mouse.....	162
Figure 5.8: Immunofluorescent labelling for GFP and CD34 cells in the neonatal skin of the mTERT-GFP mouse.....	163
Figure 5.9: anti-GFP labelled cells, of the skin of the mTERT-GFP mouse, associated with the dermis surrounding the follicular end bulb.....	164
Figure 5.10: anti-GFP labelled cells, of the skin of the mTERT-GFP mouse, associated with the inter-follicular dermis.....	165
Figure 5.11: Flow cytometric analysis of dermis, from 2 day old mTERT-GFP mouse pup, for viable GFP+ve cells.....	168

Figure 5.12: Flow cytometric analysis of dermis, from 3 day old mTERT-GFP mouse pup, for viable GFP+ve cells.....	169
Figure 5.13: Flow cytometric analysis of dermis, from 5 day old mTERT-GFP mouse pup, for viable GFP+ve cells.....	170
Figure 5.14: Flow cytometric analysis of 1 week cultured dermis, from 3 day old mTERT-GFP mouse pup, for viable GFP+ve cells	171
Figure 5.15: Flow cytometric analysis of 2 week cultured dermis, from 3 day old mTERT-GFP mouse pup, for viable GFP+ve cells	172
Figure 5.16: RT-PCR gene expression profile of FACS isolated dermal populations for cardiomyocyte-associated and stem cell-associated genes	176
Figure 5.17: Q-PCR gene expression profile of FACS isolated dermal populations for stem cell-associated genes.....	177
Figure 5.18: Flow cytometric analysis of mTERT-GFP neonatal heart for viable GFP+ve cells that are non-haematopoietic	181
Figure 5.19: Cryo-injury of heart as a model of cardiac infarct.....	183
Figure 5.20: Excised cryo-injured heart 24 hrs post-infarct.....	186
Figure 5.21: Excised cryo-injured heart 3 days post-infarct	187
Figure 5.22: Excised cryo-injured heart 8 days post-infarct	188
Figure 5.23: Excised cryo-injured heart 14 days post-infarct	189
Figure 5.24: Section of 14 day cryo-infarct showing depth of tissue damage	190
Figure 5.25: Immunohistochemical staining for GFP cells in 14 day cryo-injured myocardium of the WT mouse.....	192
Figure 5.26: Immunohistochemical labelling for GFP cells in 14 day cryo-injured heart of the mTERT-GFP mouse.....	193
Figure 5.27: Immunohistochemical labelling for GFP cells in the 14 day cryo-injured heart of the mTERT-GFP mouse	194
Figure 5.28: Immunofluorescent labelling for GFP+ve cells in the mTERT-GFP 14 day cryo-injured epicardium	195

1 Dermal follicular cells as a model for investigation of somatic cell differentiation

1.1 Stem Cell Identification

Stem cells were described in 1990 by Potten and Loeffler as being undifferentiated cells which are capable of self-maintenance, proliferation with production of a large number of differentiated functional progeny and are responsible for regeneration of tissue after injury (Potten and Loeffler 1990). This remains an accurate description of stem cells; they are also considered to be primordial with their specific differentiation potential dependent upon their anatomical location. Stem cells have been described as being totipotent or multipotent. Totipotent cells have the potential to give rise to all the three germ layers, the placenta and extra-embryonic membranes and describe the early embryonic and germinal stem cells as has been demonstrated with embryonic stem cells (reviewed by Odorico *et al.*, 2001). Multipotent cells give rise to all three germ layers and germ cells but not to the trophoblast and include the late embryonic stem cells and the neonatal stem cells, which are more differentiated than the early embryonic cells. Adult stem cells serve to maintain homeostasis of the organs they reside in, including repair after injury, and their potency is dependent upon the number of differentiated cell types they can give rise to. Adult stem cells have thought to be restricted in their differentiative and regenerative potential to the tissues in which they reside giving rise to a limited number of cell types *in vivo* for example haematopoietic stem cells (HSC) reconstituting blood after lethal irradiation. The stem cells give rise to new progeny that are less potent as the progenitor cells, however not yet as differentiated as the tissue cells; these are termed transit amplifying cells; Potten and Lajtha, in 1982, described the number of transit amplifying stages as being dependent upon the number of cells produced by that organ (Potten and Lajtha 1982).

However, the differentiation of adult stem cell progeny being described as linear and irreversible has been challenged by a number of pieces of work where adult stem cells of specific tissues have been shown to contribute to another previously unrelated tissue, giving rise to the concept of plasticity and stem cells being defined by their functionality. Enriched bone marrow populations provide the best examples; HSC can differentiate into mature hepatocytes in the liver of rodents (Petersen *et al.*, 1999; Theise *et al.*, 2000) and humans (Theise *et al.*, 2000, Alison *et al.*, 2000), as well as microglia and macroglia (Eglitis and Mezey 1997); cell lineages unrelated to that of the

HSC. Therefore the concepts and models of stem cells are frequently revised in order to accommodate new data.

The microenvironment, including contact with surrounding cells, the extracellular matrix (Hay 1991), oxygen concentrations (Studer *et al.*, 2000) as well as growth and differentiation factors are likely to play a role in determining stem cell function; now termed the stem cell niche. The niche concept was introduced in 1978 (Schofield 1978) with spleen colony forming units; however, it was largely neglected until *Drosophila* studies provided a stimulus for its resurgence (as reviewed by Lin 2002); niche cells provide a sheltering environment, normally located deep within tissues, that sequesters stem cells from differentiation stimuli, apoptotic stimuli, and other stimuli that would challenge stem cell reserves and thereby enables them to maintain tissue homeostasis. The niche also safeguards against excessive stem cell proliferation that could lead to cancer (Moore and Lemischka 2006). Stem cells periodically activate to produce progenitor or transit amplifying cells that are committed to produce mature cell lineages; maintaining a balance of stem cell quiescence and activity is therefore a hallmark of a functional niche (Moore and Lemischka 2006).

Identifying niches and determining how they are regulated is experimentally challenging. To look systematically for niches in a target tissue, stem cells first need to be identified by gene expression or cell surface antigen expression, for example, and these cells need to be marked and their progeny also tracked. When individual stem cells have been localized, evidence that they reside in a common microenvironment is sought by characterizing cellular neighbours, expression patterns of signalling molecules and local environmental factors such as extracellular matrices. If commonalities are found, then the microenvironment can be disturbed to determine which aspects, if any, affect stem cell behaviour. Evidence of cardiac stem cell clusters in the adult heart (Anversa *et al.*, 2006A) suggests a potential stem cell niche. Although these clusters are scattered throughout the myocardium, their distribution appears to be conditioned by the distinct levels of wall stress where the frequency of cardiac stem cell clusters is inversely related to the hemodynamic load sustained by those anatomical regions. These clusters accumulate in the atria and apex and are less numerous at the base and mid-portion of the left ventricle (Leri *et al.*, 2005). Stem cells and supporting cells in the niches interact structurally and functionally through specialised gap and adherent junction proteins, that mediate passage of small molecules and signals

involved in cell-to-cell communication; in the human heart these are connexin-40, connexin-43 and connexin-45 (Vozzi *et al.*, 1999). Additionally, these gap junctions interfere with the activation, commitment, and migration of stem cells out of the niches. Survival factors traverse gap junctions to oppose cell death and favour cell growth (Leri *et al.*, 2005) but the identity of these molecules at the moment is largely unknown.

Any functional test or assay that would aim to demonstrate clonogenicity, self-renewal or multilineage differentiation could alter that cell by changing its characteristics or potency (Loeffler and Potten 1997). Therefore, complex cell surface markers are more often used to isolate a number of specific stem cell populations by FACS; as yet there is no one gene or marker that absolutely defines a stem cell from any tissue or developmental stage. Side population cells have been isolated from a number of adult tissues, including skeletal muscle, bone marrow, liver, lung, kidney, and brain and are associated with stem cell or progenitor cell populations. Tissue-derived side population cells are isolated by their efflux of the DNA binding dye, Hoechst 33342 (Goodell *et al.*, 1996) which has proven useful for selecting stem cell populations including for example HSC and skeletal muscle stem cells however this is not particularly definitive (Liadaki *et al.*, 2005).

Current stem cell research is largely focusing on understanding the role of the stem cell in homeostasis and cell turnover and their regulation. This becomes the base for investigating their response to injury, regeneration and their potential for differentiating to unrelated cell types as a precursor for their potential in treatment of disease. This thesis investigates the dermal follicular cells of the skin, the dermal papilla (DP) and dermal sheath (DS), which have been attributed stem cell properties and may be capable of directed differentiation; their differentiation potential towards a cardiomyocytic lineage is investigated here. The cardiac stem cell population of the heart is investigated in response to cryo-induced injury using a mouse model whereby potential stem cells are identified by their telomerase reverse transcriptase (TERT) expression.

1.2 Significance of heart disease

Diseases of the heart and circulatory system are the main cause of death in Europe; 48% of all deaths are from coronary heart disease, accounting for over 4.30 million deaths each year (European cardiovascular disease statistics 2008). It is thus a leading cause of death throughout the Western world and the main cause of both congestive heart failure

and sudden cardiac death (Lopez 2006). Myocardial infarction (MI) results from an acute reduction of blood to the myocardium, which leads to myocardial necrosis with overloading of the myocardium and gradual loss of large numbers of cardiomyocytes. These cardiomyocytes are removed, largely by macrophages, and replaced by scar tissue that may also be surrounded by poorly contractile surviving cardiomyocytes (Frangogiannis *et al.*, 2002). Cardiac wall thinning and cardiac remodelling, among other factors, lead to diminished functional capacity of the heart and eventual heart failure and ultimately death of the patient follows.

MI results in a number of necrotic cardiomyocytes; at this time of injury the cardiac cells appear unable to regenerate the tissue that is damaged. The early inflammatory phase is marked by the necrotic cardiomyocytes being replaced by granulation tissue, with stimulation of angiogenesis and recruitment of regulatory peptides and inflammatory cells, for example macrophages, to the MI site. This is followed by the fibrogenic phase where the granulation tissue is replaced by fibrillar, collagenous tissue largely due to the interstitial fibroblasts (Sun and Weber 2000). There is as yet no evidence that a potential cardiac stem cell population, which would be expected to be responsible for regenerating the cardiac tissue, is activated in response to an MI. Proposed reasons for this may include a delay in stem cell mobilisation or a lack of signalling to the cells to be mobilised due to the fibrotic scar tissue, the hypoxic environment of the scar being too hostile for cell survival for repair, cardiac stem cells in the area of the infarct also being necrotic or simply the cardiac stem cells are just not capable of regenerating such a large area of isolated tissue.

In summary, the human myocardium is inadequate to compensate for the severe loss of functional cardiomyocytes, potentially due to limited intrinsic regenerative capacity (Angelini and Markwald 2005), in both MI and other heart diseases states with current treatment often only delaying the progression of the disease. Conventional therapies, for example drug treatment with β -blockers, an antihypertensive medication that limits the activity of epinephrine, and angiotensin-converting enzyme (ACE) inhibitors which inhibit the formation of angiotensin II responsible for artery constriction, slow the progression of the disease process in the myocardium, however they do not address the problem of cardiomyocyte loss or replacement of the myocardial scar within functioning contractile tissue. In principle three main strategies could be proposed to induce muscle regeneration following myocardial regeneration:

- The surrounding myocytes stimulated to migrate to the site of infarct and proliferate to repair the defect.

There is a little evidence that this occurs naturally; with mammalian MI there is almost always the presence of a scar with evidence of infiltrating cardiomyocytes however this is not sufficient to fully repair the infarct.

- The cardiac granulation tissue, that is rich in fibroblasts, induced to differentiate into myocytes rather than forming a scar

With better understanding into cardiac differentiation it may be possible to induce the formation of new myocardium; it has been shown that cells in cardiac granulation tissue can be induced to differentiate into skeletal muscle by transfection with MyoD, a myogenic determination gene (Murry *et al.*, 1996) however as yet there is no evidence for cardiomyocyte differentiation.

- Cardiomyocytes, or cells that will differentiate into cardiomyocytes, transplanted into the area of injury

There is preliminary data for a number of stem cell types that have potential to be used in this way; currently, it is the most promising of these three potential interventions. There is a large body of evidence suggesting that stem cells of several lineages can differentiate to cardiomyocytes and a number of them, for example bone marrow HSC, are in clinical trial phase. However, the defining criteria for successful differentiation vary from cardiomyocyte-associated gene expression to functional improvement of MI hearts; in addition a number of methods of induction of differentiation are used including, for example, co-culture. These methods will be discussed later in this section.

The challenges with transplanting any cell type into the heart will lie in the ability of the transplanted cells to home to the myocardial tissue and if they differentiate to cardiomyocytes, to remain within it. The long term fate of transplanted cells into the heart needs to be investigated; whether these cells remain viable and functional or whether they contribute to teratoma formation. Also the capability of the host tissue to promote differentiation of the engrafted cells and associated angiogenesis may be necessary for ischemic tissue to be replaced by functional cardiomyocytes. The ability of transplanted cells to differentiate to cardiomyocyte-like cells (if the cell type is not a differentiated cardiomyocyte) and the structural and functional integrity of the

implanted cells will need to be assessed to avoid arrhythmias due to uncoordinated electrical activity.

A number of different cell types have been explored as a possible source of cardiomyocytes for myocardial repair with varying degrees of success; be it by direct (into the heart) or indirect (into the bloodstream) injection of a cell suspension. Another consideration is the application of undifferentiated stem cell population e.g. HSC or a differentiated cardiomyocyte population.

A prospective donor cell would ideally have the following qualities:

1. Easy to harvest/isolate and proliferative. It is important that the donor cell can be isolated with relative ease so that a significant number of cells can be harvested. If the donor cell requires to be differentiated into a cardiomyocyte then having a large number of source cells minimises passage number in tissue culture. If the cells need to be expanded *in vitro* before being used then it is important the donor cell is proliferative in culture, without evidence of transformation events that may cause the cells to have unlimited division when transplanted into the myocardium.

If the donor cell population need to be injected/applied to the heart without further manipulation then it is necessary to harvest a sufficient amount of cells from one or a limited number of donors. From a clinical perspective it would be advantageous for the method of cell isolation/harvest to be as simple as possible so it could potentially be transferable to a hospital environment. For any external, potential sources of cardiomyocytes, there will be a limited amount of cells that can be isolated.

2. Non-immunogenic. When transplanting a cell population into a patient it is important to prevent tissue rejection, especially with an organ like the heart where immune rejection would have severe detrimental effects. If a tissue source will be immunogenic then a patient can be administered immunosuppressants (Hosenpud 2005), however the degree of immunogenicity will need to be considered to ensure organ rejection would not occur.

3. Ability to differentiate into cardiomyocytes. The donor cell should be able to differentiate into a cardiomyocyte be it *in vivo* or *in vitro*. The cardiomyocyte must be functional; if the cells are differentiated *in vitro* it is necessary that the differentiation is controlled to produce a specific population of cells and *in vivo* that the population of cells once in the patient's body will differentiate into cardiomyocytes and not a cell of a

different lineage leading to potential teratomas. Therefore a level of control is necessary be it *in vitro* by manipulation of the cells or *in vivo* by the resident cardiomyocytes or signalling pathways.

4. Integration with the resident cardiomyocytes. The donor cell must integrate with the resident cardiomyocytes improving functionality of the damaged heart. One indication of communication is evidence of the donor cardiomyocyte establishing gap junctions with the neighbouring native cardiomyocytes, namely connexin-40 and connexin-43 (Coppen *et al.*, 2003), found between cardiomyocytes *in vivo*.

5. Ability to survive. It is important that the donor cell survive in the heart long enough to improve the global cardiac function. It may not be necessarily a requirement of the donor cell to be able to survive the length of the life of the heart itself, as it may only be a temporary aid by providing for example a scaffold for resident cardiomyocytes to infiltrate. However, it is necessary that the cells survive *in vivo*.

The challenge to date has been to find a cell type that has all these qualities; many of the cell sources investigated including differentiated, undifferentiated, progenitor, precursor and adult cells, have shown evidence of limitations in the number of these qualities they express. For example to date, donor (allogenic) cells are relatively easy to obtain but involve immunosuppression for the patient. Autologous cells have no immunological problems but are more difficult to obtain and often hard to expand. Being able to generate a cardiac cell-based therapy may provide a source of functional cells that would replace normal scar formation. It has long been assumed that the reason for poor regeneration of the adult heart was the absence of endogenous progenitor cells; however this concept has been challenged with a number of pieces of evidence that support the theory of native cardiac stem cells and these will be discussed.

1.3 Development and maintenance of the heart

1.3.1 Cardiac development

The commitment of unique cellular lineages to distinct regions of the heart guides the three-dimensional events of cardiac development (Buckingham *et al.*, 2005). Understanding how stem and progenitor cells adopt cardiac-cell fate and subsequently assemble into the functional heart may lead to new approaches to repair or regenerate damaged heart muscle; insights into cardiogenesis from progenitor cells during

embryogenesis will compliment the investigation into reprogramming cells for therapeutic use.

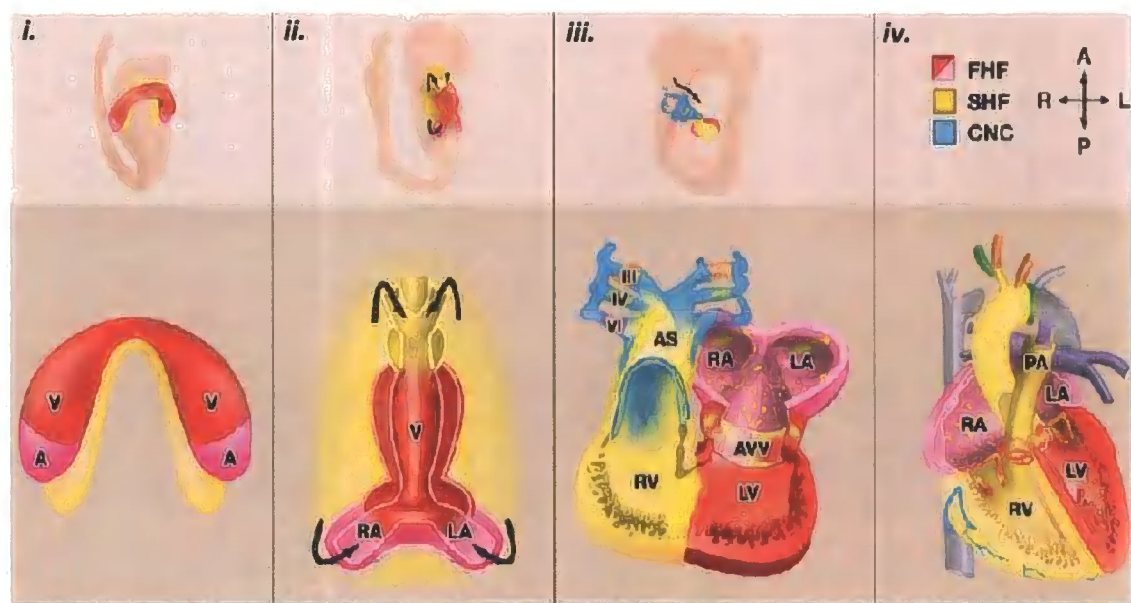
Two distinct mesodermal heart fields emerge from the primitive streak during gastrulation and contribute cells to the developing heart. The first heart field (FHF) derives cells from the anterior lateral plate mesoderm and forms a crescent shape at approximately embryonic (E) day 7.5 in the mouse embryo (week 2 of human gestation) (Srivastava 2006); by E8 (week 3 of human gestation) these cells coalesce along the ventral midline to form the primitive linear heart tube (Srivastava 2006). This structure consists of an interior layer of endocardial cells and an external layer of myocardial cells; separated by extracellular matrix which permits signalling between the layers. It is thought that the second heart field (SHF), marked by *Islet1* (*Isl1*) expression and comprising the dorsal-medial aspect of the cardiogenic plate, migrate to the scaffold provided by the FHF and contribute to chamber formation (Cai *et al.*, 2003). Interestingly *Isl1* is expressed in the post-natal heart by cells in cardiac niches and is thought to denote undifferentiated cardiac progenitor cells (Laugwitz *et al.*, 2005; Moretti *et al.*, 2006), this is discussed later. As the heart tube forms, the SHF cells migrate to the pharyngeal mesoderm at the midline. Rightward looping occurs and the SHF cells cross into the anterior and posterior portions of the tube, thought to be attracted to migrate by factors secreted by the anterior portion of the tube; these cells populate a large portion of the outflow tract, and future right ventricle, and atria with the FHF making up the majority of the cells in the left ventricle with a small contribution from the SHF; the chamber configuration is apparent by E9.5 (Srivastava 2006). Endocardial and epicardial signalling then encourages these cells to differentiate with chamber growth and expansion of the myocardium. Concurrently, the developing cardiac segments become subdivided by septa that initially are mesenchymal in composition and later in development become highly muscularised. Cardiac muscularisation is a result of two distinct mechanisms involving the growth and expansion of pre-existing myocardium and/or the recruitment of new cardiomyocytes from intracardiac and extracardiac mesenchyme located adjacent to the expanding myocardium (Srivastava 2006). Cells migrating from the neural crest septate the outflow tract of the developing heart and contribute to formation of arterial valves and the coronary arteries. These cells have been suggested to contribute to the development of the venous pole of the heart, but this process is poorly understood although there is

evidence it plays a role in nerve innervation (Hildreth *et al.*, 2008). The development of the heart is shown in figure 1.1.

A number of transcription factors are associated with early cardiomyocyte induction and commitment. These include Nkx2.5, GATA4, Mef2c and tbx5; four genes widely recognised as having roles in the developing embryonic heart as well as being expressed in the adult cardiomyocytes at lower levels. The initiation of cardiac differentiation has been vigorously investigated; however as yet there is no single transcription factor that appears responsible for the differentiation of lateral plate mesoderm into cardiac cells. The drosophila tinman gene encodes an NK-class homeodomain-containing transcription factor, identified Nkx2.5 in vertebrates (also known as Csx) and this is one of the earliest genes expressed in pre-cardiac mesoderm from both the FHF and the SHF; transcripts for murine Nkx2.5 are detected in early myocardiogenic progenitor cells at E7.5 (Srivastava and Olson 2000). Nkx2.5 is necessary for initiation of looping morphogenesis and chamber formation and its expression is maintained in the myocardium of embryonic and foetal hearts, as well as being linked to a number of downstream transcription factors (Lyons *et al.*, 1995).

The GATA family of zinc finger-containing transcription factors appear to be potentially critical in the progressive differentiation of pre-cardiac cells specifically in the formation of the linear heart tube when the FHF coalesce. GATA4 is detected at the same embryonic ages as Nkx2.5, E7.5, where it is confined to the cardiogenic crescents. GATA4 is co-expressed with Nkx2.5 in subsequent myocardial cells and by E9-10, is found in abundance in the atria, ventricles and proximal outflow where expression continues in the late foetal and adult heart. GATA4 is also responsible for controlling normal formation of the endoderm underlying the myocardial precursors (Srivastava and Olson 2000). Research into the inhibitory and activation domains indicates that Nkx2.5 undergoes conformational changes when interacting with other co-accessory factors, enabling it to become a more effective transcriptional activator (Sepulveda *et al.*, 1998). Nkx2.5 has an upstream enhancer that has a binding site for GATA4 (Brown *et al.*, 2004) and the C-terminus of Nkx2.5 has been shown to act as a transcriptional inhibitor; it is proposed that GATA4 may cause a conformational change in Nkx2.5 such that the negative constraint is eliminated.

Figure 1.1: Morphogenesis of the mammalian heart



(Adapted from Srivastava 2006)

Mammalian heart development. Myocardial progenitor cells originate in the primitive streak from where the first heart field (FHF) form the cardiac crescent; the second heart field (SHS) cells medial and anterior to the FHF (*i.*) where differentiated myocardial cells are now observed (mouse E7.5). The early cardiac tube forms through fusion of the cardiac crescent at the midline (E8). SHF cells lie dorsal to the straight heart tube and begin to migrate (arrows) into the anterior and posterior ends of the cardiac tube to form the right ventricle (RV), and part of the atria (A), known as looping (*ii.*). Following rightward looping of the heart tube, cardiac neural crest (CNC) cells also migrate into the outflow tract from the neural folds to septate the outflow tract and pattern the bilaterally symmetric aortic arch arteries (III, IV, and VI) (*iii.*). Septation of the ventricles, atria, and atrioventricular valves (AVV) results in the four-chambered heart (*iv.*).

V, ventricle; LV, left ventricle; LA, left atrium; RA, right atrium; AS, aortic sac; PA, pulmonary artery.

GATA4, in complex with Nkx2.5, associates with tbx5 promoting cardiomyocyte development (Hiroi *et al.*, 2001); together these are involved in atrial septation and left ventricular formation (Srivastava and Olson 2000).

Mef2c, a MADS-BOX transcription factor, is expressed at the late cardiac crescent stage (E7.75) medial to the crescent as well as in the SHF and subsequently throughout the linear, looping, and multi-chambered heart (Srivastava and Olson 2000). It has been identified to be important in the looping of the heart tube at the stage where the tube forms the right ventricular chamber. Mef2c also appears to be a target of Isl1 as is indicated by an enhancer element within the Mef2c gene which is regulated by Isl1 as well as GATA4 (Dodou *et al.*, 2004). GATA4 can also recruit Mef2 to GATA-dependant regulatory elements to create specific active transcriptional complexes which are likely to confer degrees of tissue specificity during heart development (Morin *et al.*, 2000). Mef2c is also thought to associate with Nkx2.5 where the two genes up-regulate each other and are thought to initiate cardiomyogenesis (Skerjanc *et al.*, 1998).

T-box transcription factor 20 (tbx20) affects expansion of FHF- and SHF-derived cells and is necessary for outflow tract development, possibly by regulating Nkx2.5 and Mef2C (Srivastava 2006). In addition tbx5 appears to be a positive regulator of early cardiogenesis and chamber specification; GATA4, tbx5, and Nkx2-5 may form a complex required for proper cardiac septation (Srivastava 2006).

These four transcription factors are central to the development of the functional, organised cardiomyocytes as is demonstrated by knock out studies; homozygous null alleles for each of these genes results in severe congenital heart malformations mostly associated with the heart tube looping morphogenesis (Lyons *et al.*, 1995; Lin *et al.*, 1997; Molkentin *et al.*, 1997). Early cardiomyocytes do form without the expression of these genes, however, their functionality and organisation is disrupted which results in embryo re-absorption. The expression of these genes are maintained in the adult heart, albeit at low levels, and has been associated with cardiac stem cells as will be discussed later in this chapter. Because these four genes are maintained in embryonic, as well as adult, cardiomyocytes they make ideal markers for investigating potential cardiomyocyte differentiation.

There are a large number of genes associated with the functional cardiomyocyte, controlled by the transcription factors described, that are associated with sarcomere

formation. The sarcomere of the cardiomyocyte is composed of thick and thin filaments; the thick filaments extend from the centre of the sarcomere and are composed of myosin heavy and light chains and supported by binding to titin molecules. The thin filament is made up of actin, troponin and tropomyosin (Takeda 2003); in the cardiomyocyte the cardiac specific sarcomere structural genes, alpha myosin heavy chain (α -MHC), myosin light chains specific to the atria (MLC1A) and ventricle (MLC1V), tropomyosin and cardiac actin are essential as well as genes associated with contractions including troponin I and titin (Wessels *et al.*, 1991; Hill *et al.*, 1992; Zammit *et al.*, 2000).

Myosin, essential for muscle contraction, is a multi-subunit protein that is made up of two heavy chains; two phosphorylated light chains and two non-phosphorylated light chains. Different myosin isoforms are found in cardiac, skeletal, smooth and non-muscle cells where myosin heavy chain (MHC) is the major contractile protein in the heart; α -MHC and β -MHC are expressed in cardiomyocytes. The myosin composition of the heart is of physiological significance; the relative distribution of α -MHC and β -MHC is in direct correlation with the contractile performance of the heart. α -MHC is associated with increased shortening of the cardiac velocity. In contrast; β -MHC is associated with hypocontractile states. α -MHC mRNA is expressed in the cardiac tube between days E7.5 and E8 but diminishes between days E8 and E9 as the ventricular chambers form (Haddad *et al.*, 2003; Kolossov *et al.*, 2005). It remains at low levels until just after birth, where β -MHC is the predominant myosin heavy chain isoforms in the ventricles during fetal development. At birth there is a dramatic increase in thyroid hormone and also a dramatic change in the expression of the myosin heavy chain isoforms; α -MHC levels increase to as much as 95% of the total MHC in the heart in humans, 90% in small mammals, and remain high throughout adult life (Haddad *et al.*, 2003). Within the α -MHC promoter are binding sites for Mef2c, GATA and KO of α -MHC results in cardiac deformities (Jones *et al.*, 1996).

Tropomyosin is an essential thin filament protein that binds to cardiac actin and troponin I which regulate the calcium sensitive interaction of actin and myosin in the heart (Adhikari and Wang 2004). The tropomyosin 1 isoform specific to striated muscle consists of 10 exons and is designated α -tropomyosin and it is expressed mainly in the heart. During fetal development α -tropomyosin represents 80% of the total tropomyosin of the heart but in the adult heart 98% (Hill *et al.*, 1992).

1.3.2 The evidence for the cardiac stem cell

Increases in cardiac mass during foetal and embryonic life arise predominantly as a consequence of cardiomyocyte proliferation, however during neonatal life there is a transition from hyperplastic to hypertrophic growth that further increases the myocardial mass as cells withdraw from the cell cycle (MacLellan and Schneider 2000; Chien and Olson 2002). This led to the long-held belief that the adult heart was a terminally differentiated organ. Hypertrophic growth is not typically accompanied by cardiomyocyte proliferation; in the adult myocardium it is generally believed that the vast majority of cardiomyocytes do not proliferate. This view is supported in part by clinical observations; functionally significant myocardial regeneration has not been documented in diseases or injuries where there is cardiomyocyte loss; the major response to myocardial damage was thought to be hypertrophy of still-viable cardiomyocytes that had exited the cell cycle (Barile *et al.*, 2007). Furthermore, primary myocardial tumours are rarely observed in adults. These observations suggest that the proliferative capacity of adult cardiomyocytes is quite low, however they do not exclude the existence of a limited degree of hyperplastic growth in either the normal or diseased myocardium.

A number of studies investigated the possibility of the cardiomyocytes having proliferative capacity, mostly by monitoring cardiomyocyte DNA synthesis as an approximation of cell division, as genome reduplication is a prerequisite for cell proliferation. One of the earliest approaches used to monitor genome reduplication was to score for the presence of mitotic figures which clearly identifies dividing nuclei (Sasaki *et al.*, 1968; Rumyantsev and Marakjan 1968; Rumyantsev 1983) however the duration of the appearance of mitosis, the M phase, is short and in a low proliferative tissue capturing a time point to identify such mitotic figures can be problematic. Direct assessment of DNA, for example by incorporation of deoxyribonucleotide analogues such as tritiated thymidine (Kuhn *et al.*, 1974; Wachtlova *et al.*, 1977; Clubb and Bishop 1984; Erokhina and Rumyantsev 1986; Marino *et al.*, 1991; Soonpaa *et al.*, 1996) and BrdU labelling in pulse chase experiments (Nakagawa *et al.*, 1988; Reiss *et al.*, 1993; Kajstura *et al.*, 1994; Cheng *et al.*, 1995; Li *et al.*, 1996A; Soonpaa *et al.*, 1996; Machida *et al.*, 1997), was employed in a number of studies to assess cardiomyocyte DNA synthesis. The reported values for cardiomyocyte DNA synthesis are in good agreement at the early stages of heart development, where a relatively large

percentage of cells are proliferating; a range of 10-46% according to mice and rat studies (reviewed by Soonpaa and Field 1998). The main discrepancies appear in the frequency of DNA synthesis in healthy and diseased hearts in late neonatal and adult animals where the level of cardiomyocyte DNA synthesis is, on average, markedly lower. A range of dividing cells have been reported in normal developmental adult hearts ranging from 0-3.5% with an average of 0.43% (reviewed by Soonpaa and Field 1998); with ranges for injury slightly higher with averages of 2.53% for spark injury, 13.22% for left ventricular infarct and 4.32% for coronary banding (reviewed by Soonpaa and Field 1998). However, these values are influenced by a number of potential factors such as nuclear misidentification, variation due to species, age of the animals (for example adolescent hearts may retain a degree of development-associated cardiomyocyte DNA synthesis), type of injury used etc., which may affect the percentage of cells demonstrating DNA synthesis as well as the possibility of these dividing cells being cell types other than cardiomyocytes, for example fibroblasts in response to injury.

This small, but evident, percentage of dividing cells was suggestive of a population of cells capable of division and offered an alternative view of cardiac homeostasis. Initial evidence of cycling ventricular myocytes in the normal and pathologic adult mammalian heart (Beltrami *et al.*, 2001; Kajstura *et al.*, 1998) following the identification of dividing cardiomyocytes, added further speculation to the existence of a proliferative population of cardiomyocytes. This raised questions over the reconciliation of the well-documented irreversible withdrawal of cardiomyocytes from the cell cycle soon after birth and the presence of cycling myocytes in the adult heart.

As a result, several independent studies described a cardiac stem cell or progenitor cells that may be responsible for the mitotically active cells and limited myocardial regeneration in response to injury. These studies took one of three approaches to isolate potential cardiac stem cells from the heart. The first was isolation of cells based upon their ability to efflux Hoechst dye, which is associated with side populations, or the presence of cell-surface markers, either c-kit, sca-1 or Abcg2 by magnetic cell sorting and flow cytometry. The second was tissue culture of cardiac explants with spontaneous cardiosphere formation *in vitro*. The third was expression of the islet-1 gene as a potential marker of embryonically derived cardiac progenitor population.

Beltrami *et al.*, isolated potential cardiac stem cells from adult rat hearts by their expression of the surface marker c-kit (Beltrami *et al.*, 2003). In sex mismatched cardiac transplants in humans, the female hearts in male hosts had a significant number of Y chromosome-positive myocytes and coronary vessels (Quaini *et al.*, 2002) potentially indicating male cells colonized the female heart after transplantation; cells of both donor and recipient origin were found to express c-kit, as well as sca-1 and moreover cells positive for these two cell surface antigens were detected in human control hearts (Quaini *et al.*, 2002; Teyssier-Le Discorde *et al.*, 1999). Beltrami identified c-kit+ve cells in the myocardium of 20-25 month old rats which were small cells, approximately one tenth the size of cardiac myocytes, arranged in clusters. These cells were negative for blood lineage markers including CD34, CD45, CD20, and CD8 (lineage-ve) (Beltrami *et al.*, 2003). FACS sorting indicated a number of these cells, 7-10% of the c-kit+ve cells also expressed Nkx2.5, GATA4 and Mef2 and <0.5% expressed sarcomeric proteins. In culture the c-kit+ve lineage-ve cells were able to divide, as demonstrated by Ki67 expression even at passage 23, they were clonogenic and demonstrated multipotent heterogeneous differentiation generating cardiomyocytes, smooth muscle cells and endothelial cells. However, these cells were morphologically and functionally immature, with disorganised structure and no identifiable sarcomeres or contractions, potentially indicating they required the terminally differentiated myocardial cells for this. To investigate whether these cells could reach maturity *in vivo*, passage 2 cultured c-kit+ve, lineage-ve cells were labelled with BrdU and injected into the border zone of experimental MI rat hearts. A band of labelled cells was identified in regenerating myocardium in all 10 treated infarcts after 20 days, the labelled cells were small relative to mature cardiomyocytes, expressed sarcomeric proteins, exhibited visible striations and the gap junction connexin-43 (Beltrami *et al.*, 2003). Ventricular function was significantly improved and contribution of labelled cells to blood vessels was observed. This was confirmed to be attributed to by the c-kit+ve, lineage-ve cells by repeating the injections with clonally derived cells. One potential caveat was the possibility that the c-kit+ve cells fused with existing host cells which would give the appearance of differentiation, however Beltrami confirmed the labelled myocytes were diploid.

Around the same time it was reported a population of cardiac progenitor cells co-purified with sca-1 expression made up 14-17% of cardiac cells, however these cells

were c-kit-ve. 0.03% of cells lacked expression of lineage markers CD45 and CD34 (markers of endothelial progenitor cells), blood cell lineage markers (CD4, CD8, TER119), markers of vascular endothelium and lacked haematopoietic transcription factors (Lmo2, GATA2 and Tal) (Oh *et al.*, 2003). Interestingly these cells were TERT+ve, a gene which has been associated with self-renewal potential. However, in contrast to the work of Beltrami these cells did not express early cardiac markers GATA4, Mef2, Nkx2.5 or sarcomeric proteins. It was reported these cells spontaneously differentiated *in vitro* however this was after treatment with 5-azacytidine, with a fraction of cells then demonstrating sarcomeric α -actin, cardiac troponin I, Nkx2.5, and MHC. As with the cells Beltrami isolated, membrane dye-marked sca-1+ve cells were injected into mice after ischemia and were identified in the border zone of the injured myocardium expressing sarcomeric α -actin, cardiac troponin I, and connexin-43 with evidence of fusion events as well as the presence of grafted cells entirely donor-derived (Oh *et al.*, 2003). Unfortunately no functional analysis was reported. A year later Matsuura also reported isolation of sca-1-ve cells, however these cells were c-kit+ve albeit at low levels. Matsuura reported that sca-1+ve cells made up 0.3% of the cardiac myocytes of which 40% expressed CD45 and 10% expressed CD34 and c-kit (Matsuura *et al.*, 2004B). These cells also expressed low levels of Nkx2.5 and GATA4. The sca-1+ve cells were treated with oxytocin in culture and spontaneous contractions were observed in approximately 1% of the cells, which also appeared spindle shaped, after 4 weeks. These cells also expressed higher levels of mRNA for Nkx2.5 and GATA4 as well as expression of Mef2c, α - and β - MHC, myosin light chain 2A and 2V, cardiac α -actin, cardiac troponin T and tropomyosin with some evidence of connexin-43+ve gap junctions. However, these cultures contained cells which were CD45+ve and CD34+ve. In an attempt to ascertain if the appearance of differentiation was attributed to the non-haematopoietic sca-1+ve cells, the sca-1+ve CD45+ve cells were cultured separate to the sca-1+ve CD45-ve cells with oxytocin treatment. The CD45+ve cells did not demonstrate evidence of cardiomyocyte differentiation while the CD45-ve cells expressed evidence of sarcomeres (Matsuura *et al.*, 2004). In addition, the sca-1+ve cells were shown to be multipotent by appearance of early markers of osteogenesis and adipogenesis after treatment with inducers in culture however the cells were not sorted for CD45 expression first, leading to the question as to whether this differentiation was due to contaminating haematopoietic cells.

The bone marrow contains cells which are haematopoietic and are c-kit+ve, sca-1+ve, lineage negative and CD34-ive/low which contribute to multilineage reconstitution of the mouse blood system (Osawa *et al.*, 1996). In addition there have been reports of c-kit+ve bone marrow and MSC transdifferentiating into cardiomyocytes *in vivo* (Orlic *et al.*, 2001; Gojo *et al.*, 2003) which suggests c-kit is an important marker for multipotent bone marrow-derived cells. In addition, skeletal muscle-derived cells highly express CD34 and sca-1 but not c-kit and CD45 (Qu-Petersen *et al.*, 2002; Torrente *et al.*, 2001). Therefore, the exclusion of CD45+ve cells is important in excluding potential bone marrow-derived contaminating cells.

Messina *et al.*, reported the isolation of undifferentiated cardiac cells that grew as self-adherent clusters termed cardiospheres (Messina *et al.*, 2004). Explants from human atrial and ventricular biopsies and mouse embryonic, foetal and adult hearts, were placed in culture. After 1-3 weeks, a fibroblastic layer of cells were generated over which small, quickly dividing, phase bright cells migrated. On collecting these cells and re-seeding, they formed clusters known as cardiospheres. Murine cardiospheres started contracting soon after generation, where human cardiospheres only contracted when co-cultured with rat cardiomyocytes. Where the cardiospheres were labelled with GFP to distinguish them from cells of rat origin, Messina reported the presence of connexin-43 which indicates communication between the two cell types most likely responsible for induced contractions. The cardiospheres were composed of clonally derived cells; when dissociated and re-plated the cells once again they generated contracting cardiospheres, at 1-10% efficiency, with expression of myosin and cardiac troponin T. The human cardiospheres were capable of self-renewal (Messina *et al.*, 2004). The initial bright, small outgrowth cells were labelled with BrdU; in the cardiosphere these cells were located in the centre of the spheres with cardiac troponin T and MHC positive cells in the external layers. 10% of the cells of the newly developed cardiosphere were c-kit+ve, sca-1+ve, CD34+ve and also positive for the endothelial marker CD31 where in larger spheres, after a period in culture, these surface antigens were expressed mostly in the cells in the centre of the sphere, c-kit was expressed in approximately 30% of the cells by day 6, with no significant up-regulation of the other 3 markers examined (Messina *et al.*, 2004). These cardiospheres were also negative for CD45 and MRD1 as well as a cocktail of blood lineage markers (Smith *et al.*, 2007).

When cells were isolated from the heart by their ability to efflux the DNA binding dye Hoechst 33342 (Goodell *et al.*, 1996; Goodell *et al.*, 1997; Matsuzaki *et al.*, 2004) i.e. the ability of side population cells, and encouraged to form cardiospheres in suspension culture, the cells were also CD45-ve with heterogeneous CD34, c-kit, flt-1 and sca-1 expression (Tomita *et al.*, 2005). Messina injected approximately 60 cardiospheres subcutaneously into mice; the cells spontaneously contracted and contained tubular formations, cardiac sarcomeres with cardiac troponin T, sarcomeric myosin and α -smooth muscle actin expression. When injected into the viable myocardium of the border zone of the MI heart, they observed bands of regenerating myocardium throughout most of the infarct area with preservation of wall thickness and significant functional improvement.

Tissue-derived side population cells isolated by their efflux of the DNA binding dye, Hoechst 33342 (Goodell *et al.*, 1996) is dependent on the expression of Abcg2, a member of the family of ATP-binding cassette (ABC) transporters (Scharenberg *et al.*, 2002; Kim *et al.*, 2002). Martin *et al.*, used Abcg2 as a marker of the side progenitor cells during embryogenesis and in the adult mouse model to attempt to define a cardiac progenitor cell population. They initially investigated the cells expressing Abcg2 during embryogenesis where it was expressed, by immunohistochemistry and PCR, in the E8.5 mouse heart expression was decreased by mid-gestational ages, E11.5-E13.5, to a subpopulation of cardiac cells (Martin *et al.*, 2004). This suggests that these cells may contribute to the development of the heart and form a pool of cardiac progenitor cells. These cells did not express desmin, which is expressed early during cardiomyocyte differentiation suggesting these cells may remain in an embryonic progenitor-like state while cardiomyocyte differentiation occurs in other cells.

The expression of Abcg2 was detected throughout cardiac development and persisted in the adult heart; these cells were sca-1+ve, c-kit+ve/low, CD34+ve/low and CD45+ve/low. In addition, endothelial cell-associated cell surface antigen Tie2 was not detectable in over 90% (6-9% were Tie2+ve) of the side population cells. The side population cells were investigated for their differentiation and proliferative capacity *in vivo* to determine if they could give rise to mesodermal derived cell populations and therefore may represent a cardiac stem cell population. The cells expressed α -actinin after co-culture with cardiac main population cells and formed haematopoietic colonies on methylcellulose media. Transcriptional analysis indicated these cells were negative

for the endothelial marker CD31 (Martin *et al.*, 2004), in contrast to the cells isolated by Oh and Messina, and had expression of Mef2C associated with early cardiomyocyte differentiation. The findings of Pfister a year later complimented those reported by Martin; Pfister claimed the CD31-ve cells exhibited functional cardiomyogenic differentiation while the CD31+ve cells did not (Pfister *et al.*, 2005). Of the side population cells, 84% expressed sca-1 and 75% expressed CD31 with <1% expressing CD45, CD34, CD44 and c-kit; however the low c-kit expression was attributed to enzyme cleavage during the digestion of the cardiac tissue. In addition the sca-1+ve cells also expressed Nkx2.5 and GATA4 as well as smooth muscle actin and desmin, both associated with early myofilament formation. Sca-1+ve, CD31+ve cells composed the majority of the total side population cells (~74%). The CD31-ve cells adhered to plastic in culture and spread out becoming spindle shaped, unlike the CD31+ve fraction which were non-adherent. In addition, after co-culture with adult cardiomyocytes, the CD31-ve cells expressed GATA4 and Mef2c and demonstrated electromechanical coupling with the cardiomyocytes with gap junction connexin-43 expression in the absence of cell fusion which was not reported with the CD31+ve cells (Pfister *et al.*, 2005).

Isl1 (Isl1) is a transcription factor that is expressed in a number of cells in the right ventricle, regions of the left ventricle, the atria and the outflow tract in the developing embryonic heart (Cai *et al.*, 2003). The population of cells that give rise to these organs are from the SHF, as discussed. In addition to Isl1, these cells also expressed Nkx2.5 and GATA4 and they remain undifferentiated until later in development, when Isl1 expression is lost with cardiomyocyte differentiation. Laugwitz *et al.*, demonstrated that Isl1+ve cells were identified in the mouse embryonic heart; their number decreases progressively from E12.5 to E18.5 and after birth an average of 500-600 Isl1+ve cells were identified in the 1-5 days old rat myocardium, indicating a very rare population. Their neonatal distribution matched that of the embryonic profile of Isl1+ve cells of the SHF; clusters of cells were identified in the atria and single cells in the ventricles (Laugwitz *et al.*, 2005). Laugwitz used a cre-recombinase triggered cell line tracing method to irreversibly label isl1 expressing cells and their differentiated progeny; when they induced cre-recombinase expression in embryos and investigated the neonatal heart; β -gal+ve cells were identified in their highest proportion in the right ventricle and made up 30-40% of the cells of the entire heart, with co-labelling of sarcomeric α -actin

with the differentiated β -gal+ve cells. Isl+ve cells isolated from the neonatal heart, and transferred into culture were analysed by FACS and were identified within the cardiac mesenchymal cell fraction where Isl1+ve cells corresponded to 0.5% of this population. The cells expressed Nkx2.5 and GATA4 but when their cell surface antigens were investigated they were negative for sca-1 and c-kit. They also did not efflux Hoechst dye, indicating these cells are distinct from side population cells. Co-culture of the cells with neonatal cardiomyocyte induced cardiac α -actin and troponin T expression, there was also a subset of contractional cells with action potentials similar to that of the neonatal cardiac myocytes with evidence of connexin-43+ve gap junction formation, properties not attributed to by fusion events (Laugwitz *et al.*, 2005). More recently, Moretti reported that these cells were multipotent, contributing to smooth muscle, pacemaker cells and vascular endothelium of the heart as well giving rise to smooth muscle and endothelial cells *in vitro* (Moretti *et al.*, 2006). In summary, the Isl1+ve cells have only been isolated from very young samples; it remains to be seen whether these cells exist in the adult heart; indeed a single human sample analysed at 148 days demonstrated no Isl1+ve cells. It is also noted that although a high percentage of cells expressed troponin I (25%) in the work described above, only 2.3% demonstrated calcium transients characteristic of cardiomyocytes. Isl1+ve cells have also not been implicated in the failing heart and therefore their role in cardiac pathology is poorly understood. Therefore, although these initial results do not exclude the possibility that some Isl1+ve cells may be present in the adult myocardium; their role here needs to be elucidated. A summary of these results are provided in the table in figure 1.2.

Figure 1.2: Table of markers associated with putative stem cell populations

Author	Number of cardiac stem cells	Species	Markers	Clonogenicity	Multipotency	Testing in vivo
Beltrami et al (2003)	1/10,000 myocytes	rat	Lin-ve CD45-ve CD34-ve c-kit+ve	Cardiosphere formation	gave rise to 3 different cardiac lineages: myocytes, endothelial cells and smooth muscle	Injected GFP+ve ckit+ve cells into myocardium and gave rise to band of regenerations after MI
Oh et al (2003)	14-17% of cardiac cells Sca-1+ve and 0.03% SP profile	mouse	Sca-1+ve Lin-ve c-kit-ve CD45-ve CD34-ve CD31+ve	not cloned	Myocyte differentiation <i>in vivo</i> and <i>in vitro</i>	ischemia/reperfusion injury. 1.5% myocyte differentiation in border zone
Matsura et al (2004)	0.3% of total myocytes in the heart	mouse	Sca-1+ve CD45+ve CD34+ve c-kit+ve	not cloned	myocyte, osteogenic and adipogenic differentiation <i>in vitro</i>	not determined
Martin et al (2004)	2% of total number of cells analysed	mouse	SP Abcg2+ve Sca-1+ve CD34+ve/low c-kit+ve/low CD45+ve/low CD31-ve	not cloned	myocyte differentiation in vitro (alpha-actin+ve cells)	not determined
Messina et al (2004)	10% of cardiac cells +ve for c-kit, CD34, Sca-1 and CD31	mouse and human	c-kit+ve Sca-1+ve CD34+ve KDR/Flk-1+ve CD31+ve	Cardiosphere formation	endothelial and myocyte differentiation in vitro and in vivo	new myocytes and capillaries in infarcted heart

Author	Number of cardiac stem cells	Species	Markers	Clonogenicity	Multipotency	Testing in vivo
Laugwitz et al (2005)	137± 23 cells right atrium, 198± 35 cells outflow tract, 67± 15 right ventricle, 25± 7 left ventricle	mouse, rat and human	Isl1+ve Sca-1-ve c-kit-ve CD31-ve Nkx2.5+ve GATA4+ve	not cloned	myocyte differentiation in vitro with sarcomere structure	not determined
Pfister et al (2005)	5000-1000/heart	mouse	SP CD31-ve Sca-1+ve CD45-ve/low CD34-ve/low CD44-ve/low c-kit-ve/low Nkx2.5+ve, GATA4+ve SMA+ve, Desmin +ve Tie2+ve	not cloned	myocyte differentiation with sarcomeric organisation and spontaneous contractions at low frequency, in vitro	not determined
Tomita et al (2005)	3.5% in 2 day heart and 0.02% in 6 week heart	mouse	SP CD11b-ve, CD13-ve CD45-ve Ter119-ve, CD29+ve CD44+ve, CD34+ve c-kit+ve, flk-1+ve Sca-1+ve, nestin+ve Musashi-1+ve, Mdr1+ve	Cardiosphere formation	beating cardiomyocytes	cardiac regeneration after injury
Ott et al (2007)		rat	SSEA-1+ve Oct4+ve	not cloned	feeder layer gave rise to cardiomyocytes, endothelial cells and smooth muscle	cardiomyocytes after injury

In an effort to try to explain why there are conflicting gene expression profiles it was proposed by Anversa that there are four classes of cardiac immature cells which progress from a more primitive to a more differentiated phenotype: cardiac stem cells, progenitors, precursors and amplifying cells (Anversa et al., 2006A). By this classification the cardiac stem cells would be self-renewing as well as producing the cardiac progenitor cells, which express c-kit, MDR1 and sca-1 on their surface as well as the early cardiac associated gene GATA4. The cardiac progenitor would then divide to produce the endothelial progenitors with GATA4 expression, the smooth muscle progenitors with GATA4 and GATA6 expression, and the myocyte progenitors with GATA4, Nkx2.5 and Mef2c expression. Each progenitor then becomes precursors; endothelial precursors that express genes such as VWF and CD31, smooth muscle precursors that express alpha-smooth muscle actin and myocyte precursors expressing sarcomeric proteins. These precursors therefore possess stem cell antigens, transcription factors, and membrane and cytoplasmic proteins typical of myocytes, endothelial cells, and smooth muscle cells. Amplifying cells have nuclear, cytoplasmic, and membrane proteins of cardiac cell lineages but are negative for stem cell antigens. The transient amplifying stem cells therefore act as a means of protection for the progenitor cells.

Not all the reports of conflicting cell surface antigen can be explained by the classification system proposed by Anversa and the ultimate cardiac stem cell remains elusive. In summary, proposed cardiac stem cells are assigned this status by expression of a variety of surface antigens and embryonic genes but generally these cells are undifferentiated, lineage negative, demonstrate proliferation and differentiation potential *in vitro* and *in vivo* as well as self-renewal and clonogenicity. They may prove to be a valuable source of cells for investigation into methods of stimulating the regenerative cardiac capacity or for comparison to propose cell types for cardiac transplantation and they continue to provide a better understanding of the regenerative role of the heart.

1.4 A source of stem cells for cardiomyocyte differentiation

The cardiomyocytic differentiation potential of a number of cell sources have been investigated in an attempt to better understand the gene expression profile and antigenic changes associated with the cardiac stem cell population giving rise to the differentiated cardiomyocyte. Unrelated cell types have been assessed for their potential as a therapeutic cell for the MI heart; to mimic cardiogenesis and improve cardiac function.

Investigated cells include skeletal muscle satellite cells, embryonic stem cells, hematopoietic stem cells, mesenchymal stem cells and crude bone-marrow cell suspensions. These will be discussed.

1.4.1 Satellite Cells

The skeletal muscle is able to regenerate itself after injury; a property attributed to the satellite cells also termed myoblasts, which are the reservoir of regenerative precursor cells for skeletal muscle tissue. These cells normally lie in a quiescent state under the basal membrane of skeletal muscle fibres, they have the ability for self-renewal and fuse with the surrounding muscle fibre and differentiate into functional skeletal muscle following skeletal muscular injury (Collins 2006). For clinical studies, the skeletal myoblasts, besides their non-cardiac origin, have ideal properties of a cardiac donor cell. They can be easily isolated from a muscle biopsy, rapidly amplified in an undifferentiated state *in vitro*, only able to differentiate into multinucleated myotubes eliminating the risk of tumour formation and have a high resistance to ischemia induced apoptosis (Hagege *et al.*, 2003).

Skeletal myoblasts have been used in a large number of experimental studies, using both small and large animal models (Dowell *et al.*, 2003) where most studies concluded that the grafted cells differentiated into multinuclear skeletal myotubes (Reinecke *et al.*, 2000, Reinecke *et al.*, 2002) incorporating into the host myocardium. These cells did not demonstrate electrophysiological coupling with the host myocardium characterised by short action potential durations, as demonstrated by their lack of expression of intercalated disk proteins N-cadherin and connexin-43 (Reinecke *et al.*, 2000). Despite this, several studies in animal models demonstrated beneficial effects including an improvement to both regional and global left ventricular function (Menasche *et al.*, 2004); improvement of the left ventricular ejection fraction along with increased wall thickness, significant reduction in fibrosis and apoptosis, and a significant increase in cell proliferation has also been reported (Hata *et al.*, 2006).

Skeletal myoblasts were the first cells to be tested in clinical trials for myocardial replacement cell therapy (reviewed by Menasche *et al.*, 2005). Several phase I safety and feasibility pilot studies have reported the use of autologous skeletal myoblast transplantation for the treatment of heart disease (Herreros *et al.*, 2003; Pagani *et al.*, 2003; Siminiak *et al.*, 2004; Smits *et al.*, 2003; Siminiak *et al.*, 2005; Menasche *et al.*, 2003). These studies suggested that myoblast transplantation was “technically feasible,

could be implemented with a low incidence of procedural complications and resulted in differentiation into myotubes whose engraftment seems to be sustained over time” (reviewed by Menasche *et al.*, 2005). A growing body of experimental data and initial clinical studies has shown not only engraftment of donor cells but also improvement in global cardiac pump function (Ghostine *et al.*, 2002; Murry *et al.*, 1996; Hagege *et al.*, 2003; Taylor *et al.*, 1998).

However, some clinical studies with myoblasts were associated with a number of patients demonstrating ventricular arrhythmias and sudden cardiac deaths, an observation that might be explained by the heterogeneity of electrical membrane properties between donor and recipient cells (Leobon *et al.*, 2003; Abraham *et al.*, 2005). This finding guided changes in future protocols involving skeletal myoblasts, which now require prophylactic defibrillator implantation and/or amiodarone therapy to prevent ventricular tachycardia. This protocol change resulted in less frequent clinically evident arrhythmias. Phase II studies of skeletal myoblast therapy are presently underway.

There seems to be an agreement in these studies concerning the functional recovery of the transplanted hearts, as indicated by an improved ejection fraction and improved regional contractility of the myoblast implanted segments. The mechanisms by which skeletal myoblasts elicit the improvement in heart function remain unclear. One possibility is that they are able to satisfactorily arrest infarct expansion and limit post-infarction remodelling. A second hypothesis is that the enhancement of contractile function could be mediated by paracrine factors secreted by the grafted cells (Murtuza *et al.*, 2004), as was also suggested by observations using bone-marrow derived cells. In addition, fusion between engrafted myoblasts and host cardiac cells has been reported (Reinecke *et al.*, 2004).

Satellite cells are committed solely to the myogenic lineage. Therefore, regardless of environmental influences, even if implanted into a scar made up mainly of fibroblasts, myoblasts differentiate into functional muscle cells. Although initial studies with injected skeletal myoblasts showed promise, this approach may not be suitable for long-term therapy owing to the failure of the injected cells to become electrically coupled to the rest of the heart and to the intrinsic differences in contractile properties between cardiac and skeletal muscle cells (Reinecke *et al.*, 2002).

1.4.2 Embryonic Stem Cells

Embryonic Stem (ES) cells are from the inner cell mass of the blastocyst-stage embryo. They are considered to be pluripotent, able to give rise to many different cell lineages, self-renewing and clonogenic (reviewed by Prella *et al.*, 2002). ES cells can differentiate into any cell present in the adult organism and have the potential to completely regenerate the myocardium; however two of the obstacles that stand in the way of the therapeutic use of ES cells are immunological rejection and the propensity of ES cells to form teratomas when injected *in vivo* (Nussbaum *et al.*, 2007). However this may be overcome by genetic selection of differentiated ES cells or differentiation of ES cells *in vitro* into cardiomyocytes or endothelial cells before injection.

Cardiogenesis is easily induced in ES cells by culture in embryoid bodies (EB) which are cell aggregates cultured in suspension. When the EB is developing, areas of spontaneous contraction are suggestive of the presence of cardiomyocytes; normally within 1-4 days after plating and with continued differentiation the number of contracting cells increases; the rate of contraction within a beating area increases with differentiation which is then followed by a decrease in average beating rate with maturation (Boheler *et al.*, 2002). Within the EB, during the early stages of development, the early-stage cardiomyocytes are round and small, situated in accumulations. Within some, the myofibrils are irregularly organised and sparse or not present at all and in others the myofibrils are arranged in parallel bundles with evidence of A and I bands. As the ES cell-derived cardiomyocytes develop they become elongated and show well-developed sarcomeres and myofibrils (Baharvand *et al.*, 2006). The ES-cell derived cardiomyocytes express cardiac gene products in a developmentally controlled manner; as in early myocardial development, GATA4 and Nkx2.5 mRNA is present in the EB before that of atrial natriuretic factor (ANF), myosin light chain-2v, α - and β -myosin heavy chain. The sarcomeric proteins also develop in the expected manner in the following order: titin (Z-disc), α -actinin, titin (M band), MHC, α -actin, cardiac troponin T, and M protein (Boheler *et al.*, 2002). Human ES cells have also been shown to differentiate into spontaneously beating cells with a cardiomyocyte phenotype. The morphology and ultra-structure of these cells are organized with sarcomeric structures, formation of intercalated disks, desmosomes, and gap junctions, characteristic of cardiomyocytes. They also demonstrate action potential propagation (Baharvand *et al.*, 2006). However, to date, no human clinical studies have been initiated because of both the ethical issues surrounding access to embryos and the

possibility of teratoma formation, suggested by a study injecting ES cells in skeletal muscle. When transplanted into infarcted myocardium of mice and rats, ES cell derived cardiomyocytes have been shown to engraft (Kolossova *et al.*, 2006), differentiate into cardiomyocytes, smooth muscle cells, and endothelial cells (Singla *et al.*, 2006), and improve cardiac function (Min *et al.*, 2002). The engrafted ES cells have demonstrated expression of proteins characteristic of cardiac phenotypes such as α - and β -MHC, α -actinin and cardiac actin, however in one study, despite the presence of N-cadherin which is important in formation of intercalated discs and gap junctions, expression of connexin-43 was not detected (Laflamme *et al.*, 2005). Recently, using cardiomyocytes derived from human ES cells injected into rats, after 4 weeks, engrafted ES cells exhibited sarcomeric structure and expressed cardiac muscle markers and connexin 43, suggesting the presence of nascent gap junctions between donor and host cells (Dai *et al.*, 2007).

There is, therefore, a growing body of knowledge from animal models regarding the steps of isolation, differentiation, and clinical application of ES cells after MI; as knowledge of pathways for ES cell differentiation and for heart embryonic development increases, ES cell differentiation might become more controllable.

1.4.3 Haematopoietic Stem Cells

Haematopoietic stem cells (HSC) are bone marrow derived cells that give rise to myeloid and lymphoid lineage. These cells are normally identified broadly by their expression of a combination of a number of cell surface antigens including CD34-ve/low, sca-1+ve, c-kit+ and lineage negative (mouse). HSC are also assigned this stem cell status by their demonstration of differentiation and proliferation using colony-forming units (Ogawa *et al.*, 2006).

There is some evidence of HSC differentiation into cardiac lineage cells; however this is almost entirely *in vivo* based work. On the occasions, HSC have been reported to differentiate *in vitro* to cardiomyocytes, they are isolated from the bone marrow but not separated from the mesenchymal stem cells (MSC) or other bone marrow derived cells. The reason for this is mostly because HSCs in culture are indistinguishable by morphology from their nuclear differentiated cell types; identifying the true stem cells is difficult which is compounded by the reluctance of HSC to proliferate in culture.

However there have been a number of investigations into the HSC *in vivo*; in 2001 Orlic *et al.*, reported that lineage-ve, c-kit+ve bone marrow HSC, after injection into the border zone of infarcted mice, differentiated into cardiomyocytes, vascular endothelial and smooth muscle cells. This led to rapid regeneration of more than 60% of the infarcted ventricle and improved cardiac function (Orlic *et al.*, 2001). Jackson *et al.*, isolated side population cells from bone marrow; these cells extruded Hoechst dye and were CD34-ve/low, c-kit+ve and sca-1+ve. When transplanted into lethally irradiated mice, rendered ischemic by coronary artery occlusion/perfusion, the engrafted cells migrated into ischemic myocardium and differentiated into cardiomyocytes and endothelial cells, and contributed to the formation of functional tissue (Jackson *et al.*, 2001). Kajstura *et al.*, in 2005 showed that lineage-ve, c-kit+ve HSCs efficiently differentiated into myocytes and coronary vessels with no detectable differentiation into haematopoietic lineages and independent of cell fusion (Kajstura *et al.*, 2005). However, a number of recent investigations have questioned whether trans-differentiation of HSCs actually occurs in damaged hearts; they suggest the transplanted HSCs did not readily acquire a cardiac phenotype in the injured heart, but adopted only traditional haematopoietic fates and that cell fusion may explain the earlier observed results (Murry *et al.*, 2004; Balsam *et al.*, 2004; Nygren *et al.*, 2004). With fusion currently being investigated within a large number of research groups it may shed light on the HSC potentiality as an independent cell population.

1.4.4 Mesenchymal Stem Cells

Mesenchymal stem cells (MSC) are found in bone marrow, muscle, skin, and adipose tissue and are characterised by their potential to differentiate into any tissue of mesenchymal origin, including muscle, fibroblasts, bone, tendon, ligament, and adipose tissue. MSC from adult bone marrow can be separated by density gradient centrifugation and adhering-cell culture in defined serum-containing medium (Boyle *et al.*, 2006). The cells isolated after adherence in culture are CD34-ve and CD45-ve, unlike HSC from bone marrow. They have been investigated by a number of groups and are proposed as the most promising cells in the bone marrow for cardiomyocyte differentiation. A large number of studies demonstrate MSC treated with 5-azacytidine, a global DNA methylating agent, induces MSC to differentiate to contracting cardiomyocyte-like cells which, when injected into injured myocardium, express

cardiac markers and appear to adopt a differentiated cardiomyocyte phenotype (Hattan *et al.*, 2005). However, the grafting of these cells has been reported to be at low frequency. The use of 5-azacytidine, although widespread in MSC cardiomyocyte differentiation studies, alters the DNA of the cells treated with such potency it is arguably not true differentiation but re-programming; such an agent will not likely make clinical trial. Although 5-azacytidine may not be suitable for clinical use in this manner, differentiation of the MSC prior to implantation appears to remain relevant.

A number of studies have indicated the potential for these cells to differentiate into other MSC lineages in the myocardium; one study demonstrated unselected bone marrow cells transplanted into acutely infarcted myocardium caused significant intra-myocardial calcification; a lineage attributed to MSC (Yoon *et al.*, 2004). However there are a number of reports of MSC trans-differentiation into cardiomyocytes and vascular-like structures *in vitro* (for example Toma *et al.*, 2002) in both normal and non-MI hearts. These cells have been characterised by immunohistochemistry and stain positively for cardiac and endothelial specific markers, as well as gap junction proteins (for example Gojo *et al.*, 2003). These results suggest that MSCs act by regenerating functionally effective, integrated cardiomyocytes and possibly new blood vessels. Allogeneic MSC have also been injected directly into the pig heart, by catheter, resulting in regeneration of myocardium, reduced infarct size, and improved regional and global cardiac contractile function and, most importantly, with no evidence of rejection (Amado *et al.*, 2005).

Rat MSC, in co-culture with adult rat cardiomyocytes, stained positively for α -actin, desmin and cardiac troponin (Wang *et al.*, 2006). In another case rat MSC, co-cultured with neonatal rat ventricular myocytes with separation by a semi-permeable membrane, demonstrated contractions and cardiac troponin T expression with additional limited expression of α -actinin, desmin and cardiac troponin I (Li *et al.*, 2007B).

MSCs also have been studied clinically; Chen *et al.*, randomized 69 patients after MI to receive intracoronary autologous MSC or placebo. They demonstrated a significant improvement in global and regional left ventricular function and a significant reduction in the size of the perfusion defect, suggesting that MSC therapy can regenerate infarcted myocardium or protect against left ventricular remodelling. (Chen *et al.*, 2004).

1.4.5 Clinical Trials

Although the experimental studies, as discussed above, demonstrate contradictory conclusions in places regarding cardiac trans-differentiation and cardiac repair of bone marrow-derived stem cells, injecting bone-marrow stem cells into an injured heart potentially represents a new therapy prompting several clinical trials.

In most clinical trials, bone marrow-derived cells or peripheral blood-derived endothelial progenitor cells were transplanted via intracoronary cell infusion in patients after myocardium infarction (reviewed by Wollert *et al.*, 2006). In several other trials, bone marrow cells were delivered to the chronic heart failure patients by direct intramyocardial injection (for example Stamm *et al.*, 2003) or catheter-based intracoronary infusion (Fuchs *et al.*, 2003). Although these clinical trials assure safety and feasibility, the initial results are ambiguous. Five separate double-blind, placebo controlled studies are described below:

- REPAIR-AMI (Reinfusion of Enriched Progenitor Cells and Infarct Remodelling in Acute Myocardial Infarction) and the TOPCARE-CHD (Transplantation Of Progenitor Cells And Recovery of left ventricular function in patients with Chronic ischemic Heart Disease) Trials

A modest 3–5% significant improvement in ejection fraction versus controls (Assmus *et al.*, 2006; Lunde *et al.*, 2006; Schachinger *et al.*, 2006). Those patients with more severe reduction of ventricular function experienced the greatest benefit (Schachinger *et al.*, 2006).

- The BOOST II (BOne marrOw transfer to enhance ST-elevation infarct regeneration) Trial

Significant improved ejection fraction after 4 months, but no significant difference between control and treated individuals at 18 months (Meyer *et al.*, 2006).

- The STEMI (ST-Elevation acute Myocardial Infarction) and the ASTAMI (Autologous Stem Cell Transplantation in Acute Myocardial Infarction) Trials

No improvement in global cardiac function (Lunde *et al.*, 2005; Janssens *et al.*, 2006; Lunde *et al.*, 2006)

There are also a number of clinical studies ongoing. Clinical trials, as listed by the government of the U.S. of trials associated with their hospitals list in excess of 50

current trials, mostly into determination of functional improvement as a result of bone marrow stem cell transplantation as well as investigations into their safe administration and effect on neogenesis, including:

- Phase I/II clinical trial at the Rigs hospital in Denmark

To evaluate safety and clinical effects of autologous MSC transplantation in 46 patients with severe chronic myocardial ischemia. This trial will end in November 2009. Patients will be treated with direct intra-myocardial injections of ex-vivo expanded MSC. Clinical and objective evaluations will be performed at baseline and at 1-year follow-up.

- Myocardial Stem Cell Administration After Acute Myocardial Infarction (MYSTAR) study

A randomized, single-blind clinical trial started in 2005 and due to end this year which was designed to compare the early and late intracoronary or combined (percutaneous intramyocardial and intracoronary) administration of bone marrow-derived stem cells to patients after acute MI. The study consists of 360 patients randomly assigned into one of four groups, Group A: early treatment (21-42 days after MI) with intracoronary injection; Group B: early treatment (21-42 days after MI) with combined (intramyocardial and intracoronary) application; Group C: late treatment (3 months after MI) with intracoronary delivery; and Group D: late treatment (3 months after MI) with combined (intramyocardial and intracoronary) administration of BM-SCs. The study was designed to determine the feasibility of the bone marrow-derived stem cell delivery modes, determined by the rates of complications, outcomes to be assessed by changes in global left ventricular ejection fraction.

- Amorocyte myocardial repair study (AMRS)- A Phase I Trial of Intra-Coronary Infusion of Bone Marrow Derived Autologous CD34+ Selected cells in Patients With Acute MI

This is a 40 patient clinical trial started in 2005 which is still recruiting patients. It is a randomized trial to evaluate the safety and efficacy of a CD34+ve stem cell population, administered through the infarct related coronary artery 6 to 9 days after successful infarct related artery stent placement, and assessment of the effect on cardiac function and infarct region perfusion.

At this time unequivocal proof of concept is still lacking, in either the clinical or experimental arena, for using bone marrow stem cells for cardiac repair through trans-differentiation into myocardial tissue. Thus, stem cell-based improvement of cardiac function may be achieved by mechanisms other than from differentiation of those cells into cardiomyocytes. The beneficial effects of cell therapy, as described above, on cardiac function following MI might be explained by a number of known variables, including host cardiomyocyte survival/death pathways, neo-angiogenesis, matrix reorganization, etc.

There are a number of problems associated with each of the proposed cells types for investigation of cardiomyocyte differentiation. ES cell isolation has ethical issues, is associated with teratoma formation and the availability of human material is limited. HSC are difficult to investigate *in vitro* as well as difficult to identify *in vivo* with debatable cardiomyocyte differentiation. MSC are capable of differentiation to a wide range of cell lineages; the risk of their differentiation into a lineage other than cardiomyocyte in the myocardium has been shown to be possible and may be too much of a risk for *in vivo* application, however it remains a promising cell source. Whole bone marrow transplantation is possibly the cell type with potential, as is reflected in its use in phase II clinical trials however it may also be associated with differentiation of cells to a lineage other than cardiomyocyte. Skeletal satellite cells have been associated with ventricular arrhythmias and in some cases sudden cardiac deaths. In addition to the cell types that have demonstrated differentiation to cardiomyocytes, native cardiac stem cells are not sufficiently mobilised after an MI. There is limited consideration as to fusion events in a lot of these studies where engraftment is reported and this may account for the problems associated with some of the clinical trials where the cells do not appear to provide a functional improvement in the heart. Due to the life span of rodents, the long term effects of stem cell transplantation and introducing new cells into the heart has not been investigated. Long-term studies in the mouse and rat rarely extend beyond 6 months. Inevitably, with human clinical trials comes the first long term results to date. Therefore the search continues for a suitable cell type for cardiac transplantation. In addition to this; the pathways involved in the cardiac stem cell role in homeostasis as well as its inability to cope with MI, are not entirely understood; an ideal cell type may only be identified when the cardiac stem cell presence and role is fully understood.

It is interesting that in the work of Beltrami (Beltrami *et al.*, 2003) where 10,000 cells were injected into the myocardium of MI hearts; there was comparable functional improvement as to that reported by Messina after injection of nearer 60 cardiospheres i.e. the number of cells being injected was not relative to the amount of repair or functional improvement. This apparent conflict in the number of cells injected and the functional improvement has been observed in a number of cases, most significantly with injection of bone marrow-derived cells. The differentiation potential of bone marrow-derived cells has been discussed in this chapter; however the uncoupling of the number of cells injected to the functional improvement, is noteworthy here. Bone marrow derived stem cells delivered to the heart were shown to transdifferentiate to cardiomyocyte-like cells and rescue cardiac function (Orlic *et al.*, 2001) in a similar manner to the cardiospheres and cells described by Beltrami, Matsuura and Messina among the others described above. These results were challenged when various groups failed to demonstrate permanent engraftment and no evidence of bone marrow cell transdifferentiation (Balsam *et al.*, 2004; Murry *et al.*, 2004; Nygren *et al.*, 2004), however there did remain significant improvement of left ventricular function. One theory was that sub-sets of the transplanted cells secreted growth factors in a paracrine fashion that may be involved in the beneficial effects or that cells may induce an inflammatory response that induces cell recruitment that in turn increases, for example, angiogenesis. When considering the value of the identification of cardiac stem cells and their therapeutic role this is an important consideration. It may indicate that the MI model may be an unsuitable method of investigation of cardiomyocyte differentiation potential, and that *in vitro* investigation will be a more accurate representation of cell source potential until a more suitable cardiac injury model is discovered or the cardiac stem cell is better understood.

It is proposed that components of the skin may be suitable for investigation of cardiomyocyte differentiation; specifically the dermal papilla (DP) and dermal sheath (DS) cells of the hair follicle. The DP and DS have both demonstrated stem cell-like properties both *in vivo* and *in vitro*; they are easily accessible and have previously demonstrated differentiation towards adipocytic and osteocytic lineages with some early spontaneous indications of myocyte differentiation. These properties are described below. It is proposed that the cells of the DP and DS may overcome problems associated with previously described stem cells as discussed above.

1.5 The skin and its appendages

The skin is derived from the ectoderm and the mesoderm during embryonic development, which gives rise to the epidermis and dermis, respectively. Within these layers are specialised appendages, also derived from the ectoderm and/or mesoderm including sweat glands, sensory nerves and hair follicles. The skin layers rest upon the subcutaneous tissue which is largely a mesh of collagen fibre, fat cells and muscle (reviewed by Prost-Squarcioni 2006). The skin has a number of functions including support where the skin acts as a flexible support for underlying tissues, and protection as the epidermis acts as a barrier to potentially dangerous absorptive materials. The sensory receptors on the skin recognise pressure, pain and temperature and the extensive blood supply and sweat glands control the body temperature. The skin excretes waste materials, e.g. excess salt and water, and melanin expression protects the lower dermal layers from UV radiation. The outer most keratinized skin layer of the epidermis, the stratum corneum, provides passive defence against entry of opportunistic organisms and the spinous layer contains epidermal Langerhan's cells for immunological surveillance (Romani *et al.*, 2006). The total number of hair follicles for an adult human is estimated at 5 million; 1 million are on the head with 100,000 on the scalp, the palms and soles of the feet are the only areas of the body that do not contain hair follicles. The basic hair follicle structure remains the same from one mammalian species to the next, with modifications for specialised functions. The hair follicle is recognised as a separate entity within the skin formed and maintained from interactions between dermal and epidermal skin components. These cells are abundant and easily accessible; a small scalp skin biopsy would yield a large number of follicular cells.

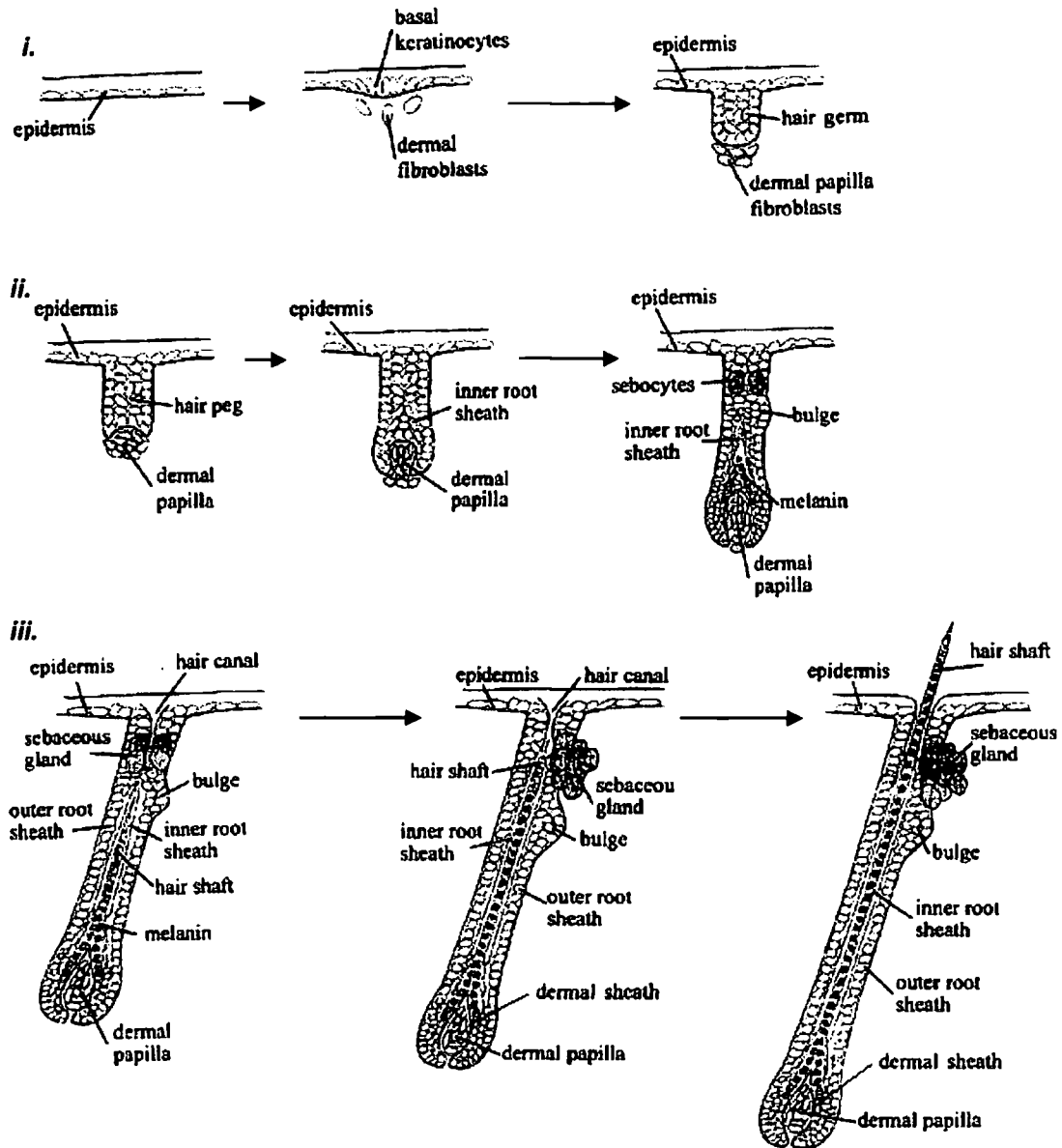
At the heart of the hair follicle is the dermal papilla (DP) which is encased in the end bulb. The DP is onion shaped in the normal hair follicle; however in disease states its shape changes e.g. in alopecia areata the DP becomes smaller and densely packed. The DP is derived from the dermal mesenchyme and consists of a highly active group of cells that are capable of inducing follicle development from the epidermis and production of hair fibre as shown in figure 1.3. The cells that lie around the DP, and are the source of hair follicle formation, are called the cortical or germinal matrix cells; they differentiate and become keratinized to form the hair cortex, which is densely packed keratinized cells, and surrounding hair cuticle of the hair shaft in a process known as induction. At the centre of the hair shaft is the medulla where the cells aren't so densely packed; cells surrounding the hair shaft comprise the inner root sheath which

is divided into the cuticle, Huxley layer and Henle layer based on structure and pattern of keratinisation (Hardy 1992). The hair follicle and hair structure is shown in figure 1.3.

At the level of the sebaceous gland the inner root sheath breaks down to leave only the hair cortex and the surrounding cuticle which protrude above the epidermis. The outer root sheath is distinct from the other epidermal components described, in that it is continuous with the epidermis, the upper part is normally keratinized although the lower part generally isn't; in the outer root sheath at the bulge region, which will be described later, is the arrector pili muscle which allows the hair to stand erect. Between the outer root sheath and DS is a basement membrane which has a protective function to divide the cells descended from embryonic ectoderm (epidermis) and embryonic mesoderm (dermis). The dermal sheath (DS) encloses the epidermal component and consists of a layer of mesenchymal cells which extends from the stratum papillaris to the DP; it runs the entire length of the hair follicle on the outside of the outer root sheath (Hardy 1992). As briefly described cells of the DP and DS are proposed as a cell types for differentiation investigation; it is apparent here that the DP and DS cells are distinct and defined populations of cells in the hair follicle; they can be isolated from the remainder of the hair follicle easily.

In embryogenesis the establishment of the DP is essential to the development of the hair follicle and associated structures. The DP is an aggregation of dermal fibroblast cells just below the epidermis which is initially established in the human embryo at 60 days old; at this stage the DP cells are loosely connected and present as long and spindle shaped; their presence indicates the site for future development of a hair follicle. Above the DP develops an epidermal plug which is a collection of cells that proliferates into the dermis, known as the hair peg, which links with the DP. There is further proliferation of the epidermal matrix cells and differentiation into the sheath and hair fibre. The DP develops into its more identifiable round structure. It is the DP that directs and dictates the embryonic generation of a hair follicle and it retains this ability throughout the life of the hair follicle. If the DP is removed, hair growth is prevented; however the lower third of the DS is capable of compensating by supplying new cells for regeneration of a new DP. If more than a third of the lower hair follicle is removed the DP cannot easily be reformed and the hair follicle is deemed destroyed (Messenger *et al.*, 1986).

Figure 1.3: The hair follicle



(Adapted from Gilbert 2006)

Early development and differentiation of the hair follicle and primitive hair shaft.

i. The epidermal epithelium, above the dermal mesenchyme, initiates proliferation of epidermal basal keratinocytes. Proliferation of these cells results in the formation of the hair germ, which signals the dermal mesenchymal cells to aggregate beneath it to form the DP. *ii.* The DP signals the continued proliferation of the hair germ producing the hair peg (primitive hair shaft). The DP cells proliferate and tightly aggregate and the primitive hair shaft engulfs it to form the inner hair root, directly above the DP. The inner root sheath elongates, about halfway up the hair follicle, and the sebaceous cells and bulge are formed. Melanin granules enter into the cortex to give the pigmentation. *iii.* The follicle growth extends at an angle to the epidermis. The sebaceous glands mature and become localized on the lateral wall of the follicle. The hair canal is formed; the hair shaft differentiates and extends into the hair canal. The hair shaft extends beyond the skin.

It has been shown that the human dermal components can induce hair growth when implanted into athymic mouse vibrissae follicles; the implanted cells interact with the follicle epithelium creating new follicle end bulbs; it was found that contact with the underlying epithelium was necessary to follicle formation (Horne and Jahoda 1992). DP and DS can also induce new hair follicles when implanted s.c. into the ears and footpads i.e. areas of skin that are normally non-hairy (McElwee *et al.*, 2003).

1.5.1 Hair cycling

The average rate of hair growth is 0.35mm a day although the rate does vary upon the site of the hair follicle and the age and sex of the individual. Sinus hairs are very large cells that are modified to act as mechanical sensors e.g. whiskers or vibrissae on rats, which are structurally identical to normal hairs except for size. Hair growth is a cyclic event consisting of three main events (Paus 1998):

1. Anagen

This is the active growth phase of the hair cycle and is the stage at which the hair fibre is produced. It is further split into the following phases:

Proanagen- This marks the initiation of growth; DNA synthesis occurs in the follicle

Mesagen – intermediate stage

Metagen – at this stage the follicle is at its maximum length and girth

This is the longest growth phase; up to 90% of follicles in the normal scalp are in this active hair growth state at any time. The length of the anagen growth phase for scalp hair is usually 6-10 years. In most young mammals, the anagen growth phase occurs in waves across the skin surface but in humans the cycles of growth can occur completely independent of surrounding follicles. Melanin is made in the hair bulb throughout this phase. The hair bulb is located in the subcutaneous fat.

2. Catagen

This marks a period of controlled regression of the hair follicle; it normally lasts 14-21 days. It is a state of quiescence and cessation of new hair growth known as the intermediate phase. The hair in catagen may detach itself from the underlying matrix which produced it and be held in place by friction, the base of the follicle moves

upwards towards the surface of the skin with the hair bulb located in the dermis; this is known as the club hair.

3. Telogen

This is a transition stage whereby the hair follicle renews itself and makes the change over back to the anagen stage again, it is known as the shedding phase. Approximately 10% of follicles of the normal human scalp are in this phase of hair cycling at any given time which normally lasts 30-90 days. In this stage, the hair bulb is located in the mid-to-upper dermis.

The fact that the DP needs to be in contact with the underlying epithelium in order to produce new hair follicles indicates that the epithelium and DP communicate via direct contact. This shows the DP responds to some sort of inductive signal in order to produce the specific cell types required which indicates that, under different inductive molecules, the DP may be able to produce a different cell type. It has been discussed that the DS can produce a new DP in its absence which indicates the DS has stem cell properties and again under specific inductive signalling can produce a cell type different to itself; it may be that under different inductive signalling the DS can be induced to producing a different cell type to that which it produces in the follicle microenvironment.

1.5.2 Stem cells of the skin

The skin contains stem cell populations that have different roles in normal homeostasis as well as in response to injury. The stem cells discussed here are those of the epidermis, briefly, and those of the dermis; namely the bulge region as well as the proposed second population in the hair follicle; cells of the DP and DS.

1.5.2.1 Epidermal stem cells

Mature epidermis is a stratified squamous epithelium whose outermost layer is the skin surface. The basal layer, which is mitotically active, secretes and assembles an extracellular matrix which constitutes much of the underlying basement membrane that separates the epidermis from the dermis. As cells leave the basal layer and move outward toward the skin surface, they withdraw from the cell cycle, switch off integrin

and laminin expression, and become terminally differentiated. The interfollicular epidermis contains its own progenitor cells to ensure tissue renewal in the absence of injury; the hair follicles contain multipotent stem cells that are activated at the start of a new hair cycle and upon wounding to provide cells for hair follicle regeneration and repair of the epidermis (reviewed by Blanpain and Fuchs 2006). The interfollicular epidermis, which generates the lipid barrier of adult skin, constantly renews its surface and undergoes re-epithelialisation after wound injuries. These renewing and repairing activities of the skin epidermis imply the existence of stem cells.

Histological analysis has shown that mouse epidermis is organized in stacks of cells with a hexagonal surface area lying on a bed of ten basal cells where the basal cells divide asymmetrically relative to the basement membrane to maintain a proliferative daughter and give rise to a differentiating daughter cell overlying it; this structure was hypothesized to function as an epidermal proliferative unit (EPU) with one putative stem cell per unit. Cultured human interfollicular epidermal keratinocytes expressing the highest level of $\beta 1$ -integrin have been shown to have the higher proliferative potential *in vitro*; these cells are located in the basal layer of the epidermis and the base of the deepest epidermal ridges of palmoplantar skin consistent with the location of slow-cycling stem cells (Jensen *et al.*, 1999). These cells, in the basal layer of the epidermis, were also found to reside in clusters; possibly indicative of an epidermal stem cell niche (Fernandes *et al.*, 2004; Jensen *et al.*, 1999). It is noted, however, that these cells have also been identified outside these zones indicating that $\beta 1$ -integrin levels may not necessarily define the stem cell population. Current research focuses on additional markers which are needed to enrich the purification and analysis of these potentially highly proliferative cells.

During injury; the hair follicle cells contribute to the healing of the interfollicular epidermis; however the functional role of these cells has not entirely been resolved. A recent investigation used the Edaradd mutant mouse, which lacks all appendageal structures in the tail skin including hair follicles, was undertaken to investigate the epidermal response to wound healing in the absence of the intervention of the hair follicle derived cells (Langton *et al.*, 2008). They observed that the wound on the hairless skin did not close as quickly, initially, as on normal hairy skin; however after a lag period of 4 days, wound reepithelialised in a similar manner to control skin. This would indicate that the hair follicle does contribute to wound closure, possibly to

accelerate the onset of wound healing, but is not necessarily essential. This in turn may help answer the questions as to why hair-bearing areas of skin tend to heal more quickly than areas lacking follicles.

The bulge region of the hair follicle has been most implicated in the hair follicle role of epidermal wound healing (Ito *et al.*, 2005). Using cre-recombinase under the promoter for keratin 15 (K-15) bulge cells were demonstrated to migrate to the epidermis following wounding; short term analysis (8 days) indicated approximately 26% of the cells in a reepithelialised wound originated in the bulge which dropped to 4% after 20 days (Ito *et al.*, 2005) indicating they may behave as transit amplifying cells.

1.5.2.2 Bulge region stem cells

The bulge region is located in the hair follicle at the level of the insertion of the arrector pilli muscle, for pelage follicles, and located well below the sebaceous glands, not at all related to the arrector pilli muscle, in vibrissal follicles. It forms a small protuberance of the outer root sheath located in the upper portion of the hair follicle; the basal layer of the bulge region rests on a thick basement membrane that separates it from the dermal sheath and, nearer the hair, is separated by a layer of stratified cells. The bulge region is widely believed to contain epithelial stem cells (Cotsarelis *et al.*, 1990) and these cells have been shown to be multipotent (Taylor *et al.*, 2000; Oshima *et al.*, 2001). The cells located in the bulge region cycle infrequently but have a highly proliferative capacity; BrdU label persists in quiescent bulge cells for more than six months (Cotsarelis *et al.*, 1990; Morris and Potten 1999). Moreover the bulge region contains 95% of the clonogenic keratinocytes, as indicated by K-15, K-19 and CD34 expression and absence of CD71 expression normally associated with actively cycling cells, where the end bulb contains only 5% (Kobayashi *et al.*, 1993).

Initiation of a new anagen cycle depends upon activation of a small number of quiescent stem cells that reside in the bulge, which is considered to be a source of stem cells for the hair follicle as well as the epidermis. These activated stem cells proliferate and differentiate into progenitor cells (matrix cells) that give rise to the differentiated lineages that comprise the hair shaft and root sheaths (Sarin *et al.*, 2005).

There is a growing body of evidence that bulge region contains pluripotent neural crest stem cells, termed epidermal neural crest cells (eNCSC). eNCSC are promising

candidates for diverse cell therapy paradigms because of their high degree of inherent plasticity (Sieber-Blum *et al.*, 2004). These bulge cells have been shown to be capable of directed differentiation towards neurons, glia, keratinocytes, smooth muscle cells, and melanocytes *in vitro* (Amoh *et al.*, 2005).

Further investigation into the specific markers of the bulge region cells, their potential to contribute to hair follicles, skin and other tissues, as well as the cellular and molecular microenvironment that maintains these cells, will elucidate the potential of the bulge cells. At the moment, although the anatomical location of these cells is known, their identification in the excised hair follicle or dermis is difficult and normally requires labelling of a number of bulge cell-associated genes to confidently identify it. Although it is an exciting population of cells with multipotency, the difficulties in its isolation and therefore poor analysis *in vitro* compared to other stem cell types, make its use in differentiation experiments limited at the moment.

1.5.2.3 Dermal follicular cells – a source of donor cells

The DP and DS follicular cells do have all the attributes that are important in a donor cells. The DP and DS are easy to isolate by micro-dissection; the different cell populations are easy to identify and isolate without significant contamination of surrounding tissue. Also a considerable amount of cells can be harvested from, for example, rat vibrissae for research and human scalp hairs for clinical application. The cells have been shown in culture to be proliferative and retain their cell viability throughout a number of cell passages. The cells are also immunologically tolerated on transplantation (Reynolds *et al.*, 1999) and have inductive and differentiation properties (Jahoda *et al.*, 2001B; Jahoda *et al.*, 2003A) The DP and DS are considered by many groups to therefore be stem cell-like in their properties and their potential applications are increasing.

A number of adult cell populations have broader stem cell capabilities than previously thought; this was examined with the dermal follicular cells and their haematopoietic stem cell activity with a view to develop the follicle as a stem cell model system. Cells within the DP and DS generated haematopoietic colonies *in vitro*; rodent hair follicle end bulbs as well as micro-dissected DP and DS cells actively produced cells of erythroid and myeloid lineages where follicle epithelial cells did not (Lako *et al.*, 2005). Cultured DP and DS cells from transgenic donor mice were transplanted into lethally

irradiated recipient mice and multilineage haematopoietic reconstitution was observed, over 70% of clonogenic precursors were derived from donor hair follicle cells, when assayed at intervals of up to one year indicating their potential primitive stem cell nature. Harvested bone marrow from primary mice then re-populated secondary, myeloablated recipients with multi-lineage haematopoietic engraftment (Lako *et al.*, 2003). These properties were not associated with blood cell contamination with DP and DS isolation as aorta and peripheral blood both failed to demonstrate haematopoietic activity *in vitro*. These observations suggest the DP and DS harbour multi-potent cells, the capacity of which is harnessed under specific environmental conditions.

Components of the hair follicles have also demonstrated inductive properties. Amputated hair follicles, where end bulb, DP or entire lower one-third is removed, have been shown to regenerate new DP and renew production of hair fibre. However, when the amount of amputated tissue exceeded this amount the vibrissae failed to reform a new DP as well as hair fibre (Jahoda *et al.*, 1992). Moreover, DP can be implanted to adult skin and will induce the formation of new hair follicles from undifferentiated epidermis; these induced hair follicles retain morphologic and hair cycle characteristics of the donor hair follicle (Reynolds and Jahoda 1991). In a similar manner, human hair follicle DP also demonstrated induction of hair growth when implanted into mouse follicle epithelium where new fibre-producing end bulbs were created (Jahoda *et al.*, 2001B).

DS cells are capable of regenerating the DP, however in a wound environment they have also demonstrated the ability to become wound healing fibroblasts and perform an important function in the repair of skin dermis after injury (Jahoda and Reynolds 2001). The dermal follicular cells have demonstrated capacity to be incorporated into skin wounds where they are capable of forming hair follicles; these cells can also create hair follicle-derived skin equivalents (Gharzi *et al.*, 2003). In a wound environment new hair follicles were formed only with the inclusion of intact DP, however DS cells combined with outer root sheath cells were capable of producing skin equivalents in organotypic chambers with characteristic dermal and epidermal architecture and a normal basement membrane (Gharzi *et al.*, 2003). Such inductive properties have been associated with stem cell types and provide further evidence as to the stem cell properties of the DP and DS.

Spontaneous appearance of muscle, lipid and bone-type cells in discretely isolated DP and DS cell primary cultures from rat vibrissa follicles were reported by Jahoda *et al.*, as well as reports that DP and DS cell lines were capable of being directed to lipid and bone differentiation. This group produced clonal cell lines, a property of stem cell populations which demonstrated extended proliferative capabilities (Jahoda *et al.*, 2003A). Clonal cell lines with differing capacity to exclude rhodamine123, an identifying feature of stem cells, were cultured in supplemented medium known to induce adipocytic and osteocytic differentiation; DP and DS derived clones both showed the capacity to make lipid and to produce calcified material. However the clones had varied behaviour that was uncoupled with dye exclusion. Interestingly, Jahoda *et al.*, also reported beating cells reminiscent of cardiomyocytes in primary follicular cell cultures and muscle cells in cultures of mixed DP and DS and in DS cultures (Jahoda *et al.*, 2003A). In addition, more recently, the myogenic differentiation potential of the bovine DP has been investigated. Bovine DP cells were reported to be capable of adopting a myogenic fate when co-cultured with murine C₂C₁₂ cells; the DP cells incorporated into myotubes and expressed muscle commitment and differentiation markers, MyoD and myogenin, in DP derived myotubules. Clonal cell lines also produced similar myogenic activity to the primary populations (Rufaut *et al.*, 2006).

Clonally derived lines of cells isolated from the entire dermis, termed skin-derived precursors (SKP), are capable of differentiating into neurons, glial cells, adipocytes, and smooth muscle cells (Toma *et al.*, 2001; Joannides *et al.*, 2004). SKPs can be derived from isolated DP and continue to express DP markers *in vitro*, suggesting they also represent a multipotent population of follicular dermis cells (Fernandes *et al.*, 2004; Richardson *et al.*, 2005); these cells may be responsible for the differentiation potential observed here.

1.6 Thesis objectives

The initial evidence for DP and DS differentiation towards a cardiomyocyte lineage is limited but encouraging and, supported by evidence of on their differentiation towards adipocytic and osteocytic lineages, suggests these cells could be manipulated to differentiate towards lineages other than their designated fate in the hair follicle. This thesis proposes the DP and DS as cell populations for somatic cell differentiation towards a cardiomyocyte lineage. In addition, in understanding the importance of

further investigation of the cardiomyocyte, it also provides analysis of the mTert-GFP mouse as a potential better indicator of cells in the dermis with differentiation potential as well as a marker for exploring the infarcted heart.

2 Methods and Materials

2.1 Materials

A list of materials and buffers is provided in Appendix 2-3. All procedures were carried out at room temperature unless otherwise specified. The grade of water used throughout was Molecular Biological (Sigma) unless otherwise specified.

2.1.1 Animals

Rats (Wistar, WST/Nhg) (denoted WT) and CD1 mice (denoted WT) were supplied by Charles River Laboratories and maintained by the Departmental Animal Facility. The mTert-GFP mouse was produced by Dr. D. Breault, Boston Childrens' Hospital and Harvard University in collaboration with Dr. N. Hole, University of Durham. The breeding colony of mice was maintained as heterozygotes on a strain 129S1/SvImJ background (denoted WT). Work was approved by local ethical review panels of Durham and Harvard University; carried out under the authority of Home Office personal and project licences.

2.2 Microscopy and centrifugation

Primary cultures were monitored using a light microscope (Olympus, ckx41); photographs of phase contrast images were taken using a Nikon digital camera attachment. Dissections were visualised using a dissection microscope (Nikon) and photographs taken with a Nikon digital camera attachment. All fluorescence was visualised on a Zeiss Axio imager.M1 microscope with a Hamamatsu digital camera attachment. All centrifugation was carried out at room temperature (Sigma and Philip Harris Scientific centrifuge) unless otherwise stated where centrifugation was carried out at 4°C (Biofuge, Heraeus).

2.3 Isolation of primary tissues

2.3.1 Isolation of vibrissae DP and DS from mouse/rat mystacial pad

The DP and DS were located in the end bulb component of the hair follicle (Reynolds and Jahoda 1991), as shown in figure 2.1. The end bulb was typically contained within the lower third of the hair follicle (figure 2.1*i*), which contains the DP on a stalk protruding from the surrounding DS (figure 2.1*ii*). It was distinguished from the rest of the hair follicle

by a slight indentation below the hair root and above where the DP resides. The DS coats the entire inner surface of the collagenous capsule of the end bulb and extends up the early part of the growing hair root where it associates with the outer root sheath.

The DP and DS were dissected from adult rat or mouse follicles of the vibrissa using previously described methods (Jahoda and Oliver 1981; Reynolds 1989). Briefly, the method is as follows:

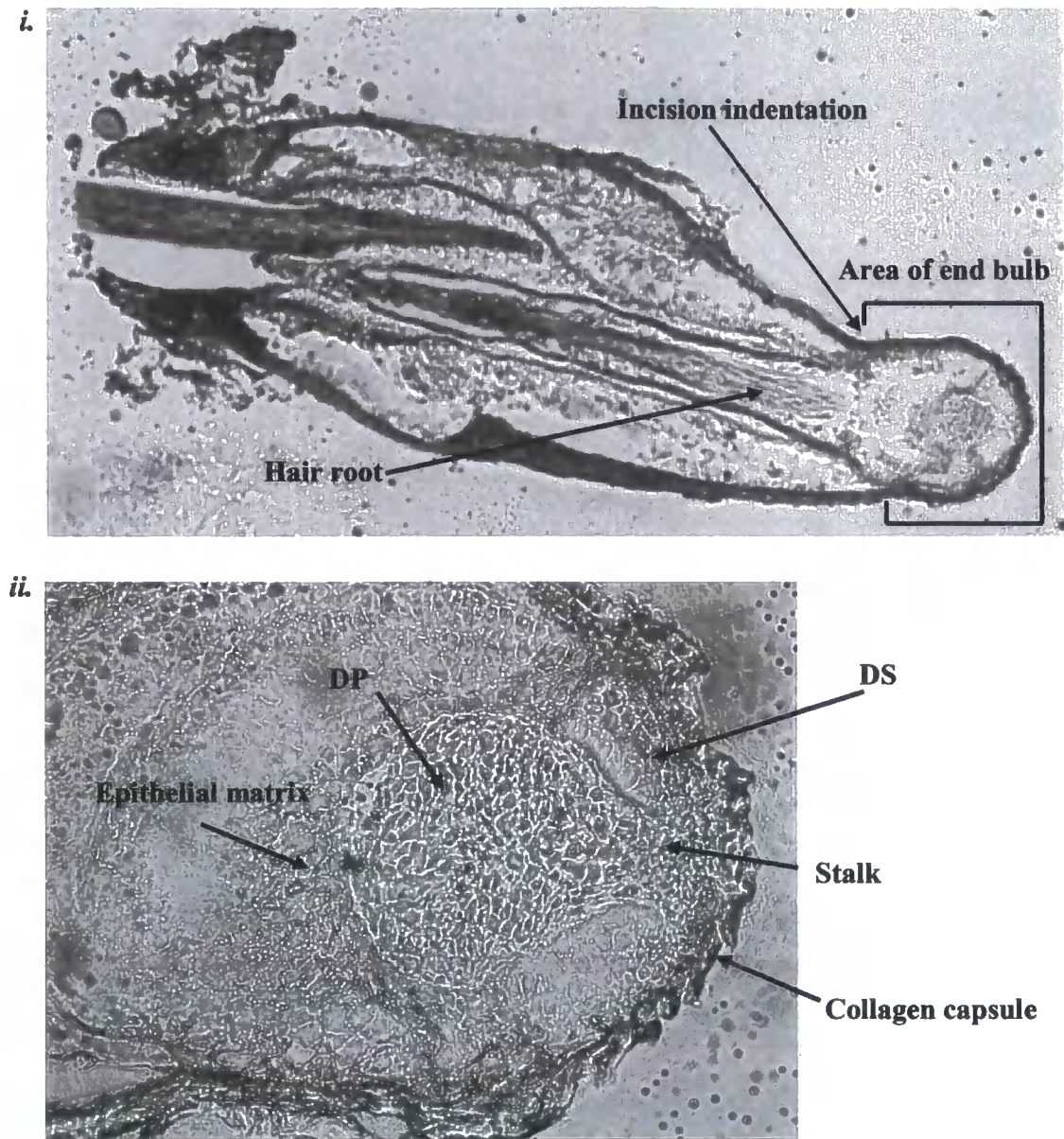
The mouse/rat was sacrificed and the mystacial pad cut open, the nerve tracts indicated the correct depth of incision (see figure 2.2i). The skin was inverted to reveal the under surface of the mystacial pad and the protruding end bulb component of the hair follicles (figure 2.2ii.). The tissue surrounding the protruding hair follicle was dissected away and the hair follicle removed from the inside of the mystacial pad and pulled back through the skin (figure 2.2iii.) so to avoid hair follicle damage and minimise contact with the skin surface. The follicles of the vibrissa were placed into a 10cm petri dish (Fisher) in 10ml of 10% MEM (Minimal Essential Media; see Appendix 5). The end bulb was excised from the hair follicle using a scalpel blade (Fine Scientific Tools, Scalpel#3); the incision was made at the indentation on the hair follicle at the end bulb (see figure 2.1). The end bulb of the hair follicle was removed into PBS (phosphate buffered saline; see Appendix 3) for DP and DS isolation or for immediate processing for RNA.

The end bulb collagen capsule was inverted using forceps (Fine Science Tools, Dumont forceps, type#5); the epithelial matrix component removed to expose the DP which was easily pinched off and isolated using forceps.

The DS was removed ensuring the collagen capsule and epithelial matrix remains. Isolated DP and DS were then processed for RNA or transferred to a 16mm tissue culture dish for culture. Typically, four DP or DS were placed into each 16mm dish.

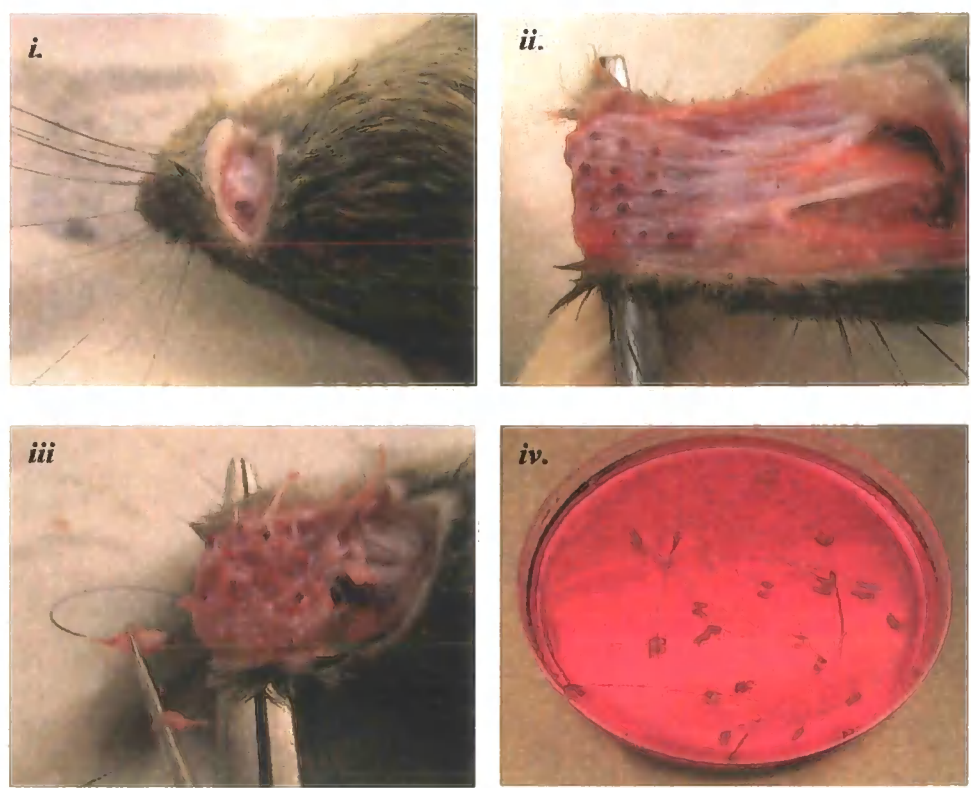
In some experiments, the DP and DS were cultured together without separating the DP from the DS; this type of mixed culture was used when investigating spontaneous cardiomyocyte-like differentiation. Typically, four mixed population primary explants were placed into each 16mm dish.

Figure 2.1: Location of the DP and DS and the end bulb in the hair follicle



Phase contrast images of the hair follicle of the mouse vibrissae at x5 magnification (i.) and x40 magnification (ii.) showing the location of the DP and DS. The end bulb is the lower one third of the hair follicle and contained the DP and most of the DS. It is excised from the hair follicle using a scalpel blade at the indentation shown (i.)

Figure 2.2: Mystacial pad excision for hair follicle exposure and vibrissae isolation



Images showing mystacial pad excision and vibrissa retrieval. The initial nerve tracts indicated the correct depth of incision (*i.*). The skin of the mystacial pad was inverted to show the underside of the hair follicles (*ii.*). The vibrissae was pulled back through the skin (*iii.*) and removed to minimal essential media (*iv.*) in preparation for removing the follicle.

2.3.2 Isolation of neonatal skin dermal cells

The mouse was sacrificed at 3-5 days post partum, when the hair was just visible. The skin from the torso of the neonate was removed in its entirety. Fat was carefully removed from the underside of the dermis using a scalpel, avoiding abrasion of the underlying dermal cell layers and the skin cut into 1cm² pieces for freezing for cryo-sectioning or for immediate processing to obtain a single dermal cell suspension for flow cytometry.

In the case of the latter, the 1cm² pieces from each neonate were transferred to a 15ml Falcon (Sigma) of 15ml Hank's Balanced Salt Solution (HBSS; see Appendix 3) containing 4mg/ml dispase (Sigma) (see Appendix 2) and incubated for 3 hrs at 37°C with gentle shaking (100rpm) in a heated incubator (Labnet). The sample was removed from the dispase and placed on a fresh petri dish, epidermis down; the dermis was stripped using forceps, leaving the epidermis adhered to the petri dish. The dermis was sliced into approximately 1mm² pieces and transferred to 5ml of HBSS containing 1mg/ml type 1A collagenase (Worthington) and incubated for 2.5hrs at 37°C with shaking (250rpm). approximately 10ml of MEM was added to the cell suspensions and then filtered through 40micron sterile filters (Sigma) twice and the cell filtrate pelleted by centrifugation (5 min, 2475g), followed by re-suspension in PBS for flow cytometry (section 2.14).

2.3.3 Removal of mouse/rat embryos

Embryos were removed from the mouse/rat uterus by tearing the mesometrium away with forceps and isolating the embryo away from the muscular walls of the uterus, Reichert's membrane and visceral yolk sac. Embryos were placed into PBS for further processing for cardiomyocyte isolation or for cryo-sectioning. For tissue typing purposes, for mTert-GFP embryos, the placentas were transferred into PBS.

2.3.4 Isolation of cardiomyocytes from embryonic hearts

Embryonic hearts were routinely isolated from E12.5 mouse embryos or E15.5 rat embryos; ages which were developmentally matched. (Kaufman 1992). The myocyte isolation method used was adapted from The Worthington Neonatal Isolation System (as described in Toraason *et al.*, 1988). In brief:

Embryos were removed from the uterus as described (section 2.3.3). The hearts were removed from the embryo, with forceps and fine scissors; following the severing of the aorta and pulmonary blood vessels, the heart was lifted from the thoracic cavity. For each experiment 30-90 embryo hearts were isolated and they were placed into ice cold HBSS for immediate processing for RNA or culture.

In the case of the latter, the hearts were finely minced in 5ml HBSS on ice and trypsin added to a final concentration of 50 μ g/ml trypsin for incubation for 16hrs at 4°C. Trypsin inhibitor (Sigma) was then added to a final concentration of 180 μ g/ml and the solution warmed to 37°C. 1500 units of collagenase (Worthington Neonatal kit) was added to further dissociate the tissue and the cell suspension incubated for 45 min at 37°C. The suspension was triturated and filtered using 40micron filters. Following centrifugation to pellet cardiomyocytes away from red blood cells (RBC) (5 min, 2178g) the pellet was re-suspended and the cells were seeded onto 35mm diameter tissue culture dishes (Nunc); 1.2x10⁶ cells/dish (equivalent to 1.25x10⁵ cells/cm²). The cells were then cultured in 10% Leibovitz culture media (L-15) (Sigma) (see Appendix 5).

2.4 Tissue culture

All plastics were sterile unless otherwise stated. All cultures were incubated at 37°C in a humidified environment under atmospheric oxygen (see Appendix 8 for incubator details) unless otherwise specified. All medium was warmed to 37°C prior to use to maintain tissue viability, unless otherwise stated. Fetal bovine serum (FBS) used was from Sigma and lot number 085k3396. In selected experiments the DP and DS explants were also incubated under hypoxic conditions. In the latter case, the cells were maintained within the incubator in a gas-tight culture container (see Appendix 8) which had been exhaustively flushed with 5% (v/v) oxygen (5% (v/v) CO₂, 90% (v/v) N₂).

2.4.1 Primary culture of isolated DS and DP

In order for the follicular cells to adhere and begin attached growth in culture, cells were undisturbed for the first three days of culture. Typically, 80% of DP and 50% of DS explants showed adherent cell proliferation after this period.

When the tissue culture dish was approximately 80% confluent (which took approximately 2 weeks) the adherent cells were transferred to a 35mm diameter tissue culture dish. The cells were removed from the dish by trypsinisation as follows: cells received a 3 min application of 1ml trypsin (0.25% (w/v) in PBS; Sigma). After the incubation period 5ml 10% MEM was added to the cells and the cell suspension was pelleted in a 15ml Falcon tubes (5 min, 2475g), the supernatant discarded. Following trypsinisation the cell pellets were re-suspended in 3ml 10% MEM and transferred into a 35mm tissue culture dish.

When the cells reached near-confluency, approximately 7 days later, they were transferred to a 25cm² culture flask (Nunc) by trypsinisation as described above; the cells were re-suspended in 5ml of 10% MEM for transfer into the culture flask. The cells were incubated in flasks until 80-100% confluent, a process which normally took a week, and then the cells trypsinised and re-suspended in 1ml 10% MEM and counted using a haemocytometer (Sigma) (see Appendix 8). Typically 1.5×10^5 cells were harvested from each flask. Cells were then seeded at 5×10^4 cells per new flask. The cell culture medium was normally changed from the flasks every three days. DP and DS primary culture cells were typically used at passage 3 when there are sufficient cells for experimentation.

2.4.2 Primary culture of isolated embryonic cardiomyocytes

The culture media (10% L-15) was changed every other day and the cultures maintained without passaging for up to 24 days. Confluency and spontaneous contractions were monitored by microscope. The cells were seen to maintain contractions for the entire period of culture.

2.4.3 Culture of ES cells

The mouse ES cell line CGR8 (see Appendix 5), originally established from the inner cell mass of a 3.5 day male pre-implantation mouse embryo of strain 129, was used for experimentation. The cell line was maintained in 10% Glasgow's Minimal Essential Media (GMEM; Appendix 5) (Sigma). The cells were grown in 25cm² flasks pre-coated with 0.1% (v/v) gelatin (Sigma) (see Appendix 2) in PBS. The cells were maintained in an undifferentiated state by the addition of 5µl/flask of leukaemia inhibitory factor (LIF) (Sigma) resulting in a final LIF concentration of 0.01µg/ml (see Appendix 2).

The cells were routinely passaged at 3 days; the cells were removed from the dish by a 3 min application of 1ml of Trypsin, Versene, Phosphate (TVP; see Appendix 3). After the TVP treatment period, 5ml of 10% GMEM was added and the cells scraped using a cell scraper (Sigma) to remove them from the flask. The cell suspension was pelleted in a 15ml Falcon tube (5 min, 2475g), the supernatant discarded and the pellet re-suspended in approximately 1ml of 10% GMEM. The cells were counted and the concentration adjusted to 2×10^5 cells/ml; 5ml was added to each new flask equating to seeding at 1×10^6 cells per new 25cm^2 flask and $5\mu\text{l}$ LIF added to each flask.

2.4.4 Hanging drop culture of ES cells

ES cells are capable of differentiation towards a cardiomyocyte lineage (Maltsev *et al.*, 1994); the ES cells were cultured as hanging drops which encourages the cells to form aggregates; when this is carried out in the absence of LIF these aggregates can differentiate into embryoid bodies (EB). The adapted method of Maltsev *et al.*, (1994) was used. In brief:

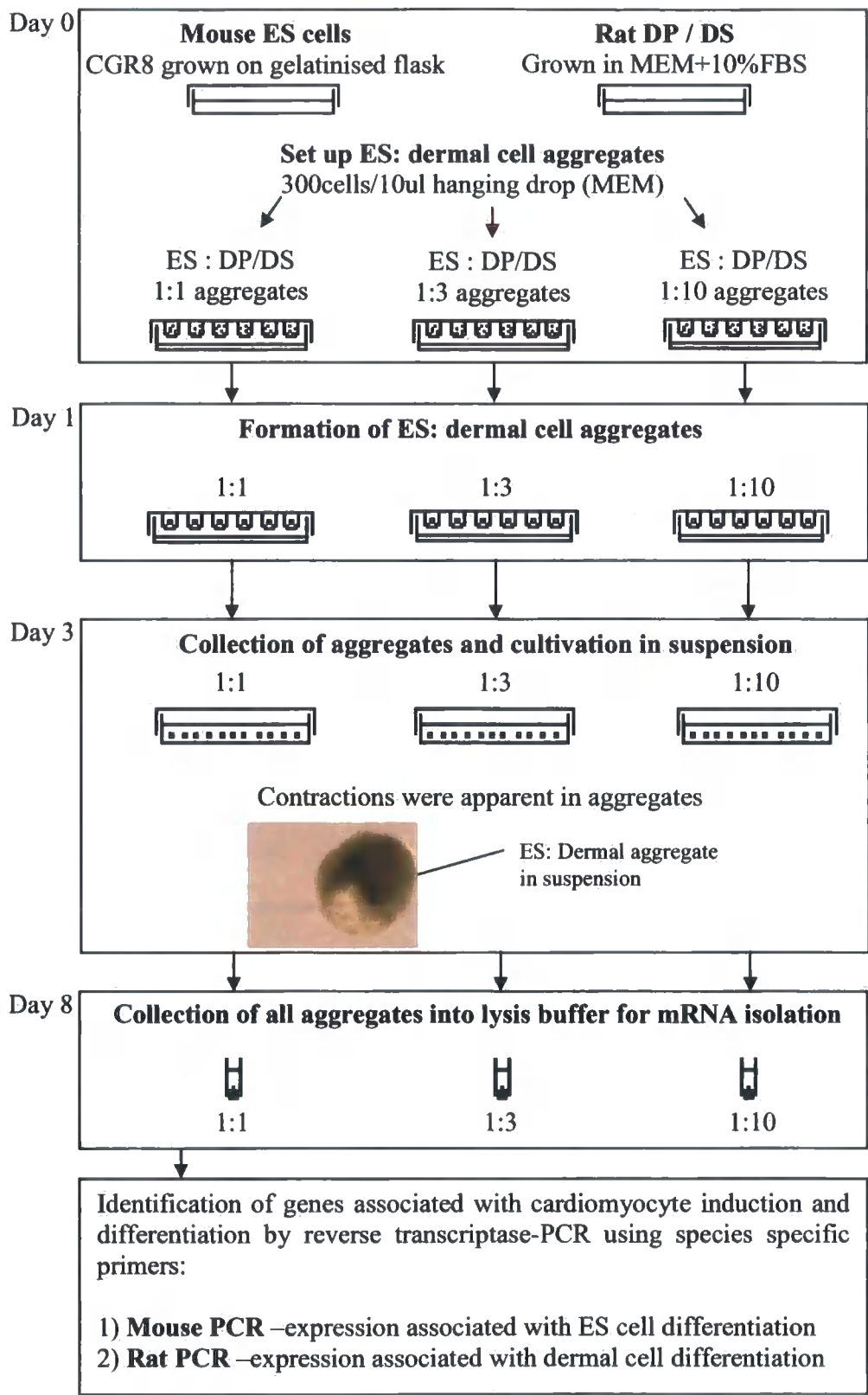
ES cells were harvested as above and concentration adjusted to 30cells/ μl of 1% GMEM in the absence of LIF. $10\mu\text{l}$ drops were created on the underside of the lid of a square dish (100cm^2 , Sigma), 100 drops per lid. 5ml water was placed in the dish, the lid was inverted and the hanging drops cultured for 3 days. EB's were then collected and transferred into petri dishes in final volume of 10ml of 10% GMEM; each dish containing approximately 100 EB's. The cell aggregates were further cultured for 5 days.

2.4.5 Co-culture of DP and DS with ES cells in aggregates

Rat dermal cells and mouse CGR8 ES cells were harvested as above and adjusted to a final concentration of 30cells/ μl in 10% GMEM in the following ES/dermal ratios; 1:1, 1:3, 1:10, ES cells alone or dermal cells alone. Aggregates were produced by hanging drop and further cultured as described for ES cells in section 2.4.4.

This co-culture procedure is summarised in the figure 2.3.

Figure 2.3: Illustration of co-culture of DP and DS with ES cells in aggregates



2.4.6 Co-culture of rat DP and DS with mouse embryonic cardiomyocytes

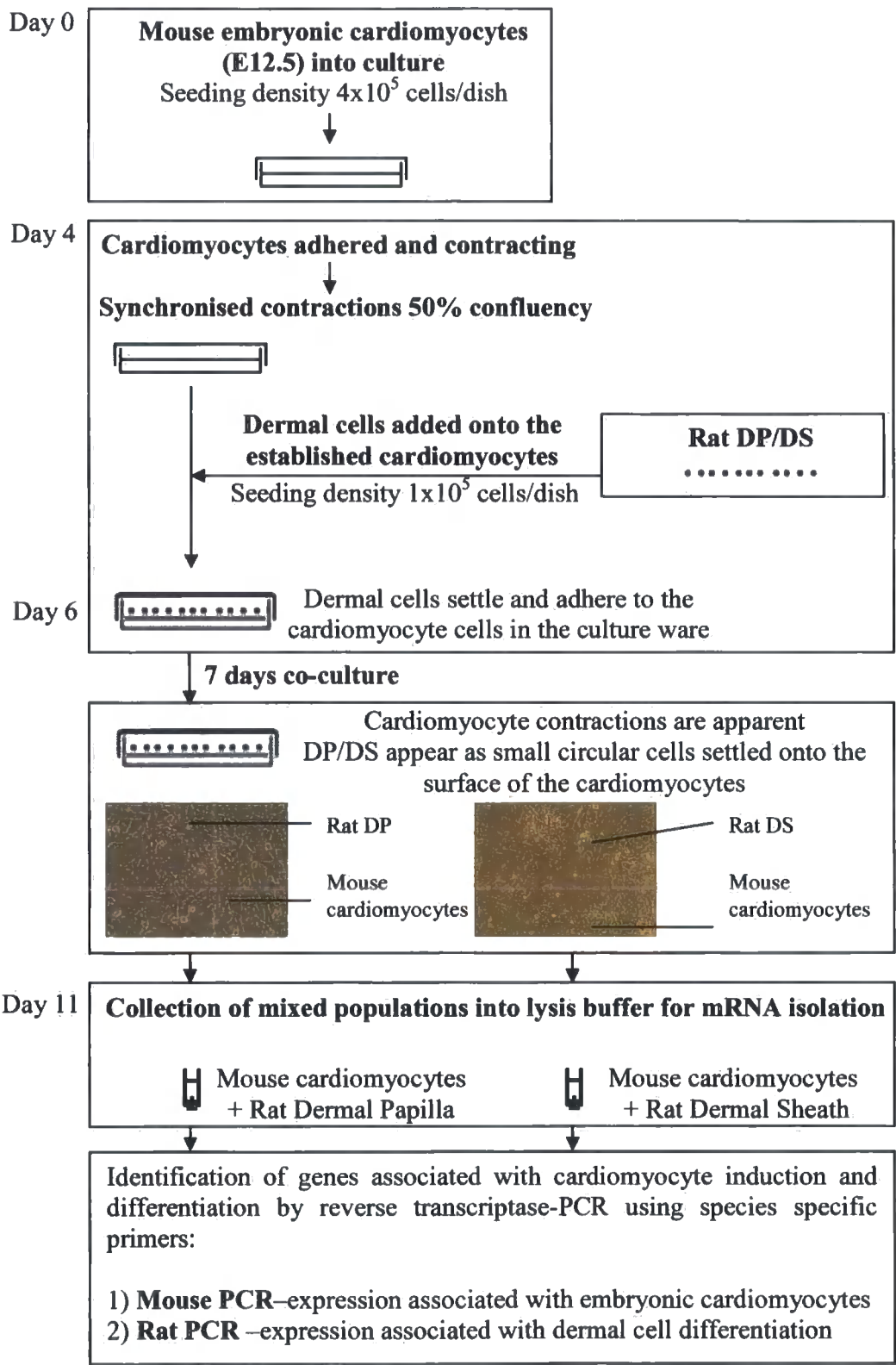
The co-culture was based upon a protocol for BM MSC (Yoon *et al.*, 2005). Briefly, mouse embryonic cardiomyocytes were isolated as described and plated into a 35mm diameter tissue culture dish at a density of 4×10^5 cells/dish; the cells were left to reach approximately 50% confluency, which normally took 6 days, at which point the cells have typically synchronized contractions. The rat DP and DS cells were removed from their tissue culture dishes by trypsinisation as described; the cell pellet re-suspended in 3ml 10% L-15 and plated onto the cardiomyocyte cultures at a density of 1×10^5 DP or DS cells/dish. The co-culture was incubated for 5 days. For RNA processing the cells were trypsinised as described above and pelleted (5 min, 2475g). A summary of this procedure is shown in figure 2.4.

2.4.7 Co-culture of DP and DS with matching species cardiomyocytes

Two co-culture experiments were set up in parallel. Both rat and mouse embryonic cardiomyocytes were isolated, plated and cultured to 50% confluency as described in section 2.3.4 and 2.4.2. As the dermal cells to be added to cardiomyocytes of the same species they needed to be pre-labelled using Carboxyfluorescein diacetate succinimidyl ester (CFSE) according to the manufacturer's instructions (see Appendix 4). CFSE can also be used to monitor cell division (Lyons *et al.*, 2000). Briefly the method was as follows:

CFSE (provided with CFSE kit) was adjusted to a concentration of 5mM with PBS, to each preparation of 5mM CFSE 18 μ l of DMSO was added (supplied with kit) and this suspension added to the cell suspensions to a final concentration of 10 μ M. The cell suspensions were incubated at 37°C for 10 min in a dry bath (Labnet). CFSE uptake was stopped by addition of 5 volumes of ice-cold MEM to the cells and incubated on ice for 5 min. Cells were pelleted by centrifugation (5 min, 2475g at 4°C), washed twice by re-suspending in ice-cold MEM and pelleted again. The cells were then re-suspended in warmed MEM. The CFSE labelled dermal cells were immediately analysed by flow cytometry, cultured for 7 days and then analysed or immediately used for co-culture with embryonic cardiomyocytes of the same species. This can be seen in figure 2.5.

Figure 2.4: Illustration of co-culture of rat DP and DS with mouse cardiomyocytes



2.4.8 Flow cytometry of CFSE labelled cells

In order to analyse cells of dermal origin from the mixed population tissue culture dishes, or from CFSE labelled cells after 7 days culture, the cells were trypsinised from the flasks as described and the cells re-suspended in 1ml PBS. The single cell suspension was subjected to flow cytometric analysis on a FACS Aria fluorescence activated cell sorter (FACS) (Becton Dickinson) by The Centre for Life flow cytometry unit (University of Newcastle). In selected experiments the fluorescein positive cells were FACS sorted into 1ml MEM. This is summarised in figure 2.5.

2.5 RNA isolation

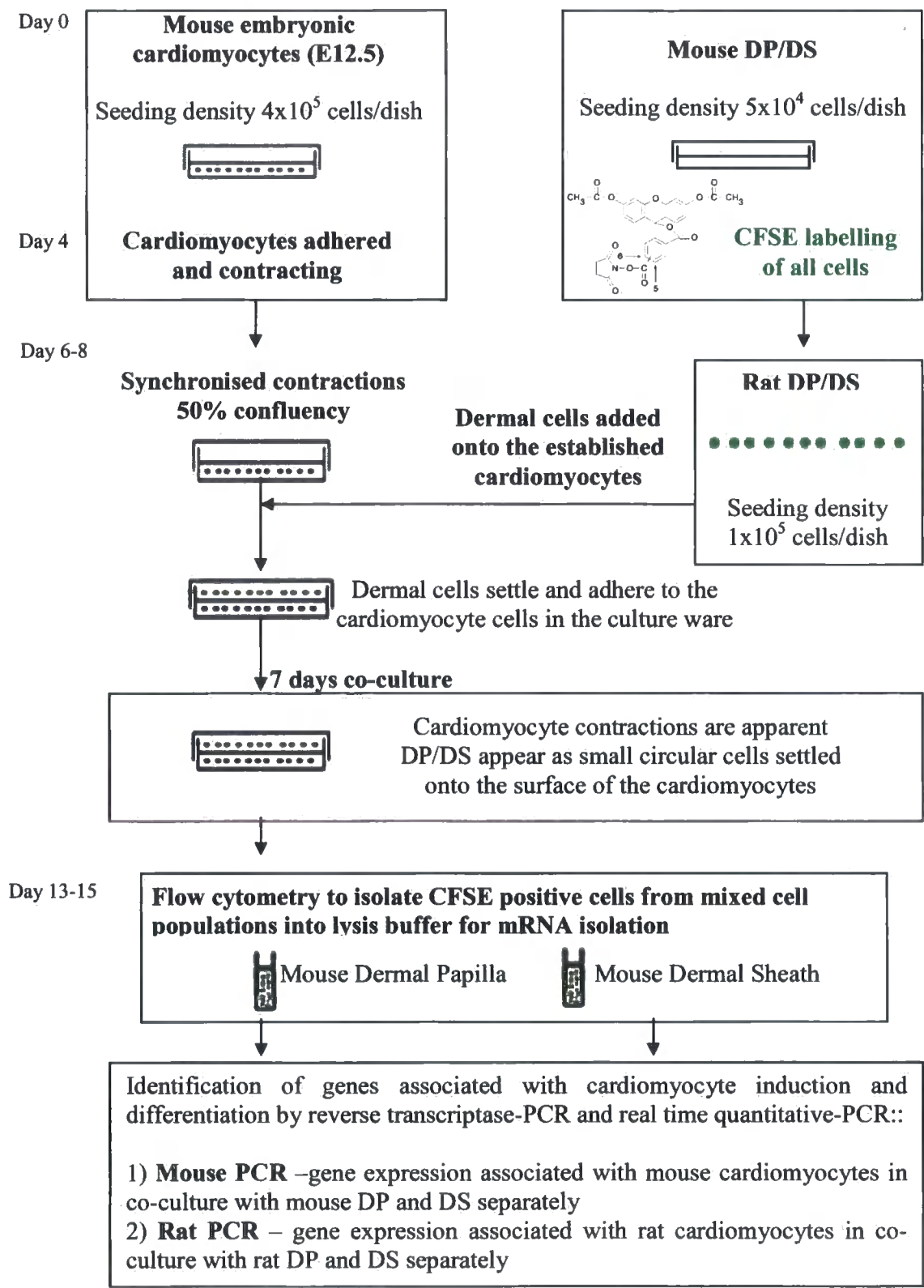
2.5.1 Harvesting cells for RNA

Cells in culture were trypsinised and pelleted as above (section 2.4.1), FACS isolated cells were pelleted (section 0) or cells were taken directly from flasks. In the latter case flasks were washed by adding 10ml PBS into culture flasks and aspirating; all liquid was removed before continuing. 500µl of denaturing solution was added directly onto cells either in 1.5ml microcentrifuge tubes or flasks and incubated for 3 minutes with agitation. The cell lysate was removed into a 1.5ml microcentrifuge tube and either used immediately or snap-frozen in liquid nitrogen (see Appendix 2) and stored at -80°C for use at a later date.

2.5.2 Harvesting tissues for RNA

RNA was isolated from tissue and cells using the Totally RNA Kit (Ambion) (see Appendix 4). Tissue was excised as described and transferred into a nitrogen filled porcelain pestle and mortar (Sigma). Tissue was ground under liquid nitrogen until it was a fine powder; this was transferred to a 1.5ml microcentrifuge tube (chilled under liquid nitrogen) after the nitrogen boiled off; tissue remained frozen. Once thawed and warmed to room temperature, 500µl of denaturing solution was added to the ground tissue and incubated for 1 minute. The lysate was snap-frozen in liquid nitrogen and stored at -80°C.

Figure 2.5: Illustration of species matched co-culture of DP and DS with cardiomyocytes



2.5.3 RNA extraction

Phenol Chloroform extraction was first carried out. 500µl of phenol chloroform (see Appendix 4) was added to the thawed cell or tissue lysate, mixed by inversion for 1 min, incubated on ice for 5 min and centrifuged for 5 min (12350g at 4°C). The top, aqueous, phase was collected and transferred into a 1.5ml microcentrifuge tube containing 50µl of 3M sodium acetate (see Appendix 4). Phenol chloroform extraction was repeated; the final aqueous phase was transferred into 500µl of isopropanol (Sigma) and chilled to -80°C for a minimum 2hrs to precipitate RNA.

The precipitated RNA was pelleted by centrifugation (5 min, 12350g at 4°C) and the supernatant discarded; the pellet was re-suspended in 300µl of 70% (v/v) ethanol, the RNA again pelleted by centrifugation (10 min, 12350g at 4°C) and the supernatant discarded. The pellet was air dried and dissolved in 20µl of Diethyl Pyrocarbonate (DEPC) treated water (see Appendix 2) and stored at -80°C.

The sample was then treated to eliminate genomic DNA using the "DNA-free kit" (Ambion) (see Appendix 4). 12µl of the thawed RNA sample was incubated at 37°C on a dry block with 1.5µl of 10x DNase-1 buffer and 1.5µl DNase-1 (see Appendix 4) for 30 minutes in 1.5ml microcentrifuge tube. 5µl of Inactivation Reagent was then added and incubated for 2 minutes, followed by centrifugation (30s, 12350g at 4°C). The supernatant containing the RNA was transferred to a new 1.5ml microcentrifuge tube and was either used immediately or stored at -80°C.

2.5.4 Agarose gel electrophoresis

1% agarose gel was prepared as follows: 0.7g agarose powder (Sigma) was added to 70ml 1xTAE buffer (Appendix 3) and heated in a microwave (Matsui 850W) at full power for 2 min. The melted agarose was left to cool to approximately 50°C before adding 7µl of 10mg/ml ethidium bromide (Sigma) (see Appendix 2). The gel was poured into the gel tank cradle (CBS Scientific) (see Appendix 8) with a 13 well comb (12µl capacity/well) and left to cool. 1µl of RNA sample was added to 5µl of Agarose Gel Load buffer (see Appendix 4) and run along side a 1kb ladder to determine product sizes (Fermentas) (ladder provided in Appendix 4). Gel Electrophoresis was carried out in 1xTAE buffer at 120 volts for 20

minutes (Consort) (see Appendix 8). The gel was visualised using a Uvidoc transilluminator (Uvitec) and the image captured.

2.5.5 RNA quantification

The RNA was quantified using a spectrophotometer (GenQuest) (see Appendix 8). 5µl of the purified RNA sample is diluted 1 in 100 with DEPC water and loaded into a UV quartz cuvette (Sigma). RNA quantitation was carried out and the concentration automatically determined.

2.6 cDNA synthesis

cDNA was synthesised from RNA for RT-PCR using the “Superscript II RNase H-Reverse Transcriptase Kit” (Invitrogen) (see Appendix 4) according to the manufacturer’s instructions. For Q-PCR the “High Capacity cDNA Reverse Transcription Kit” (Applied Biosystems) was used.

2.6.1 cDNA synthesis for reverse transcriptase PCR (RT-PCR)

For each synthesis reaction, 1µg of RNA was added to 1µl oligo(dT) primer (see Appendix 4) and made up to 12µl with DEPC water. The samples were incubated at 70°C on a dry block for 10 minutes. 4µl of 5xFirst strand buffer, 2µl 0.1M 1,4-Dithiothreitol (DTT) (see Appendix 4) and 2µl 2.5mM deoxyribonucleotide triphosphates (dNTP) (Invitrogen) (see Appendix 2) are added to each sample 1µl of reverse transcriptase (RT) (see Appendix 4) was added and incubated at 42°C on a dry block for 1 hour. The samples were either used immediately or stored at -20°C for storage. For control reactions the reverse transcriptase was substituted with 1µl DEPC water.

2.6.2 cDNA synthesis for real time quantitative PCR (Q-PCR)

For each synthesis reaction, 1µg of RNA in 10µl in DEPC water was added to 10µl of 2xRT mix (components provided with the Capacity cDNA Reverse Transcription kit) which is made up with 2µl 10xRT buffer, 0.8µl 25xdNTP Mix, 2µl 10xRT random primers, 1µl MultiScribe reverse transcriptase, 1µl RNase inhibitor, 3.2µl nuclease free water. The samples were sequentially heated to 25°C for 10 min then 37°C for 2hrs, and finally 85°C

for 5 seconds before being put on ice. For control reactions the reverse transcriptase was substituted with 1µl DEPC water.

2.7 Primer Design

2.7.1 Primers designed for RT-PCR

Primers were designed according to following rules:

- Nucleotides of gene of interest were located for species required (mouse/rat) by searching for the gene using NCBI software; BLAST (Altschul *et al.*, 1997) and GenBank (Benson *et al.*, 2000) available online (see Appendix 6)
- The open reading frame was identified within NCBI
- Forward and reverse primer sequences were designed with the following parameters:
 - Sequence length 17-25 bases long, with no more than three contiguous nucleotides with the same base or repeats of sequences of three or more bases, GC content was 50-60%, predicted product ideally be larger than 200bp, no hairpin loops or secondary structures predicted within primers as determined using the online software “Oligonucleotide Calculator”
 - Predicted melting temperatures of both primers were no more than 4°C apart and ideally be around 50-60°C
 - The primer product should span an intron so that genomic contamination can be identified by an aberrant size product
 - Primer specific for target gene and species under study

All products were of the size predicted. The image of this product was isolated for presentation. Primer details including predicted band sizes are provided in the Appendix 6.1.

2.7.2 Primers for Q-PCR

TaqMan gene expression assays were inventoried sets from Applied Biosystems. Each assay contained 2 unlabeled PCR primers (final concentration of 900nM each) and 1

FAMTM (reporter) dye-labelled TaqMan MGB (minor groove binder) probe (final concentration of 250nM). A list of the assays used is provided in Appendix 6.2.

2.8 Polymerase Chain Reaction

2.8.1 RT-PCR

RT-PCR was run using the “*Taq* DNA polymerase, recombinant kit” (Invitrogen) (see Appendix 4) according to the manufacturer’s instructions. In brief, each sample for PCR was prepared in 0.5ml PCR tubes (Sigma) and the following added to each sample in the order provided: 38.8µl RNase free water (Sigma), 5µl 10X *Taq* buffer, 1.5µl 50mM MgCl₂, 1.5µl of 2.5mM dNTP’s, 1µl each of 10µM forward and 10µM reverse primer specific to gene of interest, 1µl template (cDNA, water or positive control), 0.2µl *Taq* polymerase.

PCR was carried out in a thermocycler (Biometra, T personal) for 35 cycles. Each cycle consisted of 94°C for 5 min (1 cycle) followed by 35 cycles of 95°C for 30s, annealing temperature for 1minute followed by 72°C for 1minute. After the 35 cycles there was an extension step at 72°C for 7 min (1 cycle) and the samples were held at 4°C for use. The annealing temperatures were specific to primer sequences as detailed in Appendix 6.1. Following PCR, 10µl of loading buffer is added to each sample and 10µl run on an agarose gel described as in section 2.5.4 except it was 2% gel (1.4g agarose in 70ml 1xTAE), and run at 120v for 30 minutes.

2.8.2 Q-PCR

Q-PCR was run using the “TaqMan Fast Universal PCR Master Mix (2x)” (Applied Biosystems) (see Appendix 4) according to the manufacturer’s instructions. In brief, Q-PCR was run in a 96 well plate; each sample was run in triplicate. To prepare the reaction 10-100ng cDNA was required (routinely 100ng was used) to which was added to 1µl TaqMan gene expression assay mix (20x) (Applied Biosystems), specific to the gene of interest, 10µl PCR master mix (2x) (see Appendix 4) and made up to 20µl with DEPC water. The plate was centrifuged (30s, 10g) and subjected to Q-PCR and analysed in an 7500 Fast Real-time PCR machine (Applied Biosystems).

2.9 Induced myocardial cryo-injury

In order to investigate the effects of myocardial injury on stem cell mobilisation the method of Leferovich *et al.*, (2001) was used. In brief, as follows:

Mice were weighed using an electronic small animal weighting balance (Shimadzu) and anaesthetised using 1.25% (v/v) Avertin in sterile saline (0.9% (w/v) NaCl) by sub-cutaneous (s.c.) injection of 25µl/g body weight. Once anaesthesia was achieved, the ventral abdomen wall was shaved, using clippers, immediately caudal to the costal margin. The mouse was placed on a polystyrene tray, on its back, head facing away.

A vertical incision was made, using a scalpel, of approximately 6mm length, just left of midline. The cryo-probe (2mm rounded probe) was cooled in liquid nitrogen. The right superior epigastric artery, running caudally in the abdominal wall was visualised; the muscle was divided vertically between this vessel and midline for 5mm with “tenting” of the muscle to avoid damage to the viscera. The thorax was elevated by approximately 5mm by raising the animals back so the thoracic cavity is higher than the abdomen, by which process the medial lobe of the liver is moved out of the way. Forceps were used to hold the incision open to expose the abdominal cavity; the liver was gently manipulated away from the diaphragm. The heart was seen as a dark purple area against the diaphragm.

The cooled probe was carefully passed through the incision and applied to diaphragm adjacent to the heart surface with firm pressure for 20s. PBS pre-warmed to 37°C was dropped onto and along the probe using a disposable Pasteur pipette, to allow non-traumatic detachment of the probe from the diaphragm. Excess PBS was absorbed with cotton wool buds.

The muscle of the abdominal wall was closed with interrupted sutures using vicryl coated 4-0 suture (Ethicon) and surgical skin glue (dermabond). Analgesia was provided by s.c. injection of Buprenorphine (supplied by Dr. David Breault) at 3.3µl/g body weight and the mouse allowed to recover in a warmed box with constant monitoring until conscious. On occasion, additional analgesia was administered as necessary.

2.10 Immunohistology

2.10.1 Preparing tissue

Organs for study were washed in PBS and transferred into 4% (w/v) paraformaldehyde (Sigma) (see Appendix 2) in PBS and held on ice for a minimum of 2hrs. The tissues were then put into ice cold 40% (w/v) sucrose (Sigma) in PBS overnight at 4°C. The tissue samples were then embedded in TissueTek solution (Electron Microscopy Sciences) and snap-frozen in liquid nitrogen before storing at -80°C or using immediately.

2.10.2 Slide preparation

Tissue embedded in TissueTek solution, were cryo-sectioned using a cryostat (Leica) (see Appendix 8). 10µm sections were collected onto positively charged glass slides (Fisher). The sections were allowed to air dry for an hour after which they were stored at -20°C or used immediately. The tissue was delineated using a phthalamidoperoxydicapric acid (PAP) pen (Abcam) which formed a hydrophobic barrier around each section to aid antibody labelling. The slides were then incubated in cold 4% (w/v) paraformaldehyde in PBS for 20 minutes at 4°C with rocking on a mini-gyro-rocker (Stuart) (in refrigerated room) and used immediately for antibody labelling.

For blood smear slides, fresh blood in microcentrifuge tubes on ice was spotted onto glass slides within 2 minutes of collection and smeared using a second glass slide. All blood slides were fixed with cold methanol (Sigma) for 5 minutes rocking at 4°C and used immediately for antibody labelling.

2.11 Immunohistochemistry antibody labelling

The primary GFP antibody used was a polyclonal Rabbit anti-GFP (Abcam, ab6556). The secondary antibody was a polyclonal Goat anti-rabbit biotin (Abcam ab6720). The secondary antibody was detected using VIP (Vector) diluted in PBS according to the manufacturers instructions. The tissue was blocked with goat serum (Vector).

This method is used for sections of testes, adult mystacial pad, embryos and adult heart (section 2.10.1) using the GFP antibody. Details of the antibodies and detection chemicals are provided in Appendix 7. The method was as follows:

Day 1

1. Wash slides twice in PBS-TritonX-100 buffer (PBS-T100; see Appendix 3), rocking (Sigma rocker at room temperature) for 5 min each
2. Wash slides twice in PBS, rocking for 5 min
3. Apply 0.3% (v/v) hydrogen peroxide (Sigma) in methanol (Sigma) for 30 minutes, rocking
4. Wash slides twice in PBS, rocking for 5 min
5. Block with streptavidin (Vector) (see Appendix 4) for 1 hour , rocking
6. Wash slides twice in PBS, rocking for 5 min
7. Block with biotin (Vector) (see Appendix 4) for 1 hr , rocking
8. Wash slides twice in PBS, rocking for 5 min
9. Block with blocking buffer (1% (v/v) serum specific to serum suitable for antibody combination as described above – in this case rabbit anti-GFP) for 1 hr , rocking
10. Shake off excess blocking buffer and apply primary antibody (specific to antibody as indicted above – in this case goat serum) diluted in 1% (v/v) serum blocking buffer (as above) at 4°C overnight

Day 2

1. Wash slides in PBS-T100, rocking for 5 min
2. Wash slides in PBS, rocking for 5 min
3. Apply biotinylated secondary antibody (specific to antibody as indicted above) diluted in 1% (v/v) serum blocking buffer as above – in this case goat) rocking for 30 min
4. Prepare ABC solution (Vector) required for step 7 30 min prior to use (see Appendix 4)
5. Wash slides twice in PBS, rocking for 5 min
6. To inactivate endogenous peroxidase activity, application of 1.6% (v/v) H₂O₂ (see Appendix 2) in PBS for 10 min rocking
7. Wash slides twice in PBS, rocking for 5 min
8. Incubate in ABC solution rocking for 1hr
9. Wash slides twice in PBS, rocking for 5 min
10. Make VIP stain (Vector) (see Appendix 4)
11. Apply VIP stain for 1 minute monitoring under the microscope constantly
12. Stop reaction by placing slides in running tap water for 5 min
13. The nucleus was counterstained with methyl green staining solution (Vector) on a 60°C slide warmer (Fisher) for 5 min
14. Wash slides in water for 1 minute then dip 10 times in acetone (Sigma) containing 0.05% (v/v) acetic acid (Sigma)
15. Dehydrate slides for 2 min in each sequential step:
 - 70% (v/v) ethanol
 - 90% (v/v) ethanol
 - 100% (v/v) ethanol
 - Xylene
16. Mount in permount (Fisher) and coverslip (Fisher) and leave to dry

2.12 Immunofluorescence antibody labelling

The primary GFP antibody used was a polyclonal Rabbit anti-GFP (Abcam, ab6556). The secondary antibody was a polyclonal goat anti-rabbit FITC (Abcam, 7086). For this combination the tissue was blocked with goat serum (Vectastain).

The primary anti-CD45 and anti-CD34 antibodies used were a monoclonal Rat anti-mouse CD45 (Abcam, ab25386) and a monoclonal Rat anti-mouse CD34 (Abcam, ab8158). The secondary antibody used for both was a biotinylated monoclonal Chicken anti-rat (Abcam, ab6835). The secondary antibody was detected using streptavidin-7-amino-4-methylcoumarin-3-acetic acid (streptavidin-AMCA) (Vector, SA-5008). For this combination the tissue was blocked with chicken serum (Abcam ab7477).

Details of the antibodies and detection chemicals are provided in Appendix 7.

2.12.1 Single labelling methods

A single labelling method was used for GFP antibody labelling of neonatal skin. The method was as follows:

Day 1

1. Wash slides twice in PBS, rocking for 5 min
2. Block with 1% (v/v) serum blocking buffer (specific to serum suitable for antibody combination as described above – in this case goat) for 20 min, rocking
3. Remove block and apply primary antibody (specific to antibody – in this case ANTI-GFP) diluted in 1% (v/v) serum blocking buffer (as above) at 4°C overnight

Day 2

1. Wash slides twice in PBS, rocking for 5 min
2. Apply secondary antibody (specific to antibody as indicated above – in this case goat anti-rabbit FITC) diluted in 1% (v/v) serum blocking buffer (as above) rocking for 1hr
3. Wash slides twice in PBS, rocking for 5 min
4. Shake off excess PBS
5. The nuclei are labelled with 4',6-diamidino-2-phenylindole (DAPI) (Vector) and the slide mounted with a glass cover slip

A single labelling method was used for anti-CD45 and anti-CD34 antibody labelling of neonatal skin. The method was as follows:

Day 1

1. Wash slides twice in PBS-T100 rocking for 5 min

2. Wash slides twice in PBS, rocking for 5 min
3. Apply 0.3% (v/v) H₂O₂ in methanol for 30 minutes, rocking
4. Wash slides twice in PBS, rocking for 5 min
5. Block with streptavidin for 1 hour , rocking
6. Wash slides twice in PBS, rocking for 5 min
7. Block with biotin for 1hr , rocking
8. Wash slides twice in PBS, rocking for 5 min
9. Block with 1% (v/v) serum blocking buffer (specific to serum suitable for antibody combination as described above – in this case either goat or chicken) for 1hr , rocking
10. Remove block and apply primary antibody (specific to antibody as indicted above – in this case either anti-CD45 or anti-CD34) diluted in 1% (v/v) serum blocking buffer (as above) at 4°C overnight

Day 2

1. Wash slides in PBS-T100, rocking for 5 min
2. Wash slides in PBS, rocking for 5 min
3. Apply biotinylated secondary antibody (specific to antibody as indicted above) diluted in 1% (v/v) serum blocking buffer as above – in this case goat anti-rabbit) rocking for 30 min
4. Wash slides twice in PBS, rocking for 5 min
5. To inactivate endogenous peroxidase activity, application of 1.6% (v/v) H₂O₂ in PBS for 10 min rocking
6. Wash slides twice in PBS, rocking for 5 min
7. Incubate in streptavidin-AMCA for 30 min
8. Wash slides twice in PBS, rocking for 5 min
9. Shake off excess PBS
10. The nuclei are labelled with Propidium Iodide (PI) (blood smears for all antibodies) at 1 in 5000 dilution; 20µl per section and the slide mounted with a glass cover slip.

2.12.2 Dual labelling method

A dual labelling method was used for GFP antibody labelling in combination with anti-CD45 and anti-CD34 for neonatal skin and adult heart. The method was as follows:

Day 1 – anti-GFP antibody labelling

1. Wash slides twice in PBS, rocking for 5 min
2. Block with 1% (v/v) serum blocking buffer (specific to serum suitable for antibody combination as described above – in this case goat) for 20 min , rocking
3. Remove block and apply primary antibody (specific to antibody – in this case GFP) diluted in 1% (v/v) serum blocking buffer (as above) at 4°C overnight

Day 2

1. Wash slides twice in PBS, rocking for 5 min
2. Apply secondary antibody (specific to antibody as indicted above – in this case goat anti-rabbit FITC) diluted in 1% (v/v) serum blocking buffer (as above) rocking for 1hr
3. Wash slides twice in PBS, rocking for 5 min

Day 2 – anti-CD45 or anti-CD34 antibody labelling

4. Wash slides twice in PBS-T100, rocking for 5 min
5. Wash slides twice in PBS, rocking for 5 min
6. Apply 0.3% (v/v) H₂O₂ in methanol for 30 minutes, rocking
7. Wash slides twice in PBS, rocking for 5 min
8. Block with streptavidin for 1 hour, rocking
9. Wash slides twice in PBS, rocking for 5 min
10. Block with biotin for 1 hr, rocking
11. Wash slides twice in PBS, rocking for 5 min
12. Block with 1% (v/v) serum blocking buffer (specific to serum suitable for antibody combination as described above – in this case chicken) for 1 hr, rocking
13. Remove block and apply primary antibody (specific to antibody as indicated above – in this case either anti-CD45 or anti-CD34) diluted in 1% (v/v) serum blocking buffer (as above) at 4°C overnight

Day 3

1. Wash slides in PBS-T100, rocking for 5 min
2. Wash slides in PBS, rocking for 5 min
3. Apply biotinylated secondary antibody (specific to antibody as indicated above) diluted in 1% (v/v) serum blocking buffer as above) rocking for 30 min
4. Wash slides twice in PBS, rocking for 5 min
5. To inactivate endogenous peroxidase activity application of 1.6% (v/v) H₂O₂ in PBS for 10 min rocking
6. Wash slides twice in PBS, rocking for 5 min
7. Incubate in streptavidin-AMCA (as described above) for 30 min
8. Wash slides twice in PBS, rocking for 5 min
9. Shake off excess PBS
10. The nuclei are labelled with PI (blood smears for all antibodies) (1 in 5000 dilution 20µl per section) and the slide mounted with a glass cover slip.

2.13 Cell preparation for flow cytometry immunofluorescence analysis

2.13.1 Adult heart

The adult heart was isolated and dissociated to single cells as described with the embryonic hearts (section 2.3.4). The final cell pellet was re-suspended in PBS and concentration adjusted to approximately 1×10^6 cells/ml for flow cytometry antibody labelling

2.13.2 Neonatal skin

The neonatal skin was dissociated to single cells as described (section 2.3.2). The final cell pellet was re-suspended in PBS and concentration adjusted to approximately 1×10^6 cells/ml for flow cytometry antibody labelling.

2.14 Flow cytometry

Native GFP expression is able to be detected by flow cytometry without the need for antibody labelling. The cells are labelled with the following:

The mouse lineage antibody cocktail (BD Pharmingen) is APC conjugated (see Appendix 7.2); it labels CD3 ϵ chain, CD11b, CD45R/B220, Erythroid Cells (Ly-76/TER-119), Ly-6G and Ly-6C. Cells expressing these genes were considered to be associated with cells that may be present in the blood or of haematopoietic lineage such as T lymphocytes, B lymphocytes, monocytes/macrophages, NK cells, erythrocytes, and granulocytes. Cells positive for APC were therefore excluded when sorting for cells that are GFP+ve. 10 μ l of the lineage cocktail solution was added to a maximum of 1x10⁶ cells in 1ml PBS and incubated on ice for 30 min then pelleted by centrifugation (5 min, 1235g at 4°C). The cells were re-suspended in 5ml PBS to wash and pelleted before being re-suspended in 1ml PBS for FACS.

7-AAD (BD Pharmingen) is a viability dye. 7AAD only enters membrane-compromised cells and binds to DNA. Cells positive for 7AAD were therefore excluded when sorting for cells that are GFP+ve. The 7-AAD fluorescence is detected in the far red range of the spectrum at 650 nm using a long-pass filter. 10 μ l of 7-AAD solution was added to a maximum of 1x10⁶ cells in 1ml PBS 5 min prior to FACS.

2.15 Statistical analysis

Any statistical analysis was using a students t-test; statistical significance is assigned when $p \leq 0.01$ unless otherwise stated; where significance is still attributed but at a higher p value.

3 Characterisation of dermal follicular cells

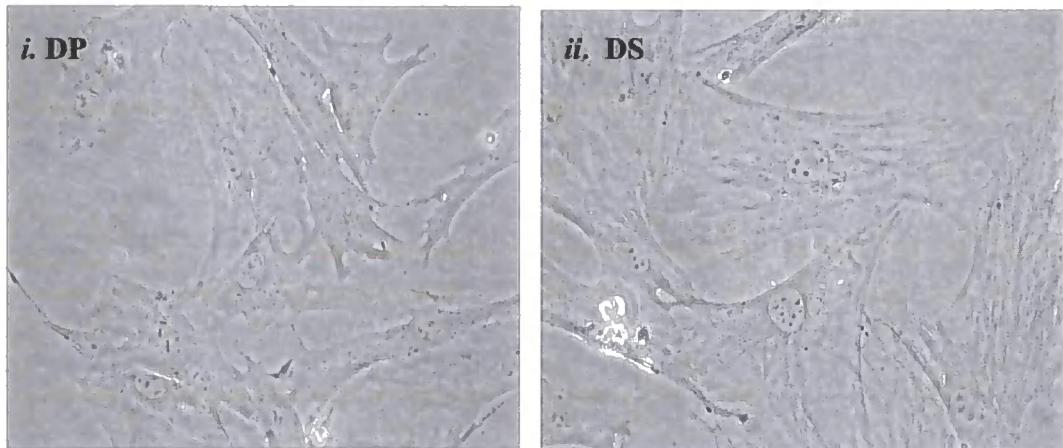
The use of primary cultures of stem cell populations as a tool for investigating their developmental and differentiation potential has a number of advantages; the lack of tissue culture adaptation reduces the risk of aneuploidy (Baker *et al.*, 2007); they are more useful in the development of tissue engineering strategies and they are more likely to be representative of the *in vivo* condition (Polak *et al.*, 2006). However, such cultures normally have a limiting lifespan in tissue culture (Rubin *et al.*, 1997) and this affects their utility for extended biological studies. One approach to extend their *in vitro* culture lifespan has been to immortalise primary cultures however this has been associated with cellular transformation; such examples include over expression of telomerase (Cerni 2000), human papilloma virus (Takeuchi *et al.*, 2007) or T antigen activation by simian virus 40 (Sv40) (Potter and Potter 1975). Such transformation limits interpretation of cellular physiology and normally precludes their use in tissue engineering. The alternative approach has been to develop conditions for the reproducible isolation and culture of primary tissues.

This chapter describes the isolation and culture of dermal papilla (DP) and dermal sheath (DS) cell populations and demonstrates that these primary cultures show reproducible patterns of cell morphology, gene expression and population doublings, indicating that these cell populations are suitable for further study of their developmental potential.

3.1 Morphological characteristics of the dermal follicular cells in adherent culture

The DP and DS were isolated from the hair follicle by manual dissection (section 2.3.1) and cultured as described (section 2.4.1). The adherent DP and DS monolayers were seeded to a 25cm² culture flask for expansion after a period of proliferation in a 16mm then 35mm dish to expand the isolated DP and DS primary explants. Cells were routinely passaged at 80% confluency, a cell density of approximately 6x10³ cells/cm², and seeded into subsequent flasks at a density of 2x10³ cells/cm²; cells were maintained in 25cm² flasks until use. In total in excess of 20 primary cultures were set up and monitored for up to 10 passages.

Figure 3.1 Morphology of DP and DS *in vitro* culture



Gross morphology of DP (i) and DS (ii) cultures *in vitro* at passage 3. DP and DS cultures were similar in cellular appearance; broadly fibroblastic in appearance and had a high cytoplasm to nucleus ratio. Morphology was maintained over 10 passages as assessed by phase microscopy at x40 magnification

The images in figure 3.1 show representative images of DP and DS primary culture cells *in vitro*; the morphology of these both cell types in culture was consistent with previous suggested descriptions:

- The first outgrowth of cells from the primary explant were closely packed together, irregularly shaped and often granular in appearance at the perinuclear area which grew in a monolayer, this was maintained to sub-confluency (Jahoda and Oliver 1981)
- The cells on the periphery of the primary outgrowth from the DP and DS explants were fibroblastic, flattened, polygonal shaped cells with a single speckled nucleus and a number of cellular processes; this morphology defined the DP and DS after the first passage (Jahoda and Oliver 1981) and was maintained throughout the period of culture which was up to 10 passages; a total of approximately 4 weeks
- Both the DP and DS had phase-dark microfilament bundles (Jahoda and Oliver 1981)
- At confluency multilayered aggregates were often observed (Messenger *et al.*, 1986; Jahoda and Oliver 1984)

Although the cells demonstrated limited morphological changes throughout investigation, there may have been gene expression changes in the cells associated with culturing which would be undetectable by microscopy. In order to address this and confirm their DP and DS identity, the gene expression profile of dermal follicular associated genes was examined.

3.2 Expression of dermal follicular genes in DP and DS primary cultures

Dermal follicular cell populations have a characteristic gene expression profile which includes nexin, versican and LEF-1. *In vivo*, nexin is expressed in the DP and lower DS (Sonoda *et al.*, 1999; Yu *et al.*, 1995), versican is expressed in the DP, DS, bulb matrix and epithelial column (Harris and Jahoda 2001; Fernandes *et al.*, 2004) and LEF-1 is expressed in the DP, DS and matrix cells of the lower hair follicle (DasGupta and Fuchs 1999; Merrill *et al.*, 2001). Nexin is the most useful of these genes as its expression is not detectable in

dermal fibroblasts, mast cells, adipocytes, endothelial cells or keratinocytes *in vivo* (Xiang and Yang 1998). Therefore when nexin is expressed in conjunction with LEF-1 and versican in cells isolated from the hair follicle *in vitro*, it allows the very specific identification of the DP and DS; an important tool when these cell populations are isolated by manual dissection from surrounding tissue, this method of identification has proved useful in identifying the DP and DS primary culture cells *in vitro* and investigating their differentiation into adipocytic and osteocytic lineages (Jahoda *et al.*, 2003).



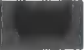



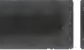





























Expression of these genes were assessed in the DP and DS primary cultures to confirm their identity and investigate culture associated changes as shown in figure 3.2. Cells were sampled at passage 1; considered early passage, and passage 3; the stage at which there was sufficient cells for experimentation (see Methods section 2.4.1). DP and DS primary cultures were investigated along with three independent DP and DS clonal cell lines (gift of Prof. Colin Jahoda).

The end bulb was also analysed; as described the end bulb is the lower one third of the hair follicle and contains the DP and DS in an un-manipulated state. However, the dermal populations have not been excised from other structures, such as the epithelial matrix of the hair follicle or capillaries containing haematopoietic or endothelial progenitor cells, and are less useful in defining DP and DS properties. An alternative approach is to examine primary cultures from surgically excised dermal populations. Representative samples are shown in figure 3.2.

Expression of the genes characteristic of the dermal follicular cells was reproducibly detected across all the samples investigated. This expression pattern is consistent with the maintenance of the dermal follicular cell type in the DP and DS primary culture cells and the clonal cell lines.

The gene expression of the entire DP and DS primary cultures were sampled and there was detectable expression of all three genes. These primary cultures are considered to be a mixed population of biochemically distinct cells (Jahoda *et al.*, 2003) therefore not all of the cells may express nexin, LEF-1 and versican at the same time.

Figure 3.2: Gene expression profile of DP and DS primary cultures and clones

				Clones					
	End Bulb	DP	DS	DP1	DP2	DP3	DS1	DS2	DS3
Nexin									
LEF-1									
Versican									
GAPDH									

RT-PCR of genes characteristic of the follicular dermal cells. Nexin, LEF-1 and versican were consistently expressed in isolated whole end bulb, cultured populations of DP and DS and dermal clonal cell lines. Representative bands are shown from passage 1, 2 and 3 primary culture DP and DS cells and passage 6 clonal cell lines GAPDH was used as a loading control.

The clonal cell lines, derived from single DP and DS primary culture cells, did express all three genes indicating those individual founder cells had a similar gene expression profile. This can be extrapolated back to the DP and DS primary cultures, suggesting there are cells isolated that must be capable of expressing all three genes simultaneously, as is observed *in vivo*. In summary, this indicates there are cells present in the DP and DS primary cultures that are representative of the cells *in vivo* by dermal follicular cell gene expression profiling.

Although the expression of genes characteristic of *in vivo* dermal follicular cells were consistently observed in the DP and DS primary cultures, this does not exclude the possibility of these cells having undergone tissue culture adaptation *in vitro* which may not be apparent by gene expression or morphology. Indeed, clones of single cells from DS and DP cultures can show a similar gene profile to the *in vivo* cells (figure 3.2) despite having undergone such cellular transformation. Transformation of other mesenchymal stem cell types demonstrates a characteristic shift in population doubling times (Zhou *et al.*, 2006). In order to monitor whether such changes occurred during the duration of primary culture of DS and DP, the population doubling times were assessed.

DS and DP established cell lines, cultured from primary explants, were typically used at passage 3. The effects of extended culture by changes in cell doubling time from passage 3 to passage 5 were therefore studied for comparison to passage 3. Any changes would potentially indicate tissue culture adaptation or transformation, as has been used to indicate if a bone marrow derived mesenchymal stem cell (MSC) population has become senescent (Kern *et al.*, 2006).

3.3 Dermal follicular cell population doubling time as determined by cell counts

The population doubling time of untransformed primary DS and DP cultures has been reported to range from 1.1 days (Hoogduijn *et al.*, 2006) to 3.8 days (Bassukas *et al.*, 1993). Clonal cell line doubling times also vary in a similar manner from 1 day to 3.8 days (Jahoda *et al.*, 2003).

The population doubling times across the three passages, as calculated by cell counts, were comparable with published data for both DP and DS primary cultured cells (2.5 to 2.8

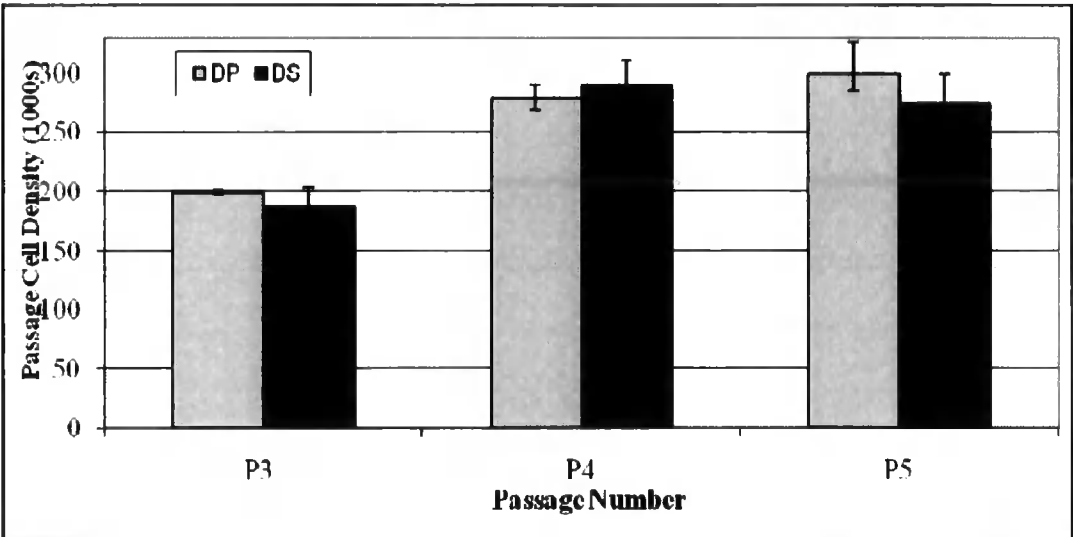
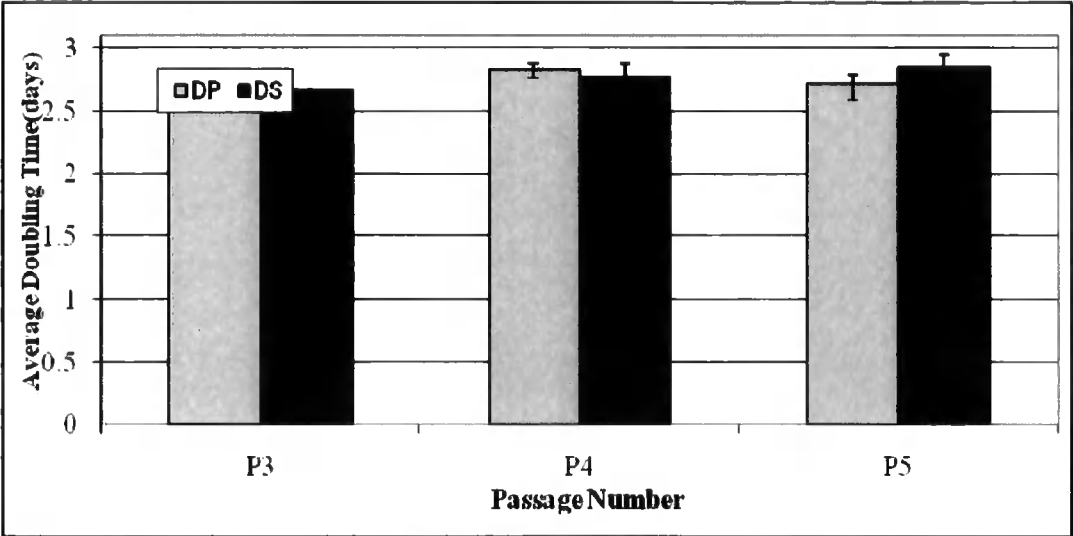
days) as shown in figure 3.3. The effect of cellular transformation would be to shorten this significantly as the cells rapidly proliferate. Mouse bone marrow derived MSC have demonstrated spontaneous transformation, starting at passage 3, as indicated by rapid proliferation which correlated with karyotype changes and loss of contact inhibition (Zhou *et al.*, 2006). As can be seen from figure 3.3, the time taken for the population to double in these three independent cultures actually increased modestly from 2.5 days to 2.8 days over the period of study. These results were consistent with an absence of frequent cellular transformation in the cell populations; however it would be possible that heterogeneity in cell division rates in this large cell population could mask the effects of a rapidly dividing minority. In order to address this, the cell division profile of the whole population was examined.

3.4 Pulse chase proliferation assay to examine cell division

CFSE can be used in a pulse-chase experiment to monitor cell division (Lyons 2000). The principle of this assay is shown in figure 3.4. Cells incubated with CFSE take up and retain this fluorescent dye independent of cell type; subsequent cell divisions can then be monitored throughout a period of culture. Cell division results in daughter cells retaining half of the fluorescence of the parental cell type, which is halved again when these cells in turn divide. Preliminary experiments demonstrated that labelling by CFSE of dermal cells at passage 3 was very efficient (less than 6% (DP) or 10% (DS) unlabelled cells (data not shown) making CFSE suitable for labelling of these cell types; the fluorescence of the cells labelled with CFSE was detectable and distinguishable from non-labelled cells as shown in figure 3.5.

Figure 3.3: Cell population doubling time and passage cell density

	P3 doubling time	P3 Cell Density (1000s)	P4 doubling time	P4 Cell Density (1000s)	P5 doubling time	P5 Cell Density (1000s)
DP	2.51	199	2.82	279	2.72	299
DS	2.66	187	2.77	289	2.85	275



Average population doubling times and cell yields for DP and DS primary cultures across three passages with standard deviation error bars. Primary DP and DS cultures showed similar cell population doubling times over three passages; passage 3, 4 and 5 from three independent experiments.

Figure 3.4: Illustration of method of CFSE labelling

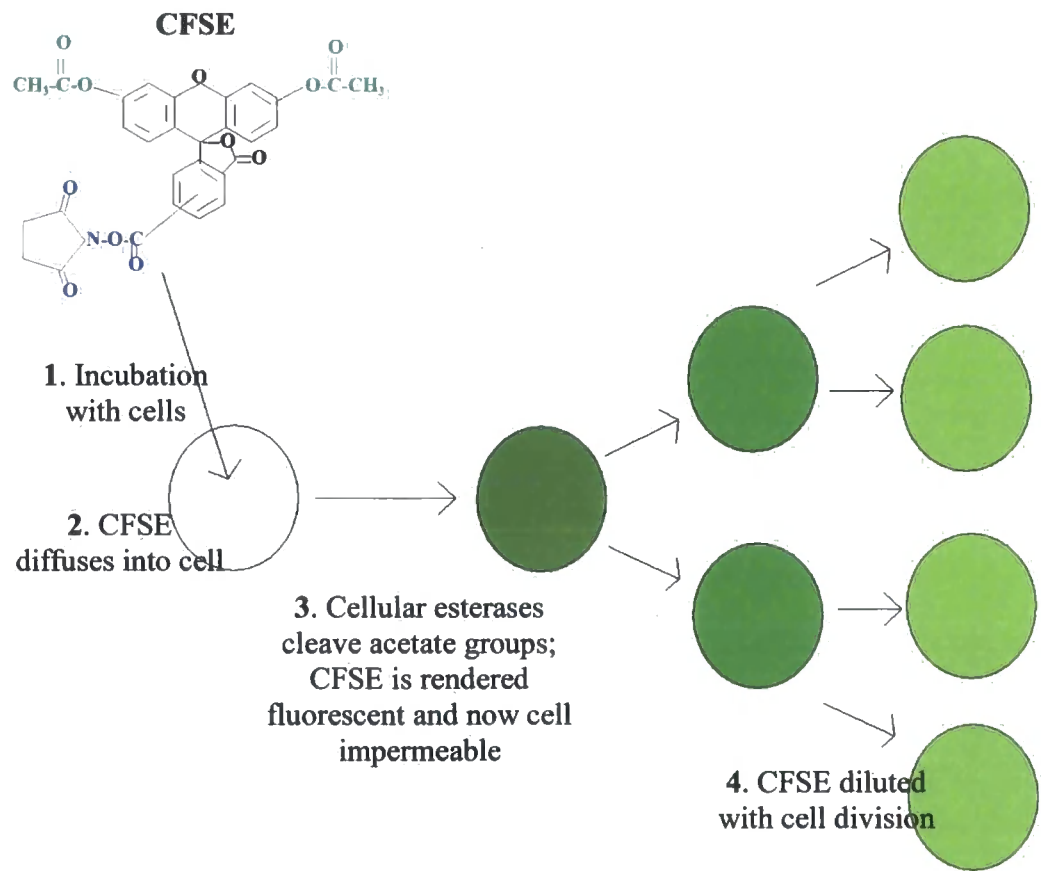
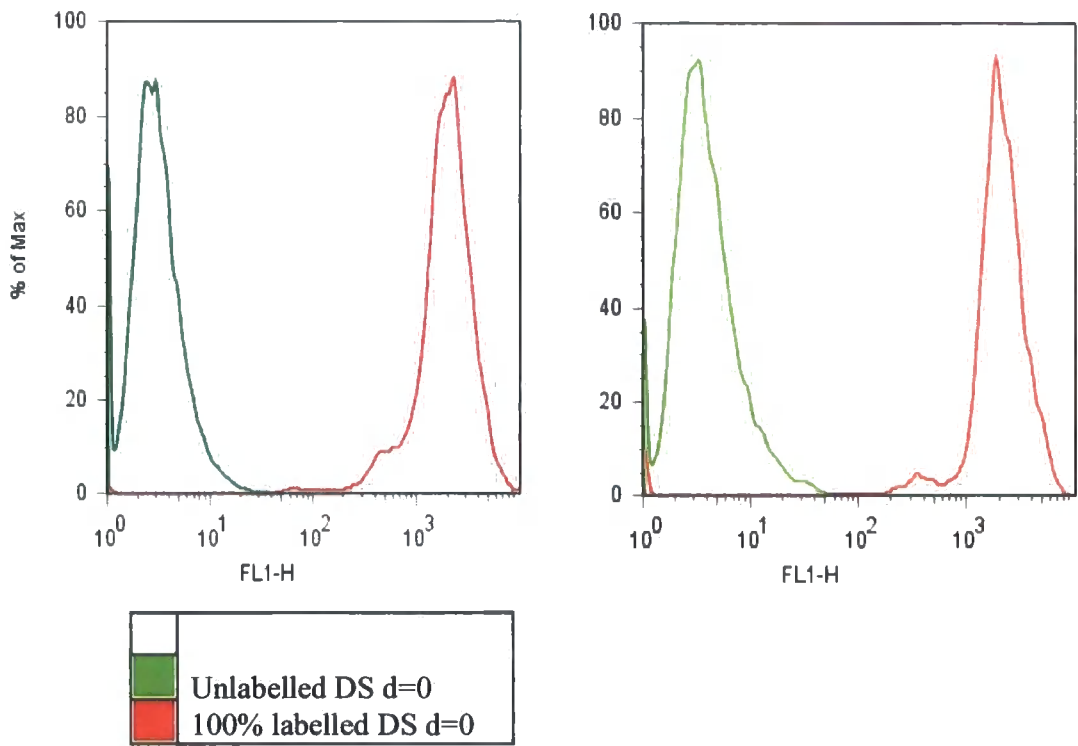


Illustration to show the mode of action of CFSE. Non-fluorescent CFSE enters the cells where it is cleaved and becomes fluorescent and cell impermeable which then prevents it from leaving the cell. On cell divisions, the CFSE fluorescence signal is diluted as the CFSE is passed to daughter cells.

Figure 3.5: Pulse chase CFSE labelling of DP and DS in culture: control CFSE labelling of DP and DS primary cells



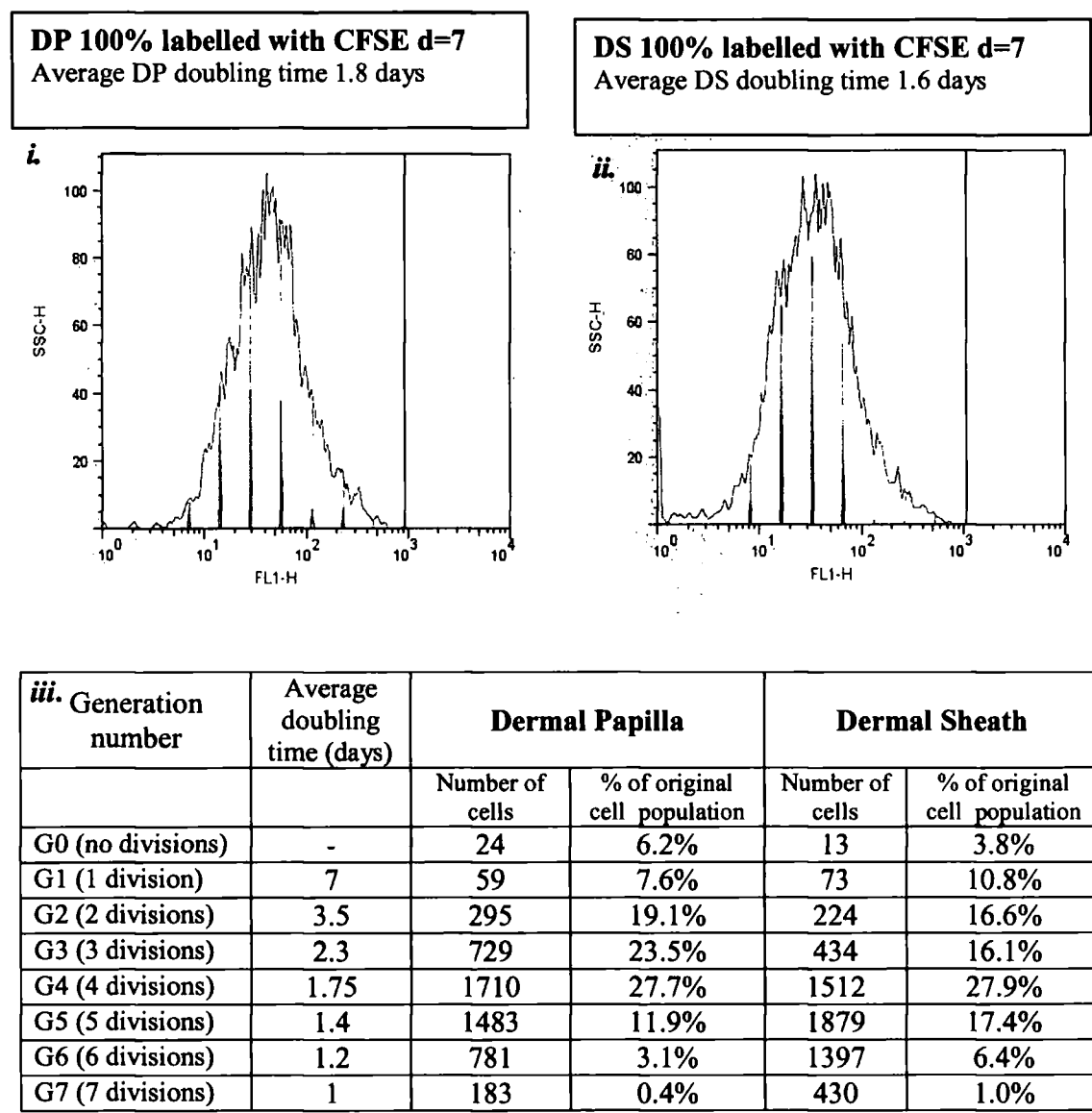
FACS analysis of control samples for CFSE proliferation assay. Unlabelled DP and DS primary cultures had a low level of autofluorescence. CFSE labelled cells had a peak fluorescence of 10^3 . When the DP and DS cells were labelled with CFSE their initial peak fluorescence was as above; reductions in fluorescence were correlated to generation number as shown in figure 3.6.

The majority of the DP and DS primary culture cells have an average doubling time between 1.4 days and 3.5 days; average of 1.8 days for DP and 1.6 days for DS as shown in figure 3.6. This is within the published range of 1.1 days to 3.8 days (Hoogduijn *et al.*, 2006; Bassukas *et al.*, 1993), although the average doubling time calculated by pulse chase is lower than the cell count-calculated doubling time. One explanation for this is that the cells show different population dynamics in bulk culture (figure 3.3) compared to low density analysis necessitated by the CFSE approach; however, the fact that population doubling times both fell within published range gave confidence that these cultures were suitable for study.

A spread of cell division history was observed, varying from cells that had not undergone division (DP 6.2%, DS 3.8%) to cells that had 7 divisions over 7 days with an average doubling time of 1 day (DP 0.4%, DS 1.0%). This distribution of cell division rates was consistent with other mesenchymal stem cell types, for example human bone marrow MSC have demonstrated a range of doubling times from 1.6-6.7 days with an mean of 4 days (Suva *et al.*, 2004).

Having established that the isolated DP and DS populations may contain populations of cells with stem cell properties, one approach to facilitate stem cell culture *in vitro* is to use low oxygen tension.

Figure 3.6: Pulse chase CFSE labelling of DP and DS in culture: CFSE proliferation assay of DP and DS primary culture cells



A proliferation assay using CFSE to examine the cell division profile of the DP (i.) and DS (ii.). The cells were CFSE labelled and cultured for 7 days then FACS analysed; this sensitive technique allowed each cell to be evaluated and assigned a generation number based on fluorescence. The percentage of cells dividing (iii.) and the original percentage of cells which gave rise to the final generation cell counts (iii.) were broadly similar. The graphs are generated by the flow cytometry FlowJo software (Tree star, Ashland, Oregon).

3.5 Investigation of hypoxic culture on population doubling time

The quantity of cells that can be harvested from tissues is limited; one constraint with using primary tissue is that cell numbers need to be increased prior to experimentation. However, extensive passaging, as well as storage, can cause cellular damage such as karyotypic changes, cell culture adaptation and inability for cell cycle exit (Mather and Roberts 1998). The number of primary DP and DS cells that can be isolated from the hair follicle is limited, therefore the ability to expand these cells *in vitro*, in the absence of accumulated damage, is necessary. It may be possible to alter the dermal follicular cell culture conditions to necessitate this. The *in vitro* growth of cells is subject to many culture-related factors one of which is oxygen tension. Standard culture oxygen levels (20-21%) have been described as being “hyper-physiologic” for many cell types (Moussavi-Harami *et al.*, 2004), including cells such as MSC which are adapted to relatively low oxygen levels *in vivo*; higher oxygen levels can cause sufficient oxidative stress to induce premature senescence. In order to investigate whether low oxygen tension had an effect on dermal follicular cells in culture, DS and DP populations were isolated from the hair follicle and cultured in normoxic (20-21% O₂) or hypoxic (5% O₂) conditions.

3.5.1 Outgrowth from primary explant: day 1-14

The DP and DS primary explants were placed into culture as described in the Method section 2.4.1.

The cells were observed to grow in a monolayer, in a roughly spherical area of outgrowth from the primary explant in DP (n=4) and DS (n=4) cultures in both normal (figure 3.7i.) and low (figure 3.7ii.) oxygen culture. The cell morphology between the two oxygen concentrations was similar. The area of confluency was observed to spread further from the primary explant material for low oxygen culture; the diameter of the outgrowth in hypoxic culture was significantly larger than that of the cells in normoxic culture ($p < 0.01$) (DP n=4 and DS n=4); this result was independent of primary material diameter. At day 14 (passage 1) the cells were seeded into fresh dishes and grown as monolayers.

3.5.2 DP and DS primary culture: day 14-30

From day 14 the DP and DS cells were allowed to proliferate to sub-confluency.

The DP and DS primary culture cells both appeared more densely packed in the low oxygen (figure 3.7iv.) compared to normal oxygen (figure 3.7iii.) (DP n=4 and DS n=4). The cell morphology was similar between the two oxygen conditions. The final cell count is higher in hypoxic culture compared to normoxic culture; the doubling time was significantly lower for the low oxygen compared to the normal oxygen ($p<0.01$) (figure 3.8) (DP n=4 and DS n=4).

This first monolayer culture was then passaged at day 30 (passage 2) and further cultured.

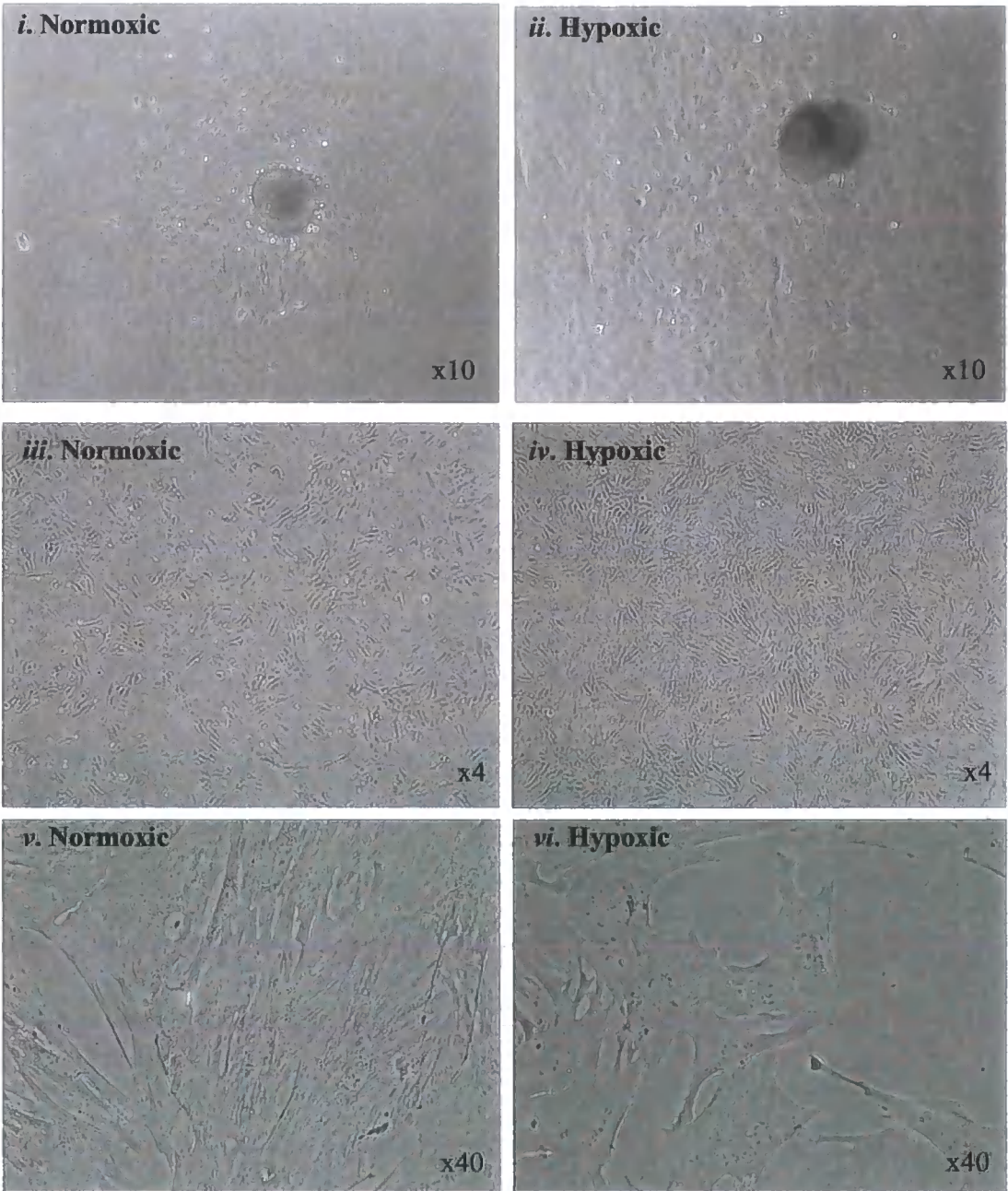
3.5.3 DP and DS primary culture: day 30-46

The cells were grown in dishes from day 30 to day 46, the time point at which they would normally be used for expanding at flasks.

The DP and DS primary culture cells both appeared more densely packed in the normal oxygen compared to low oxygen (DP n=4 and DS n=4). The cell morphology was similar between normal oxygen (figure 3.7v.) and low oxygen (figure 3.7vi.) culture conditions. The final cell count was higher in normoxic culture compared to the hypoxic culture; the doubling time was significantly lower in the normoxic culture ($p<0.01$) (figure 3.8) contrary to previous sampling times (figure 3.8i.-iv.). The doubling time for the normoxic DP and DS primary culture cells is consistent with published cell doubling times of 2.5 days for the dermal cells

For *in vitro* experiments, DP and DS primary cultures were routinely used at passage 3; culturing the cells under hypoxic conditions resulted in a significantly increased cell doubling time at this passage, however the numerical value lies within previously published ranges for dermal follicular cells. Cell morphology was identical between the different oxygen concentrations, and no overt differences in sub-populations were observed. However, at passage 3 the hypoxic culture doubling time was significantly longer indicative of cell death or cellular senescence. Given this, and that cell numbers were limiting for further experiments, the normoxic conditions were selected for further work as they delivered the significantly greater yield of cells at passages where hypoxia was having a detrimental effect upon the cell population.

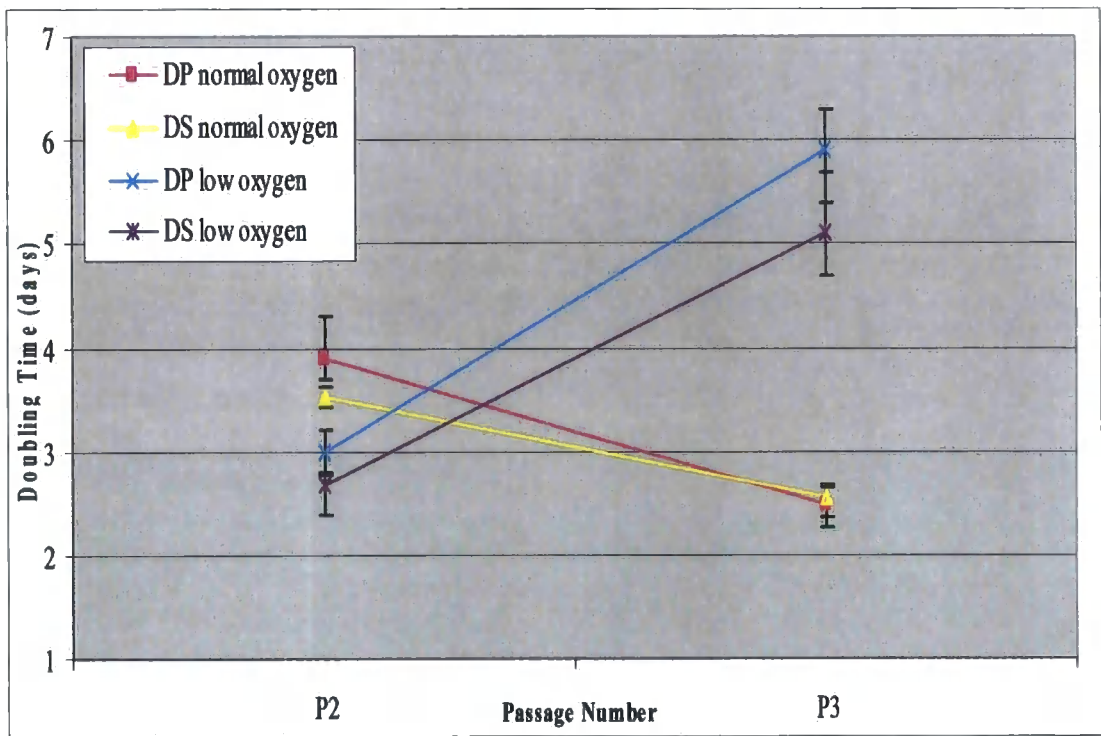
Figure 3.7: Morphology of DP and DS primary cells in normoxic and hypoxic *in vitro* culture



Primary explant cell outgrown, confluency and gross morphology of DP and DS primary cells in normoxic and hypoxic *in vitro* culture. The outgrowth of DP and DS cells from primary explants spread further for cells under hypoxic culture (ii); by passage 2 the DP and DS primary cells were more confluent under hypoxic culture (iv). Morphology of the DP and DS primary cells were broadly similar (v,vi) throughout; by passage 3 the cells were more confluent under normoxic culture (v). Cell images are representative of the DP and DS cultures analysed.

Figure 3.8: DP and DS primary culture population doubling time changes from passage 2 to passage 3 in normoxic and hypoxic *in vitro* culture

Sample	Passage 2	Passage 3
DP normal oxygen	3.9	2.5
DS normal oxygen	3.5	2.6
DP low oxygen	3.0	5.9
DS low oxygen	2.7	5.1



Population doubling times for DP and DS primary culture at passage 2 and passage 3 for normoxic and hypoxic culture with standard deviation error bars. At passage 3 the DP and DS primary cells in normoxic culture had a significantly lower doubling time compared to hypoxic culture ($p<0.01$). The change in doubling time for DP and DS primary cells, in both normoxic and hypoxic culture , from passage 2 to passage 3 was also significant ($p<0.01$). This indicates DP and DS cells under normoxic culture at passage 3 were most suitable for experimental purposes. Average doubling times shown for DP and DS passage 2 (day 30) and passage 3 (day 46) (n=8)

Should low oxygen culture have been conducive for a stem cell population, in the absence of significant cell death or senescence, there would be a decrease in average population doubling time as the stem cells proliferate and the overall cell number in culture increase. This in turn would make the final cell count, taken at passage, greater or the flasks would reach confluency earlier, either of which would result in a lower average population doubling time. The cell counts indicated a significant increase in population doubling time, as shown in figure 3.8; suggesting hypoxia had a detrimental effect upon the population. Should low oxygen have in fact been conducive for a small number of potential stem cells present, it was masked by the detrimental effect of hypoxia upon the population. Therefore, there was no evidence that hypoxic culture promoted stem cell proliferation within the DP and DS culture populations.

3.6 Spontaneous appearance in DP and DS culture cardiomyocyte-like cells

In analysing the potential for the dermal cells to differentiate to a cardiomyocyte-like population, the first step in their investigation was the spontaneous *in vitro* differentiation of the DP and DS primary cultures to this lineage. Cells in DP and DS primary cultures have been reported to spontaneously differentiate to cell lineages such as adipocytic and osteocytic (Jahoda *et al.*, 2003). Contractions consistent with cardiomyocytic differentiation were observed. However, this latter differentiation was less well defined. Gross morphology and contracting areas of dermal cells in primary culture have been reported (Jahoda *et al.*, 2003) as well as myotubules like cells (Rufaut *et al.*, 2006) but systemic analysis has not been published. Further, the expression of genes characteristic of cardiomyocyte commitment has not been studied with the exception of general myocyte markers: MyoD and myogenin (Rufaut *et al.*, 2006). This was therefore investigated further.

The DP and DS were cultured together producing a mixed DP and DS primary culture by removing the dermal follicular cells from the end bulb and, instead of separating the two populations, putting them into culture while they are still attached to one another. The cells grew out from the explant in a monolayer as seen in individual DP and DS primary culture making it impossible to determine which cells were DP or DS derived. However, with this

type of culture, on occasion, spontaneous appearance of cells with cardiomyocyte and myotube morphology have been observed as well as cells with synchronised contractions, a hallmark of cardiomyocytes, were also observed.

3.6.1 Spontaneous appearance of myocyte-like cells

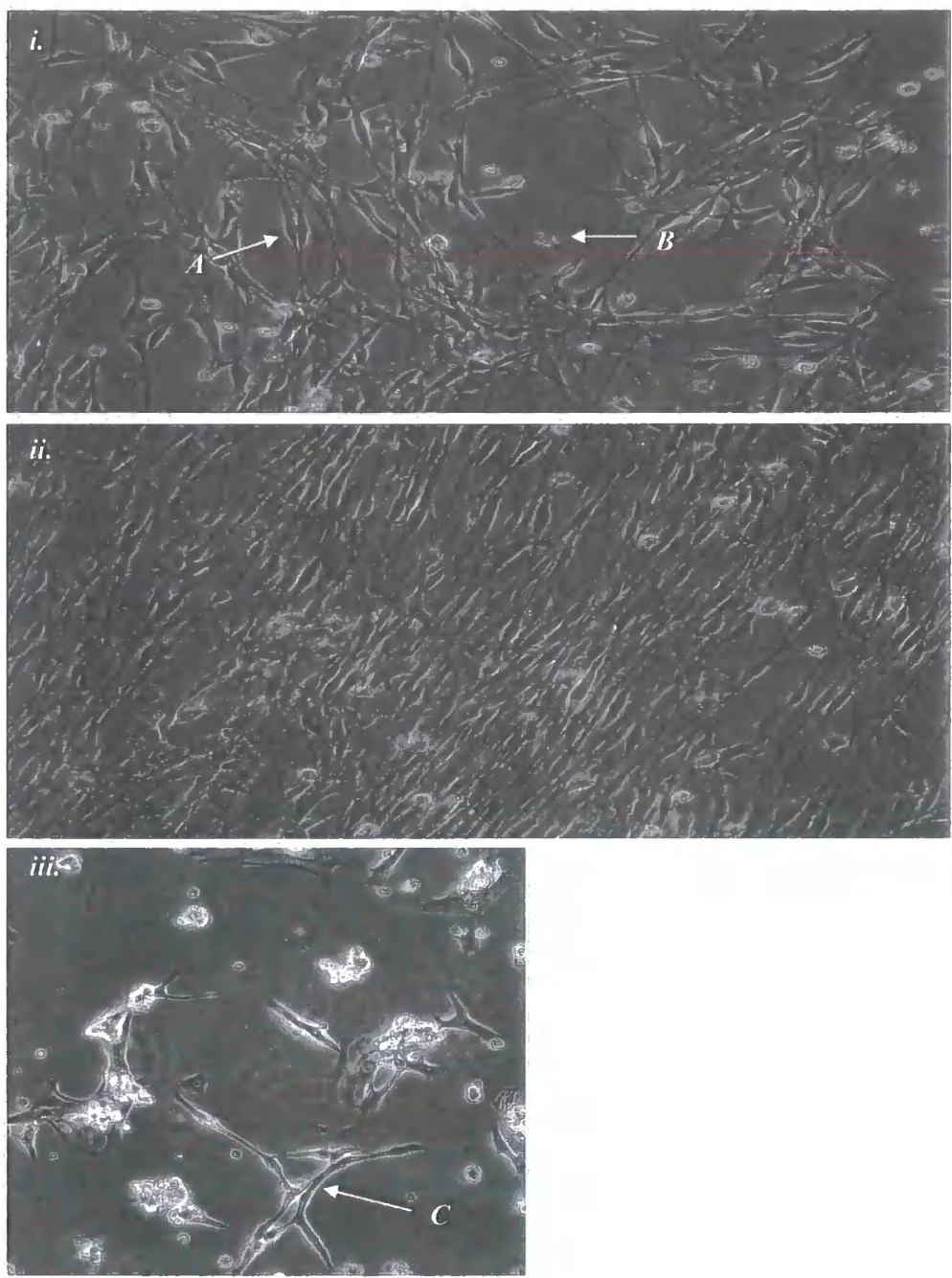
As a comparator for expected morphology of cardiomyocytes *in vitro*, cell cultures of embryonic cardiomyocytes were set up. As seen in figure 3.9iii, these have rod shaped morphology, a single nucleus and a small number of cytoplasmic processes overlapped with neighbouring cells, a result consistent with published studies (Maltzev *et al.*, 1993).

Cells with morphology similar to adipocytes spontaneously developed in several cultures under sub-confluent conditions, a result consistent with that reported by Jahoda *et al.* (2003). However, in at least 5 of the 40 cultures examined, cells indicative of individual myocytes were observed (figure 3.9). These latter cells did not spontaneously contract but had morphology similar to embryonic cardiomyocytes from an early *in vitro* culture time point as described above (figure 3.9iii). Over time (typically seven days) the numbers of these cardiomyocyte-like cells increased in some cultures, whereupon they developed into more organised structures (figure 3.9ii.) in a manner reminiscent of myotube formation.

3.6.2 Spontaneous appearance of myotube-like cells

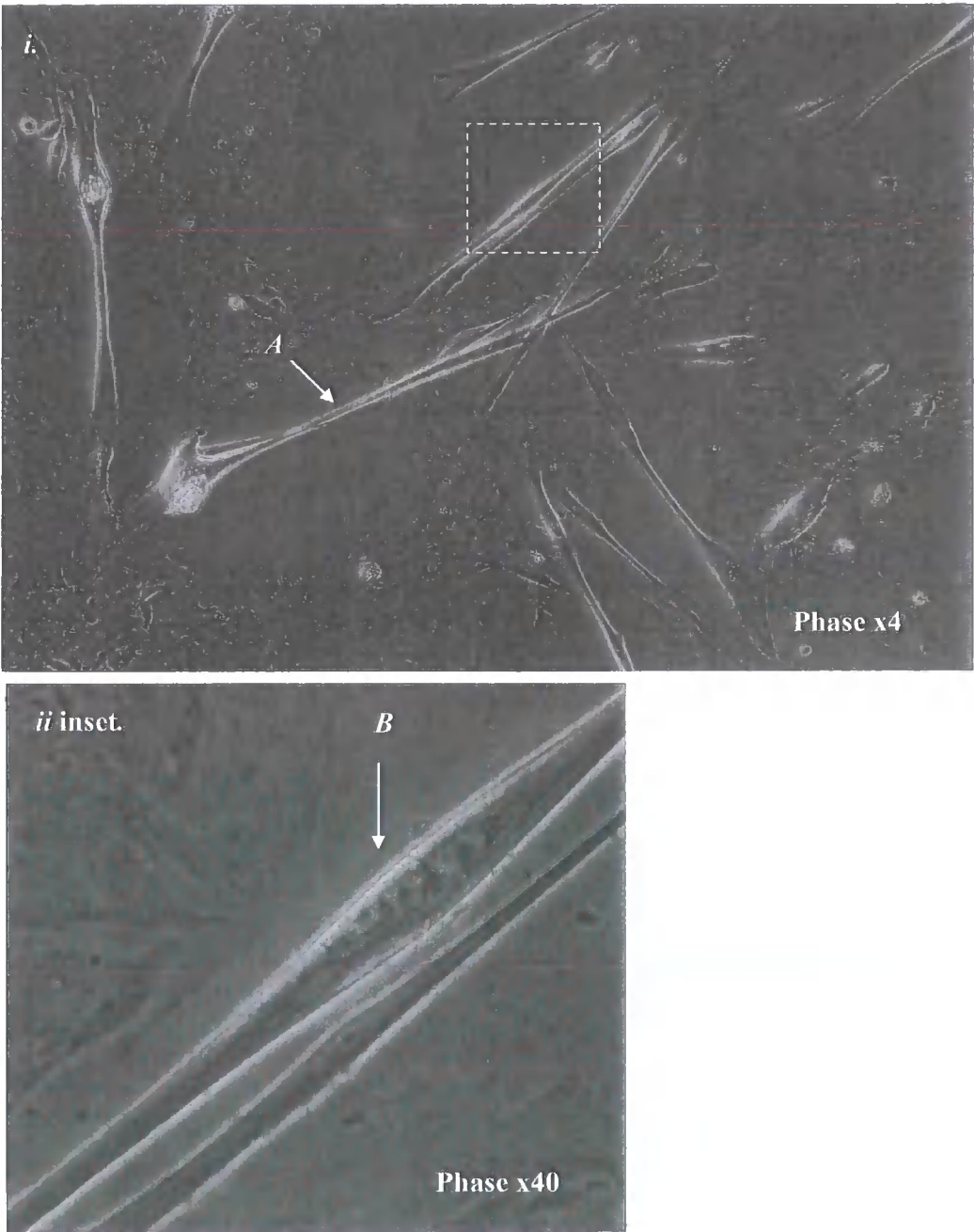
In at least two of the 40 cultures examined, larger cellular structures were observed in mixed DP and DS primary cultures that appeared morphologically similar to conventional myotubes formed *in vitro*. These are characterised by having a narrow spindle shape, a dense cytoplasm and with a conspicuous bulge in the portion of the cell occupied by the nucleus; individual myoblasts fusing to form larger, multinuclear cells (Capers 1960). As can be seen in figure 3.10, such structures appeared in some of the DP and DS mixed cultures, extending across many undifferentiated DP and DS cells. They were not observed to produce spontaneous contraction over the period of observation. These cells were typically observed after 14 days of culture.

Figure 3.9: Morphology of cells similar to cardiomyocytes spontaneously appearing in mixed DP and DS primary cultures *in vitro*



Morphology of cardiomyocyte-like cell in mixed DP and DS culture *in vitro*. In primary cultures of mixed DP and DS, cells similar to cardiomyocytes (A) and adipocytes (B) appeared disorganised (i.) or highly organised (ii.). The morphology of these cells appeared very similar to E12.5 embryonic cardiomyocytes (C) after 6 days in primary culture (iii.). Representative image shown; cardiomyocyte-like cells were observed after 7 days in mixed DP and DS primary culture. Images at x20 magnification.

Figure 3.10: Morphology of cells indicative of myotubules, spontaneously appearing in mixed DP and DS primary cultures *in vitro*



Morphology of myotubules-like cells in mixed DP and DS primary culture *in vitro*. There spontaneously appeared cells indicative of myotubules (A) These long tubular cells were multi-nucleated (B) with the nucleus to the centre of the cells; a quality consistent with myotubules. Representative image shown; myotubules-like cells were observed after 14 days mixed DP and DS primary culture.

3.6.3 Synchronised contractions

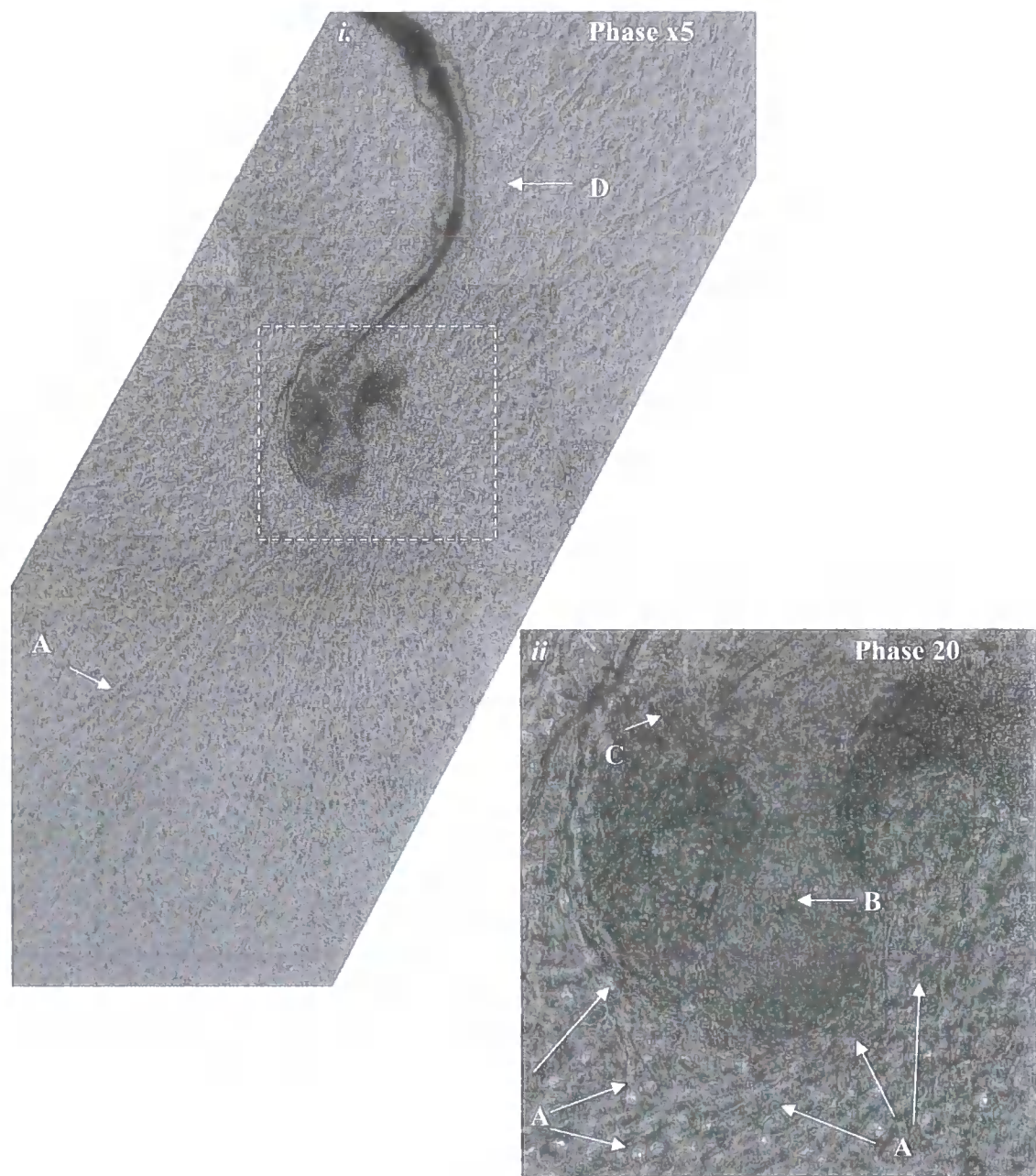
Large areas of contractile cells were also observed in more than 5 mixed DP and DS cultures (figure 3.11), although not in those areas of culture where the myotube-like cells described above were present. In these instances the contracting cells were co-located with non-contracting cells and appeared to orientate their axes parallel to one another but were otherwise indistinguishable from surrounding non-contracting cells. The contracting cells appeared to radiate from the primary explant across the entire culture dish and contraction was synchronised across all the cells.

The spontaneous appearance of contractions and myotube-like cells in the dermal cultures does not distinguish between a skeletal myocytes which spontaneously contract (Florini *et al.*, 1991) and cardiomyocyte lineages. Makino *et al.*, showed that bone marrow stromal cells, treated with 5-azacytidine, which formed myotube-like structures, began spontaneously beating after two weeks, and beat synchronously after three weeks. These cells, although appearing more like skeletal cells *in vitro*, displayed a cardiomyocyte-like ultrastructure by electron microscopy analysis including typical sarcomeres, a centrally positioned nucleus. In addition, the cells expressed the contractile protein genes, myosin heavy chain, myosin light chain, and α -actin, in a phenotype indicated that similar to that of foetal ventricular cardiomyocytes (Makino *et al.*, 1999).

Skeletal myoblasts do not normally synchronise their contractions in culture (Itabashi *et al.*, 2005); the appearance of cells with synchronised contractions in the dermal cultures indicates that cells capable of cardiomyocyte differentiation were present within these cultures.

The genes controlling conventional cardiomyocytic differentiation have been described, as discussed in Chapter 1. In order to examine whether cells with this profile were present within the primary cultures, DP and DS cultures were subjected to RT-PCR analysis.

Figure 3.11: Morphology of spontaneous appearance of contractile cells in mixed DP and DS primary culture *in vitro*



Large areas of spontaneous contractile cells (A) in mixed DP and DS primary culture. The areas of contracting cells were arranged in a linear manner radiating from the primary explant material; the DP (B) and DS (C); in this instance there was induction of hair shaft growth (D). Representative image shown; contracting cells were observed after 14 days mixed DP and DS primary culture.

* This is a composite image consisting of 6 separate photographs (i.)

3.7 Directed cardiomyocytic differentiation potential of DP and DS cultures by gene expression analysis

The gene expression of the transcription factors associated with early cardiomyocyte induction and commitment; Nkx2.5, GATA4, Mef2c and tbx5, a number of genes associated with the functional cardiomyocyte; cardiac specific sarcomere structural genes: alpha myosin heavy chain (α -MHC), myosin light chains specific to the atria (MLC1A) and ventricle (MLC1V), tropomyosin and cardiac actin as well as genes associated with contracting cardiomyocytes: troponin I and titin were investigated as an indicator of cardiomyocyte differentiation potential. These genes are discussed in Chapter 1. In addition, sca-1, which is implicated in the identification of native cardiac stem cells (Tateishi *et al.*, 2007) and Tert, associated with stem cells and important in increased proliferative capacity (Serakinci *et al.*, 2008) were also investigated. Tropoelastin, an extracellular matrix protein associated with vessels (McKee *et al.*, 2003) was also investigated.

The expression of these three groups of genes were investigated in the *in vitro* DP and DS primary culture cells at passage 1 and passage 3. The end bulb represents the intact DP and DS structures before isolation and culture. These primary cultures could contain a small number of contaminating cell types. In order to further characterise the gene expression profiles of DP and DS cells, independent clonal cell lines isolated from individual dermal follicular cells were also analysed.

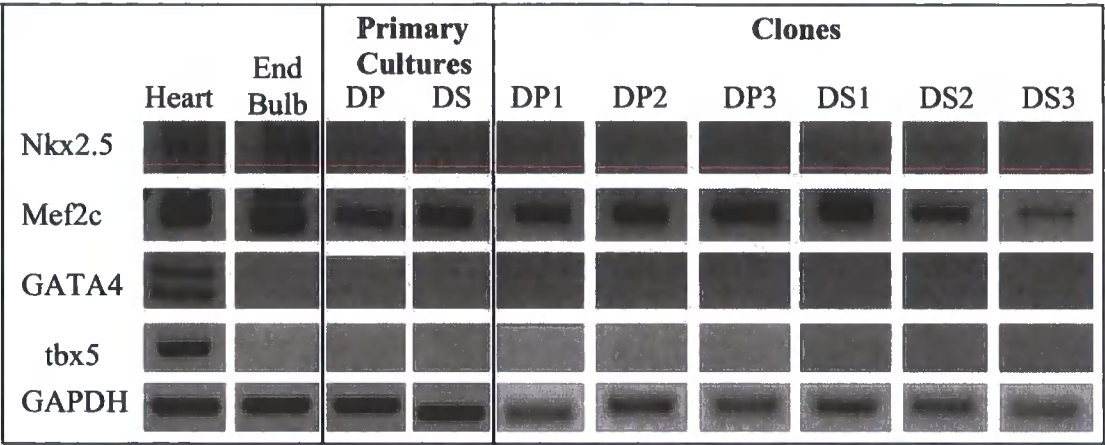
The adult heart produced a positive signal for all of the PCR targets, confirming their suitability. Interestingly, the adult heart consistently produced PCR products specific for mTert and sca-1, genes characteristic of stem cells.

Of the cardiac transcription factors investigated, the DP and DS primary culture samples expressed only Mef2c (figure 3.12). Of the functional genes, tropomyosin and troponin I were detected, albeit at very low levels in the latter case (figure 3.13). Tropoelastin was detected as well as Tert at very low levels, but transcripts for sca-1 were not present at levels sufficient to produce a PCR product (figure 3.14). That such detectable gene expression was a product of the dermal cells and not any contaminating cell type is supported by the expression of these genes in a number of the clonal cell lines.

The end bulb sample expressed a number of cardiomyocyte transcription factors (Nkx2.5 and Mef2c), functional genes (cardiac actin, tropomyosin, titin, MLC1A and possibly MLC1V) and low level expression of tropoelastin and Tert. By definition of isolation, the end bulb may contain contaminating cells that could attribute the gene expression observed here however the level of expression is in some instances relatively high and may represent the gene expression of the DP and DS *in vivo* or when the DP and DS are combined, however the end bulb sample does express a number of genes not detected in the DP and DS primary cultures or in the clones namely Nkx2.5, cardiac actin and titin. In addition, elastin is expected to be abundant in the skin and has previously been identified in the DP, its stalk and the peribulbar mesenchyme (Young *et al.*, 1980).

The clonal cell lines were also investigated; these cell lines were established from single DP and DS primary culture cells. These cell lines have previously been investigated for their differentiation potential to adipocytic and osteocytic lineages (Jahoda *et al.*, 2003) where their doubling times were monitored and were within published ranges, indicating the cells had not undergone transforming events. The expression of troponin I and tropoelastin varied between clonal cell lines, suggesting that this may not be a property common to all follicular dermal cells. In addition, all clonal cell lines examined expressed α -MHC, MLC1A and Tert, despite an absence of strongly detectable expression in the primary cultures. This may indicate the clones are representative of a small population of cells within the DP and DS primary culture which are then undetectable when in primary culture.

Figure 3.12: Cardiac transcription factor-associated gene expression profile of DP and DS primary cultures and clones



RT-PCR analysis of genes associated with early induction and commitment of cardiomyocytes. The dermal follicular cells did not consistently express genes associated with cardiomyocyte induction. RT-PCR analysis indicated the expression of Mef2c in the DP and DS primary cultures, confirmed by clonal cell lines, with expression of Nkx2.5 detected in the end bulb alone. Representative samples are shown; the results were confirmed by three independent DP and DS primary cultures at passage 1 and 3 and three independent clonal cell lines.

Figure 3.13: Cardiac function-associated gene expression profile of DP and DS primary cultures and clones

			Primary Cultures		Clones					
	Heart	End Bulb	DP	DS	DP1	DP2	DP3	DS1	DS2	DS3
α -MHC										
Cardiac actin										
Tropomyosin										
Troponin I										
Titin										
MLC1A										
MLC1V										
GAPDH										

RT-PCR of genes associated with cardiomyocyte function. The dermal follicular cells did not express the entire profile of genes associated with cardiomyocyte function. The DP and DS primary cultures expressed tropomyosin and troponin I, at low levels, which were confirmed by clonal cell lines. At this level of analysis the end bulb expressed all the cardiac genes investigated with the exception of α -MHC and troponin I. In addition, a number of the clones expressed α -MHC, atrial MLC (MLC1A) and titin at varying levels. Representative samples are shown; the results were confirmed by three independent DP and DS primary cultures at passage 1 and 3 and three independent clonal cell lines.

Figure 3.14: Gene expression profile of DP and DS primary cultures and clones for genes associated with stem cells; sca-1 and Tert and vessel-associated gene tropoelastin

			Cultured		Clones					
	Heart	End Bulb	DP	DS	DP1	DP2	DP3	DS1	DS2	DS3
Sca-1										
Tropoelastin										
Tert										
GAPDH										

RT-PCR of stem cells associated genes and tropoelastin. The DP and DS primary cultures expressed tropoelastin and Tert at low levels alone which was confirmed by expression in a number of the clonal cell lines. Tert was expressed in all of the clones and sca-1 was undetectable. The end bulb expressed tropoelastin and Tert at very low levels. Representative samples are shown; the results were confirmed by three independent DP and DS primary cultures at passage 1 and 3 and three independent clonal cell lines.

3.8 Chapter 3 Discussion

The DP and DS primary culture cells were investigated to determine if they had reproducible culture characteristics as determined by monitoring morphology, population doubling times and gene expression. The DP and DS cell populations were easily isolated and readily available from the vibrissae. The cells isolated had morphology consistent with previously described DP and DS culture populations; population doubling times were within range of published results and indicated the cells proliferation rate was clinically relevant; DP and DS isolates were reproducibly produced. The population dynamics and gene expression profile did not substantially change over the period of *in vitro* culture. These data indicate that the DP and DS cultures were suitable for further study. Furthermore, these features were evaluated to determine if the cells were suitable as a model system investigating for somatic cell differentiation specifically of commitment towards a cardiomyocyte lineage.

Given the similarity of the behaviour of the two cell populations *in vitro*, the question arises as to which to study further. Evidence suggests that the DP and DS have different roles in the hair follicle and surrounding dermis. The DP has hair and dermal follicular inductive properties (Jahoda *et al.*, 2001) and these cells have also demonstrated the ability to form new hair follicles even in undifferentiated epidermal tissue (Reynolds and Jahoda 1991) and is a necessary component for follicle formation in wounded skin (Ghazi *et al.*, 2003). The DS has been suggested to play a role in wound healing in the dermis where it has demonstrated fibroblastic properties (Jahoda and Reynolds 2001). The DS is also capable of inducing new follicles as well as skin substitutes with outer root sheath (Ghazi *et al.*, 2003). The overlapping but distinctive *in vivo* capabilities of the DP and DS may have an effect upon their potential to differentiate to cells of a cardiomyocyte lineage *in vitro*. The DP has demonstrated properties that are more involved in normal skin homeostasis e.g. induction, whereas the DS appears to be more significant in a wound healing environment in an adaptive response. The infarcted heart is considered to be a hostile, hypoxic, *in vivo* wound healing environment therefore the DS, as demonstrated by its role in the skin, may be more adaptive in this environment. However, the method of *in vitro* differentiation of cells may be more suited to the properties of the DP where the cells

are being induced to differentiate to a new cells type. In addition to this, the DP and DS have different alkaline phosphatase activities *in vivo*; the DP having high alkaline phosphatase activity with the lower DS, as used here, having low alkaline phosphatase activity; expression of which is associated with stem cells and may suggest the DP is more stem-cell like where the DS is more proliferative, this may play an important role in induction and differentiation potential, respectively (McElwee *et al.*, 2003). The proposed differences between the two cell types suggest investigating the DP and DS as separate cell populations.

Cells of the DP and DS can show properties of mesenchymal stem cell types, but have some discrepancies with other MSC. Those MSC originating from bone marrow, umbilical cord blood and adipose tissue do show comparable morphology in culture; the cells are adherent, mononuclear and grow to a monolayer although they do have more elongated spindle-shaped cell morphology than the DP and DS primary cells in culture (Kern *et al.*, 2006). During *in vitro* culture, MSC have an average doubling time of 3 days (Bertani *et al.*, 2005) which is comparable to the DP and DS primary culture cells (2.5-2.8 days). MSC possess a limited life span and finally undergo replicative senescence, as indicated by loss of proliferation and altered morphology. For bone marrow MSC, this is at passage 7, for adipose tissue MSC at passage 8 and umbilical cord blood MSC at passage 9 (Kern *et al.*, 2006). Other reports suggest that replicative arrest for these stem cell types can occur slightly later, between passage 10 and 12 (Bertani *et al.*, 2005). Interestingly, both DP and DS demonstrated changes in morphology and incidence of cell death at passage 8. These data suggest that both these cell types may show a similar limit to cell expansion *in vitro*. This similarly extended to the rate of cell division. The population doubling times were first investigated by whole population cell counts. These data demonstrated a predicted population doubling time that was within range of previously published reports. However, whole-population studies cannot discriminate between a fast-dividing sub-population and a slow-dividing bulk population; the net effect is the same.

A CFSE-based proliferation assay allowed the generation status of each cell to be determined where the grouping of cells based on doubling times can be appreciated; CFSE has been shown to be a reliable method for studying the proliferative activity of MSC sub-populations (Urbani *et al.*, 2006) however a CFSE profile of the dermal follicular cells has

not been published. Pulse chase analysis resulted in a lower average doubling time for the DP (1.8 days) and DS (1.6 days) primary cells in culture than had been calculated by cell counts (2.5-2.8 days); interestingly a doubling time closer to that of the dermal clones, as described in figure 3.2 (Jahoda *et al.*, 2003). Consistent with the DP and DS clones in comparison to the primary populations; MSC clonal cell lines have demonstrated an average doubling time of 1.5 days (Suva *et al.*, 2004) as indicated by CFSE labelling. Adherent cells from bone marrow have demonstrated a doubling population time of 1.6-6.7 days with a mean of 4 days (Suva *et al.*, 2004), however when the MSC are specifically isolated by FACS and analysed by CFSE 65% of the population were mature MSC and 35% were a re-cycling population of MSC; these re-cycling cells had a higher proliferative potential as suggested by CFSE proliferation analysis (Urbani *et al.*, 2006). This complex CFSE profile is comparable with the DP and DS profiles. When the MSC profile was split into two separate profiles representing the recycling and more mature MSC as identified by FACS, it was demonstrated that the majority of the mature MSC (99.6%) and recycling MSC (70%) had a population doubling time of 1.5 days however 30% of the recycling cells had a population doubling time of 0.6-1 days (Urbani *et al.*, 2006). Therefore MSC doubling times based on bulk cell counts do suggest a higher proliferation than that calculated with CFSE labelling as was demonstrated with the DP and DS cells however CFSE-calculated doubling times do not indicate this is due to a small, transformed population of cells which suggests experiments with different primary isolated would have little variation.

This adds further evidence to the theory of the DP and DS cultures being a mixed population of cells. It poses the question: in order to use a population of DP and DS primary cells for differentiation investigation, indeed any type of primary cell, will a sub-population of cells with stem cell capabilities need to be identified and isolated within the culture system first? One possible approach to investigate a potential sub-population is to first identify it by way of stem cell markers. This was investigated with the expression of Tert which may allow identification of a cell population with a higher proliferative capacity as described in Chapter 5. In the first instance the bulk population was investigated.

Several studies have suggested that low oxygen tension can be conducive for proliferation of a number of cell populations. For example, osteoblasts show increased cellular

proliferation rate with decreased differentiation under hypoxic *in vitro* culture (Tuncay *et al.*, 1994). In a similar manner, Warren showed hypoxia affected rat primary osteoblast controlled osseous healing by increasing expression of cytokines and bone-specific extracellular matrix molecules and their regulators (Warren *et al.*, 2001). However, bone marrow MSC showed induction of differentiation under hypoxic conditions, resulting in accelerated differentiation, proliferation and morphological changes (Ren *et al.*, 2006), a result consistent with that of published work on osteoblastic established cell lines cultured under low oxygen; hypoxia appears regulate gene expression, cellular proliferation and cellular differentiation (Steinbrech *et al.*, 1999, Park *et al.*, 2002).

DP and DS appeared not to show these properties. DP and DS cells demonstrated unchanged morphology in culture suggesting an absence of gross differentiation. In addition, by passage 3 there was increased population doubling time inconsistent with accelerated proliferation. The culture stage of the cells in question, as well as the length of hypoxic exposure, may play an important role in the effect of the hypoxia; Potier showed that human MSC exposed to prolonged hypoxia resulted in cell death however temporary hypoxia had no detectable effect on MSC survival (Potier *et al.*, 2007). The pulse chase experiments suggested the DP and DS primary culture cells to be a mixed population of cells, of which one group may be stem cell-like in their properties and differentiation ability. One suggestion was that culturing the cells under hypoxic conditions could have been conducive for differentiation as well as proliferation of a stem cell population as indicated by the MSC work described. However, the morphology of the DP and DS primary cells remained unchanged; suggesting an absence of gross differentiation, and population doubling time was significantly increased. Cell counts from the hypoxic cultures were significantly higher within the first two passages as compared to normoxic culture conditions; this initial burst of cellular activity could be the result of hypoxia-induced increased motility. MSC have demonstrated increased migration in tumour angiogenesis environment as induced by hypoxia (Annabi *et al.*, 2003). One explanation is that the cells are responding to the hypoxia in a similar manner to a wound healing environment as has been shown with dermal fibroblasts. Li showed that hypoxia promoted dermal fibroblast motility by inducing their secretion of heat shock protein 90alpha (HSP-90α) via hypoxia-inducible factor 1alpha (HIF-1α); this secreted HSP-90α in turn executes

the pro-motility signal of hypoxia (Li *et al.*, 2007B). The dermal follicular cells may act in a similar manner as they have been attributed wound healing capabilities (Jahoda and Reynolds 2001). However, the extended period of hypoxic culture resulted in a reduced cellular doubling time as would be seen with the outcome of hypoxic cell death (Zhu *et al.*, 2006). Low oxygen, for these reasons was deemed an unsuitable for further investigation, including for promoting differentiation.

Cells similar in morphology and behaviour to myocytes, myotubes and cardiomyocytes developed spontaneously in a small number of mixed DP and DP primary cultures. Due to the nature of the isolation of the primary material for these cultures there is a greater possibility of contaminating cell types. The DP and DS were isolated from the hair follicle with precision to ensure surrounding cells were not transferred into culture, however in any *in vitro* system where more than one cell is studied; there remains a small, but finite, risk of contamination with other cell types. This is a problem for studies of stem cell fate of a specific cell type. With this type of culture there is also the risk of blood being transferred into culture with the isolated DP and DS; components of the blood, such as HSC, have been reported to contribute to cardiomyocyte lineage *in vivo* (Orlic *et al.*, 2001). The frequency of these events is very low (possibly zero), and indeed the physiology of such cardiomyocyte commitment from HSC that may occur remains unclear. However, the possibility formally remains. Other circulating stem cell types have been suggested to commit to cardiomyocytes such as MSC (Toma *et al.*, 2002), endothelial progenitor cells (Anversa *et al.*, 2006B) and potentially, circulating adult cardiac stem cell types as may exist (Weissman *et al.*, 2001).

Myocyte differentiation has been previously suggested by the spontaneous appearance of contracting cells in dermal cultures (Jahoda *et al.*, 2003) however this was not investigated further. Contracting cells, as well as cells of myocyte morphology, spontaneously appearing in culture has not been identified in MSC cultures to date except in response to 5-azacytidine, which is a potent de-methylation agent (for example Hattar *et al.*, 2005). Specific culture media supplemented with growth factors has been demonstrated to induce myocytic differentiation of ear MSC (Gawronska-Kozak *et al.*, 2007) with the appearance of spontaneous contractions however contractions were not synchronised and gene expression analysis was limited to general myocyte genes. Therefore Gawronska-Kozak *et*

al., could only conclude that the cells identified did not display a definitive cardiomyocyte or skeletal myocyte phenotype but a heterogeneous mixture of cells with a partially differentiated myogenic phenotype.

Mixed cultures of DP and DS did show spontaneous appearance of cells with myotube-like morphology similar to cells differentiated from bone marrow stromal cells (Makino *et al.*, 1999), suggesting cardiomyocyte commitment. This morphology is not unique to cardiomyocytes, as skeletal muscle cells can show similar forms (Capers 1960). However, the spontaneous, synchronised contraction of the myotubes in the dermal cultures indicates the presence of differentiated cardiomyocytes. One approach is to study primary cells on a single cell basis (Short *et al.*, 2003). However, given the slow population doubling time of primary DP and DS, and the potential limit before replicative senescence (see above), this approach would prove very challenging for *in vitro* differentiation studies. However, using dermal clones would be a potential route of investigation. These cell lines are derived from single DP or DS cells therefore they would overcome the possibility of contaminating cell types and any differentiation would be attributed to the dermal follicular cells.

RT-PCR analysis demonstrated that the clones investigated had a gene profile consistent with that of follicular dermal cells (section 3.7). Gene expression analysis showed expression of *Mef2c*; a gene associated with cardiomyocyte commitment. This could suggest that these cell types have propensity for cardiac commitment, in a fashion similar to, for example, undifferentiated ES cells which express genes associated with mesodermal lineages and spontaneously differentiate towards mesoderm lineage (Heo *et al.*, 2005). However, this may not be the case. Of the transcription factors, only *Mef2c* had detectable expression in the primary culture DP and DS and clonal cell line. *Mef2c* is normally expressed in developing striated muscle playing an important role in efficient differentiation of heart precursor cardiomyoblasts into cardiomyocytes (Karamboulas *et al.*, 2006) by being upstream of a subset of cardiac genes essential for contraction. *Mef2c* is regulated by *Nkx2.5* and *GATA4* however the dermal cells did not express these transcription factors at baseline. *Mef2c*, *Nkx2.5* and *GATA4* are upstream of tropomyosin (Reddy *et al.*, 2000) and elastin; which both the DP and DS express, as well as α -MHC (Molkentin *et al.*, 1993) and troponin I (Di Lisi *et al.*, 1998). *Mef2c*, associated with muscle regulation and cardiovascular development, has also been reported to control bone



development by activating chondrocyte hypertrophy and was detected in developing chondrocytes (Arnold *et al.*, 2007), and the expression of this gene may be associated with osteogenic potential in dermal cells. Previous work has confirmed that at least some cells in the follicular dermis can demonstrate bone formation *in vitro* (Jahoda *et al.*, 2003).

Genes characteristic of functional cardiomyocytes appeared to be expressed by primary cell types; these included tropomyosin in the DP and DS, and cardiac actin in end bulb. In respect of the latter, recent work suggests that the primer pairs used may cross-react with specific actin isoforms found in fibroblasts (Yasuda *et al.*, 2006), suggesting that inclusion of these cell types in the whole end bulb may be responsible for the production of the PCR product. The absence of detectable expression in follicular dermal cells explanted from the end bulb supports this. In respect of tropomyosin, in a similar manner to Mef2c, the products of this are expressed in osteoclasts and up-regulated during osteoclastogenesis where it has been suggested to play a role in determining the dynamic properties of the actin cytoskeleton and thus osteoclast activity (McMichael *et al.*, 2006). Therefore this expression may be associated with the osteogenic potential of the dermal cells (Jahoda *et al.*, 2003).

A number of the genes investigated were expressed in the dermal clones but not in the end bulb or DP and DS primary cultures; these were α -MHC, troponin I and MLC1A. The clones are considered to be representative of the primary cells as has previously been suggested with bovine DP clonal cell lines (Rufaut *et al.*, 2006). This pattern of expression may indicate that these genes are expressed in a limited number of the cells present in the DP and DS, the expression of which may be diluted in the entire end bulb sample and in the primary cultures; it may be that these genes were expressed in the cells used for clonal cell line establishment and therefore they are expressed in the clones but not primary material. The primary cells may be more representative of the tissue or origin, as non-representative sub-populations may be selected during the cloning process. If this were the case, this would explain the α -MHC, troponin I and MLC1A expression detected in the clonal cell lines but not in the primary cell lines.

Tert, which adds telomeric repeats to the ends of chromosomes, is associated with the maintenance of stem cell populations and extended culture *in vitro* (reviewed by Hiyama

and Hiyama 2007). Tert expression in the clonal cell lines may be associated with the proliferate potential of these cells. The clonal cell lines have high proliferative potential; they have been shown to be maintained for up to 26 passages, (Jahoda *et al.*, 2003). Expression of Tert is unsurprising as it correlates with the lack of cellular senescence. Interestingly there was low level in the end bulb suggesting that at least some cells within these cultures may have equally high proliferative potential. This possibility is investigated later, in Chapter 5, where the Tert expression is examined in the DP and DS with the used of the mTert-GFP mouse model. Sca-1, a potential marker of cardiac stem cells and was detected in the end bulb, but not in DP or DS or any of the clones. However sca-1 is not exclusively expressed by potential cardiac stem cells, but by other cells types as has been demonstrated with the bone marrow, endothelial progenitor cells and HSC.

The appearance of three distinct cell types in culture: myocytes, myotubules and cells with synchronised cardiomyocyte-like contractions, are indicative of there being cells present within the DP and DS primary cultures which are capable of differentiation towards a myocyte lineage and under specific conditions, cardiomyocytic lineage. On no occasion did these three cell types appear when DP and DS were cultured alone nor in the same culture dishes to one another. This was observed by Jahoda *et al.*, (2003) when investigating the adipocytic and osteogenic differentiation potential of the DP and DS primary cultures. It appears the microenvironment determines the differentiation response of the dermal follicular cells into adipocytes and osteocytes, as suggested by activation or inhibition of the MAP kinase ERK (Jaiswal *et al.*, 2000), regardless of their multipotency (Jahoda *et al.*, 2003). This would indicate that in order to direct the differentiation of the DP and DS primary cells towards a cardiomyocytic lineage, an inductive microenvironment is necessary as has been suggested with their differentiation towards adipocytic and osteocytic lineage. The gene expression profile of the dermal follicular cells suggests an inductive environment that would switch on the expression of early cardiomyocyte-associated genes. Although isolated populations contain cells with the potential to produce cardiomyocytes, they only express that potential spontaneously in mixed cultures and the end bulb is not a suitable model for study. The consistent isolation of the end bulb would be complicated; variation in follicle sizes would make the end bulb section more difficult to reproducibly identify. It would be expected that there would be variations from one

primary culture to the next for example in the morphology of the mixed population of cells, the proliferative rates of sub-populations, spontaneous contraction rates and spontaneous differentiation rates *in vitro* as well as the possibility of contaminating cell types. In addition to this, there is no evidence of spontaneous differentiation *in vivo* in the end bulb. In order to examine whether DP and DS have the potential for cardiomyocytic differentiation and expression of cardiomyocyte-associated genes, an inductive approach is necessary. Co-culture provides an inductive micro-environment; intimate cell contact allows gap junction communication which may lead to efficient transduction of autocrine and paracrine factors secreted by an inductive cell type which would induce cardiomyocytic differentiation (reviewed in Christoforou and Gearhart *et al.*, 2007). This type of method has been shown to be successful in differentiation of MSC to cardiomyocytes (for example Li *et al.*, 2007) as well as differentiation of bovine DP cells to myotubules-like structures (Rufaut *et al.*, 2006). Differentiation of cells to cardiomyocytes has been shown to be dependent on communication with an inductive cell (Xu *et al.*, 2004), co-culture is therefore the most suitable next step in the investigation of the DP and DS and their potential towards cells of cardiomyocyte lineage.

4 *In vitro* cardiomyogenic differentiation potential of the dermal follicular cells

Work described in Chapter 3 indicated that cells of the follicular dermis expressed genes characteristic of functioning cardiomyocytes, and could spontaneously demonstrate differentiation consistent with the formation of these cell types. However, the level of gene expression and spontaneous differentiation was comparatively modest. In order to examine whether this potential could be enhanced, an inductive approach was adopted. There is evidence from other mesenchymal cell types that such an approach can help demonstrate cardiomyocytic potential *in vitro*.

The bone marrow (BM) contains several populations of stem cells including HSC, which are responsible for forming blood, as well as MSC or stromal cells. These cells are capable of differentiating to osteocytes, chondrocytes, adipocytes and skeletal myoblasts; there is also a large body of evidence that they can commit to a cardiomyocyte lineage. For example, Wang showed that rat MSC in cell contact with rat adult cardiomyocytes differentiated to cells of cardiomyocyte phenotype as indicated by expression of α -actin, desmin and troponin T (Wang *et al.*, 2006). Human MSC are also capable of differentiating *in vivo* in murine heart where they have demonstrated a similar gene expression profile of α -actinin, desmin, cardiac troponin T and β -MHC (Toma *et al.*, 2002). This differentiation has also been shown to have function attributes, Beeres showed human MSC restored experimental conduction blocks in rat cardiomyocytes (Beeres *et al.*, 2005).

In attempting to differentiate the dermal follicular cells a similar method of induction was implemented as described for MSC. At least two sources of inductive cell could be used. Embryonic cardiomyocytes, as has been successfully used with MSC (Yoon *et al.*, 2005), and ES cells.

4.1 Inducing the dermal follicular cells to differentiate to cardiomyocytes by hanging drop co-culture with ES cells

When cultured in suspension, under conditions favourable for differentiation, ES cells spontaneously form cells aggregates termed embryoid bodies (EB) which is required for *in vitro* differentiation of the cells towards cardiomyocytes (Wei *et al.*, 2005). During this differentiation, cells similar to those of the three primary germ lines are identified namely

the endoderm, ectoderm and mesoderm; the cardiomyocytes that form in the EB are located between the outer epithelial layer and the basal mesenchymal cells (Boheler *et al.*, 2002). The cells of the EB expressed a number of cardiogenic lineage markers (Boheler *et al.*, 2002) and have been seen to contract with a similar action potential to that of the early chamber myocardium (Fijnvandraat *et al.*, 2003).

The EB inductive microenvironment is therefore crucial to the commitment of the ES cells to cardiomyocytes. The ability of EB formation, from ES cells, to facilitate the cardiomyocyte differentiation of the dermal follicular cells was examined. In order to confirm reproducible cardiomyocyte differentiation of ES cells, the method of Fijnvandraat was followed (Fijnvandraat *et al.*, 2003). In brief, the mouse ES cell line CGR8 was used; hanging drop culture was set up with 30cells/ μ l in 10ul drops as described in the methods section 2.4.4. EB were produced by differentiation for 8 days consisting of 3 days in hanging drop culture and 5 days in suspension culture and routinely demonstrated spontaneous contractions, a result consistent with Fijnvandraat (data not shown). Gene expression profiles of these differentiating ES cells confirmed cardiomyocytic potential (as integrated into figure 4.2). Having demonstrated that cardiomyocytic differentiation of ES cells was consistently observed, their effects upon dermal follicular cells were investigated.

4.1.1 Morphological comparison of ES cell embryoid bodies with DP and DS co-culture cell aggregates

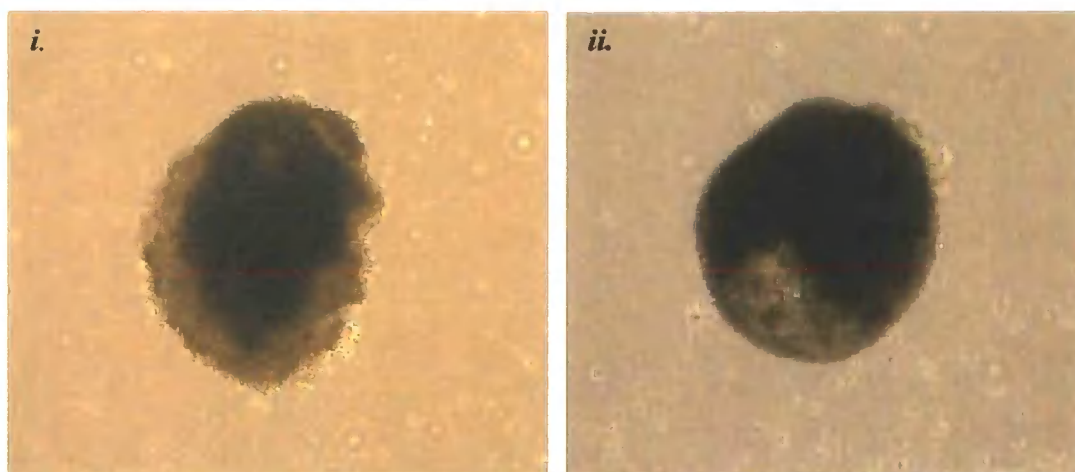
ES cells and dermal follicular cells were added together in different ratios and co-cultured in hanging drop and suspension culture as described above for ES cells. In order to discriminate the differentiation attributed to the two different cell types, rat dermal follicular cells were cultured with mouse ES cells. This type of co-culture relies upon the cross-species communication between the mouse ES cells and the rat dermal follicular cells. Previous experiments have indicated these two species are capable of communicating with one another in co-culture and inducing differentiation towards a myocyte lineage. Fukuhara *et al.*, showed rat cardiomyocytes in cell-to-cell *in vitro* co-culture with mouse BM stromal cells produced myotubules formation with cardiomyocyte associated gene expression in cells of mouse origin that had synchronised contractions with surrounding rat cardiomyocytes (Fukuhara *et al.*, 2003). Macdonald *et al.*, showed this communication was also possible *in vivo* by injecting mouse BM MSC into the peri-infarct zone of rat hearts

after induced myocardial infarction (MI). They observed mouse cells with cardiomyocyte associated gene expression and improved cardiac function (Macdonald *et al.*, 2005). In these two cases rat cells induced mouse cells to differentiate towards cardiomyocytes, the opposite has also been reported; mouse neonatal cardiomyocytes *in vivo* co-culture with a rat liver stem cell line has shown to induce contractile cardiomyocytes, expressing cardiogenic proteins, of rat origin; differentiation that was not attributed to cell fusion (Muller-Borer *et al.*, 2004).

Previous work therefore indicates the two species are capable of communicating as well as inducing cross-species cardiomyogenic differentiation when cultured together. Cell ratios were set up as described in the methods at the following ratios of ES: dermal ratios; 1:1, 1:3, 1:10, ES cells alone or dermal follicular cells alone. The mouse ES cells and rat dermal follicular cells were distinguished from one another post-culture with species-specific primers.

100 hanging drops were set up for each culture ratio; randomly selected samples of approximately 20 were monitored by phase microscopy throughout suspension culture. All cell ratios produced cell aggregates after 3 days in hanging drop culture. The cell aggregates were roughly spherical with the cells appearing to be tightly attached to one another; aggregates did not break apart upon transferring from hanging drop to suspension culture consistent with EB observations. Figure 4.1 shows a representative photograph of an EB and a cell aggregate in suspension culture after 3 days in hanging drop culture. Contractions were observed in aggregates that contained ES cells however there were no contractions observed in any of the cell aggregates made entirely of DP cells or DS cells alone. The centre of the co-culture aggregates appears darker than the outer layer of cells which may indicate there is a cell dense core or a degree of cell death; this was comparable with the EB (Wei *et al.*, 2005).

Figure 4.1: Morphology of ES cell embryoid bodies and ES: dermal cell aggregates



Gross morphology of (i) mouse ES cell embryoid bodies (EB) and (ii) aggregates of mouse ES cells and rat dermal follicular cells. The aggregates/embryoid bodies were cultured for 8 days; 3 day in hanging drop culture and 5 days suspension culture. Areas of contractions were observed in both EB and mixed cell aggregates. Bright field image, x5 magnification.

The morphology of an early EB, i.e. after 2 days into hanging drop culture, is a spherical aggregate of cells with a defined cell surface where individual cells cannot clearly be distinguished from one another. An EB after approximately 10 days in culture remains roughly spherical, however the aggregates have a less well defined edge as individual clumps of cells appear raised from its surface (Wei *et al.*, 2005). The morphology of the ES cell EB after 8 days in hanging drop and suspension culture, figure 4.1, was consistent with this morphology. However, the appearance of the aggregates of mixtures of ES and dermal follicular cells after 8 days co-culture appeared more morphologically similar to that of an early EB (Wei *et al.*, 2005) as seen in figure 4.1, as was the case for the cell aggregates of dermal follicular cells alone (data not shown).

Although the mixed population aggregates (ES and dermal follicular cell) were seen to contract, the cellular origin of the contractile cells was not known. In order to address this, species-specific PCR for cardiomyocyte-characteristic markers was used.

4.1.2 Expression of cardiomyocyte associated genes in DP and DS primary cells after ES cell co-culture

The hanging drop method of culturing cells promotes tight gap junctions to be formed between cells (Oyamada *et al.*, 1996). On washing the cell aggregates after co-culture, the cells do not dissociate from one another; it would therefore be difficult to isolate single cells for analysis without causing damage. Species-specific PCR allows the gene expression of cells of ES and dermal origin to be investigated following co-culture without the need to separate them post-culture.

The species-specificity of the PCR primers was first confirmed. As can be seen in figure 4.2, mouse-specific primers generated a PCR product from mouse cDNA but never from rat cDNA; similarly the rat specific-primers generated a PCR product from rat cDNA but never from mouse cDNA. This provided confidence that this method of detection was suitable for investigating single species-specific gene expression changes in a sample of mixed populations of cells.

Figure 4.2: Expression of genes characteristic of cardiomyocyte lineage during ES cell differentiation and dermal cell aggregate culture.

	Mouse -specific primers				Rat -specific primers			
	Mouse heart	ES cell EB	Rat DP aggregate	Rat DS aggregate	Rat heart	ES cell EB	Rat DP aggregate	Rat DS aggregate
Nkx2.5								
Mef2c								
GATA4								
tbx5								
α- MHC								
Cardiac actin								
Tropomyosin								
Troponin I								
Titin								
Tropoelastin								
GAPDH								

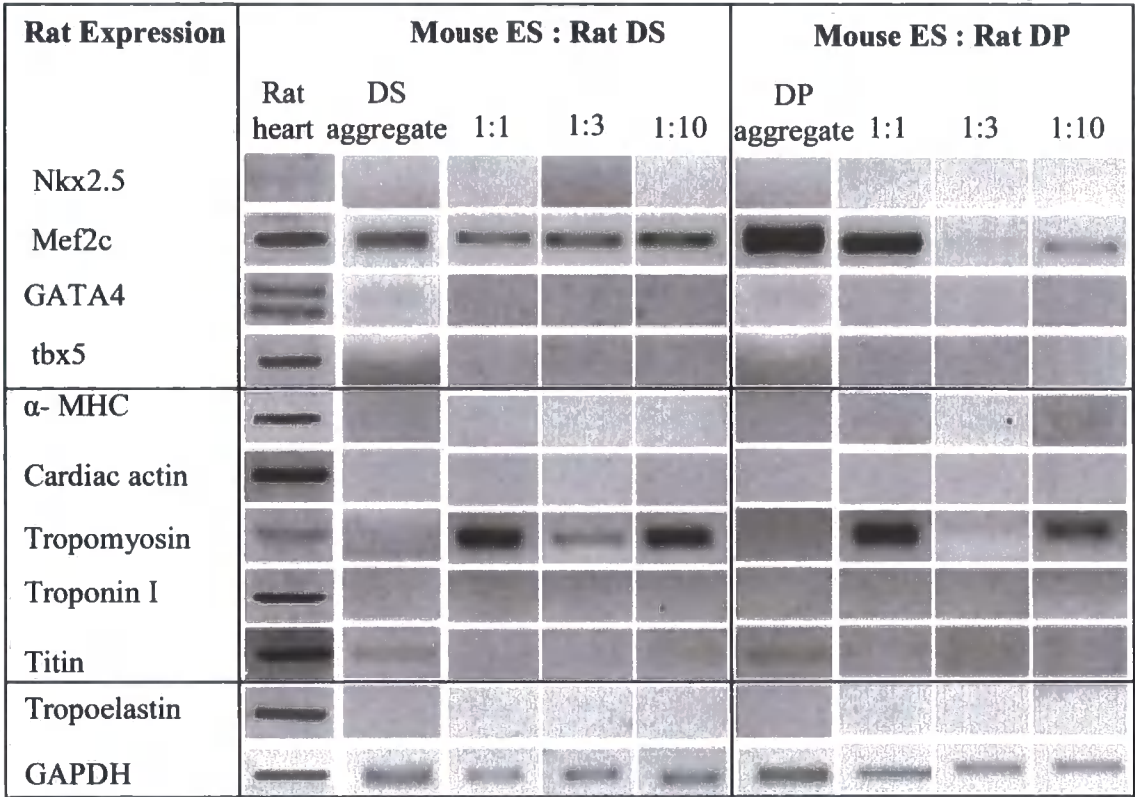
Expression of genes characteristic of cardiomyocyte lineage in mouse EB and rat dermal aggregates as assessed by species-specific RT-PCR. The species specificity of both sets of primers was confirmed by the presence or absence of PCR product from the positive and negative control species, respectively. Note that expression of Nkx2.5 was only just detectable even in the positive controls. The expression of this panel of genes is consistent with cardiomyocyte differentiation of the murine ES cells, but the rat dermal aggregates did not express detectable levels of the majority of genes characteristic of cardiomyocytes. The GAPDH primer set was common to both rat and mouse and acted as a loading control in this and subsequent RT-PCR analyses.

When the DP and DS cells were cultured in cell aggregates in the absence of ES cells, the only detectable gene expression was *Mef2c* with very low expression of titin and possibly *GATA4* as can be seen in figure 4.3. DP and DS primary culture cells expressed *Mef2c* when in conventional culture in flasks; however *GATA4* was previously undetectable (figure 3.11) as was titin (figure 3.12). This may indicate that culturing the DP and DS primary cells in hanging drop culture, and promoting them to have close contact with one another in suspension, induces the expression of additional cardiomyocyte-associated genes, however the level of expression was consistently very low and very substantially less than the positive control heart.

After co-culture with mouse ES cells, the rat dermal follicular cells maintained detectable expression of both *Mef2c* and tropomyosin as can be seen in figure 4.3; both of which were previously identified in conventional DP and DS primary cell cultures (figure 3.11 and 3.12). There was low level expression of α -MHC which was previously undetected in dermal primary cell cultures (figure 3.12). α -MHC is expressed in EB at this stage of differentiation but normally precedes *Nkx2.5* and *GATA4* expression (Boheler *et al.*, 2002) of which neither are detectable here. This may indicate the expression of α -MHC is not associated with cardiomyocyte lineage commitment. Interestingly, tropomyosin is normally expressed in the EB very early in their differentiation; of the genes investigated here it is normally the first to be expressed in the EB at day 1 of differentiation (Boheler *et al.*, 2002); its expression here may indicate the start of the network of genes important to development of cardiomyocytes.

One possible outcome of co-culture of rat dermal follicular cells with ES cells is that it could interfere with endogenous ES commitment to, and induction of, the cardiomyocytic lineage. The differentiation of ES cells in the EB has previously been shown to be affected by the co-culture cell type. For example murine EB cultured in contact with embryonic pulmonary mesenchyme showed appearance of structural organisation of epithelial lined channels throughout the EB that expressed early developmental markers of pulmonary epithelium (Van Vranken *et al.*, 2005). In order to confirm that such commitment was not affected or suppressed in the ES cells, the expression of genes characteristic to ES-derived cardiomyocytic differentiation was examined.

Figure 4.3: Expression of genes characteristic of cardiomyocyte lineage by dermal follicular cells cultured in the presence of differentiating ES cells.



Rat dermal follicular cells were cultured as aggregates with differentiating mouse ES cells in different ratios, and species-specific expression of genes examined by RT-PCR. The dermal follicular cells, as detected with rat-specific primers, maintained expression of Mef2c when cultured with the differentiating ES cells. These culture conditions also produced detectable expression of tropomyosin and low level α-MHC.

As can be seen in figure 4.4, transcription factors characteristic of early cardiomyocyte commitment (Mef2c, GATA4 and tbx5) were consistently detected in differentiating ES cells in the presence or absence of rat dermal follicular cells at any ratio. Nkx2.5 was difficult to detect in EB cultures, but was just detectable in some ES follicular dermal co-cultures. Genes characteristic of functional cardiomyocytes were detectable, a result consistent with observations that contractility was observed in all aggregates. Although there was some dose-dependant variability in gene expression, the consistent detection of characteristic genes suggested that the inductive environment of the EB was maintained.

In summary, the expression profile of the rat dermal follicular cells after co-culture with ES cells was almost identical to that of dermal follicular cell primary cultures. Although a modest level of α -MHC was detected in one culture condition, the absence of detectable expression of any of the other cardiomyocyte-characteristic genes indicates that there was no substantial inductive event. This data suggests that although ES cell commitment was not compromised, such inductive signals as were present were unable to induce substantial cardiomyocyte commitment of the dermal follicular cells. However, an alternative approach that has been successfully used with mesenchymal stem cells is co-culture with cardiomyocytes (Yoon *et al.*, 2005).

Figure 4.4: Expression of genes characteristic of cardiomyocyte lineage by differentiating murine ES cells cultured in the presence of rat follicular dermal cells

Mouse Expression			Mouse ES : Rat DS			Mouse ES : Rat DP		
	Mouse heart	ES cell EB	1:1	1:3	1:10	1:1	1:3	1:10
Nkx2.5								
Mef2c								
GATA4								
tbx5								
α- MHC								
Cardiac actin								
Tropomyosin								
Troponin I								
Titin								
Tropoelastin								
GAPDH								

Differentiating mouse ES cells were cultured as aggregates with rat follicular dermal cells at different ratios, and species-specific expression of murine genes examined by RT-PCR. With the exception of tropoelastin in aggregates with rat DS cells, the mouse ES cells demonstrated a pattern of gene expression consistent with the cardiomyocytic differentiation observed in embryoid bodies.

4.2 Inducing the dermal follicular cells to differentiate to cardiomyocytes by co-culture with embryonic cardiomyocytes

In order to assess whether co-culture would induce dermal follicular stem cells to a cardiomyocyte phenotype, E12.5 mouse embryonic cardiomyocytes were used in co-culture with rat dermal follicular cells. The *in vitro* culture of embryonic cardiomyocytes is not well described in the literature; therefore a better understanding of the cell's behaviour in culture is necessary in order to analyse co-culture results.

Yoon described co-culture of neonatal and adult cardiomyocytes with BM MSC concluding that the age of the cardiomyocytes was important in the success of the differentiation of the MSC. The results suggested that the ability of the cardiomyocytes to act as inducers of cardiomyocyte differentiation was dependant on their age; that inducing agents may be progressively lost through the cardiomyocyte post-natal life (Yoon *et al.*, 2005). Embryonic cardiomyocytes express all of the genes under investigating here; the expression of the early transcription factors may be reduced in post-natal hearts therefore the use of embryonic heart may be preferential in this set of experiments. The embryonic age of the hearts used E12.5, at a time point when the contracting four chamber heart has atrial and ventricular formation (Christoffels *et al.*, 2000) and expression of all the genes investigated.

4.2.1 Establishing embryonic cardiomyocytes in adherent culture for co-culture with DP and DS primary cells

Ten separate groups of mouse embryonic cardiomyocytes were isolated and cultured *in vitro* and a time course of their proliferation, contractile activity and baseline gene expression analysed over a period of 24 days at which point the contractions had ceased and the cells were considered to no longer be typical of *in vivo* cardiomyocytes.

The cardiomyocytes were isolated from the embryonic heart and transferred to adherent culture as described in methods section 2.3.4, the cells took 24hrs to settle on the plastic; all settled cells monitored were seen to contract within the first 24hrs in culture. The cardiomyocytes were small, spherical, refractive, non-contracting cells in suspension which settled onto the plastic, where they were multi-nucleated with a fibroblastic morphology

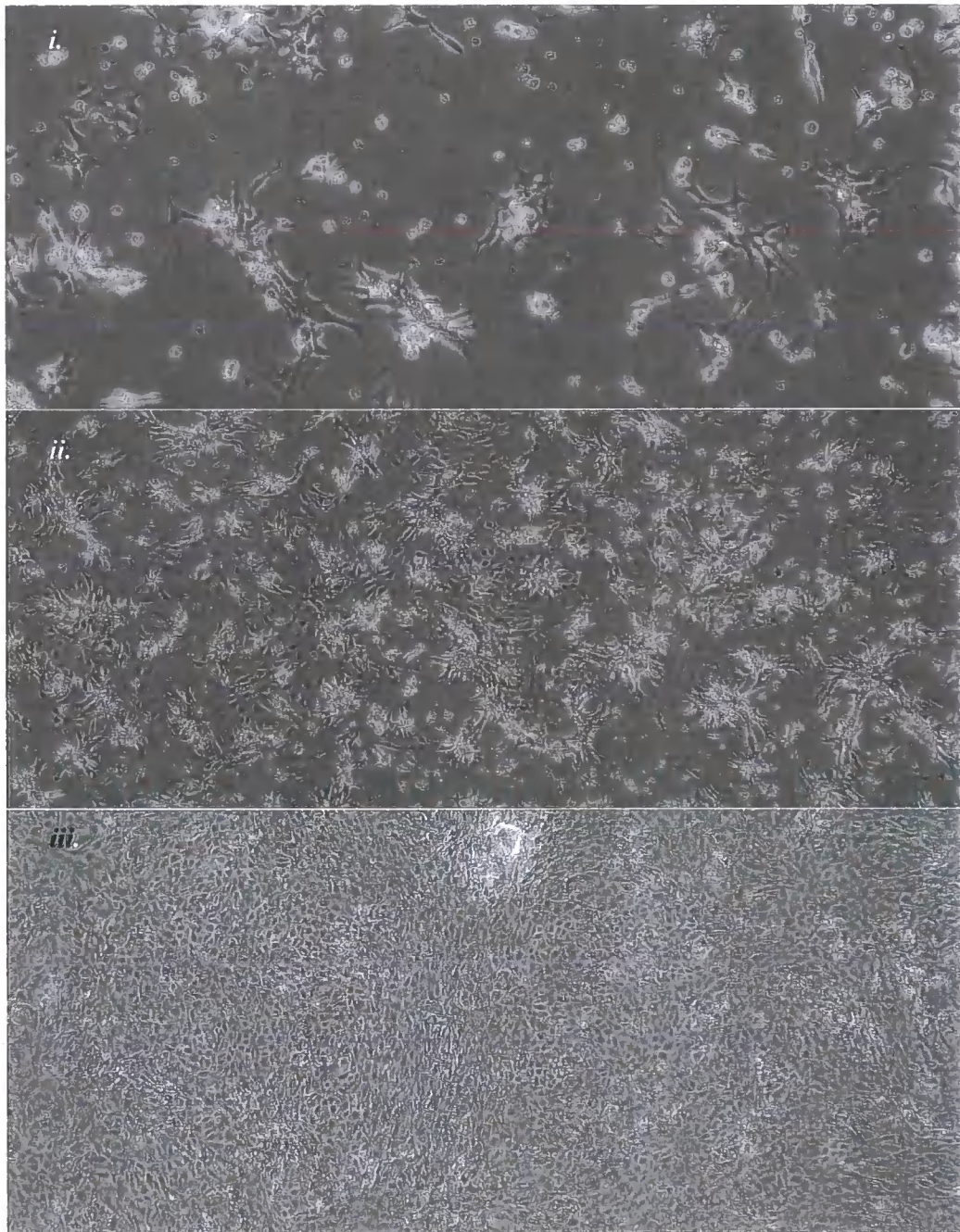
and were phase-dark. The adherent cardiomyocytes had many cytoplasmic processes, a raised appearance and contracted independently of one another. Within the first three days the cells reached 40% confluency; representative images are shown in figure 4.5*i*.

By day 10 in culture the cells had increased to approximately 70% confluency; the individual cells were distinguishable from one another and arranged in raised clumps of cells. Within each group the cells could be seen to contract rhythmically in unison, independent to other collections of cells on the culture dish. Representative images are shown in figure 4.5*ii*.

At day 16 the cells were 100% confluent; individual cells were barely distinguishable from one another with cells overlapping, as seen in figure 4.5*iii*. Rhythmic contractions were synchronised across the entire culture dish.

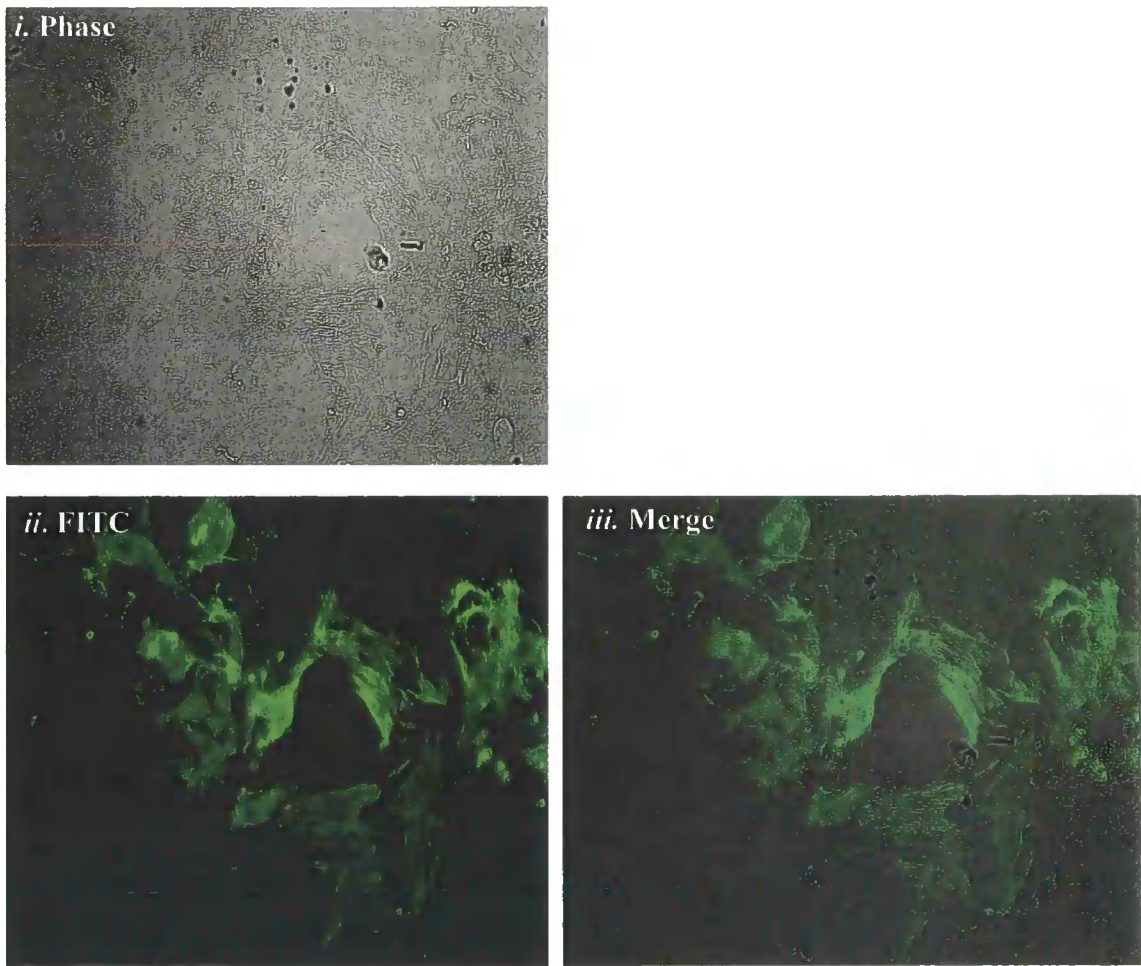
After day 16 the cells remained at 100% confluency however nuclei became less distinguishable from the overlaying cytoplasmic processes until at approximately day 20 nuclei were barely visible. This made it impossible to monitor individual cells to determine the surface area of each cell or determine if there was any cell death. Contractions remained consistent across the entire dish, however individual contracting cells could not be identified making the percentage of contracting cells still present impossible to determine. For this reason, at day 25 the cells were labelled with cardiac α -actin. Contracting cells would express this gene and any cell not expressing cardiac actin was considered to no longer be representative of an *in vivo* cardiomyocyte i.e. have ceased contractions. Representative images are shown in figure 4.6. Approximately 30-40% of the surface area labelled positive for cardiac actin indicating, by this time point, cells may no longer be representative of *in vivo* cardiomyocytes or those cells in early *in vitro* culture. All contractions ceased by day 26 of culture in all sample cultures.

Figure 4.5: Morphology of embryonic cardiomyocytes in adherent primary culture



Morphology of mouse E12.5 embryonic cardiomyocytes in adherent culture. At day 3 (*i.*) cultures were approximately 40% confluent with individual cells arranged in small groups which contracted independent of one another. By day 10 (*ii.*), at 70% confluence, the cells were clumped together in larger groups with unified rhythmical contraction. At day 16 (*iii.*) the cells were 100% confluent. However, the cells could still be distinguished from one another. Synchronised contractions rippled across the entire culture dish. Representative phase images are shown at x10 magnification.

Figure 4.6: Identification of individual embryonic cardiomyocytes at day 25 in adherent primary culture by cardiac actin immunofluorescence



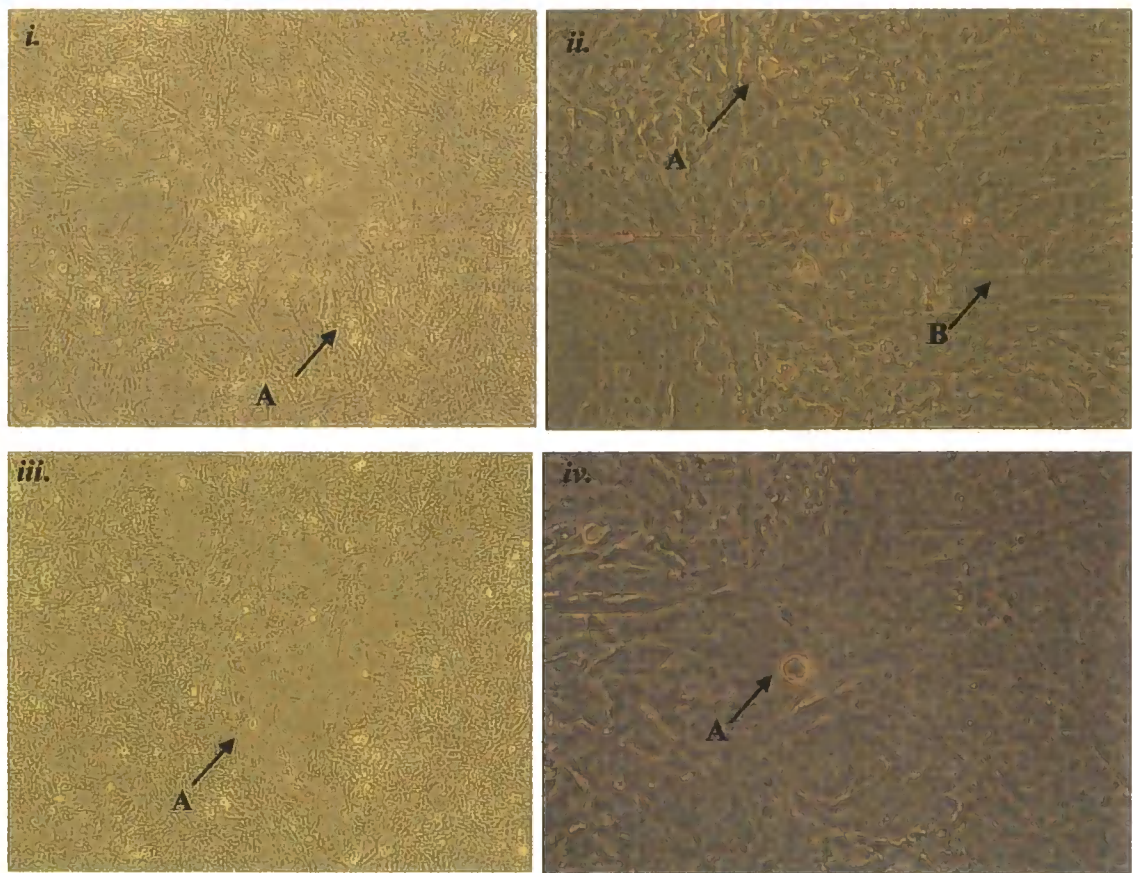
Cardiac actin fluorescent labelling of individual embryonic cardiomyocytes at day 25 of adherent culture. At day 25, the individual cardiomyocytes could not be distinguished from one another; contractions ceased at day 26. The cells were visualised with fluorescent antibody labelling for cardiac actin to establish the presence of typical cardiomyocytes at this late culture time point when contractions were about to cease. Representative images are shown at x20 magnification.

4.2.2 Co-culture of rat dermal follicular cells with mouse embryonic cardiomyocytes

The method described by Yoon for culturing BM MSC with neonatal cardiomyocytes was followed (Yoon *et al.*, 2005) with alterations as described in method section 2.4.6. Cell-to-cell contact is an important factor for transdifferentiation of adult stem cells into cardiomyocytes possibly by gap junction formation and thereby electrical coupling. Taking this into consideration, the mouse embryonic cardiomyocytes were allowed to proliferate to 50% confluency before the addition of rat dermal follicular cells thus allowing plastic for the dermal follicular cells to adhere to and sufficient contracting cardiomyocytes for cell-to-cell contact. In order to detect specific changes in commitment of the DP and DS primary cells, as induced by mouse embryonic cardiomyocytes, species-specific PCR primers were used.

The rat dermal follicular cells were added to the E12.5 mouse cardiomyocytes and allowed 7 days co-culture. Representative images in figure 4.7 show the appearance of the cardiomyocytes which were distinguishable from the dermal follicular cells. Although the dermal cells were added to cardiomyocytes when they were at 50% confluency the cells appeared at close to 100% confluency after the 7 days co-culture which was consistent with the time course for the cardiomyocytes as pre-determined (figure 4.5). Interestingly, the dermal follicular cells appeared as small, spherical cells quite unlike the morphology of DP and DS in conventional adherent culture. The DP and DS were adherent to the surface of the cardiomyocytes and, in no instance observed, adherent to the culture ware. This would indicate the dermal follicular cells were prevented from adhering to the plastic ware or preferentially chose the cardiomyocytes to attach to. Visually, on seeding the dermal cells, there was sufficient plastic clear of cardiomyocytes as well as sufficient time for the dermal cells to adhere before the cardiomyocytes reached 100% confluency. The uncharacteristic culture behaviour of the DP and DS in this case may have to be taken into account when analysing gene expression changes

Figure 4.7: 2D co-culture of mouse embryonic cardiomyocytes with rat dermal follicular cells



Morphology of dermal follicular cells (A) and embryonic cardiomyocytes (B) in 2D co-culture under phase microscopy. At low magnification (x10) the DP (i.) and the DS (ii.) were observed to be on the surface of the confluent cardiomyocytes. At higher magnification (x40) the DP (iii.) and DS (iv.) were distinguishable from the cardiomyocytes with a morphology unlike that seen in normal primary dermal follicular cell culture. The cells appeared round and refractive with no cellular processes.

4.2.3 Expression of cardiomyocyte associated genes in DP and DS primary cells after embryonic cardiomyocyte co-culture

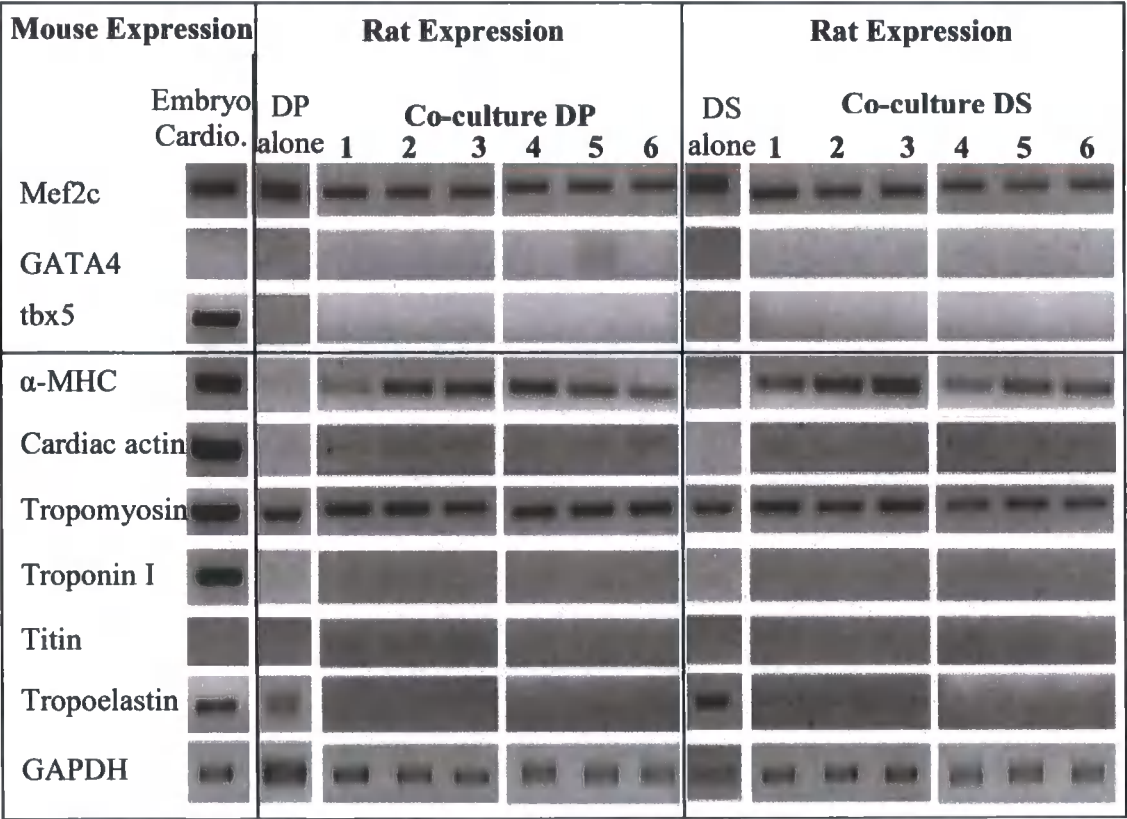
As can be seen in figure 4.8, the embryonic cardiomyocytes in co-culture demonstrated detectable expression of all the genes investigated with the exception of GATA4 and titin. The dermal follicular cell expression was consistent between all three DP and DS and detectable expression of tropomyosin; both of which were previously identified in conventional dermal follicular cultures (figure 3.11 and 3.12). However, there was detectable expression of α -MHC and cardiac actin both of which were not expressed in DP and DS primary culture cells (figure 3.12). In summary, there remains absence of expression of a number of the transcription factors and sarcomeric-associated functional genes.

This may indicate that complete differentiation has not occurred. The data suggests that the approach of using co-culture for cardiomyocyte commitment was capable of inducing a more complete molecular profile consistent with cardiomyocyte differentiation than using ES cells; using an inducing cell from a species that does not match that of the dermal stem cells may be inadequate to the task of full cardiomyocytic commitment. Therefore embryonic cardiomyocytes from the same species were investigated to determine if they would be better able to induce the DP and DS primary cells.

4.3 Inducing the dermal follicular cells to differentiate to cardiomyocytes by co-culture with embryonic cardiomyocytes of matching species

As discussed, the dermal follicular cells do not express the entire cardiomyocyte gene profile. Previous experiments have indicated that mouse and rat cells are capable of communicating with one another; expecting cells of different types as well as species may not be suitable for this experiment. Therefore the co-culture was repeated using mouse embryonic cardiomyocytes with mouse DP/DS, and rat embryonic cardiomyocytes with rat DP/DS. Species-specific primers were not suitable for this type of co-culture, therefore the dermal follicular cells needed to be labelled in order to identify co-culture cells that were of dermal origin.

Figure 4.8: Expression of cardiomyocyte lineage genes in rat primary dermal follicular cells after co-culture with murine embryonic cardiomyocytes



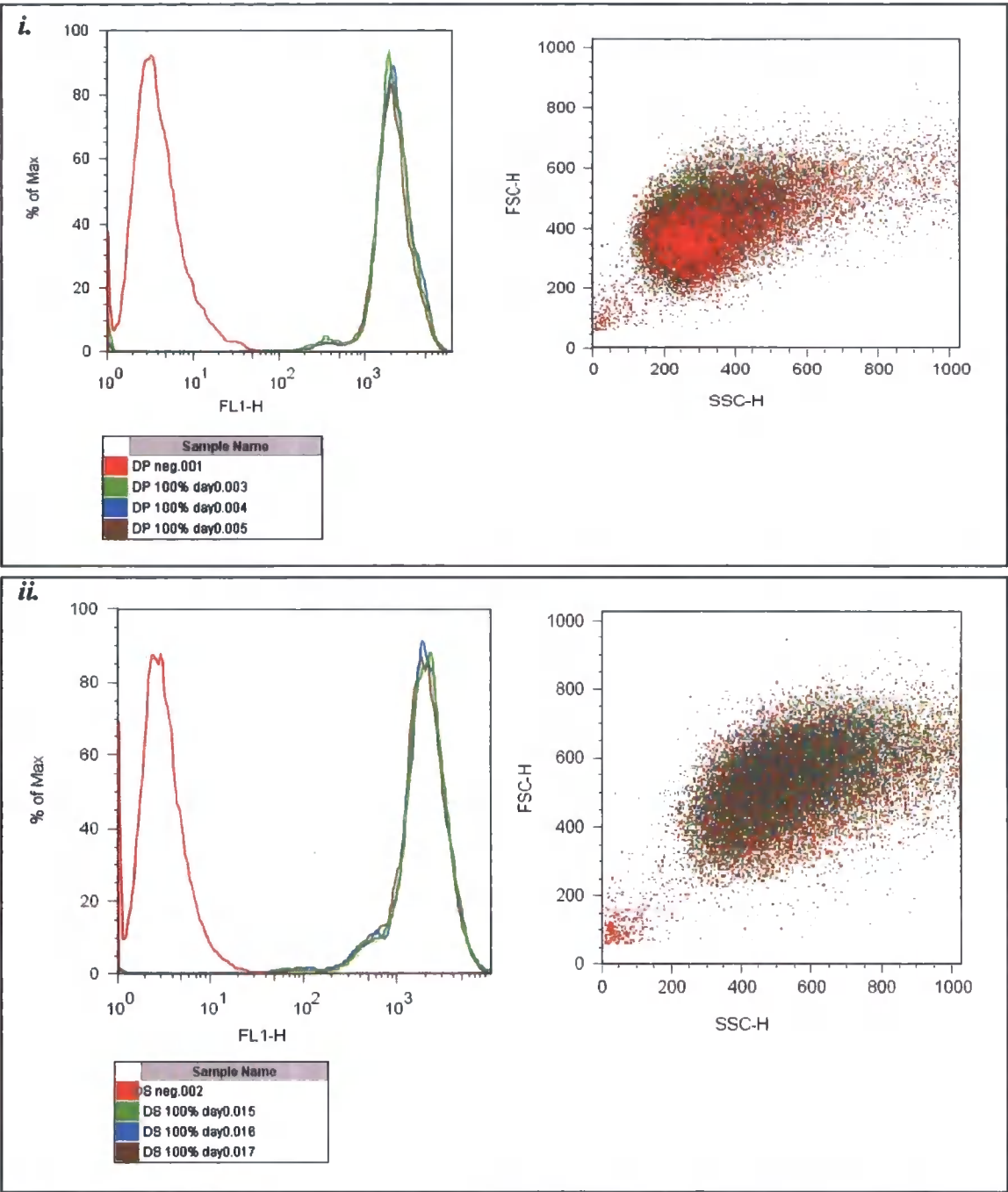
Expression of cardiomyocyte lineage genes by rat follicular dermal cells after 5 days co-culture with murine E12.5 embryonic cardiomyocytes, as assessed by species-specific RT-PCR. Results from two sets of six independent co-cultures (1-6), DP and DS cultured alone and mouse embryonic cardiomyocytes alone are shown. DP and DS were broadly similar in their gene expression profile, with detectable levels of Mef2c, α-MHC, low level cardiac actin and tropomyosin, as detected using rat-specific primers. The expression of cardiomyocyte lineage genes in the co-culture embryonic cardiomyocytes was confirmed using mouse specific primers.

4.3.1 Identifying cells of dermal origin in same species co-culture

Carboxyfluorescein Succinimidyl Ester (CFSE) was used to track the cells of dermal origin. CFSE is a harmless, fluorescein derivative which is cell permeable and non-fluorescent. Upon entering cells, CFSE undergoes esterase cleavage and diffuses throughout the cytoplasm making the molecule fluorescent and cell impermeable. As cells divide, the CFSE is split equally between the daughter cells resulting in diminished CFSE signal detection. This division, and resultant signal diminishment occurs with each subsequent cell division (Lyons 2000).

There is no evidence of CFSE being used on dermal follicular cells previously; therefore in the first instance it was important to investigate its suitability for co-culture purposes. The CFSE fluorescence must be detectable above, and distinguishable from, the autofluorescence of the embryonic cardiomyocytes. The method dictates 100% of the dermal follicular cells were labelled with the CFSE prior to co-culture, according to this the CFSE positive cells collected post-co-culture would represent cells of dermal origin. Should the efficiency of the labelling be less than 100% then the isolated cells may not represent the entire population of dermal origin which would need to be considered in analysing gene expression results. It is imperative that the CFSE cannot pass from one cell to another in co-culture, with the exception of cell division, as this may lead to contaminating cardiomyocytes in the cells assigned dermal follicular cell origin status. CFSE, by its nature, should not do this however it is important to investigate the efficacy and efficiency of dermal follicular cell CFSE labelling. The effect of incubation on the dermal follicular cells with CFSE, as described in methods section 2.4.7, was first analysed to determine if it affected the cells viability as determined by the side scatter (SSC) and forward scatter (FSC) of the cells by flow cytometry. This is shown in figure 4.9 where the FSC and SSC for the CFSE labelled cells were consistent for both DP (figure 4.9i.) and DS (figure 4.9ii) with the unlabelled dermal follicular cells. There was no indication of CFSE-associated detrimental effect upon the cell size or complexity indicating cell viability after labelling. It is noted that the fluorescence of the CFSE labelled cells was distinguishable from the unlabelled cells with nominal overlap of cell populations by fluorescein fluorescence analysis; a result confirmed in three DP and DS replicates.

Figure 4.9: CFSE labelling of dermal follicular cells



Flow cytometric analysis of DP (*i*) and DS (*ii*) cells after CFSE labelling. Results from three independent labelling experiments are shown (green, blue and brown). Results from unlabelled control dermal cells are shown in red. The left hand histograms indicate the log fluorescence (FL1-H), the right hand dot plots show the forward (FSC) and side (SSC) scatter patterns. CFSE labelling was highly efficient and produced little discernable change in FSC and SSC profiles.

CFSE-labelled dermal follicular cells were allowed a period of 7 days culture and analysed by flow cytometry for FSC and SSC to estimate if the CFSE throughout this period of culture had a detrimental effect upon the cells and to ensure the fluorescence of the day 7 cells remained distinguishable from the unlabelled cells. As can be seen in figure 4.10, the SSC and FSC were sufficiently consistent to indicate there was no detrimental effect of 7 days culture on the cells. The fluorescence of the CFSE was reduced, as expected, to a level of closer to that of the unlabelled cells however an acceptable proportion of labelled cells remained distinguishable from the unlabelled cells indicating the technique suitable for co-culture.

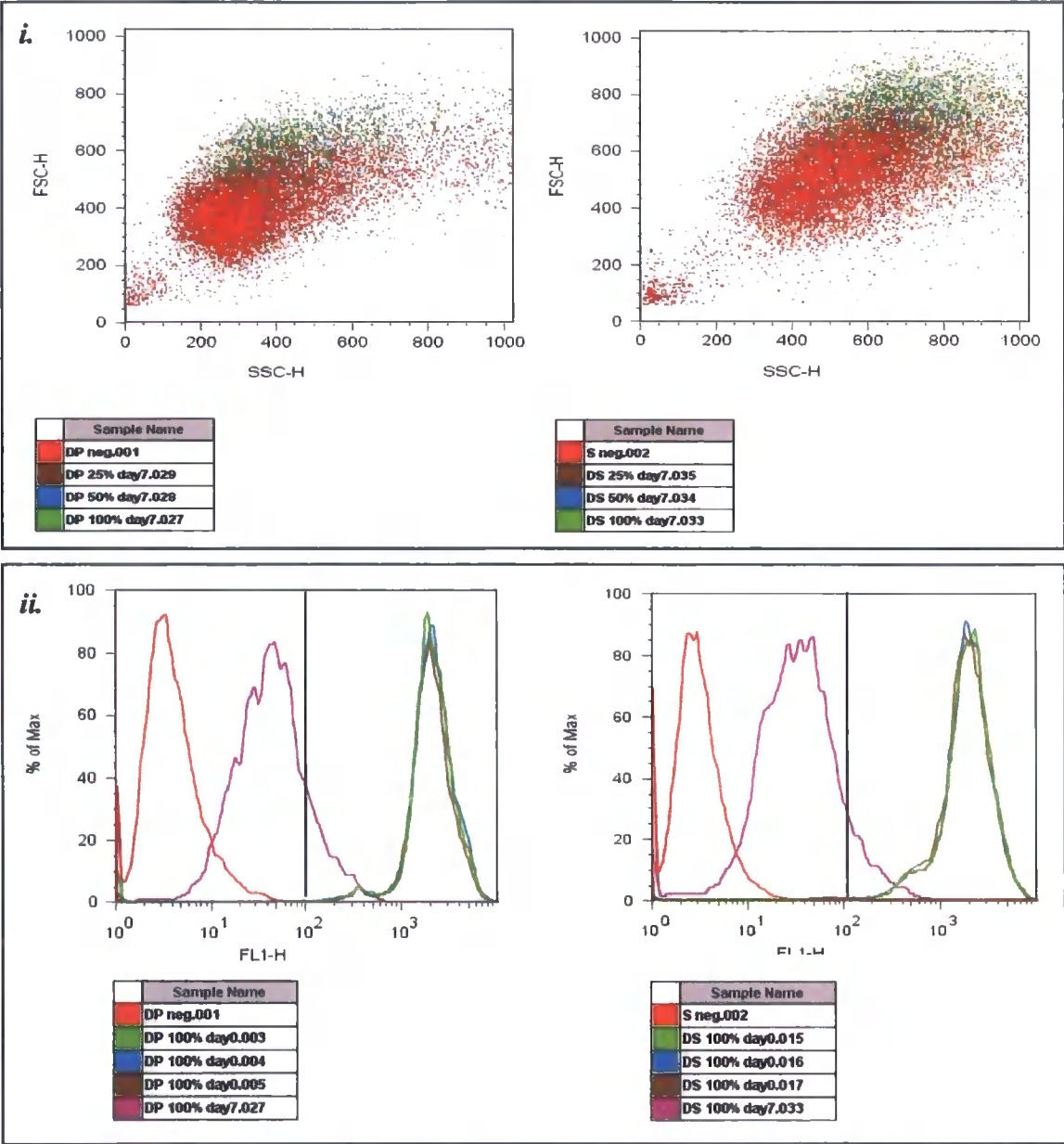
The CFSE labelling did not cause any detectable alteration to the dermal follicular cell's FSCvs.SSC scatter and fluorescence after 7 days was sufficiently distinguishable from the unlabeled cells. Therefore the efficiency of labelling was investigated; the labelled dermal follicular cells were mixed with non-labelled cardiomyocytes to determine there was no transfer CFSE between the two populations.

The dermal follicular cells were labelled with CFSE as described; labelled cells were then mixed with unlabelled dermal follicular cells at the following ratios of unlabelled: labelled; 75%:25% 50%:50% and 75%:25%. The cell mixes were analysed immediately as well as after 7 days culture. Figure 4.11 shows the proportions of positive fluorescence cells at each percentage mix; the level of fluorescence for each percentage of DP or DS CFSE labelled cells were within the same range and distinct from non-labelled cells. The graphical representation of cells analysed immediately after labelling shows the percentage of positive cells was consistent with the actual labelling for both the DP and DS cells at 25%, 50% and 75% percentages. Positive fluorescence was assigned to cells at a fluorescence level of $\geq 10^2$ as was indicated with 100% labelling (figure 4.10). The actual numbers of cells sorted at both time points, immediate and after 7 days culture, are shown in figure 4.12. The cell counts taken immediately after CFSE labelling were very closely matched to the actual percentage mixes with the labelling of DP cells appearing to be more efficient than the DS cells. After 7 days the number of cells with detectable fluorescence was reduced compared to the immediate samples as would be expected due to cell division. If the d=0 samples represent the number of cell taking up the CFSE and the d=7 samples represent the number of those initial CFSE cells that are able to be sorted away from the

assigned negative cells, then the percentage of cells able to be recovered was 44.1% for the DP primary culture cells and 51.2% for the DS primary culture cells. When analysing the sorted cells from co-culture this will have to be considered however at this level of analysis the percentage of cells able to be recovered is acceptable. The fluorescence of cells after 14 days was also investigated in a similar manner however the autofluorescence of the cells was reduced to the level of the unlabelled cells and was therefore unsuitable for co-culture purposes (data not shown).

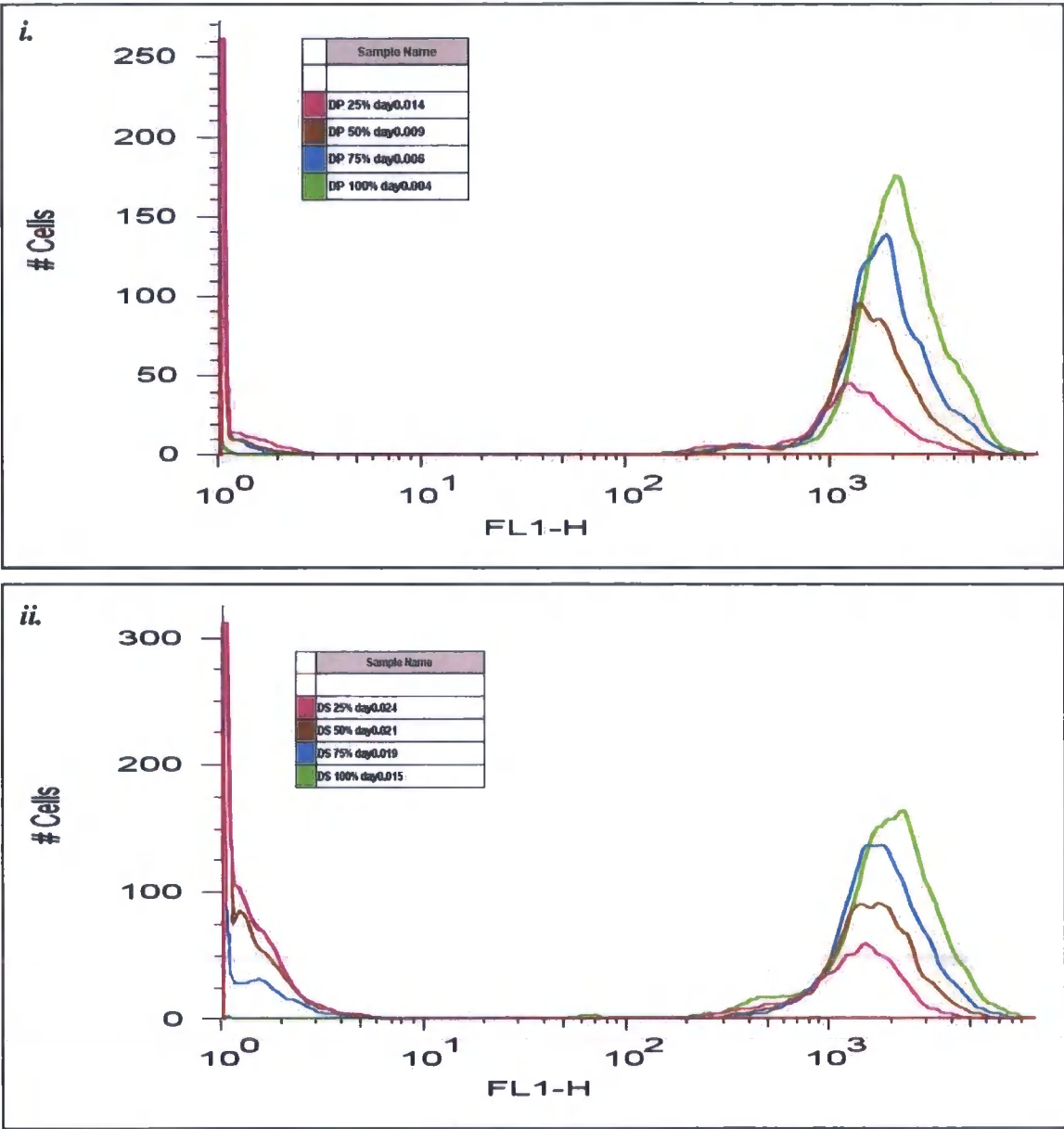
CFSE was confirmed suitable for co-culture application and was therefore used to label rat and mouse dermal follicular cells prior to co-culture with embryonic cardiomyocytes of matching species.

Figure 4.10: Flow cytometry analysis of CFSE labelled dermal follicular cells after 7 days culture



Flow cytometric analysis of dermal follicular cells after CFSE labelling before and after 7 days culture. (i) dot plot of forward scatter (FSC) and side scatter (SSC). There was no substantial change in forward/side scatter profile after seven days culture (green) compared with unlabelled controls (red). (ii) Fluorescence histograms. Data shown from unlabelled (red), CFSE-labelled with no culture period (green) and CFSE-labelled cells cultured for seven days in vitro (purple) for DP (left) and DS (right) cells. The level of detectable fluorescence decreased with 7 days culture, however a substantial number of cells continued to be contained within a gate which excluded unlabelled cells (fluorescence above 10^2 , shown by the black bar) (ii.).

Figure 4.11: Quantitative detection of CFSE-labelled cells in mixed populations.



Flow cytometric analysis of populations of mixed populations of CFSE-labelled and unlabelled dermal follicular cells. The histogram plots show 100%, 75%, 50% and 25% CFSE labelled cells for DP (i.) and DS (ii.) samples. This data demonstrated that flow cytometry could detect CFSE-labelled dermal cells in a quantitative fashion against a background of unlabelled cell types.

Figure 4.12: Percentage recovery of CFSE labelled cells following FACS sorting immediately after labelling or after seven days culture.

CFSE Sample	% recovery from d=0 (3 sample average)	% recovery from d=7 (3 sample average) at sorting	Cells retrieved at d=7 as a percentage of d=0
DP 100%	93.8 \pm 0.7	40.4 \pm 1.2	43.1
DP 50%	44.4 \pm 1.5	19.9 \pm 2.4	44.7
DP 25%	22.9 \pm 2.1	10.2 \pm 4.1	44.4
Average DS			44.1
DS 100%	85.2 \pm 0.9	48.9 \pm 0.7	57.4
DS 50%	44.8 \pm 1.7	22.7 \pm 3.7	50.7
DS 25%	25.5 \pm 0.4	11.6 \pm 5.3	45.5
Average DS			51.2

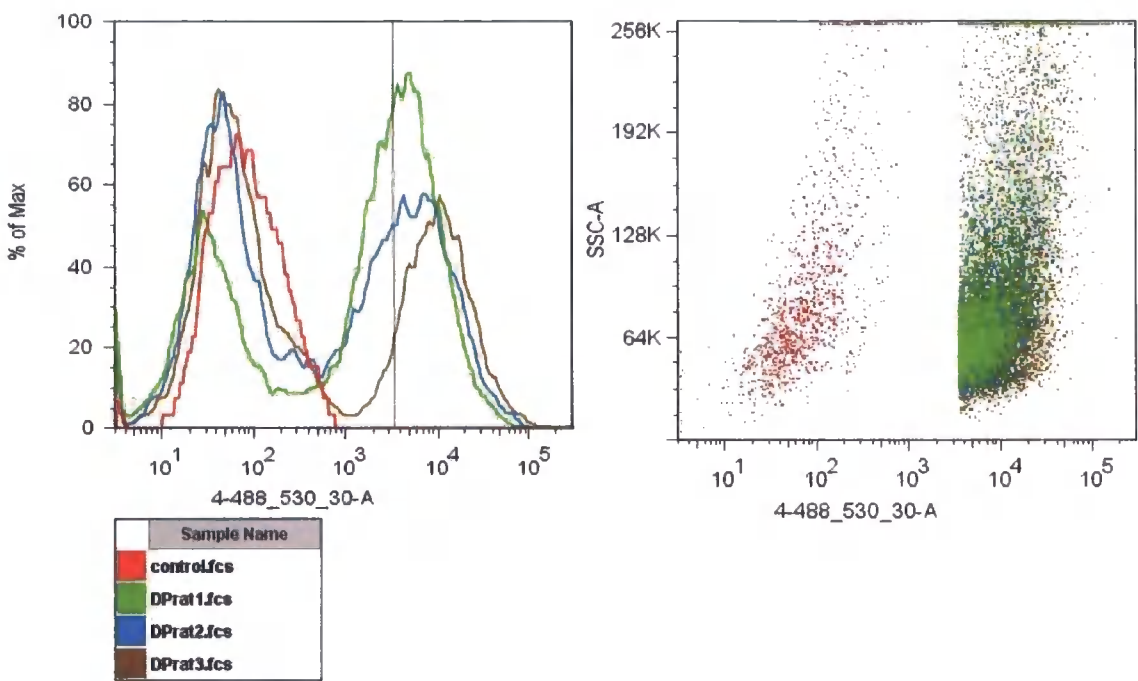
Labelled dermal follicular cells were mixed with non-labelled cells at the ratios indicated, and the cultures either subjected to FACS sorting for positive cells immediately afterward or after seven days culture (d=7) . The percentage of positive cells was determined and compared to the original number of cells labelled to determine the yield of cells. After seven days of culture, more than 40% of labelled DP and 45% of DS cells were recovered, regardless of starting ratios. Peak yields were 44.7% and 57% for labelled DP and DS cells respectively.

4.3.2 Expression of cardiomyocyte associated genes in DP and DS primary cells after same species embryonic cardiomyocyte co-culture

The DP and DS CFSE labelled cells were co-cultured on the embryonic cardiomyocyte cells (methods figure 2.5). The morphology of the dermal follicular cells on the cardiomyocytes was similar to that of the cells on cardiomyocytes of mis-matching species namely small, spherical, refractive cells (data not shown). After 7 days co-culture the cells were FACS analysed; unlabelled dermal follicular cells and cardiomyocytes were used as a negative control; the cardiomyocytes had a higher autofluorescence than the dermal follicular cells therefore the fluorescence level for sorting was set higher than in the CFSE test experiments at $10^{3.5}$ to ensure there were no cardiomyocytes in the sorted population. CFSE positive cells of fluorescence $\geq 10^{3.5}$ were retained representing cells of dermal origin; only viable cells were included in the sorting as determined by 7-AAD uptake (method 2.15.1). In total, three DP and three DS co-culture samples were sorted of both rat and mouse species; representative FACS images are shown in figure 4.13. The example shown is rat DP primary co-culture cells with the negative control sample in red. As can be seen each co-culture sample (DPrat1, DPrat2 and DPrat3) had two fluorescence peaks; the first overlapping with the negative cells, this was the cardiomyocytes and potentially a number of dermal follicular cells that either did not take up the CFSE in the first instance or have undertaken a number of cell divisions thereby diluting their CFSE fluorescence. The second peak is within the fluorescence range assigned to CFSE labelled dermal follicular cells. As can be seen by the level of sorting, the labelled cells retained were those that were the brightest although this did result in losing up to half of the population of CFSE positive cells.

The difference between peak fluorescence of the unlabelled cells to peak fluorescence of CFSE labelled cells, is 100 fold; although the yield of cells collected is reduced by this fluorescence sorting level, the purity of the cells was ensured. The gene expression changes in the mouse and rat dermal follicular co-culture cells was analysed to determine if same species co-culture induced a better dermal differentiation response towards a cardiomyocyte lineage.

Figure 4.13: FACS identification of cells of dermal origin in co-culture with embryonic cardiomyocytes of matching species



FACS analysis of co-culture mixed cell population and isolation of CFSE positive cells of dermal origin. After co-culture, the CFSE labelled cells were sufficiently fluorescent for the cells to be isolated from non-labelled cells; the fluorescence level of sorting was set high to ensure there were no negative cells included. A representative sample (rat DP after co-culture with rat cardiomyocytes) is shown, where the control (red) represents the autofluorescence of unlabelled DP, DS and embryonic cardiomyocytes. The fluorescence sorting level is shown at $10^{3.5}$; cell yield was sacrificed at the expense of purity.

4.3.3 RT-PCR analysis

Rat and mouse dermal follicular cells were analysed by RT-PCR as shown in figure 4.4 and figure 4.5 respectively. The genes investigated were those used previous; those indicative of cardiomyocyte induction and functional ability as well as a number of stem cell genes and genes that may prove important in a cardiomyocyte. Within these figures the gene expression for DP and DS primary culture cells prior to co-culture is included for comparison.

Both rat and mouse DP and DS demonstrated maintained expression of the transcription factor Mef2c and the functional associated gene, tropomyosin, as was previously seen in primary cultures. However the remaining gene expression profile of the two species was quite different with a number of differences.

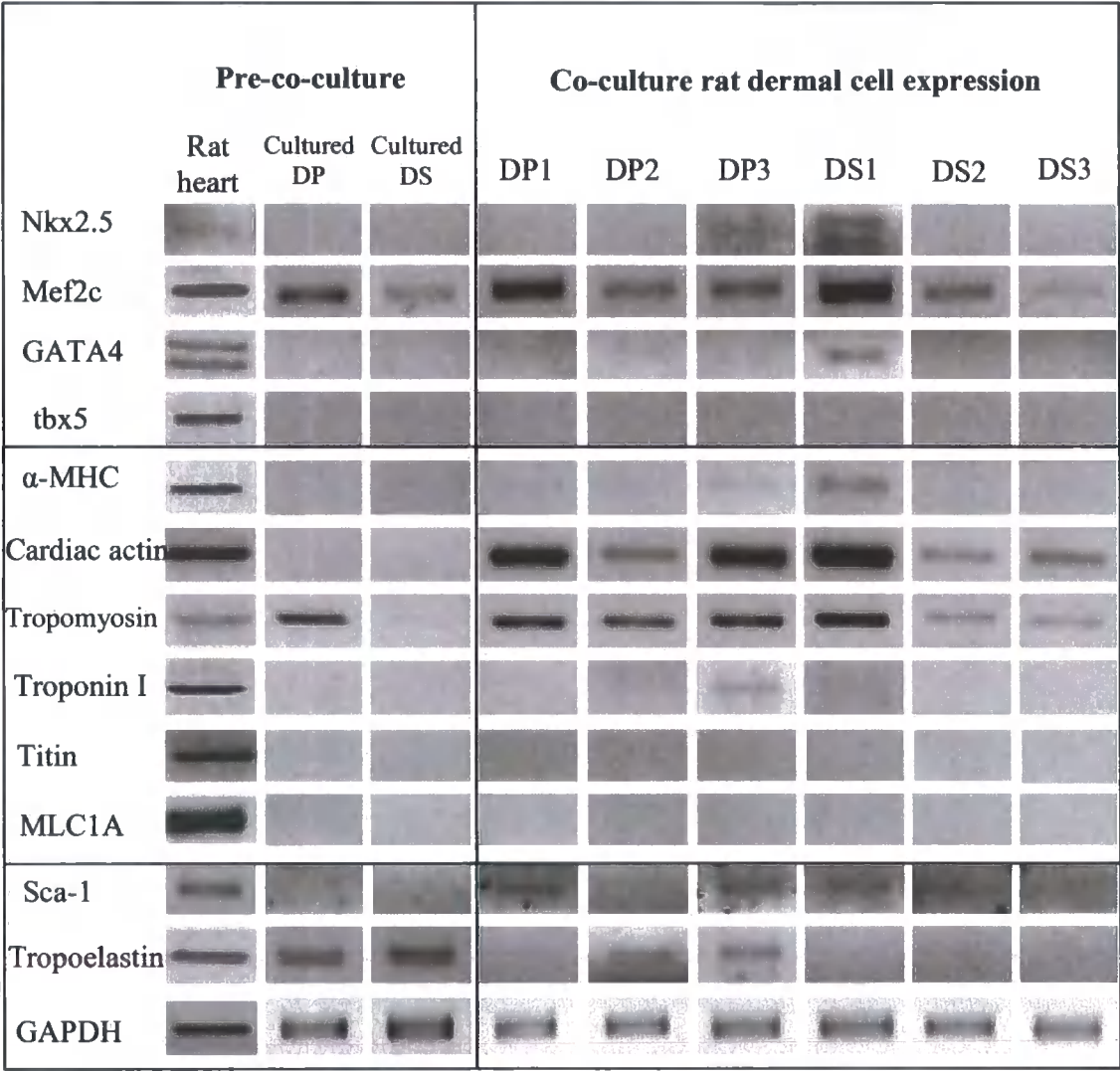
The rat DP and DS primary co-culture cells, figure 4.1, showed limited expression of the transcription factors, Nkx2.5 and GATA4, with one DS sample expressing both (DS1) however tbx5 was not detectable in any of the dermal follicular cells. The mouse DP and DS primary co-culture cells had an opposite expression profile of no detectable Nkx2.5 or GATA4 but low level expression of tbx5 in all replicates.

Of the function associated genes, the rat DP and DS primary co-culture cells had limited expression of α -MHC and troponin I, with cardiac actin expression in all replicates. The mouse DP and DS primary co-culture cells had limited expression of α -MHC, cardiac actin, troponin I and titin, with MLC1A in all replicates.

The rat DP and DS primary co-culture cells had limited expression of sca-1 and tropoelastin. The mouse DP and DS primary co-culture cells had similar expression of tropoelastin with expression of sca-1 in all samples. Tert was also investigated in the mouse DP and DS where it was expressed in a number of the samples.

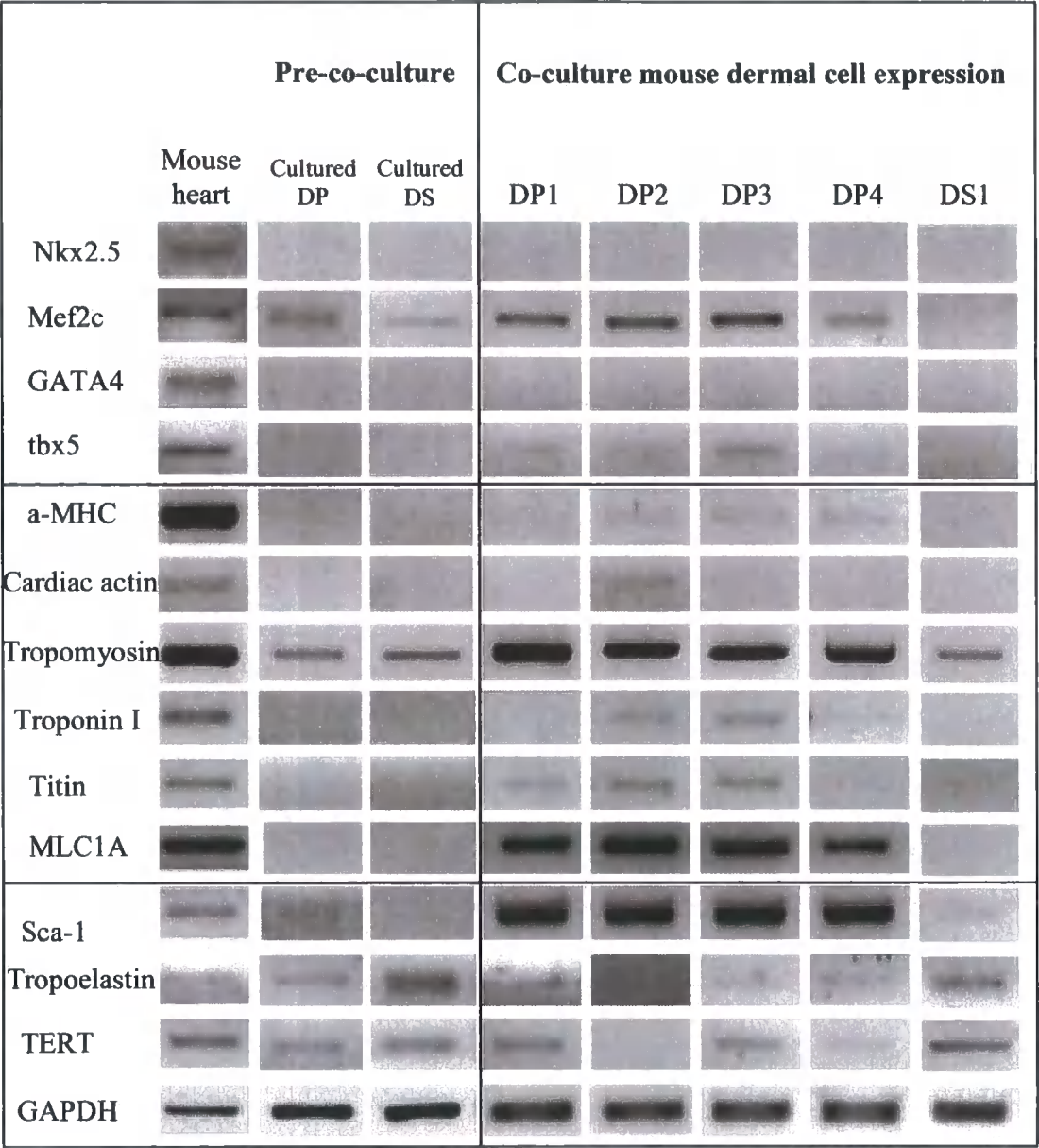
These data indicated that definitive cardiomyocytic commitment of follicular dermal cells was not observed. However, there were substantial changes in expression of genes associated with a stem cell phenotype.

Figure 4.14: RT-PCR Gene expression profile of CFSE+ve rat dermal follicular cells after co-culture with rat embryonic cardiomyocytes.



Dermal follicular cell expression of cardiomyocyte lineage genes after co-culture with embryonic cardiomyocytes. The CFSE labelled rat dermal follicular cells were isolated from rat embryonic cardiomyocytes by FACS; RT-PCR analysis showed dermal cell expression of a number of cardiomyocyte function and induction genes: Nkx2.5, Mef2c, GATA4, α-MHC, cardiac actin, tropomyosin, troponin I and stem cell associated gene sca-1, as well as tropoelastin.

Figure 4.15: RT-PCR Gene expression profile of CFSE+ve mouse dermal follicular cells after co-culture with mouse embryonic cardiomyocytes.



Dermal follicular cell expression of cardiomyocyte lineage genes after co-culture with embryonic cardiomyocytes. The CFSE positive mouse dermal follicular cells were isolated from mouse embryonic cardiomyocytes by FACS; RT-PCR analysis showed dermal cell expression of a number of cardiomyocyte function and induction genes: Mef2c and tbx5, α-MHC, cardiac actin, tropomyosin, troponin I, titin, MLC1A and the stem cell associated genes sca-1 and Tert, as well as tropoelastin.

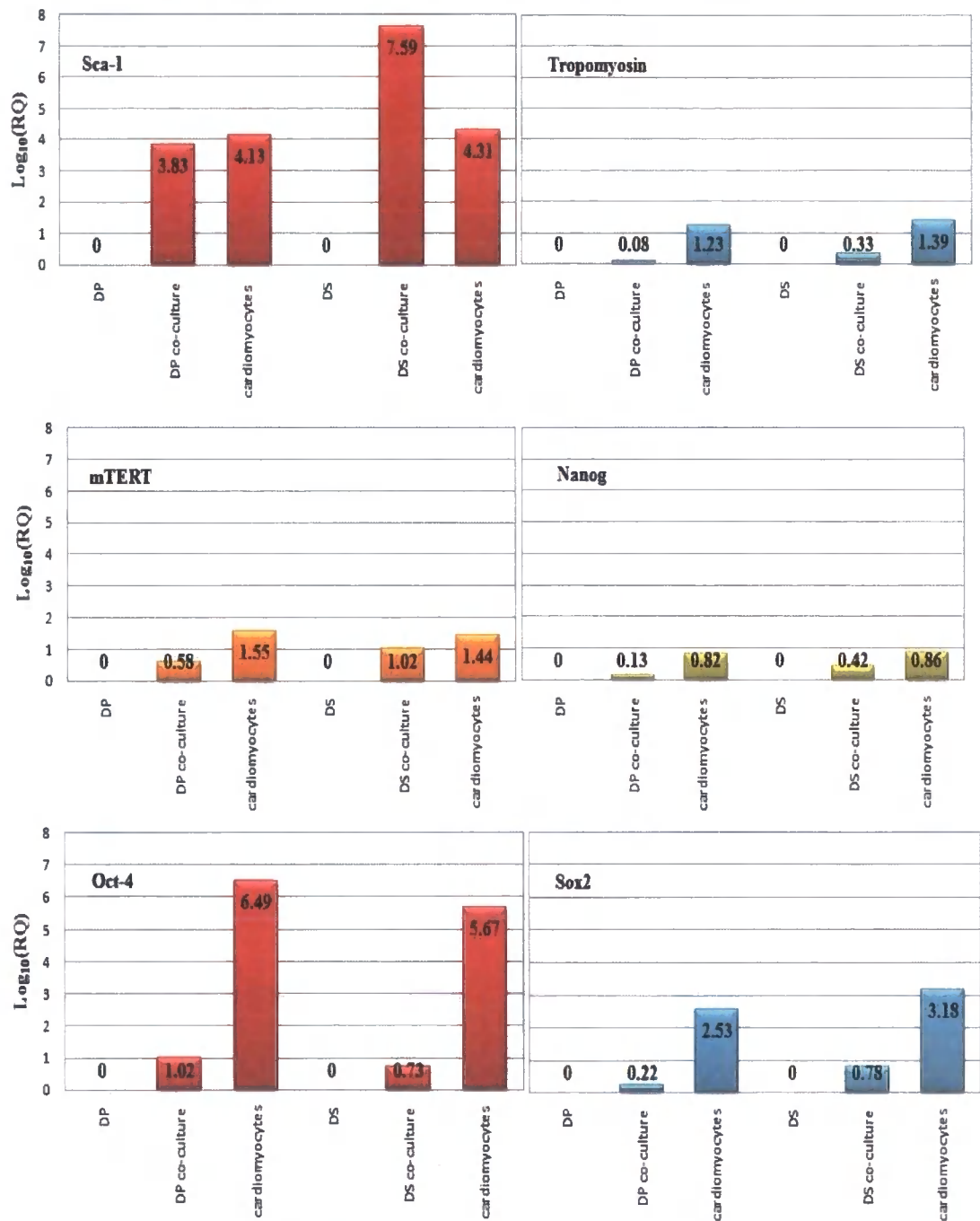
Following co-culture, the DP and DS primary cells showed dramatically increased levels of both sca-1, a surface antigen marker characteristic of a number of different stem cell types, potentially including cardiac stem cells (Matsuura *et al.*, 2004), as well as Tert, a gene product which is a phenotypic marker of proliferative stem cells (Breault *et al.*, 2008). These data could suggest that co-culture changed the numbers or properties of stem cells in the DP and DS cultures. One approach to investigate this is to examine the expression of stem cell-characteristic transcription factors. However, the low level of transcripts for this class of gene products is typically that which is amenable to routine detection by RT-PCR. However, Q-PCR can detect transcripts at low levels and with high reproducibility (reviewed by Ginzinger 2002), and thus this approach was used to investigate expression of stem cell associated gene products.

4.3.4 Q-PCR analysis

The RT-PCR analysis indicated there may be significant changes in the expression of a number of the genes investigated; therefore Q-PCR was completed to attempt to determine if the observed differences in genes were significant, as well as to try to better establish evidence of differentiation.

RT-PCR analysis indicated that the most marked gene changes were in the mouse dermal follicular cells when they are cultured with mouse embryonic cardiomyocytes. Therefore, these samples were prepared for Q-PCR and probed for number of genes associated with the cardiomyocyte and stem cell phenotype. The genes investigated in the DP and DS primary cells included Sca-1, tropomyosin, mTert, Nanog, Oct4, Sox2, tbx5 and α -MHC (figure 4.16)

Figure 4.16: Q-PCR Gene expression profile of CFSE+ve mouse dermal follicular cells after co-culture with mouse embryonic cardiomyocytes



Q-PCR gene expression analysis of selected genes in embryonic cardiomyocytes and dermal follicular primary cells before and after co-culture. Results are presented as log₁₀ of the relative quantitation (RQ) with respect to the control gene GAPDH. Results are normalised with respect to expression of each gene in DP or DS in the absence of co-culture; log₁₀zero indicates a relative expression of one, i.e. identical to that found in DS or DP. Each sample was run in triplicate.

Sca-1

As mentioned previously, Sca-1 is a surface antigen expressed by a number of cell types, including stem cell types, as well as those of the adult heart (Matsuura *et al.*, 2004); if the dermal follicular cells were capable of differentiating towards a cardiomyocytes lineage they may change their expression of Sca-1 in this process. In contrast to RT-PCR analysis (figure 4.15), Sca-1 expression was detectable by Q-PCR in both in the DP and DS primary cells. There was a significant increase in expression in both DP and DS following co-culture, showing a relative increase of approximately 130 ± 20 and 4200 ± 100 respectively (fold changes $p < 0.01$ in both cases)

Tropomyosin

Tropomyosin, a structural gene which is important in the formation of the sarcomere was detectable in the DP and DS primary cells by Q-PCR; it was also detectable by RT-PCR. Q-PCR analysis suggested a modest increase in the level of tropomyosin expression in the DP and DS after co-culture; however this change was not statistically significant.

mTert

mTert, associated with stem cells and proliferative capacity, was detectable in the DP and DS primary cells by Q-PCR, confirming the RT-PCR expression. Q-PCR analysis indicated the level of mTert in the DP and DS increased after co-culture increased by 3.8 fold and 10.4 fold respectively; this change was statistically significant ($p < 0.02$).

Nanog

Nanog is a gene whose expression is associated with embryonic stem cells; co-expression of Nanog with Oct4 and Sox2 has been argued to be definitive for ES cells (Reviewed by Pan and Thomson 2007). Nanog was detectable in the DP and DS primary cells by Q-PCR; its level of expression in the DP and DS after co-culture increased by 1.4 fold and 2.6 fold respectively; this change was only statistically significant for the DS sample at a $p < 0.03$.

Oct4

Oct4 was detectable in the DP and DS primary cells by Q-PCR and the reported level of expression after co-culture increased by 11.5 fold and 5.4 fold respectively. The very low

level of expression was associated with increased variation in replicates, such that these apparently large changes were not statistically significant.

Oct4 expression was detectable in the heart; its level of expression similar to the DS and DP primary cells pre-co-culture which was at a lower level than the embryonic cardiomyocytes and the dermal follicular cells after co-culture.

Sox2

Sox2 was detectable in the DP and DS primary cells by Q-PCR; its level of expression in the DP and DS after co-culture increased by 1.9 fold and 6 fold respectively. This relatively modest change was statistically significant (DP $p < 0.04$ and DS $p < 0.01$).

Sox2 expression was detectable in the heart; its level of expression similar to the DS and DP primary cells pre-co-culture which was at a lower level than the embryonic cardiomyocytes and the dermal follicular cells after co-culture, in a similar manner to Oct4.

tbx5 and α -MHC

The expression of these genes were not detectable in the DP and DS primary cells before co-culture following Q-PCR for 60 cycles. However, *tbx5* expression was detected in DP primary cells (but not DS) after co-culture (data not shown). As a minimum, this reflects an increase in gene expression of at least 10^2 - 10^4 fold, although this is from a very low assumed level.

Tbx5 was expressed by both adult and embryonic heart at very similar levels between the two with the level of expression in the DP co-culture samples was less. α -MHC was expressed in both the DP and DS primary cells after co-culture. This reflected an increase in expression, admittedly from a very low level, of at least 10^4 - 10^5 fold.

In summary, there was increase in gene expression of all of the genes investigated from mouse dermal cells pre-co-culture compared to cells after co-culture with mouse cardiomyocytes. The expression of these genes was lower than the expression of the cardiomyocytes with the exception of *sca-1*. However, the gene changes were consistent with the RT-PCR findings and whilst dermal cell commitment to cardiomyocyte lineage may have been incomplete, there was increase in expression of a number of stem cell genes consistent with the development of the stem cell phenotype

4.4 Chapter 4 Discussion

Work described in Chapter 3 demonstrated that DP and DS did not spontaneously produce myotubes and spontaneous contraction when cultured independently, but that an inductive environment, such as may be found in the end bulb, could express this potential. Cells similar to cardiomyocytes, as determined by gene expression, have also been demonstrated in dermal follicular cell cultures as a result of 5-azacytidine treatment (Hoogduijn *et al.*, 2006). However, the use of such a potent de-methylation agent would not allow for investigation of any physiological cardiomyocyte differentiation and understanding of the pathways involved. In order to examine the molecular changes during commitment, DP and DS were co-cultured in an inductive environment; differentiating embryoid bodies.

ES cells spontaneously differentiate to cardiomyocytes, but only do so with high efficiency in hanging drop culture (Maltsev *et al.*, 1994). Dermal follicular cells were mixed with the ES cells to determine if this microenvironment promoted their differentiation towards a cardiomyocyte lineage as determined by gene expression. RT-PCR analysis indicated that, despite possessing an inductive environment suitable for ES cell commitment to a gene profile consistent with that of cardiomyocytes, the gene expression profile of both the DP and DS primary culture cells in these embryoid bodies remained substantially unchanged. Only one or two of the cardiomyocyte-associated genes increase their expression and some actually went down. This data suggested that the inductive environment in embryoid bodies was not suitable for this lineage commitment of DP and DS. One explanation for this is that recent work suggests that DP and DS may directly influence the embryoid body inductive environment; Liu have recently investigated the interactions between the dermal follicular cells and ES cells in 2D adherent and embryoid body co-culture. In 2D culture the DP and DS cells maintained ES cells in an undifferentiated state; the ES cells settled onto the dermal monolayer as they would on a MEF feeder layer and demonstrated maintenance for the entire observation period; up to 4 weeks/8 passages with no loss of colony formation with passaging (Lui *et al.*, 2008; in publication). The ES cells also maintained their pluripotent potential as indicated by differentiating towards neural, adipogenic and endoderm lineages following co-culture. The DP and DS cells were reported to express cytokines which were involved in the support of the ES cell e.g. LIF. The expression of these cytokines in the embryoid body were not sufficient to maintain the

ES cells in an undifferentiated state; as was observed here by gene expression consistent with ES cell cardiomyocyte differentiation and the apparent contractions in developing cell aggregations of mixed cells. This suggests that such inductive signals that are present within the embryoid body are insufficient to induce the dermal cells to adopt a cardiomyocytic fate.

An alternative approach was investigated. Co-culture has previously been shown to be inductive for cardiomyocyte differentiation; co-culture of dermal follicular cells with ES cells and embryonic cardiomyocytes of different species allowed the dermal follicular cells to be identified with species-specific primers for PCR without question of contamination, as has been previously used with co-culture of bovine DP with murine C2C12 cells (Rufaut *et al.*, 2006). This method of cross-species co-culture has been demonstrated to induce differentiation. Human MSC, after co-culture with embryonic rat cardiomyocytes, have been reported to express cardiac specific β -myosin indicate of differentiation, proposed to be as a result of communication between the two cells types cardiomyocytes supported by evidence of gap junctions (Plotnikov *et al.*, 2007). Therefore the rat dermal follicular cells were co-cultured with mouse embryonic cardiomyocytes and differentiation determined by changes in expression of the early transcription factors and function associated genes. Following co-culture, there was very little evidence of up-regulation of inductive genes. This absence strongly indicates that there was no substantial differentiation to the cardiomyocyte lineage. There was evidence of up-regulation of some structural genes in the DP and DS. The dermal follicular cells had up-regulated gene expression of α -MHC and cardiac actin both of which were undetectable in DP and DS primary cultures, genes that are essential to functioning cardiomyocytes (Jones *et al.*, 1996; Buckingham *et al.*, 2005). One explanation is that a cellular stretch response is responsible for the up-regulation of these genes. Sadoshima demonstrated that expression of sarcomeric MHC and smooth muscle α -actin were both induced to detectable levels in rat neonatal cardiomyocytes exposed to stretch (Sadoshima *et al.*, 1992). This was supported by the work of Fink which demonstrated α -sarcomeric actin RNA/DNA expression increased by 98% and protein by 40% in response to chronic mechanical stretch (Fink *et al.*, 2000). This may explain the induction of expression of these genes in the DP and DS cells after co-

culture with contracting embryonic cardiomyocytes; the cells may be expressing these genes in response to stretch in the absence of differentiation.

Therefore, the work described here indicated that cardiomyocytes from one rodent species did not induce cardiomyocytic commitment of dermal cells from a different rodent. Successful cross-species induction of stem cell differentiation has been reported for rat cardiomyocyte induction of mouse MSC differentiation (Fukuhara *et al.*, 2003). In this system, murine MSC co-cultured with rat cardiomyocytes went on to demonstrate contractions and myotube formation, associated with the expression of myosin heavy chain, troponin I and gap junction connexin-43. However, this study did not exclude fusion as a potential mechanism for apparent mouse differentiation; in addition there is little evidence for mouse cardiomyocytes inducing cardiomyocytic differentiation in MSC. It is noted that co-culture of the dermal cells with cardiomyocytes was dependant on cross-species communication; previous experiments by other groups have indicated that mouse and rat cells of other tissues can communicate in a similar co-culture system. Condorelli showed primary endothelial cells from E9 mouse dorsal aorta could communicate with rat cardiomyocytes; the endothelial cells differentiated into contracting cardiomyocytes and expressed a limited number of cardiac markers as well as contributing to myocardium formation in a post ischemic heart (Condorelli *et al.*, 2001). Xu also showed that mouse bone marrow stromal cells could communicate with rat neonatal cardiomyocytes; the bone marrow stromal cells trans-differentiated into cells with a cardiac phenotype and gap junctions between the two cell types (Xu *et al.*, 2004). Although rat and mouse cells are therefore capable of communicating with one another, especially in a differentiation setting, this may not be suitable for the dermal follicular cells and the mouse cardiomyocytes may not be capable of inducing cardiomyocyte expression in a mesenchymal-like cell population. In order to determine whether the dermal follicular cells are capable of significant differentiation by this method, without the added complication of cross-species communication, the DP and DS were co-cultured with embryonic cardiomyocytes of the same species.

When the rat dermal follicular cells were cultured with the rat embryonic cardiomyocytes there was detectable increase in expression of some cardiomyocyte-associated genes as shown by RT-PCR, the incomplete profile indicated that the embryonic cardiomyocytes

failed to induce complete cardiomyogenesis. The expression of Nkx2.5 and GATA4 were detectable in some, but not all, co-cultured DP and DS. In addition to the previously detected α -MHC expressed in some of the rat DP and DS co-culture samples, and cardiac actin in all the DP and DS samples, troponin I was detectable in one of the DP samples. However, there was evidence that some induction may be occurring but there was no detectable *tbx5* expression. It is noted that the number of RT-PCR product bands for GATA4 and Nkx2.5 differed when comparing the rat heart to the rat dermal cells after co-culture. GATA4 has two isoforms which were detected with the primers used here; these are shown on figure 4.14. This is consistent with previous findings, as detected by immunoblot analysis by Morimoto, where the larger size isoform was predominantly found in cellular nuclear extracts and was phosphorylated; GATA4 phosphorylation promotes transactivation ability in cardiomyocytes (Morimoto *et al.*, 2000). This isoform correlated with one of the RT-PCR bands in the heart sample in figure 4.1.4; however, this band was not detected in the rat dermal cells indicative of an absence of full cardiomyocyte commitment. The identity of the second RT-PCR product band associated with Nkx2.5 as was detected in one of the dermal co-culture samples is unknown. There are isoforms associated with human Nkx2.5 but not yet reported for rat Nkx2.5 therefore this could be an, as yet unidentified, isoform. However, the difference in detected gene products between the heart and dermal cell samples is supportive of a lack of contamination of cardiomyocytes into the cells sorted as being dermal in origin. If this were the case you would expect to see the same gene product in both samples. In summary, although a number of cardiomyocyte structural genes were detected, the entire dermal co-culture cell population were sampled and therefore it is not possible to determine if the genes detectable were expressed within the same cells.

When the mouse DP and DS were cultured with the mouse embryonic cardiomyocytes there was a different expression profile detected to that of the rat dermal cells. There was detectable expression of a number of the structural genes, in one instance expression of all of the function-associated cardiomyocyte genes as detected by RT-PCR at low level, however there was an incomplete gene expression profile with absence of a number of inductive genes indicative of a failure to induce cardiomyogenesis.

There was detectable low-level expression of *tbx5* in a number of dermal co-culture samples no detectable expression of *Nkx2.5* and *GATA4*. Of the structural genes, one sample demonstrated expression of all of the genes investigated and a number of these were investigated by Q-PCR to determine quantitation of these genes; Q-PCR indicated that the level of these genes in the DP and DS samples was so low that if there is indication of differentiation it is a very rare event.

It is noted that the mouse co-culture cells did not express *Nkx2.5* but had low level *tbx5* expression while the rat dermal co-culture cells did not express *tbx5* but had low level *nkx2.5* expression. *Nkx2.5* and *tbx5* synergistically activate cardiac genes and are necessary for cardiomyocyte differentiation (Hiroi *et al.*, 2001) and therefore the absence of expression of one gene; either *tbx5* or *Nkx2.5* is suggestive of failure of cardiogenesis in the rat dermal cells.

With the mouse co-culture dermal cells changes in gene expression appeared to be very modest except for *sca-1* expression. *Sca-1*, a cell surface antigen which has been implicated in cardiac stem cell populations, was expressed in all samples which suggested investigation of stem cell markers. *Sca-1*, *Oct4*, *Sox2*, *Nanog* and *Tert* were investigated by Q-PCR where all of these stem cell markers were apparently up-regulated post-co-culture. *Nanog*, *Oct4* and *Sox2*, all expressed by the mouse dermal follicular cells following co-culture, are considered markers of pluripotency and are normally expressed by undifferentiated ES cells.

The expression of these genes is consistent with co-culture changing the properties and/or numbers of stem cells from the DP and DS. However, it is not possible to determine if all the transcripts were detected in the same cells. There is the question of contamination; data from FACS experiments indicated that the maximum level of possible spill over, i.e. cardiomyocytes collected as being dermal in origin was less than 1 in 10,000. However, the level of expression of *Oct4* and *Sox2* in the embryonic cardiomyocytes could account for the detected level of expression in the dermal cells with a contamination level of 1 in 100,000 cells. Thus contamination cannot be excluded as one explanation. However, such very minor levels of contamination cannot explain the *sca-1* expression, *Nanog* (which would require contamination levels of near 1 in 6 cells) or *Tert* (which would require

contamination levels of near 1 in 3 cells). In addition, the difference in isoform bands, as described for *nkx2.5* and *GATA4* with rat dermal cells, is not consistent with contamination.

Sca-1 expression cannot be due to contaminative cell types as the expression in the co-culture cells is greater than the cardiomyocytes as determined by Q-PCR analysis which is supported by RT-PCR results with strong evidence of an absence of contamination. It is unlikely that this is due to more cells being examined after co-culture compared to before co-culture which are expressing the same amount of sca-1 as the expression change, 7.5fold for the DS cells, is higher than the number of cells being put into the co-culture. This therefore suggests that there is induction of expression of sca-1 in cells and potentially an increase in cell number.

Cells expressing sca-1, as well as c-kit and *Isl1*, have been identified in the adult heart and are suggested to be capable of differentiation into cardiomyocytes, such cells are proposed to represent a cardiac progenitor cell sub-population that is capable of self-renewal and differentiation into mature, contracting cardiomyocytes (Pfister *et al.*, 2005); sca-1 is therefore proposed as a putative marker to identify cardiac progenitor cells (Oh *et al.*, 2003). In the work of Oh, it is noted that cardiac sca1+ve cells express none of the cardiac structural genes that were investigated including α -MHC, atrial and ventricular MLC or α -actin among others, however they did express the cardiac transcription factors *GATA4* and *Mef2c* as well as having high levels telomerase activity not detected in the cardiac sca1⁻ fraction (Oh *et al.*, 2003). This profile may be comparable to the rat dermal follicular cells after co-culture with the embryonic cardiomyocytes as shown in figure 4.14.

Oh also showed sca1+ve cells were capable of homing to site of myocardium injury (Oh *et al.*, 2003). In addition, bone marrow-derived adult MSC expressing sca-1 have been demonstrated to differentiate into cardiomyocytes (Gojo *et al.*, 2003). Skeletal muscle-derived cells express sca-1 and are capable of differentiating into myogenic cells (Asakura *et al.*, 2002) as well as, on over-expression of sca-1, contributing to muscle regeneration (Qu-Petersen *et al.*, 2002). Most interestingly, sca-1 has been implicated in cellular commitment to myocyte differentiation; using C₂C₁₂ cells, sca-1 was expressed at low levels on the surface of proliferating myoblasts but was up-regulated when the cells left the

cell cycle and differentiated to cardiomyocytes; expression then down-regulated in differentiated myotubes. Removing sca-1 from the cell surface or blocking it resulted in proliferation, interference with myotube formation and persistent expression of early markers of myogenic differentiation indicating defective myogenesis (Epting *et al.*, 2004). As noted by Epting, mice null for another Ly-6 super family members, of which sca-1 is one, resulted in a primary defect of myocardial development and embryo lethality (Zammit *et al.*, 2002). These observations suggest an important role for Ly-6 family members in muscle development. Sca-1 expression in the dermal follicular cells, especially at the high levels detected in the mouse DP and DS primary culture cells is therefore very interesting and may confer these properties described.

Nanog requires expression of Oct4 and Sox2 for cardiomyocyte commitment which may suggest the detectable expression Oct4 and Sox2, although small and possibly due to contamination, may be real. However, this population based study cannot indicate if the expression of these three transcripts were in the same cells. In addition, somatic cells do not express telomerase and the primary cells used for experimentation here were not transformed therefore there is a high probability that the expression of Tert in these cells was from cycling stem cells, an increase in the number of stem cells or increasing expression levels of Tert in existing stem cells. mTert, expressed in the co-culture samples, is a key gene in the investigation of stem cells and their progeny; it is expressed in the stem cell compartment of several adult tissues (reviewed by Sarin *et al.*, 2005; Flores *et al.*, 2006; Siegl-Cachedenier *et al.*, 2007).

The overall level of expression of gene expression for the DP and DS, as determined by quantitative PCR, was generally of a level lower than that detected for the embryonic cardiomyocytes but higher than that of the adult heart. For analysis of successful differentiation, if the profile of the dermal cells is reminiscent of the adult cardiomyocyte, then this is suggestive that these cells if used clinically, having a profile close to that of the embryonic cells i.e. a more progenitor, stem cell-like, may indicate they will be capable of proliferation and may be recognised in a similar manner to the native stem cell population and mobilised more efficiently.

In current literature there are a significant number of studies into the differentiation of other MSC, as well as various other types of stem cells, into cardiomyocytes. A lot of these investigations conclude successful differentiation based on the expression of a small number of cardiac associated genes, which are included here, however these genes only represent a very small selection of the genes important in the cardiomyocyte. Yoon concluded that rat bone marrow MSC had undergone trans-differentiation after co-culture with neonatal cardiomyocytes based upon the induction of expression of sarcomeric alpha-actinin alone (Yoon *et al.*, 2005). Wang also concluded that rat bone marrow MSC had differentiated into cardiomyocytes after co-culture with adult rat cardiomyocytes based upon the induction of expression of α -actin and troponin T as well as desmin and calponin however it is noted these latter two genes are not specific to cardiac tissue (Wang *et al.*, 2006). Moscoso concluded that pig bone marrow MSC differentiated into cardiomyocytes suitable for transplantation, after treatment with 5-azacytizine, based upon induction of expression of α -actin in a fraction of the cells (Moscoso *et al.*, 2005). Xu concluded adult human bone marrow MSC has differentiated to cardiomyocytes, after treatment with 5-azacytizine, based upon desmin, β -MHC, troponin T and α -cardiac actin as well as the morphology of the cells (Xu *et al.*, 2004). In all of these cases the number of genes investigated is only a fraction of cardiomyocyte-associated functional genes important without the inclusion of any transcription factors. If conclusions made in this chapter were based upon such a limited gene expression profile, then the dermal follicular cells would be deemed capable of differentiating to cardiomyocytes. We detected, by RT-PCR, expression of cardiac actin, α -MHC and troponin I in the dermal follicular cells after co-culture with species matched embryonic cardiomyocytes, and two of these after cross-species co-culture in addition to the genes mentioned above there was also demonstration in once co-culture sample of tropomyosin, titin and MLC1A (DP2 in figure 4.15). In same species co-culture, particularly with mouse dermal follicular cells and mouse embryonic cardiomyocytes, there was evidence of induction of expression of genes by RT-PCR relevant to cardiomyocytes, including stem-cell associated genes, which were not significant as determined by Q-PCR. However, under this less stringent system of identification and confirmation of cell differentiation, as is demonstrated in a number of pieces of current literature, the conclusion would be successful differentiation of the dermal follicular cells to

cardiomyocytes. Further investigation, as shown here by Q-PCR and indeed a larger gene expression profile being examined by RT-PCR, indicates the dermal cells are not expressing all the genes expressed by a native cardiomyocyte. Furthermore when the genes are detected they are not at comparable expression levels to the cardiomyocyte and in some instances could be a result of contamination. This suggests potential for cardiomyocytic differentiation, however full differentiation has not occurred.

It is therefore vital in future studies investigating cardiomyocyte differentiation, especially when the cells are cited as having functional and contractile capabilities based on gene expression, that an extensive array of genes are probed for. It poses the question: do we need to reconsider how cardiomyocyte differentiation is defined and, considering the impact of this area of research, revisit a number of pieces of work. It is of concern that the investigations by others do not show that this has been taken into consideration and, in a number of cases, ongoing clinical trials and *in vivo* work is based upon such limited results.

Based on the results presented here, we cannot conclude with confidence that the dermal follicular cells have demonstrated full differentiation as they do not express basic genes expressed in the embryonic, as well as adult, cardiomyocyte. In summary, when the dermal follicular cells are co-cultured with embryonic cardiomyocytes of the same species we see the most marked expression profile alteration of cardiac inductive and function associated genes, with an increase in the levels of expression to detectable levels or above that previously identified. The dermal follicular cells are proposed here as a potential cell type for investigating somatic cell differentiation towards a cardiomyocyte lineage. The results shown here of gene expressing changes in co-culture are exciting and promote further investigation into the dermal follicular cells and their place in cardiomyocyte stem cell research.

These data suggest that there may be a stem cell population resident within the dermal follicle. The absence of definitive differentiation of the dermal follicular cells to cardiomyocytes may indicate the differentiation potential of the cells only applies to a sub-population of the DP and DS; the spontaneous differentiation and gene expression changes may be attributed to these cells. Population based studies can't be used to examine a sub-population of stem cells therefore it is necessary to use a method of investigation that will

allow for the identification of sub-populations that may be responsible for the gene expression changes observed here. Existing stem cell models that use surface antigen expression have been demonstrated to not be entirely reliable as there is possibility of loss of antigens or presence of contaminating cell types. Therefore, considering there is suggestion of up-regulation of Tert in the dermal cells, a phenotypic marker of stem cells, the mTert-GFP transgenic mouse was investigated to determine if it could be useful in studying stem cells of the dermis and their relationship with stem cells involved in cardiogenesis. The mTert-GFP mouse is an animal model that has recently been indicated to identify populations of adult cells with stem cell like capabilities (Breault *et al.*, 2008); it may allow identification of a stem cell population within the DP and DS structures, or the dermis, that is better suited to differentiation.

5 The mTert-GFP mouse model

Complex combinations of cell surface antigens are used to identify and isolate stem cells from adult and foetal tissue. This is not always a reliable method of isolation as cell surface antigens can change or be degraded by enzyme activity when dissociating cells from tissues. An alternative method of isolation, which defines side population cells, is by detecting the functional properties of stem cells by, for example, their ability to efflux Hoechst dye. However, this does come with caveats such as potential contaminating cell types. As a result the two methods are often used in combination as tools to enrich stem cell populations from tissues.

One common feature of stem cells is their long term relative resistance to cellular senescence despite multiple rounds of cell division. Telomerase is a ribonucleic protein complex that helps maintain the telomeric ends of chromosomes; these telomeres are normally shortened with each cell division in somatic cells, until a critical threshold length is reached which induces cellular senescence. Therefore maintenance of telomeres or induction of telomerase activity is a means of preventing senescence which is associated with the self-renewal of stem cells. Telomerase is normally undetected in most somatic cells but is expressed in adult male germ cells and proliferative stem cells of renewing tissues.

In the mouse, the transcription of mTert is tightly regulated and its gene expression profile correlates with telomerase activity; the expression of mTert is down-regulated with somatic cell differentiation. Furthermore, mTert has been reported to have a direct role in regulating adult stem cell proliferation and mobilization. Telomerase regulation in stem cells is primarily controlled by Tert. In the mouse a reporter gene system using the mTert promoter may allow for the identification of telomerase expressing cells; a biomarker for stem cells in adult tissues. In order to examine this, transgenic mouse lines expressing GFP under the control of the mTert promoter was produced; the mTert-GFP mouse model (Breault *et al.*, 2008). Preliminary data showed that, in a manner similar to the *in vitro* studies, cells expressing native Tert also expressed GFP, and that when GFP was absent, Tert was also undetectable. In the tissues studies so far (gut and blood), somatic stem cells could be identified on the basis of their expression of GFP using immunofluorescence or FACS. In the peripheral blood, cells expressing GFP included B-cells (~45%), T-cells (~25%), myeloid cells (~25%), as well as a rare

population of circulating haematopoietic progenitor/stem cells, which in culture formed GFP+ve CFU-GEMM colonies (Breault *et al.*, 2008).

Analysis of the germ cell populations indicated that the largest percentage of GFP+ve cells were found in the mitotically active primary spermatocytes. In comparison, a smaller fraction spermatogonia and/or secondary spermatocytes as well as spermatids also expressed GFP. These data were consistent with previous reports of telomerase activity and validated GFP expression as a marker of male germ cells in mTert-GFP mice. GFP mRNA and protein were localized within the seminiferous tubules and corresponded to primary and secondary spermatocytes, consistent with the FACS analysis (Breault *et al.*, 2008).

To functionally confirm that GFP expression marked the HSC subset of mTert-GFP BM, the capacity of high GFP+ve cells from whole bone marrow to exhibit long-term, serial, multilineage reconstitution was assessed. Long-term engraftment, defined as persistence of donor cells for more than 5 months following transplantation, was demonstrated in recipient mice receiving GFP+ve cells by FACS analysis of bone marrow. Serial bone marrow transplantation into secondary female recipients was performed using GFP+ve bone marrow cells obtained from a primary bone marrow transplant recipient 5 months after the initial transplantation. The female recipient received GFP+ve cells which demonstrated long-term HSC engraftment, surviving 5 months following serial transplantation, and peripheral blood chimerism was confirmed indicating multilineage reconstitution (Breault *et al.*, 2008).

The mTert-GFP transgenic mouse is therefore a model system to facilitate the identification, isolation and functional characterisation of putative stem cells using a functional as opposed to an antigenic marker.

5.1 Characterisation of the hair follicle and dermis of the mTert-GFP mouse

The mTert-GFP mouse was used to investigate the DP, DS and bulge region to determine if Tert could identify stem cell populations of the dermis. The DP and DS primary culture cells demonstrated low level detectable expression of Tert by RT-PCR (Chapter 3 figure 3.14), however the end bulb had low level expression and the clonal cell lines expressed Tert, therefore the DP and DS were investigated in hair follicle sections to determine Tert gene expression *in vivo*. The theory that a sub-population of

the DP and DS may be more stem cell-like in their properties may be indicated by a proportion of these structures expressing Tert.

Therefore the initial step in investigating the mTert-GFP mouse model was to consider the cells of interest in the hair follicle, the DP and DS, to determine if they could be located by their GFP expression and distinguished from surrounding hair follicle structures as well as the surrounding inter-follicular dermis. According to RT-PCR analysis (shown in Chapter 3, figure 3.14) the DP and DS primary culture cells expressed low level Tert however this expression was higher in the end bulb; the theory that a sub-population of the DP and DS may be more stem cell-like in their properties may be indicated by a proportion of these structures expressing Tert. Identifying cells expressing Tert from the hair follicle may provide a better method of isolation of cells for differentiation investigation rather than the manual dissection method that has previously been used.

mTert-GFP status was assigned to adult mice by blood typing for GFP+ve cells; in GFP+ve mice there was approximately 4% of the blood cells positive for GFP-associated fluorescence which, using the same gating, was 0% for WT mice (data not shown). Embryos were assigned GFP status by placenta removal and PCR tissue typing (Methods section 2.5.2).

5.1.1 Histological investigation of the mTert-GFP vibrissae follicles

Follicles from mTert-GFP mice were investigated and compared to WT littermates:

1. Vibrissae follicles

Vibrissae follicles were examined initially as they are the largest follicles in the mouse and a range of follicles at different cell cycle stages are typically present simultaneously (Davidson and Hardy 1952) as discussed in Chapter 1.

2. Smaller hair follicles on the face pad

The bulb region is an area of the hair follicle which has previously demonstrated Tert expression as indicated by its role here in the transition of hair from telogen (resting) to anagen (growing) (Sarin *et al.*, 2005). The bulge region of the vibrissae follicles is difficult to identify in cross sections of the follicles; the smaller hair follicles of the face pad, surrounding the vibrissae, were in sagittal sections and thus allowed potential identification of the bulge region in the same plane as the end bulb.

3. Developing vibrissae follicles in the E14.5 embryo

Tert plays an important role in the hair follicle, one which is independent of its role in telomere lengthening. Tert over expression, in the absence of telomere length changes, was found to be associated with stem cell mobilisation, hair growth with promoted transition of hairs from telogen to anagen, with increased skin thickness and increased stem cell proliferation (Flores *et al.*, 2005). Telomerase deficiency was associated with a larger number of stem or progenitor cells in the epidermal and hair follicle compartment i.e. the presence of more inactivated stem cells (Flores *et al.*, 2005). The E14.5 mouse was chosen for investigation of the vibrissa follicles; developing embryonic follicles, where the progenitor cells are proliferating and differentiating to produce the cells of the bulge as well as DP and DS structures may represent a time of stem cell mobilisation that requires Tert expression. At E10-11 there are no vibrissa follicles in the face pad; at E12 follicle plugs form as epidermal down growths surrounded by dermal sheath. The DP is formed at E14 and within a day later the hair cones form; these are hollow cones that give rise to the inner root sheath which develops by hardening of certain cells from the hair matrix. The cone extends upwards to form the hair canal at E15 (Davidson and Hardy 1952). Therefore, at E14.5 the DP and DS are both present with the follicles, as the hair canals are formed. Therefore the E14.5 mouse embryo was chosen for investigation of the developing vibrissa follicles.

4. Neonatal skin

Recently it has been reported that Tert triggers a rapid change in gene expression that significantly overlaps with the program controlling natural hair follicle cycling; it is thought that Tert activates the expression of hair growth genes and inhibits expression of anti-hair growth genes (Choi *et al.*, 2008). These gene expression changes, which are linked to changes in Tert levels, appear to be independent of alterations in hair follicle cycling. This may indicate Tert plays a more important role in the follicle during hair growth and, therefore, Tert expression may be associated with hair formation, and increase in expression to detectable levels in neonatal skin when the hair is formed and growing. Hair emerges through neonatal skin at age 2-3 days old (9-10 days after embryonic age E14) and secondary follicles form at 5-8 days old (Davidson and Hardy 1952) therefore, the dermis of the neonatal torso skin was investigated in the mTert-GFP mouse neonates at 5 days old, when the skin was expected to be particularly active.

The hair follicles contain a dense network of blood vessels, therefore discriminating between cells that may be present in the circulating blood from the dermal derived cells is necessary. CD45 and CD34, identified by antibody labelling, were used for this purpose. CD34 is expressed on haematopoietic cells including the HSC where it expressed most strongly on the primitive cells and lost with differentiation; it plays a role in cell to cell adhesion and signal transduction where it is involved in regulating other haematopoiesis associated genes (Holyoake and Alcom 1994). CD34 is also expressed by vascular endothelial cells (Fina *et al.*, 1990). CD45 is expressed exclusively by haematopoietic cells including HSC (Trowbridge and Thomas 1994). Co-labelling immunofluorescence techniques are described in method section 2.12.2. GFP was detected using an anti-GFP antibody to indicate cells which were Tert+ve at the time of tissue sampling as described in methods section 2.12.1.

5.1.1.1 GFP epifluorescence of adult vibrissae follicles

GFP epifluorescence was initially investigated on entire sectioned hair follicles to determine if GFP expression in the hair follicle was detectable above auto-fluorescence.

Over 20 vibrissa follicles from the mTert-GFP mouse were compared to sex matched, WT littermate follicles were taken from matched vibrissa locations to ensure cell cycle staging was also matched. 10µm sections were collected from each vibrissa follicle and in excess of 5 sections per follicle were visualised for GFP fluorescence (data not shown).

There was no fluorescence detectable above autofluorescence in the follicles investigated (data not shown); autofluorescence is a common problem with the skin and the follicles which is overcome by signal amplification with antibody labelling.

GFP expression may have been present but too low to be detectable above autofluorescence; the hair follicles were investigated using antibody labelling which would amplify any GFP signal present.

5.1.1.2 Antibody labelling of adult vibrissae follicles

The testes of mTert-GFP mice were antibody labelled as a positive control to confirm GFP status of the mouse, as assigned by blood typing. GFP antibody specificity was also confirmed as present to a detectable level in an organ known to be Tert+ve. Representative testes sections, from 5 mTert-GFP mice and 5 WT littermates are shown in figure 5.1. In mice assigned GFP+ve status, anti-GFP labelling was detectable in the

region of mature sperm heads, spermatids and the stem cells of the seminiferous tubules; the spermatogonium (figure 5.1iv) as described in the analysis of the germ cells when the mTert-GFP mouse was first established (Breault *et al.*, 2008).

With confirmation of the GFP status of the animals and anti-GFP antibody labelling correlating with known stem cells of the testes, the vibrissa follicles were investigated. 5 mTert-GFP mice and 5 WT littermates were used. Both face pads were excised and sectioned in their entirety; sections of the end bulb were antibody labelled. Figure 5.2 shows matched hair follicles.

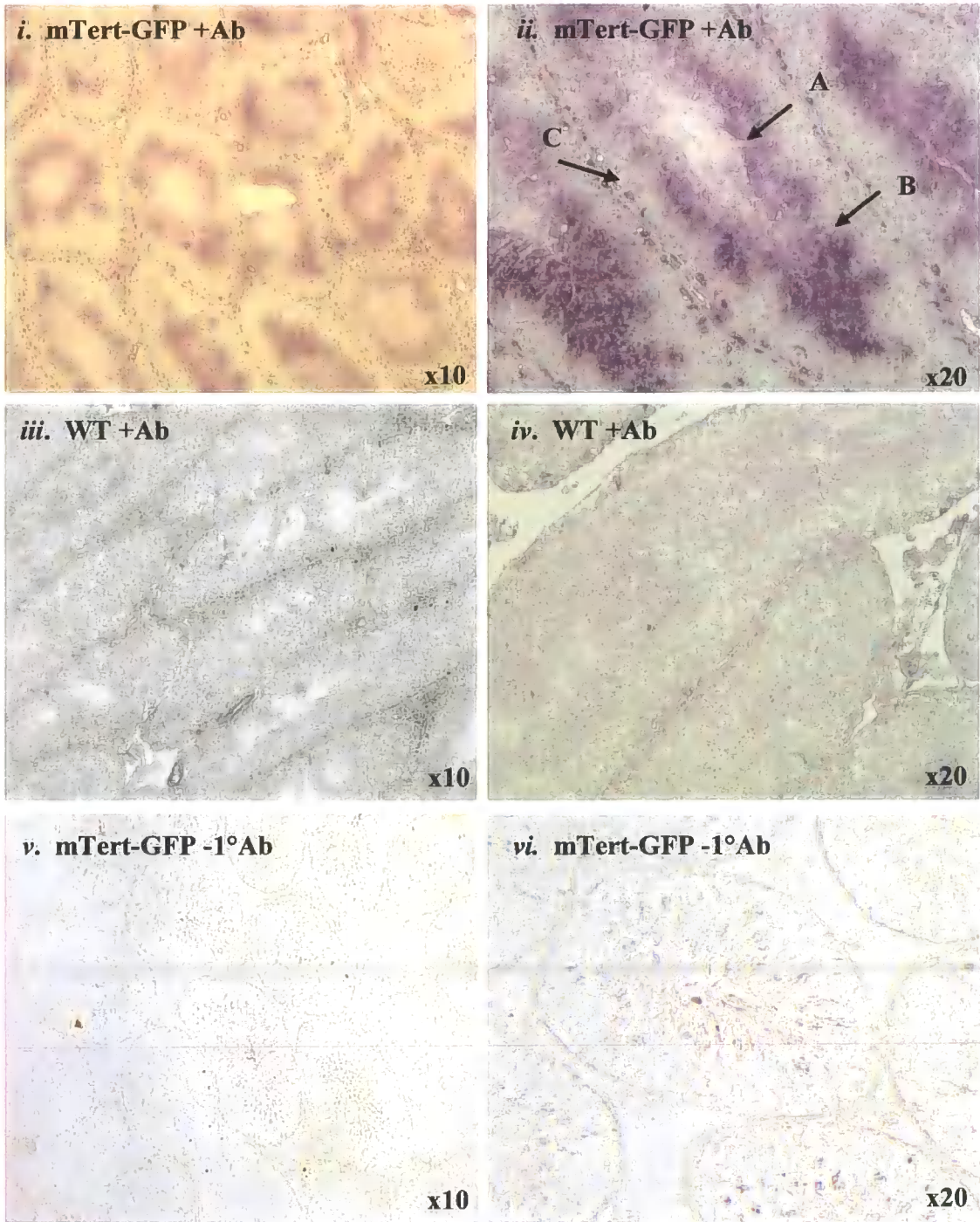
Anti-GFP labelling was identified in approximately 10% of the vibrissae follicles; these were the larger of the vibrissae follicles where the DP and DS were discernable. Relatively strong anti-GFP labelling was associated with the DP and DS, with less intense staining seen in the cortex and medulla.

5.1.1.3 Antibody labelling of adult face pad

Of the 5 mTert-GFP mice and 5 WT littermates, where both face pads were excised and sectioned, the hairy skin surrounding the vibrissae follicles were assessed for anti-GFP labelling. Representative images are shown in figure 5.3.

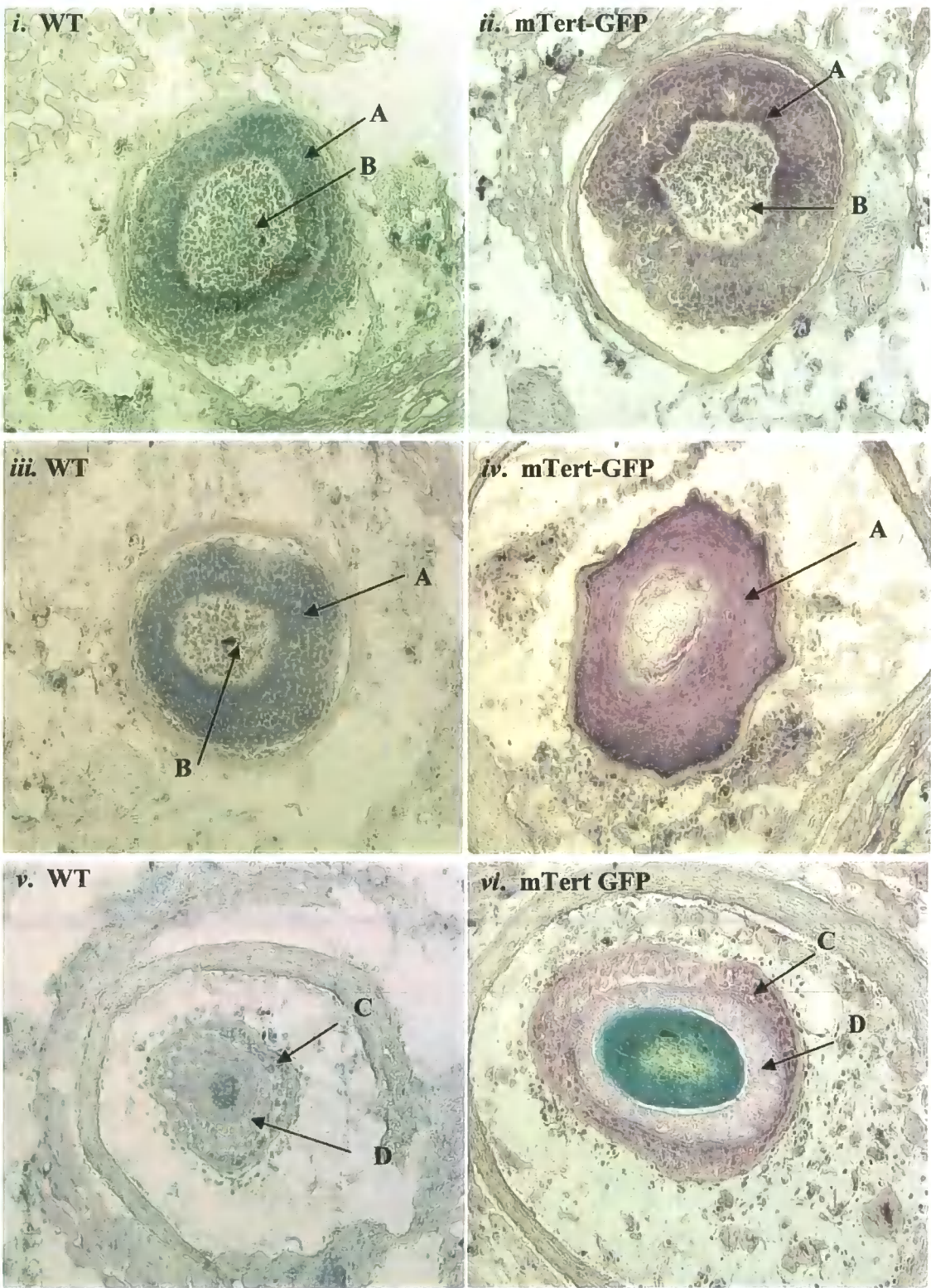
The dermis of the WT mice indicated non-specific binding of the GFP antibody associated with the region of the sebaceous gland. In the dermis of the mTert-GFP mouse there was positive labelling of the end bulbs of developing follicles however the DP and DS could not be distinguished within these structures. GFP positive cells were visualised in just 10% of distinguishable follicles present.

Figure 5.1: Immunohistochemical labelling for GFP cells in the testes of the mTert-GFP mouse



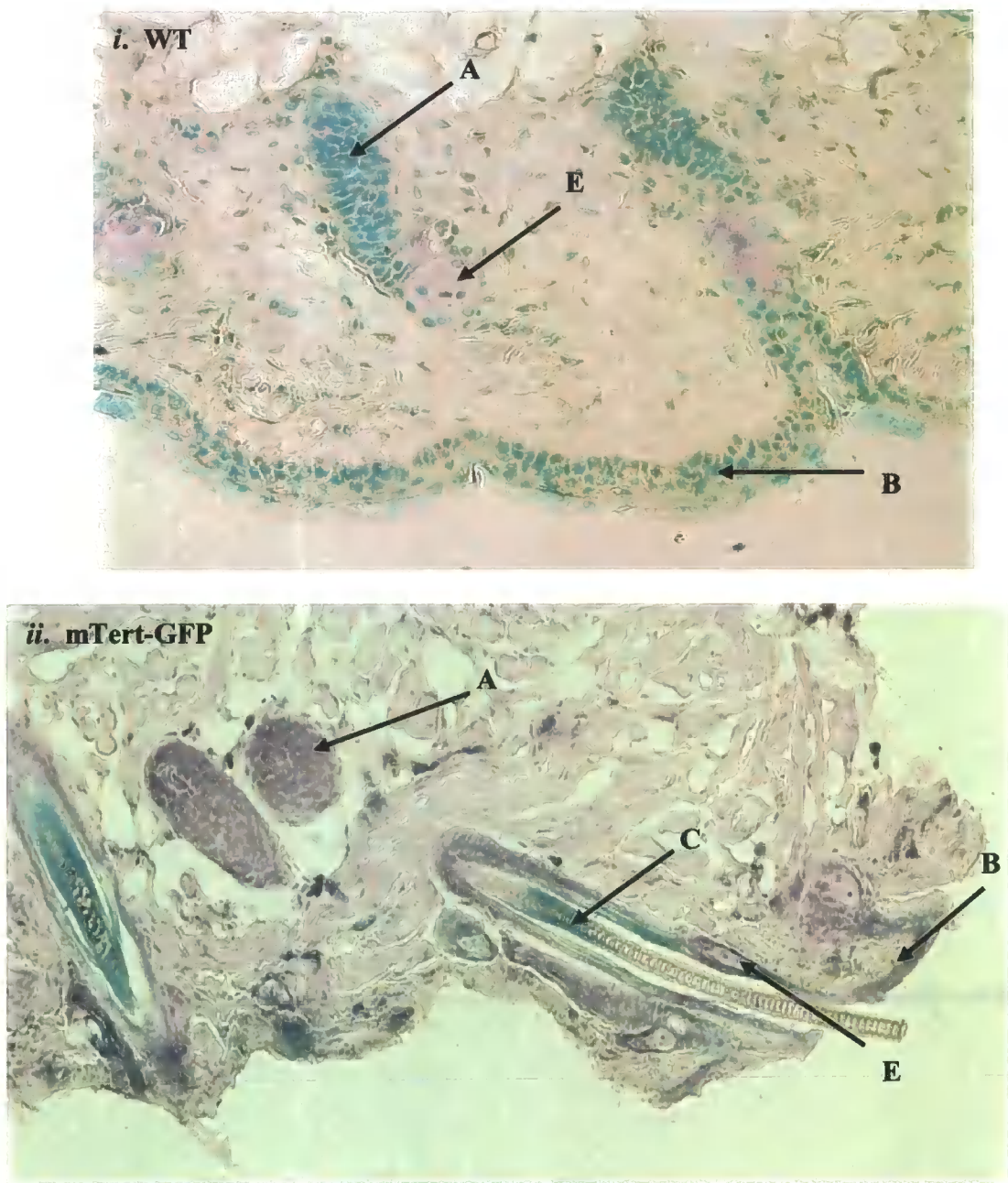
Anti-GFP antibody labelling detected by VIP (purple) (as described in Methods 2.11) on testes from an mTert-GFP mouse (i,ii,v,vi) and testes from a WT littermate (iii,iv). VIP was detectable in the region of mature sperm heads (A), spermatids (B) and a number of the spermatogonium (C) closely associated with the basement membrane. Compared with the WT mouse (iii, iv), substantive and specific labelling was seen in the testes of the mTert-GFP mouse. Representative phase images.

Figure 5.2: Immunohistochemical labelling for GFP+ve cells in vibrissae follicles of the mTert-GFP mouse



Anti-GFP antibody labelling detected by VIP, counterstained with methyl green, on hair follicles from an mTert-GFP mouse (ii,iv,vi) and developmentally matched follicles from WT littermates (i,iii,v). Relatively strong anti-GFP labelling was associated with the DP (B) and DS (A), but less intense staining was seen in the inner root sheath (D) and outer root sheath (C). Bright field images at x20 magnification.

Figure 5.3: Immunohistochemical labelling for GFP+ve cells in the vibrissae of the mTert-GFP mouse



Anti-GFP antibody labelling detected by VIP, counterstained with methyl green, on skin surrounding the vibrissa follicles from the mTert-GFP mouse (ii) and developmentally matched skin of WT littermates (i). There was relatively strong anti-GFP labelling of the end bulb structures (A) of the mTert-GFP hair follicles. The hair shaft (C) of the mTert-GFP mouse was negative with a degree of labelling in the epidermis (B). There was non-specific labelling in the region of the sebaceous gland (E) as shown on the follicles of the WT skin. Representative bright field images at x20 magnification.

5.1.1.4 Antibody labelling of embryonic vibrissae

E14.5 embryos from two unrelated females were investigated; sagittal sections of 5 mTert-GFP embryos and 5 WT littermate embryos were examined. The developing vibrissae follicles were apparent in rows and in excess of 10 sections from each embryo were antibody labelled.

There were no GFP+ve cells associated with the follicles or the surrounding dermal tissue in any of the embryo sections investigated (data not shown).

5.1.1.5 Antibody labelling of neonatal dermis

Five mTert-GFP neonates and 5 WT littermates were used for dermal cell preparation. Approximately 4cm² of skin was removed from each neonate yielding a total of 20cm² dermis; in excess of 200 sections of skin were antibody treated for both mTert-GFP and WT neonates.

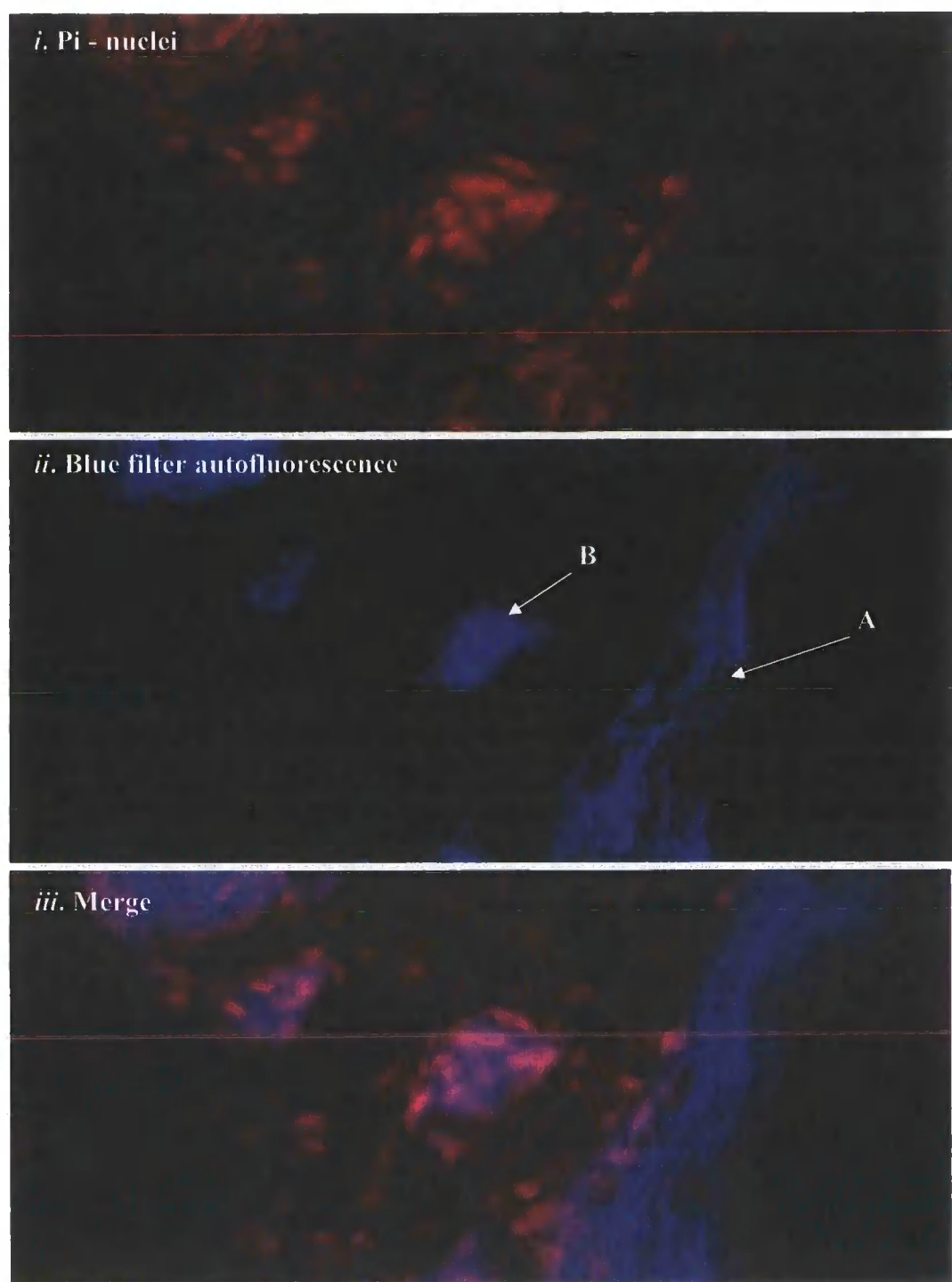
A number of GFP+ve cells, associated with the hair follicles, were identified in the dermis. Representative images are shown in figures 5.5-5.10. Figure 5.4 shows there was blue filter autofluorescence, in the absence of antibody labelling in both mTert-GFP and WT sections, of the epidermis and the cell-dense follicles, this was taken into account when analysing the mTert-GFP skin sections.

Figure 5.5 shows WT dermis with CD45 staining; there were no detectable GFP+ve cells. A representative image of a similar mTert-GFP section of dermis shows the identification of a dermal GFP+ve cell which was CD45-ve, as shown in figure 5.6. Figure 5.7 shows WT dermis with CD34 staining; there were no detectable GFP+ve cells. A representative image of a similar mTert-GFP section of dermis shows the identification of a dermal GFP+ve cell which was CD34-ve, as shown in figure 5.8.

On occasion GFP+ve cells were identified in the dermis which co-labelled for anti-CD45 (figure 5.6). These cells were associated with the end bulbs where there was a network of capillaries and appeared to be located in a blood vessel-like structure indicative of HSC.

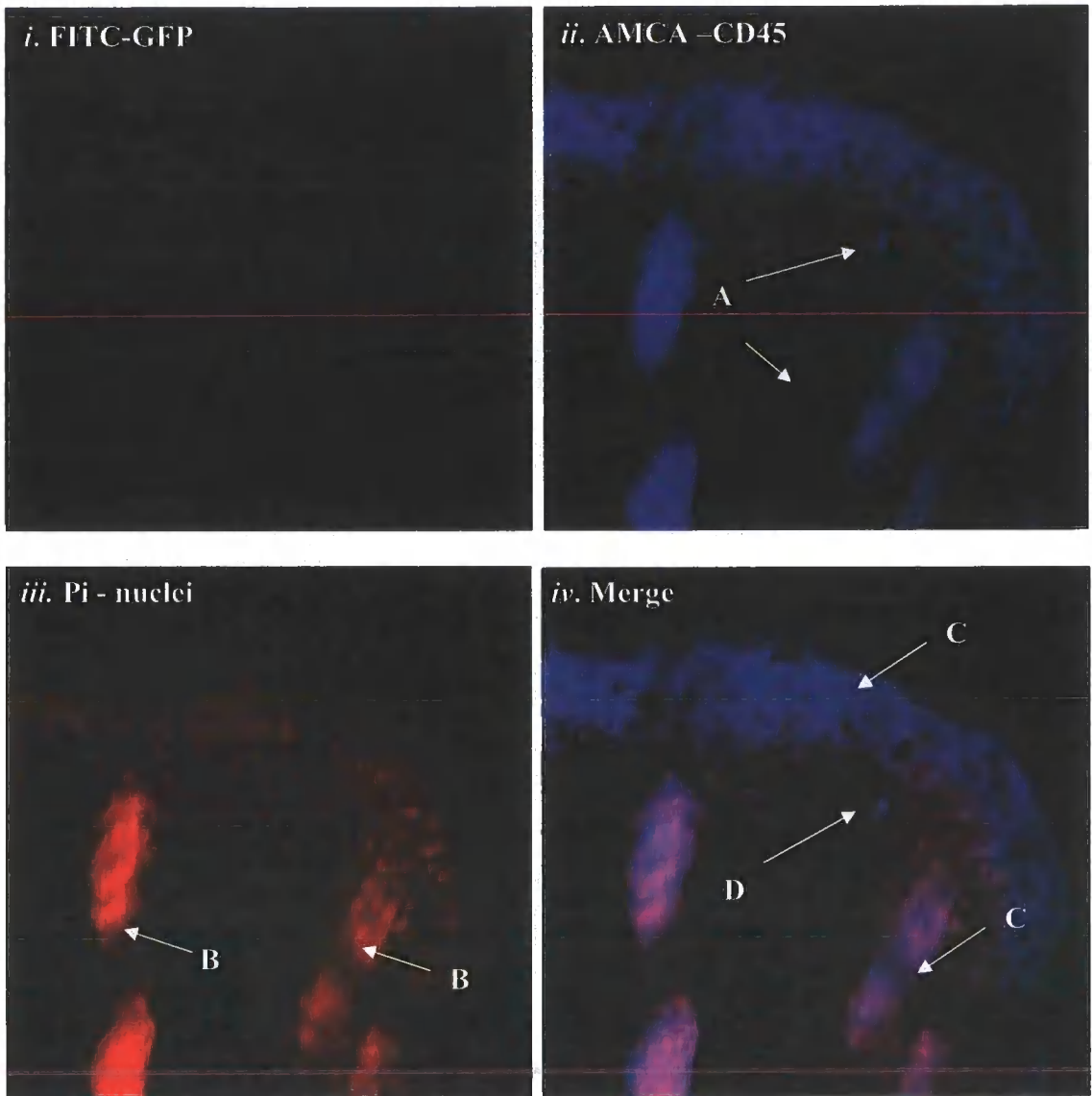
GFP+ve cells were identified in one of two locations in the dermis. The first was the dermis surrounding the follicular end bulb as demonstrated in figure 5.9. The second was the inter-follicular dermis where cells were located higher up the follicle as demonstrated in figure 5.10. These cells were CD45-ve and CD34-ve.

Figure 5.4: Neonatal skin of the WT mouse showing epidermal autofluorescence



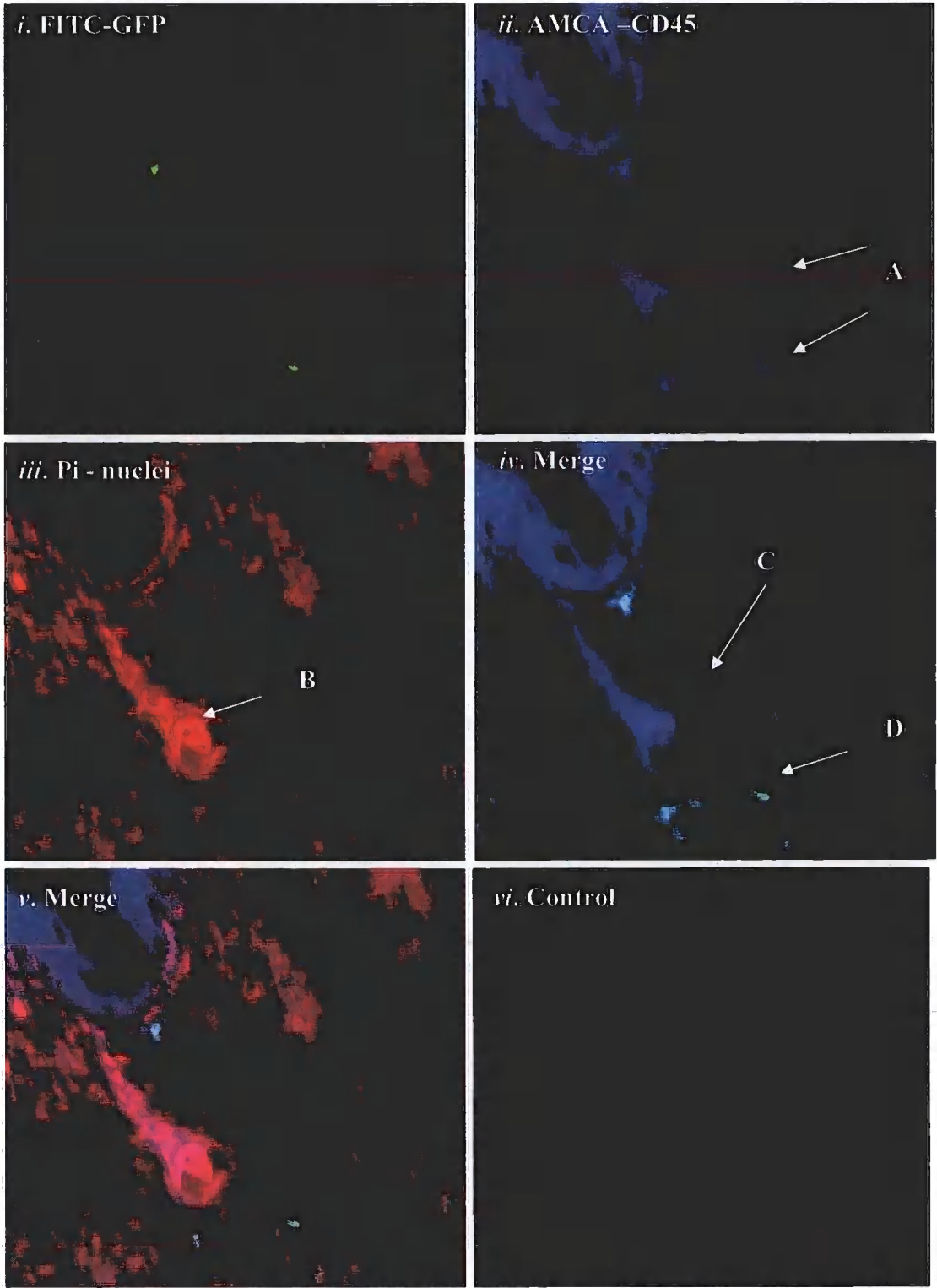
Blue filter autofluorescence of the epidermis of the WT mouse. In the absence of antibody labelling, there was autofluorescence of the epidermis (A) and the cell-dense follicles (B) with the blue fluorescence filter.

Figure 5.5: Immunofluorescent labelling for GFP and CD45 cells in the neonatal skin of the WT mouse



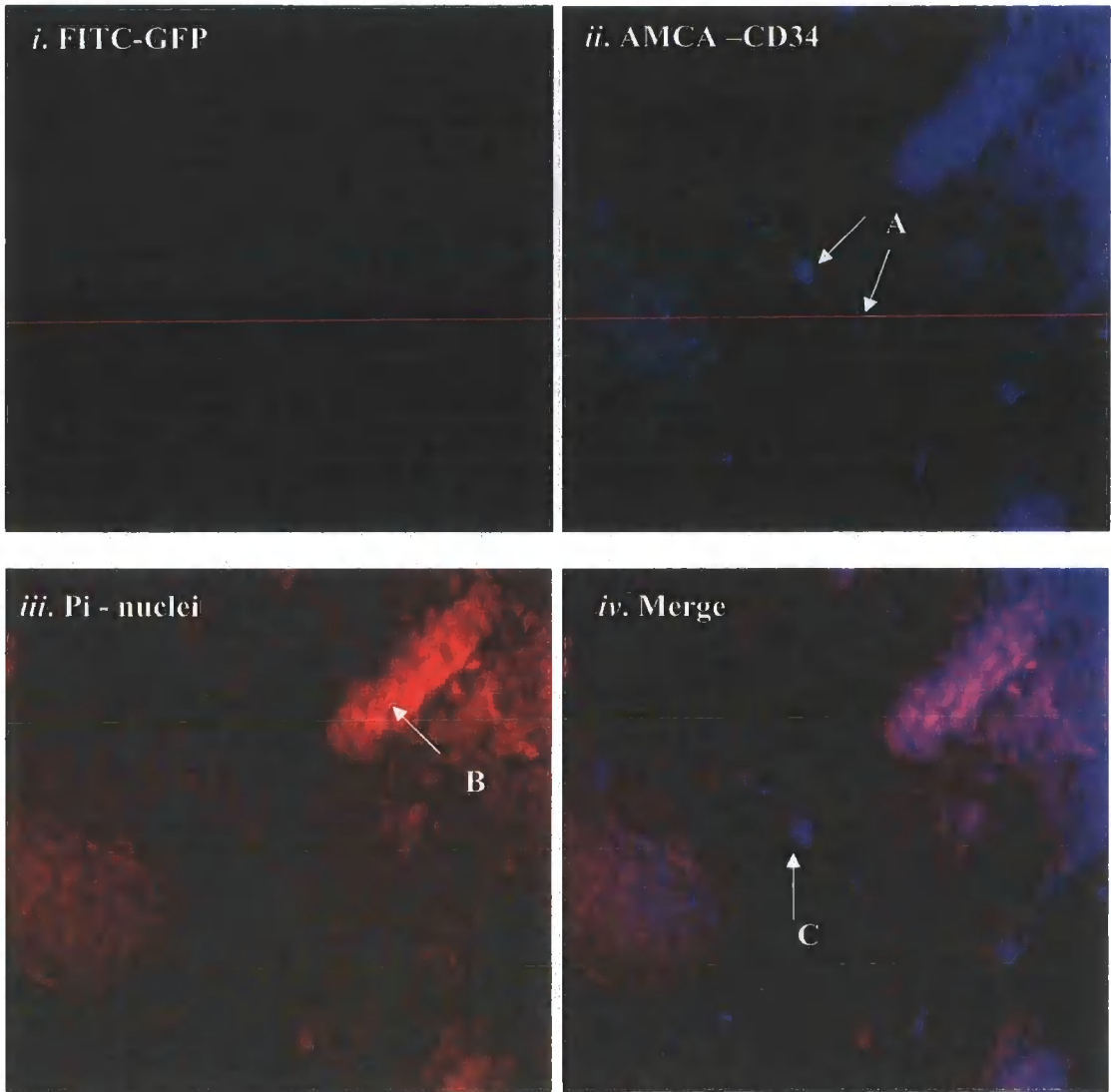
Immunofluorescent labelling of neonatal dermis of WT mouse. There was no detectable anti-GFP expression (*i*). Anti-CD45 labelling (*ii*) indicated a number of haematopoietic cells (A). Nuclei were identified by Pi labelling (*iii*) where the individual hair follicles can be seen (B). The epidermis and the dense areas of the follicles were autofluorescent under blue filter fluorescence (C). There were a number of cells which appeared to be CD45+ve (D). Images shown at x40 magnification.

Figure 5.6: Immunofluorescent labelling for GFP and CD45 cells in the neonatal skin of the mTert-GFP mouse



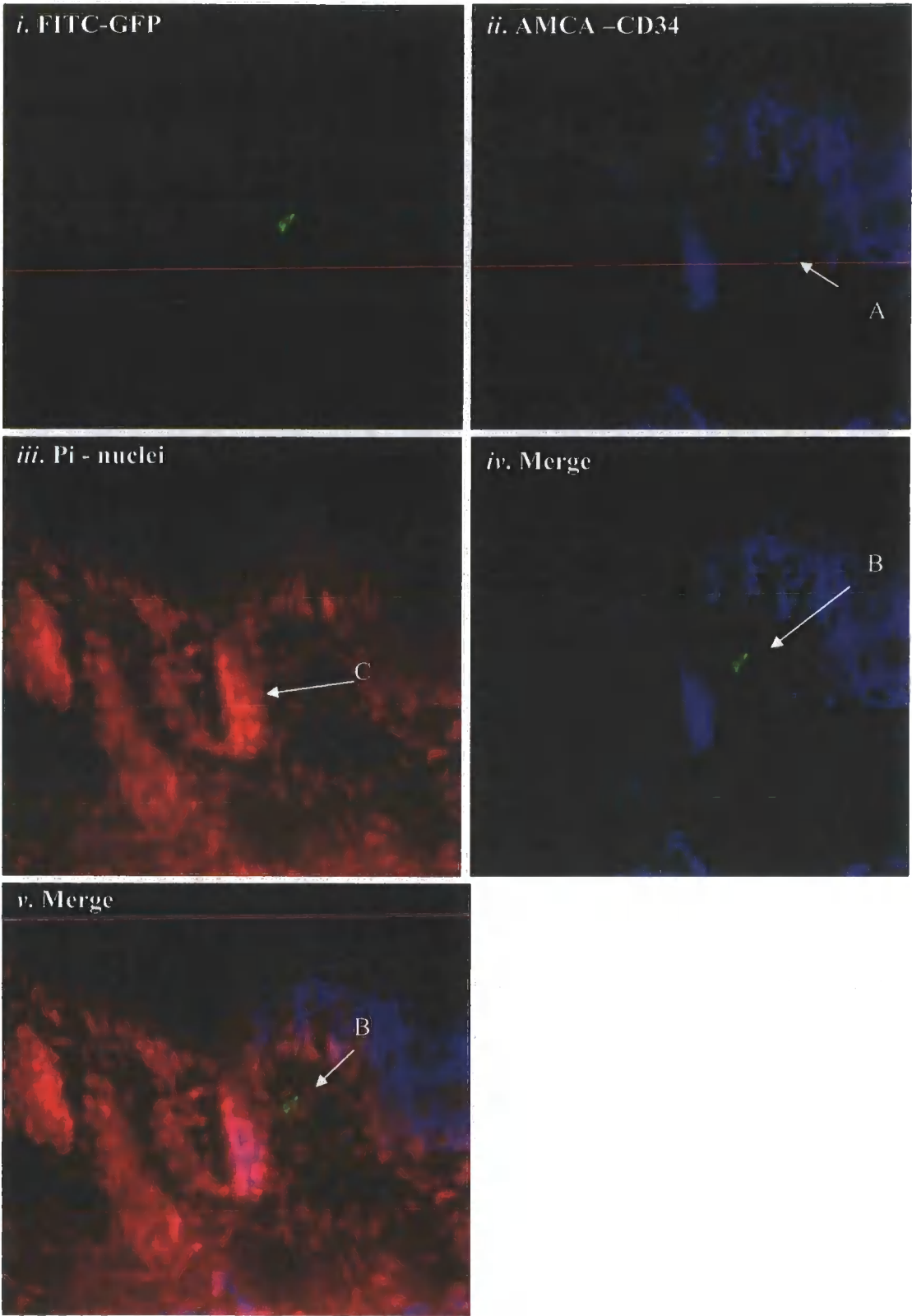
Immunofluorescent labelling of neonatal dermis of mTert-GFP mouse. There were a number of GFP+ve cells (i) and CD45+ve cells (A) (ii) in the dermis. A single GFP+ve, CD45+ve cell (C) was observed amongst cells that were GFP+ve and CD45+ve (D) indicative of haematopoietic cells in a blood vessel. The GFP+ve cell was located in the dermis associated with the hair follicle (B). Antibody specificity was confirmed by a no-primary antibody control (vi). Images shown at x40 magnification.

Figure 5.7: Immunofluorescent labelling for GFP and CD34 cells in the neonatal skin of the WT mouse



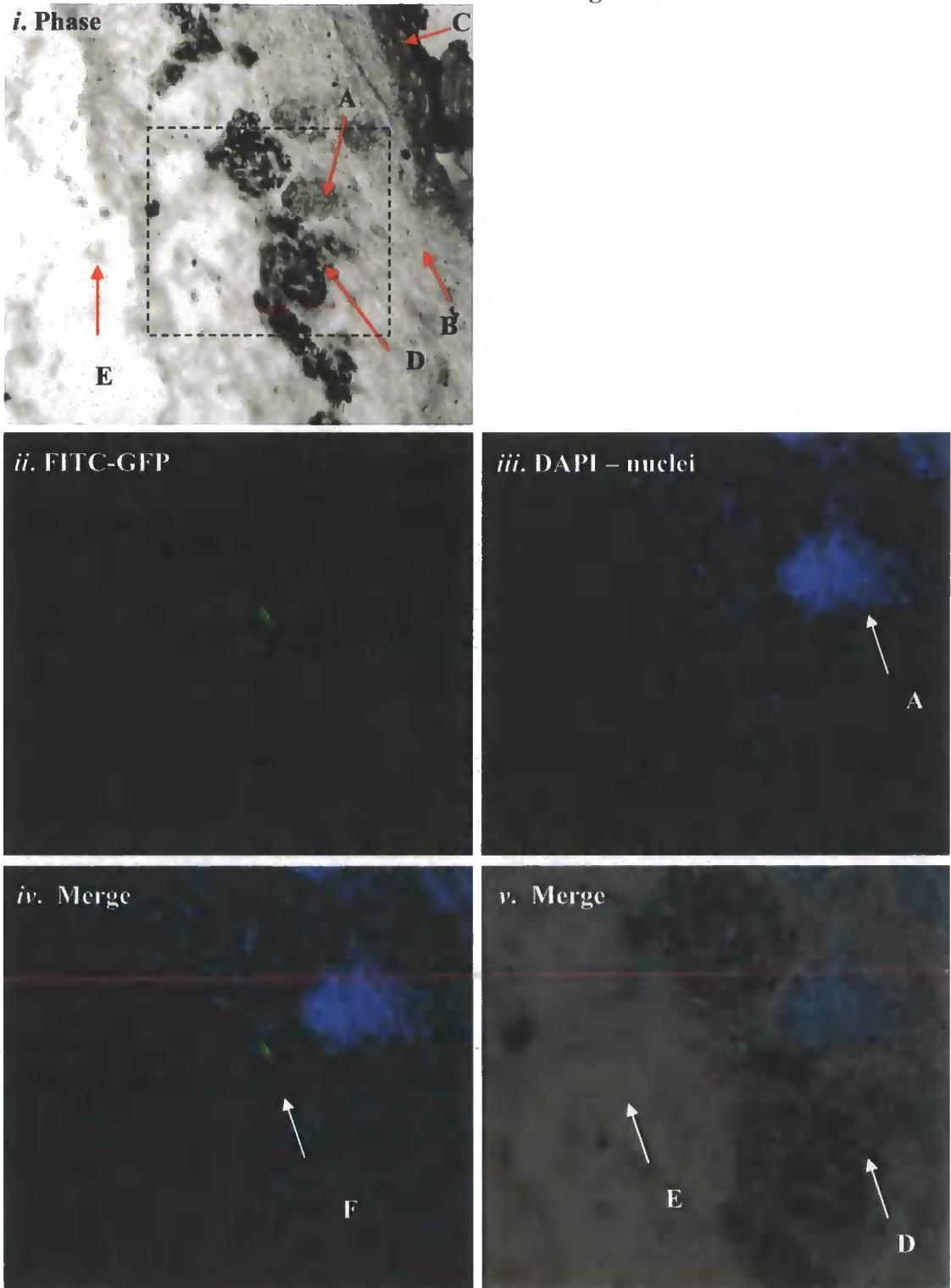
Immunofluorescent labelling of the neonatal dermis of the WT mouse. There was no detectable anti-GFP expression (i). Anti-CD34 labelling (ii) indicated a number of cells that were CD34+ve (A). Nuclei were identified by Pi labelling (iii) where an individual hair follicle can be seen (B). There were a number of cells, as indicated by Pi+ve nuclei, which were CD34+ve (C). Images shown are at x40 magnification.

Figure 5.8: Immunofluorescent labelling for GFP and CD34 cells in the neonatal skin of the mTert-GFP mouse



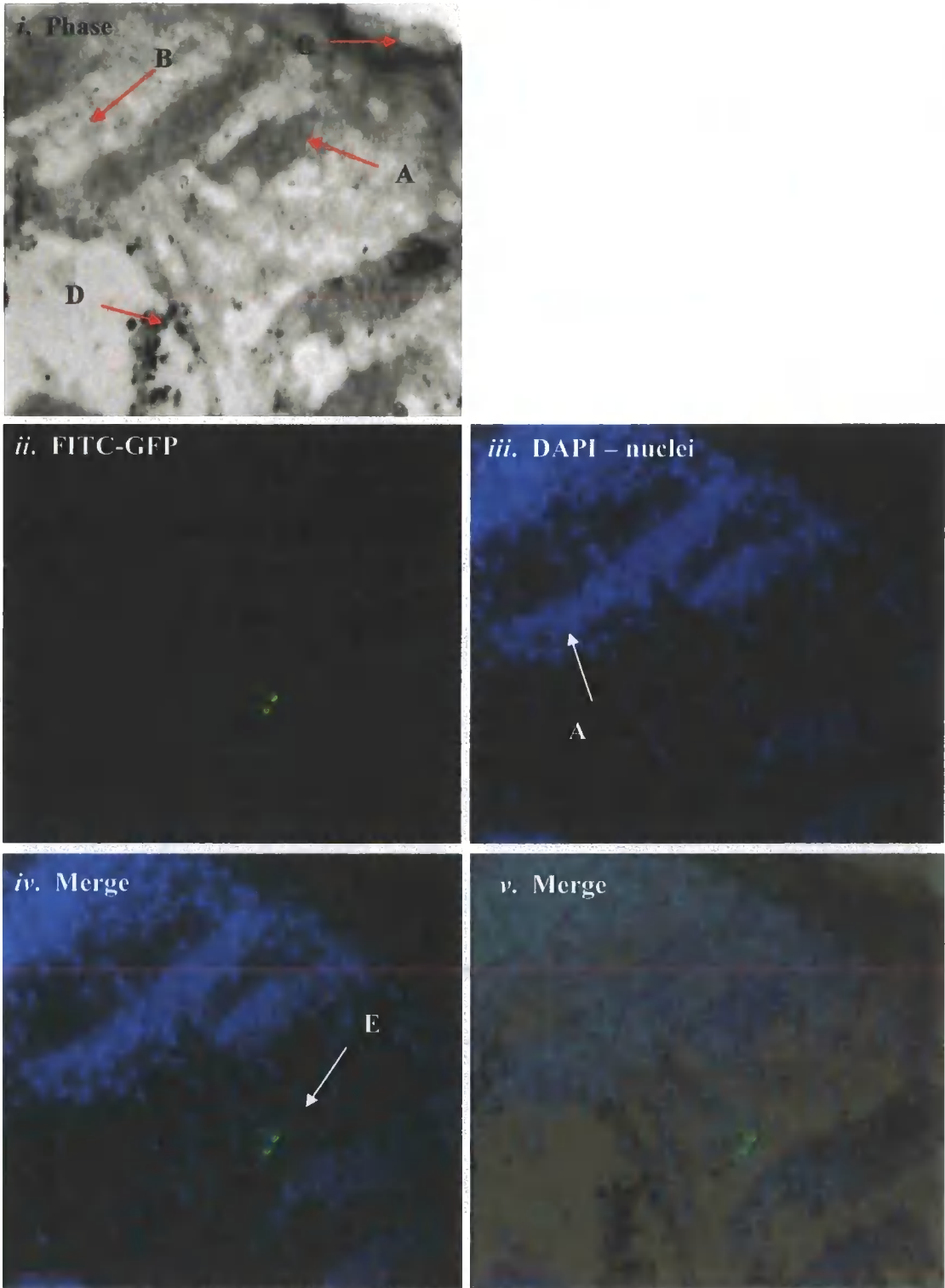
Immunofluorescent labelling of the neonatal dermis of the mTert-GFP mouse. There was one GFP+ve cell identified in the dermis (i) as well as a number of CD34+ve cells (A) (ii). The GFP+ve cell was CD34-ve (B) and was located in the dermis associated with the hair follicle (C). Images shown are at x40 magnification.

Figure 5.9: Anti-GFP labelled cells, of the skin of the mTert-GFP mouse, associated with the dermis surrounding the follicular end bulb



Immunofluorescent labelling of the neonatal dermis of the mTert-GFP mouse showing a GFP+ve cell associated with the follicular end bulb. The phase image (*i*) shows the location of the hair follicle end bulb (A), dermis (B), epidermis (C), fat (D) and muscle (E) (x5 magnification). Nuclei labelling with DAPI (*iii*) showed the GFP+ve cell associated with the end bulb of the hair follicle (F). Images *ii,iii,iv* and *v* are at x40 magnification. GFP+ve cells, associated with the end bulb, were CD45-ve and CD34-ve.

Figure 5.10: Anti-GFP labelled cells, of the skin of the mTert-GFP mouse, associated with the inter-follicular dermis



Immunofluorescent labelling of the neonatal dermis of the mTert-GFP showing an inter-follicular GFP+ve cell associated with the hair shaft region of the hair follicle. The phase image (i) shows the location of the hair follicles (A), dermis (B), epidermis (C) and fat (D) (x5 magnification). Nuclei labelling with DAPI (iii) showed the GFP+ve cell associated with the hair follicle (A). Images are shown at x40 magnification. GFP+ve cells, associated with the interfollicular dermis, were CD45-ve and CD34-ve

The identification of GFP+ve cells in two different locations in the dermis, both of which were negative for haematopoietic lineage surface antigens CD45 and CD34, is suggestive of two separate dermal cell populations, potentially one associated with the end bulb of the follicle and the other with the bulge region.

Considering there were two GFP+ve cells locations within the dermis, both associated with the hair follicle, further analysis of these GFP+ve cells was undertaken by investigating the entire dermis by flow cytometry and FACS isolating the GFP+ve populations for further analysis.

5.1.2 Isolation and characterisation of the mTert-GFP neonatal dermis

GFP+ve cells associated with the hair follicle, as identified in the dermis by immunofluorescence, were investigated by flow cytometry as described in methods sections 2.3.2 and 2.14. GFP expression was previously identified by antibody labelling however, native expression was sufficient to be captured by flow cytometry without the need for further amplification of the signal.

As demonstrated above, GFP+ve dermal cells were identified in the dermal compartment of the skin by immunohistochemistry from 5 day old neonatal skin when there is appearance of hair on the skin. Freshly isolated dermis from 5 day old neonatal skin was investigated by flow cytometry. In addition to this time point, the freshly isolated dermis of earlier aged neonates were also investigated; from 2 day old neonates and 3 days old neonates to correlate with initial hair appearance and initial secondary hair follicle formation. In order to potentially be able to correlate findings from the dermal GFP+ve cell population with the DP and DP primary cells in culture, the entire dermis was also put into culture and the adherent cells, after 1 week culture and 2 weeks culture, were FACS investigated in a similar manner to the “fresh” sorts, which were the cells isolated immediately after tissue processing as described above.

5.1.2.1 Flow cytometric analysis of the dermis

The dermis from neonates aged 2 days, 3 days and 5 days old were isolated. 10 mTert-GFP neonates and 10 WT neonates were used for each time point, equating to a sampling total of 40cm² of dermis for each time point. The fresh dermal samples were analysed by flow cytometry for viable cells, 7-AAD-ve, that were lineage-ve and GFP+ve (Methods section 2.14). To minimise any effect of FACS method, the

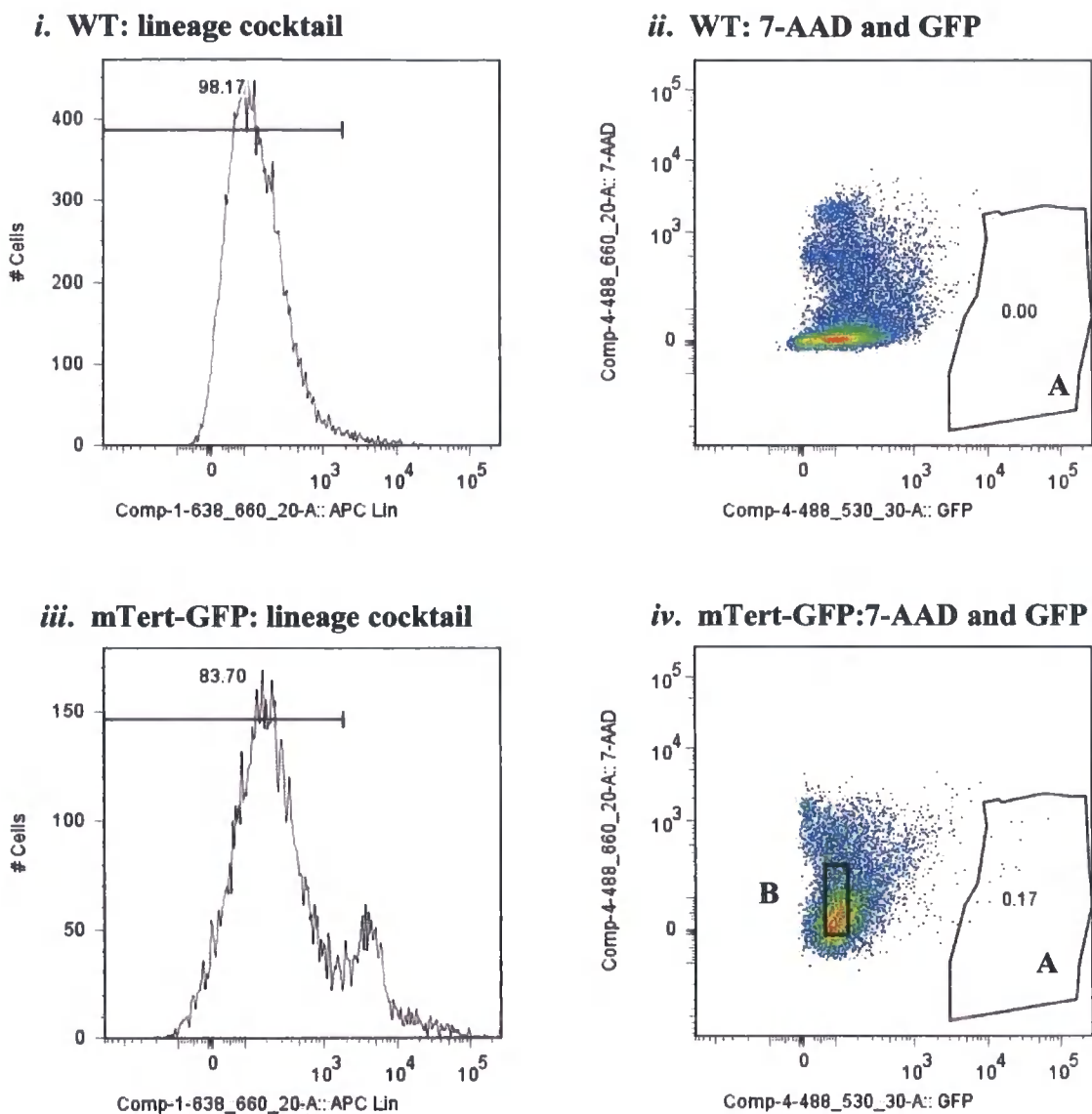
experiment was ran on three separate days with 3-4 mTert-GFP neonates and matching WT littermates for each time point run on each day (figures 5.11-5.13).

The mean proportion of GFP+ve lineage-ve cells identified in the dermis from 2 day and 5 day old neonates were similar; the dermis from the 2 day old neonates contained 0.19% GFP+ve lineage-ve cells (n=10) (representative sample is shown in figure 5.11) and the dermis from the 5 day old neonates contained 0.20% GFP+ve lineage-ve cells (n=10) (representative sample is shown in figure 5.12). However the mean proportion of GFP+ve lineage-ve cells identified in the dermis from 3 day neonates was higher at 0.45% (n=10) (representative sample is shown in figure 5.13); this may correlate with the time of secondary follicle formation and with the GFP+ve cells seen by immunofluorescence associating with the end bulb and developing DP. The flow cytometric analysis profile was similar for all ages of the dermis with similar percentages of viable lineage-ve cells. The GFP+ve cells were gated for lineage negativity according to lineage positive control samples. The level of expression of lineage cocktail in the GFP+ve cells was re-checked and on every occasion these cells were within the range of 10^0 - 10^1 APC fluorescence confirming they were well within the assigned lineage-ve cells (data not shown). In summary, the flow cytometric profile for the mTert-GFP dermis shows there is a clear population of cells that are GFP+ve, distinct from the GFP-ve cells and negative for lineage markers, which may represent a population of dermal stem-like cells.

Due to the increased number of GFP+ve cells in the 3 day old neonatal fresh dermis sample, this age of neonate was used for further analysis of the dermal cells after a period of *in vitro* culture. The entire dermis from 5 mTert-GFP and 5 WT littermates were transferred into a 25cm² flask each and adherent cells, after 7 days (figure 5.14) and 14 days (figure 5.15), were analysed for viable GFP+ve lineage-ve cells.

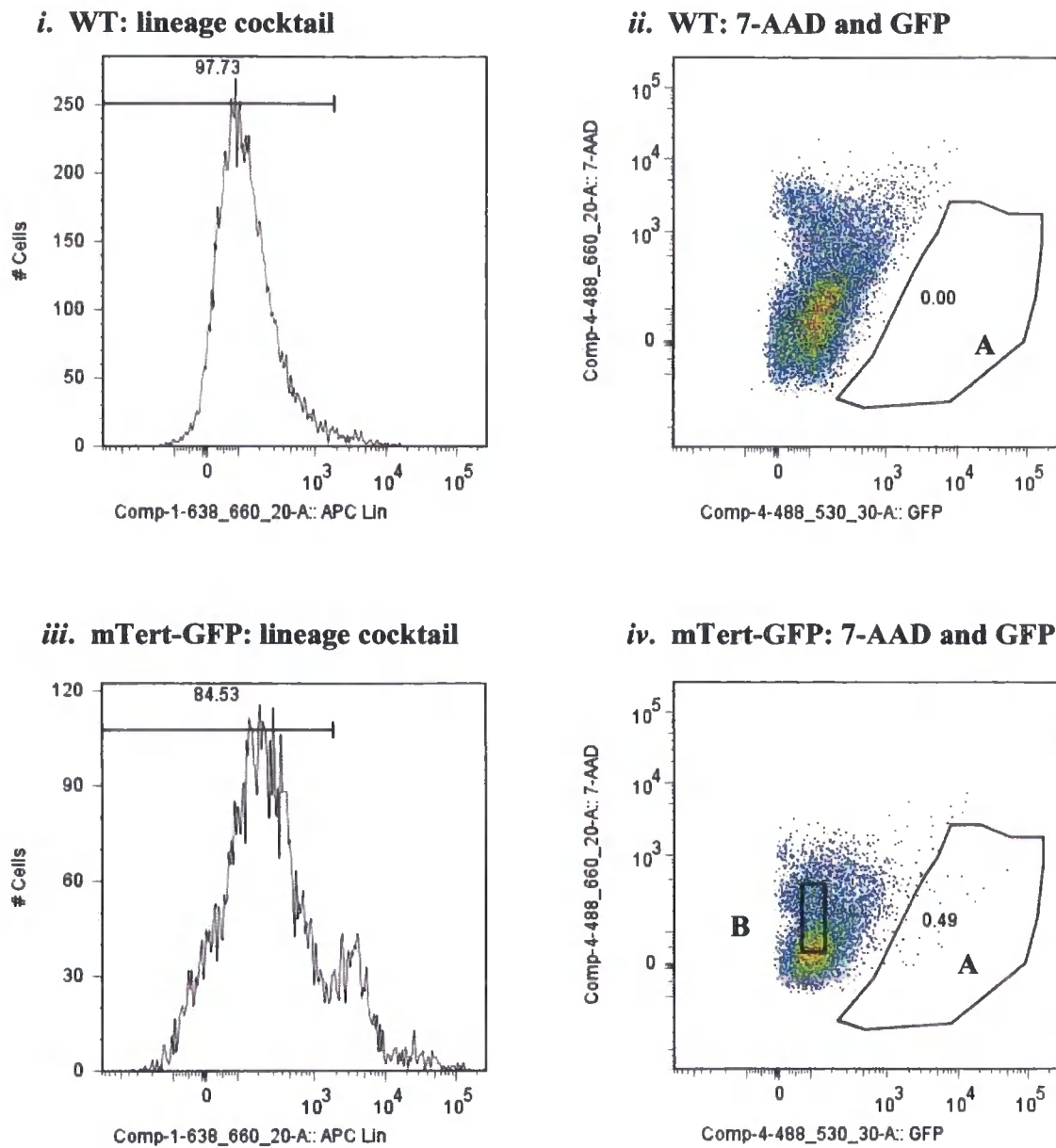
The flow cytometric profile for the 1 week cultured dermis was different to the 2 week cultured dermis with 0.30% and 0.13% of cells GFP+ve lineage-ve respectively (fresh sorts demonstrated 0.49% GFP+ve lineage-ve as described above).

Figure 5.11: Flow cytometric analysis of dermis from a neonatal WT and mTert-GFP mouse neonates



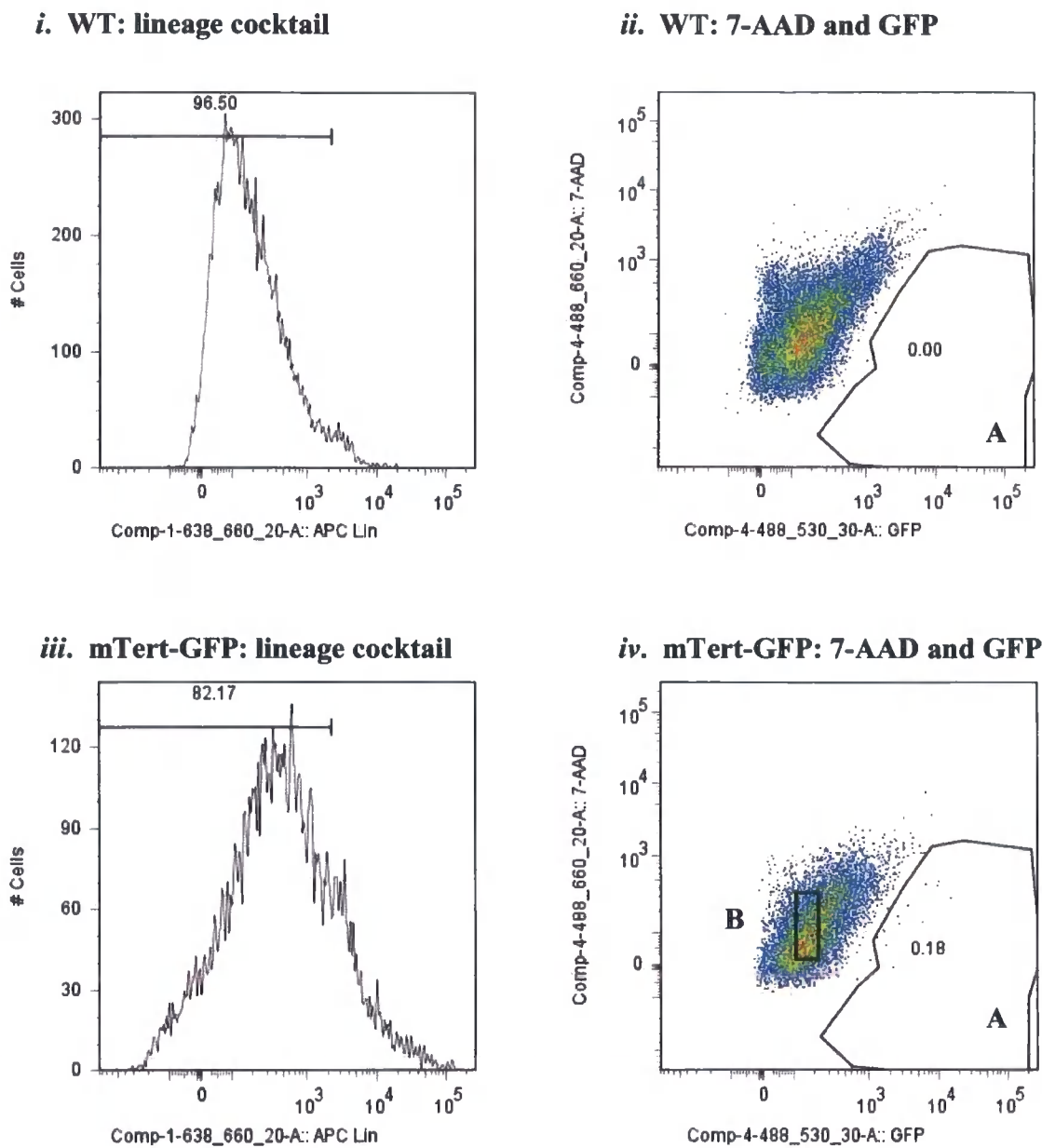
Flow cytometric analysis of neonatal dermis from 2 day old littermates. Gating for flow cytometric analysis was set according to WT neonatal dermis (*i* and *ii*) of matching age and sex to the mTert-GFP neonates (*iii* and *iv*). Only cells negative for lineage cocktail (method section 2.14) were analysed so to exclude any cells that may be blood derived. These gates were confirmed as negative for lineage positive control samples. Of these cells, viability was determined using 7-AAD (methods section 2.14) and viable cells positive for GFP (gating A) were counted and FACS sorted for further investigation. A matching GFP-ve population of cells from the mTert-GFP dermis were also collected (B). The number of viable GFP+ve, lineage negative cells is shown in the gating (A) as a percentage of the entire sorted dermal population of the mTert-GFP neonates; from four experiments the average was 0.19%, in this experiment this was 0.17%.

Figure 5.12: Flow cytometric analysis of dermis, from a neonatal WT and mTert-GFP mouse neonates



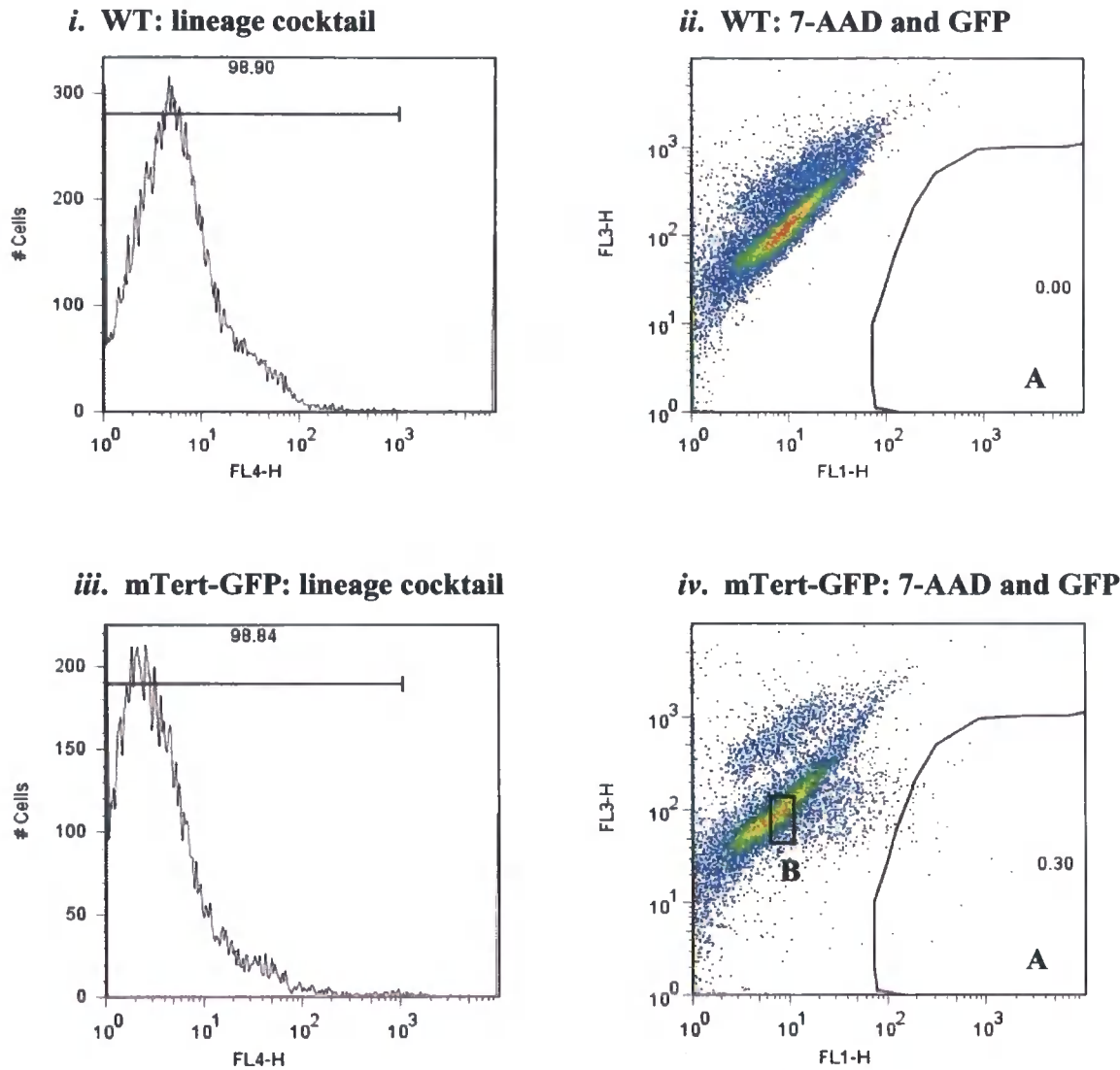
Flow cytometric analysis of neonatal dermis from 3 day old littermates. Gating for flow cytometric analysis was set according to WT neonatal dermis (*i* and *ii*) of matching age and sex to the mTert-GFP neonates (*iii* and *iv*). Only cells negative for lineage cocktail (method section 2.14) were analysed so to exclude any cells that may be blood derived. Of these cells, viability was determined using 7-AAD (methods section 2.14) and viable cells positive for GFP (gating A) were counted and FACS sorted for further investigation. A matching GFP-ve population of cells from the mTert-GFP dermis were also collected (B). The number of viable GFP+ve, lineage negative cells is shown in the gating (A) as a percentage of the entire sorted dermal population of the mTert-GFP neonates; from four experiments the average was 0.45%; in this experiment this was 0.49%.

Figure 5.13: Flow cytometric analysis of dermis, from a neonatal WT and mTert-GFP mouse neonates



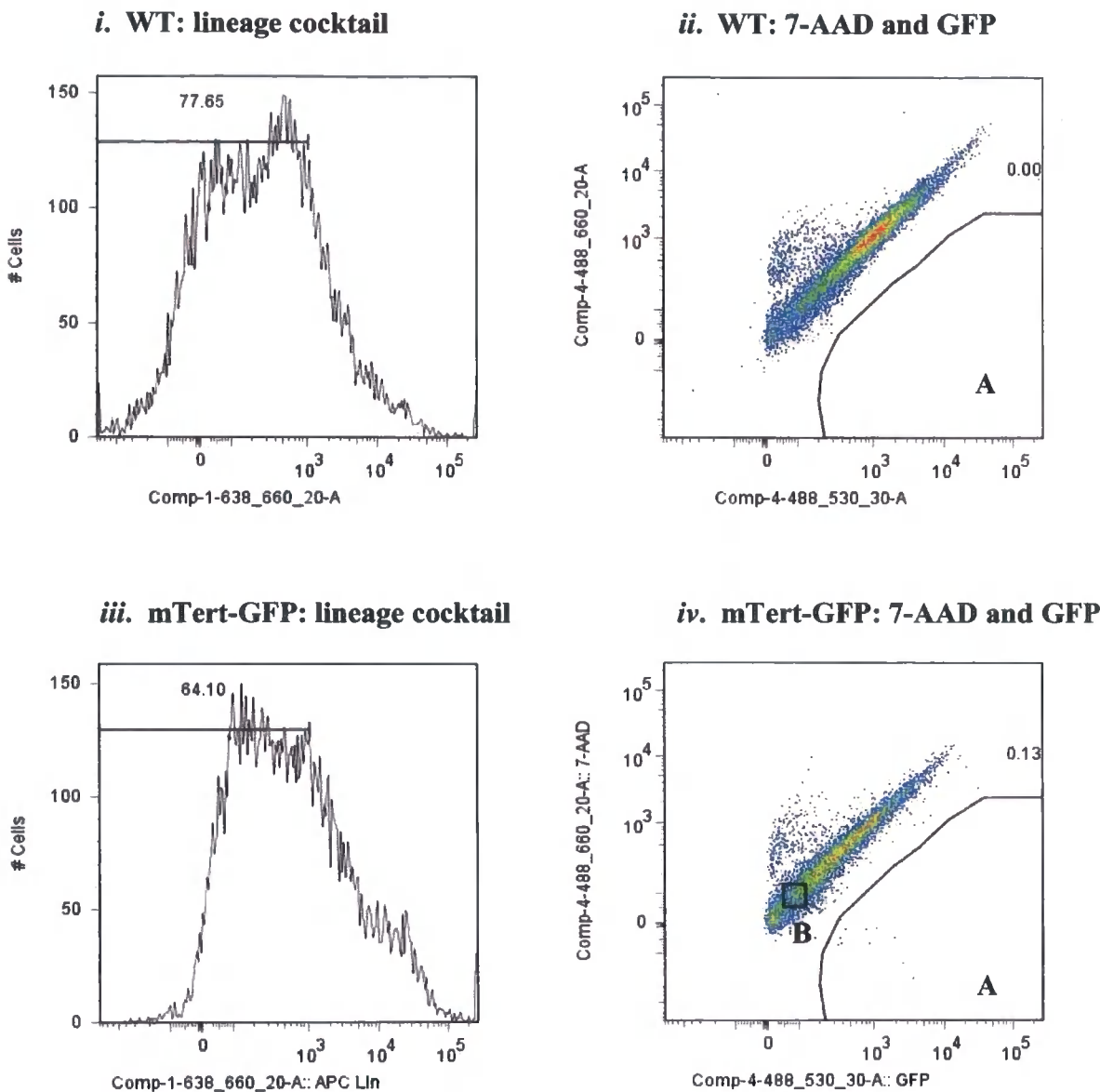
Flow cytometric analysis of neonatal dermis from 5 day old littermates. Gating for flow cytometric analysis was set according to WT neonatal dermis (*i* and *ii*) of matching age and sex to the mTert-GFP neonates (*iii* and *iv*). Only cells negative for lineage cocktail (method section 2.14) were analysed so to exclude any cells that may be blood derived. Of these cells, viability was determined using 7-AAD (methods section 2.14) and viable cells positive for GFP (gating A) were counted and FACS sorted for further investigation. A matching GFP-ve population of cells from the mTert-GFP dermis were also collected (B). The number of viable GFP+ve, lineage negative cells is shown in the gating (A) as a percentage of the entire sorted dermal population of the mTert-GFP neonates; from four experiments the average was 0.20%, in this experiment this was 0.18%.

Figure 5.14: Flow cytometric analysis of dermis from 3 day old mTert-GFP mouse neonates, cultured in vitro for 7 days



Flow cytometric analysis of the 1 week cultured dermis. Gating for flow cytometric analysis was set according to WT neonatal dermis (*i* and *ii*) of matching age and sex to the mTert-GFP neonates (*iii* and *iv*). Only cells negative for lineage cocktail (method section 2.14) were analysed so to exclude any cells that may be blood derived. Of these cells, viability was determined using 7-AAD (methods section 2.14) and viable cells positive for GFP (gating A) were counted and FACS sorted for further investigation. A matching GFP-ve population of cells from the mTert-GFP dermis were also collected (B). The number of viable GFP+ve, lineage negative cells is shown in the gating (A) as a percentage of the entire cultured dermal population of the mTert-GFP neonates; from four experiments the average was 0.35%; in this experiment this was 0.30%.

Figure 5.15: Flow cytometric analysis of dermis from 3 day old mTert-GFP mouse neonates, cultured in vitro for 14 days



Flow cytometric analysis of the 2 week cultured dermis. Gating for flow cytometric analysis was set according to WT neonatal dermis (*i* and *ii*) of matching age and sex to the mTert-GFP neonates (*iii* and *iv*). Only cells negative for lineage cocktail (method section 2.14) were analysed so to exclude any cells that may be blood derived. Of these cells, viability was determined using 7-AAD (methods section 2.14) and viable cells positive for GFP (gating A) were counted and FACS sorted for further investigation. A matching GFP-ve population of cells from the mTert-GFP dermis were also collected (B). The number of viable GFP+ve, lineage negative cells is shown in the gating (A) as a percentage of the entire cultured dermal population of the mTert-GFP neonates; from four experiments the average was 0.10%; in this experiment this was 0.13%.

On occasion with flow cytometric analysis, there was a small peak of dermal cells that were located within the lineage positive range of cells, as shown in figures 5.11-5.13(iii) and 5.15iii. On every occasion this was observed, these cells also expressed 7-AAD with a fluorescence of 10^3 upwards indicating that these cells were dead or dying and most likely accumulated the lineage cocktail fluorescent molecules with cell debris giving false positive expression (data not shown). The percentage of cells assigned lineage-ve decreased between 7 days and 14 days culture from 98.8% to 64.1%; the WT samples also decreased in a similar manner. The number of cells in this category was amplified in the dermis after 14 days of culture at a time point where the culture flask was confluent, and in the absence of passaging, which would lead to increased cell death.

5.1.2.2 Culture of FACS isolated GFP+ve and GFP-ve cells of the dermis

The freshly isolated dermis from 2 mTert-GFP neonates aged 2 days old, 2 mTert-GFP neonates aged 3 days old and 2 mTert-GFP neonates aged 5 days with an equal number of WT littermates were sorted into three populations of cells: GFP+ve lineage-ve, GFP-ve lineage-ve and a mixed, lineage-ve population. The mixed population represented dermal cells that were passed through flow cytometer with population sorting for lineage-ve cells only and therefore contained both GFP+ve and GFP-ve cells at the time of sampling. Passing all the cells through the flow cytometer allowed any differences between the three populations to not be attributed to the FACS method. The freshly sorted cells were investigated in adherent culture to investigate adherent cell morphology, division and to compare to cultures of DP and DS cells. Cells were also investigated in suspension culture to investigate aggregation events or proliferation, and in hanging drop which encourages aggregation formation.

Adherent and suspension culture

Adherent cultures were set up for each of the three, freshly sorted, dermal populations from mTert-GFP and WT neonates aged 2 days old, 3 days old and 5 days old. 300 cells were plated into 16mm individual adherent culture dishes and observed for 2 weeks *in vitro* culture:

GFP+ve lineage-ve sorted population: On every occasion, approximately 2% of cells adhered with atypical fibroblastic morphology. These cells did not divide or increase in cell size once settled.

GFP-ve lineage-ve sorted population: On every occasion, approximately 50% of cells adhered in culture with atypical fibroblast morphology comparable to the GFP+ve population. There was no evidence of substantive proliferation and the dishes did not increase in confluency within the 2 weeks of *in vitro* culture.

Mixed, lineage-ve population: On every occasion, cells adhered in culture with atypical fibroblast morphology comparable to the GFP+ve and GFP-ve populations. The dishes were confluent within 1 week of *in vitro* culture.

To determine if the sorted cells would aggregate in suspension culture, the sorts were repeated and the same groups of cells cultured in petri dishes. After approximately 2 days the cells no longer appeared refractive, with the presence of a significant degree of cell debris, in all populations, none having aggregated.

Hanging drop culture

Adherent cultures were set up for each of the three, freshly sorted, dermal populations from mTert-GFP and WT neonates aged 2 days old, 3 days old and 5 days old. 300 cells were plated into 16mm individual adherent culture dishes and observed for 2 weeks *in vitro* culture:

Individual hanging drops were set up for each of the three, freshly sorted, dermal populations from mTert-GFP and WT neonates aged 2 days old, 3 days old and 5 days old. Each cell aggregated contained 300 cells/10µl media; 5 hanging drops were set up per sort population for each neonatal age as described above. Hanging drops were allowed 5 days undisturbed *in vitro* culture.

The cells did not aggregate in any of the hanging drops, including those of the mixed dermis.

5.1.2.3 PCR analysis of FACS isolated dermal populations

The freshly isolated cells analysed and collected by flow cytometry (as demonstrated in figures 5.11-5.13) were sorted into three populations as described above; these populations were GFP+ve lineage-ve, GFP-ve lineage-ve and mixed lineage-ve cells, at the three neonatal ages. In addition, the adherent cells from the 7 day (figure 5.14) and

14 day (figure 5.15) cultured dermis were also sorted into three populations. cDNA suitable for RT-PCR (method 2.6.1) and Q-PCR (method 2.6.2) was produced for each population, with triplicate samples, apart from the GFP+ve lineage-ve and GFP-ve lineage-ve populations of both the 7 day and 14 day *in vitro* cultured dermis, where there was insufficient RNA to produce RT-PCR quality cDNA.

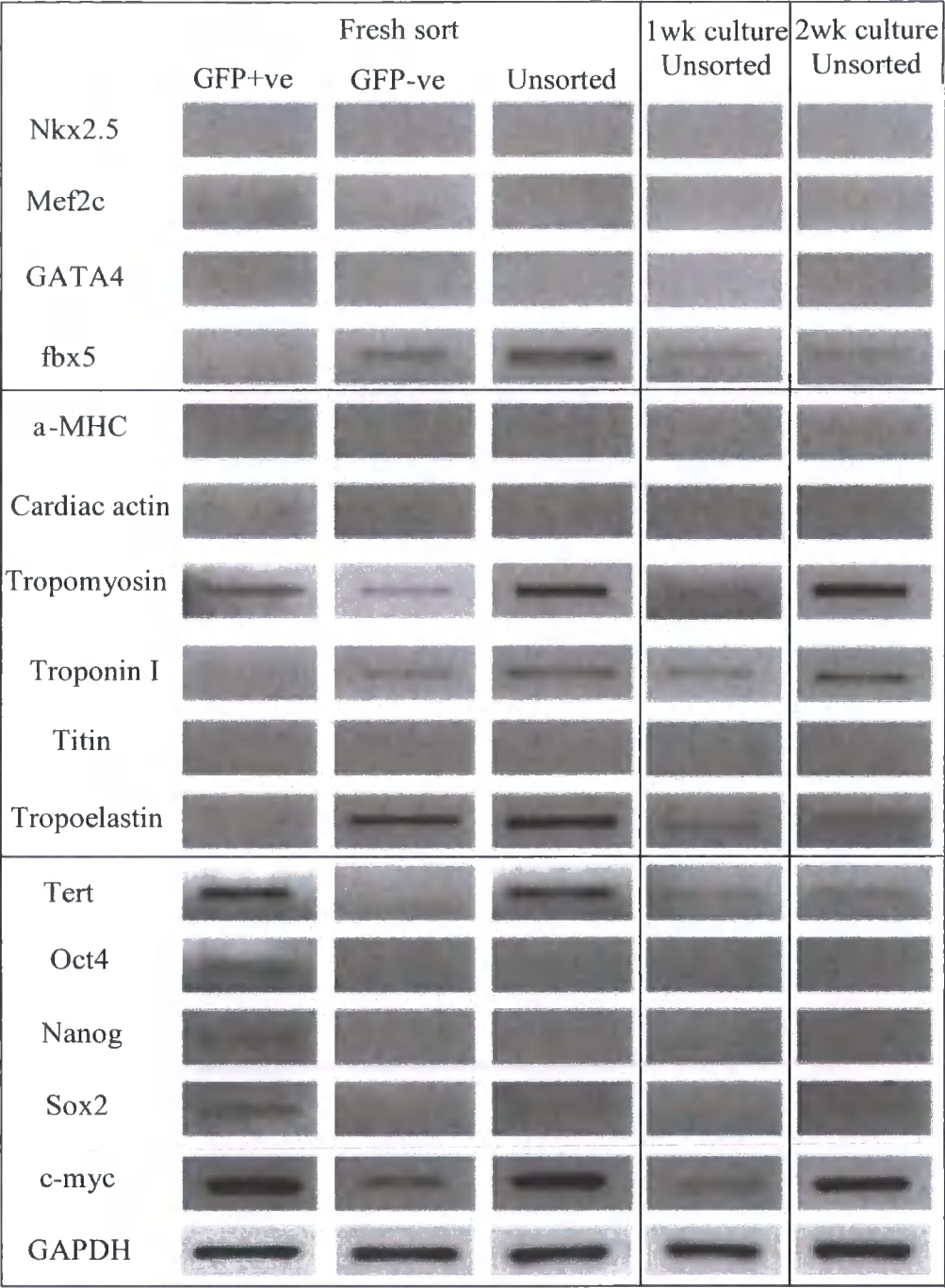
Figure 5.16 shows RT-PCR analysis of representative samples of the dermal cell populations. Included is GFP+ve, GFP-ve and mixed samples (denoted 'unsorted') from fresh sorts. Dermal cells from 2 day old, 3 day old and 5 day old neonates all displayed a similar gene expression profile; representative bands are shown in figure 5.16. There were insufficient cells for RNA amplification for the 7 day and 14 day cultured GFP+ve cells therefore only unsorted cells are shown in figure 5.16.

The GFP+ve population contained all the detectable Tert expression from the mixed sample confirming the mTert-GFP model. This which allows properties associated with GFP expression to be linked to Tert expression. The GFP+ve population contained all the detectable stem cell associated gene expression; Oct4, Nanog and sox2 with c-myc expressed in GFP+ve and GFP-ve populations. Cardiomyocyte associated genes were also investigated, as previously described when investigating DP and DS cells (Chapter 3, figures 3.12-3.14). The GFP+ve population of cells was not enriched for detectable expression of the cardiomyocyte associated genes. Examination of cardiomyocyte associated transcription factors in lineage-ve, dermal cells obtained by this method did not express detectable Nkx2.5, GATA4, or Mef2c. Tbx5 was enriched in the GFP-ve population. Of the cardiomyocyte associated functional genes troponin I was enriched in the GFP-ve cells. Tropoelastin was also enriched to the GFP-ve population. These dermal cells did not express detectable α -MHC, cardiac actin and titin. This suggests that the expression of the stem cell genes is uncoupled from the expression of the cardiomyocyte genes in the dermis.

Q-PCR was completed on the GFP+ve, GFP-ve and unsorted populations for fresh, 1 week culture and 2 week culture cells for mTert, Nanog and Sox2 expression to confirm the RT-PCR expression profile. These are shown in figure 5.17.

The GFP+ve populations contained all the mTert, Nanog and Sox2 expression; a property maintained from fresh sort samples to 2 weeks *in vitro* culture samples.

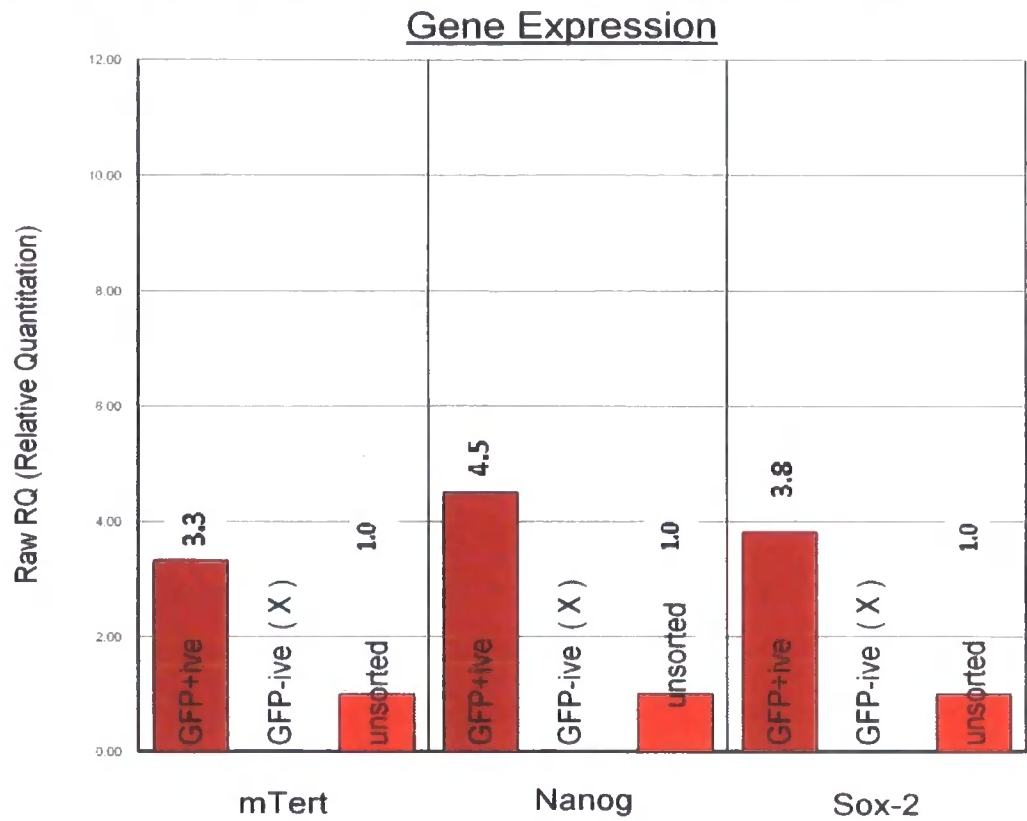
Figure 5.16: RT-PCR gene expression profile of FACS isolated dermal populations for cardiomyocyte-associated and stem cell-associated genes



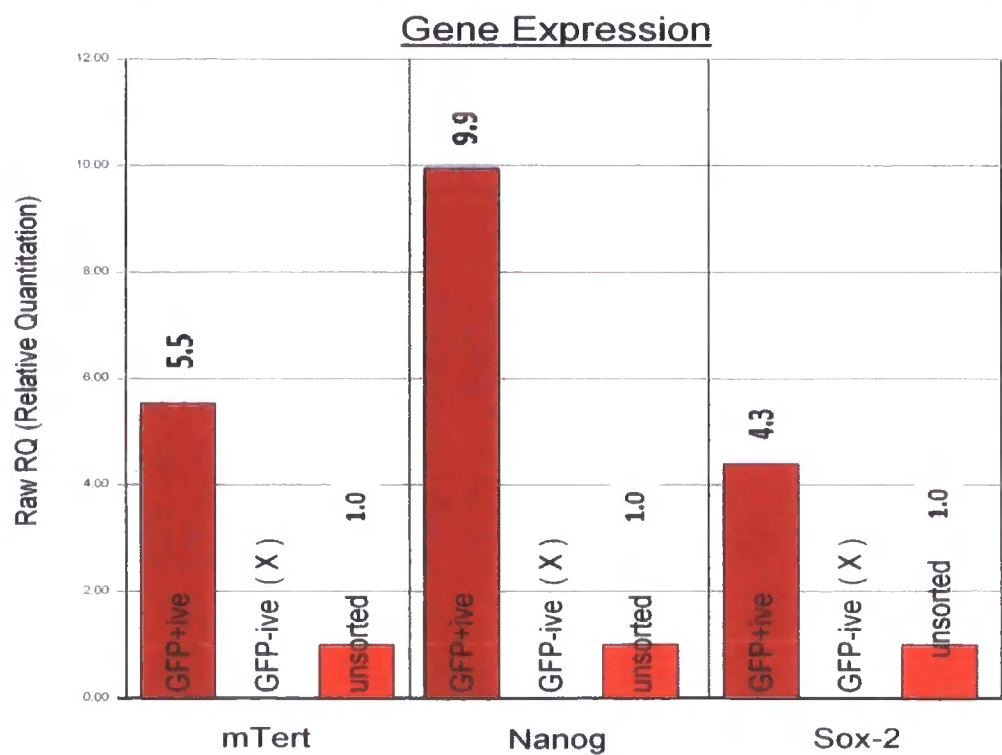
RT-PCR analysis of mTert-GFP sorted populations for cardiomyocyte and stem cell associated genes. The GFP+ve cells contained all the detectable Tert expression which confirms the mTert-GFP mouse model. GFP+ve cells contained all the Oct4, Nanog and Sox2 detectable expression and was enriched for c-myc expression which was also detected in the GFP-ve cells. Of the cardiomyocyte associated genes, tbx5 appeared enriched to the GFP-ve population with no detectable expression of Nkx2.5, Mef2c and GATA4. Tropomyosin was detectable in all dermal populations, with detectable troponin I and tropoelastin expression enriched in the GFP-ve cells. There was no detectable expression of a-MHC, cardiac actin or titin. The gene expression profile for the mixed cells (denoted unsorted) appears to remain consistent over the periods of culture investigated. Representative bands are shown.

Figure 5.17: Q-PCR gene expression profile of FACS isolated dermal populations for stem cell-associated genes

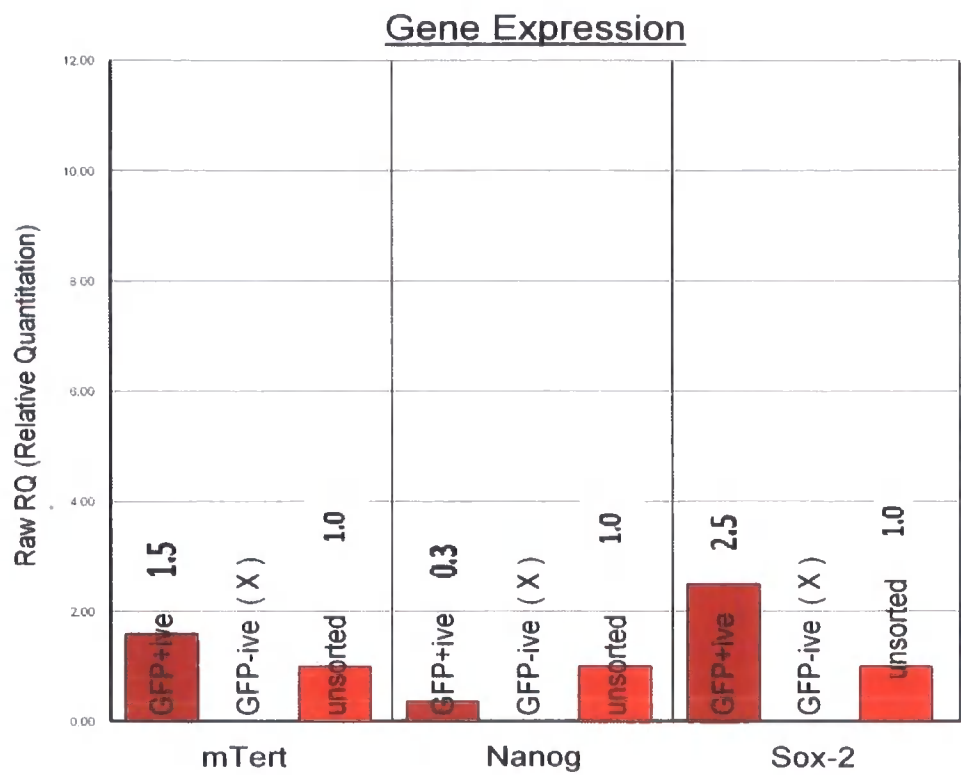
i. Fresh dermis sort samples: GFP+ve, GFP-ve and unsorted cell samples



ii. 1 week cultured dermis samples: GFP+ve, GFP-ve and unsorted cell samples



iii. 2 week cultured dermis samples: GFP+ve, GFP-ve and unsorted cell samples



Q-PCR gene expression analysis of dermal cells freshly isolated, after 1 week culture and after 2 weeks culture, samples were then sorted. The graphs show fresh sorted samples (i) representative of dermis from neonates aged day 2, 3 and 5 after 1 week cultured dermis (ii) and 2 week cultured dermis (iii). Gene expression fold changes were significant for the fresh and 1 week sorted samples only ($p<0.01$) when the GFP+ve cells were compared to the unsorted samples (mixed population) from the same time point. The expression results were relative to GAPDH and normalised with respect to mixed (denoted unsorted) samples (mixed GFP+ve and GFP-ve cells). A no-transcript control ensured detectable gene expression changes were not as a result of the assays used.

In summary, GFP+ve cells were identified in the DP and DS adult vibrissae follicles by immunohistochemistry. In the smaller pelage follicles, anti-GFP labelling was identified in the end bulb. With dual labelling, GFP+ve CD45-ve and GFP+ve CD34-ve cells were identified in the dermis associated with the end bulb and the bulge region. GFP+ve lineage-ve cells were isolated by FACS and were found to not adhere or proliferate in culture unless in contact with GFP-ve cells. The GFP+ve cells contained all detectable Tert expression, by Q-PCR and RT-PCR analysis, and this population was also enriched for the pluripotency-associated stem cell genes namely Oct4, Nanog and Sox2 demonstrating the mTert-GFP mouse model identifies cells with stem cell markers. This suggests that the mTert-GFP mouse model may provide a tool for the isolation of a similar stem cell population from the heart.

5.2 Characterisation of GFP expression of the heart in the mTert-GFP mouse

Having demonstrated a GFP-expressing population of dermal cells in this model that contained all the detectable Tert activity and which expressed a pattern of markers characteristic of embryonic stem cells, the heart was then examined to evaluate whether the mTert-GFP mouse could potentially be a model to identify native cardiac stem cells. Furthermore, comparison of selected gene expression between GFP-marked candidate stem cells from each of these tissues could aid in identification of molecular markers that could involved in cardiomyocyte differentiation.

There is evidence for the presence of undifferentiated cells with stem cell properties within the adult heart (Beltrami *et al.*, 2003; Matsuura *et al.*, 2004; Laugwitz *et al.*, 2005). However, as outlined earlier, the characteristics, physiology and absolute numbers of these cells remains unclear. Some reports indicate that primitive cells with stem cell properties make up as much as 2% of all cells, whereas others studies suggest that this fraction is as low as 0.005-0.0125% (as reviewed by Anversa *et al.*, 2006); differences potentially accounted for by the use of different markers for these cell types. One approach to overcome this is to use a marker system that is driven by the phenotype of stem cells; such a marker system could be mTert-driven expression of GFP. It has been also been suggested that to increase the number of cells with stem-like properties to a level more suitable for investigation, such cells types may need to be 'activated', for example in response to disease or growth. In the heart, the use of models of acute injury has been used to investigate the 'activation' of candidate stem

cells (Urbanek et al., 2005). The utility of the mTert-GFP mouse in identifying candidate stem cells in the heart was thus investigated in both normal adults and in mice which received acute cryo-injury to the ventricle.

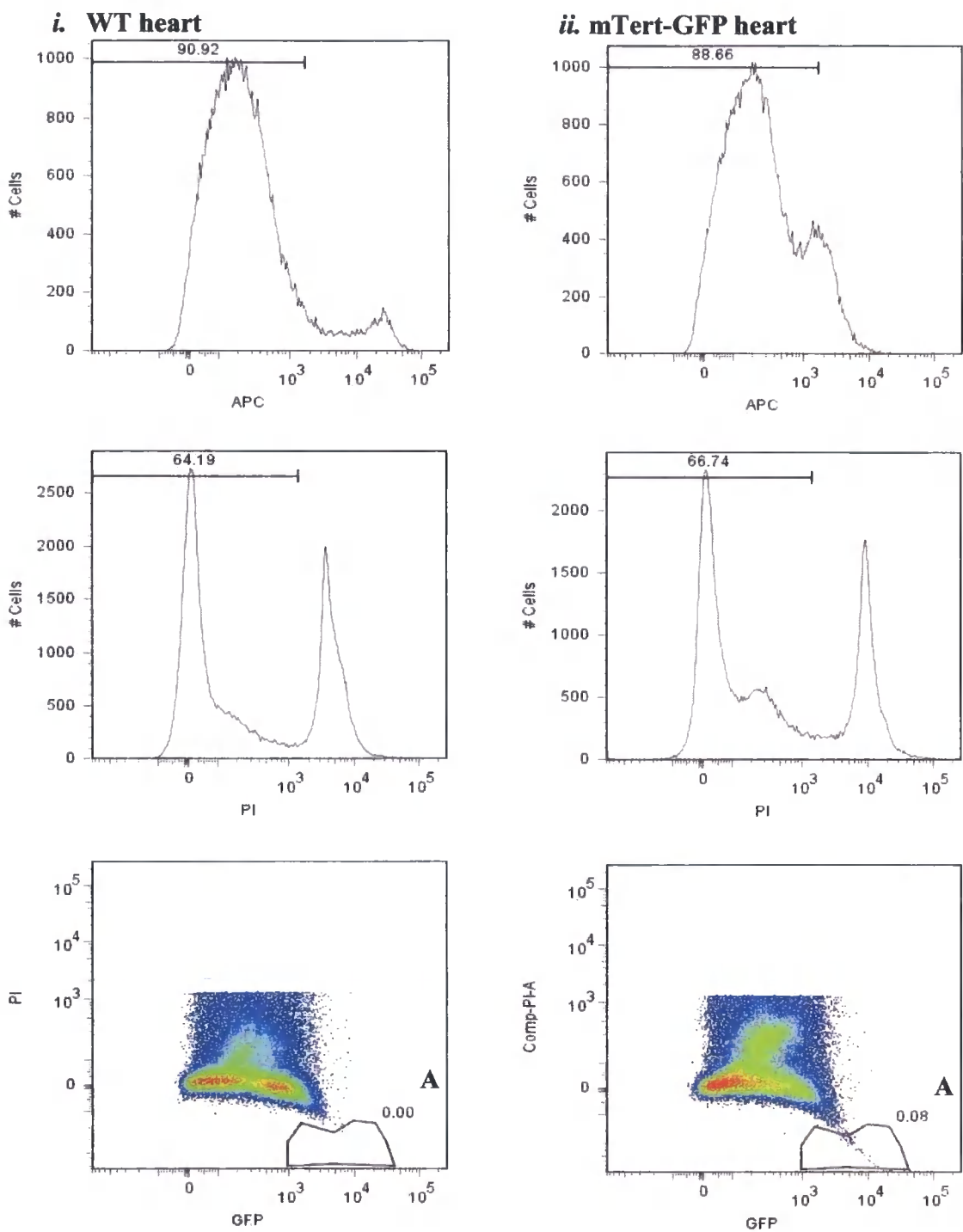
5.2.1 Histological investigation of the mTert-GFP heart

GFP expression in the heart was initially investigated by specific immunofluorescence and immunohistochemistry, as with the dermis. Age and sex matched hearts from 3 mTert-GFP mice and 3 WT neonatal littermates as well as E14.5 embryonic hearts from 3 mTert-GFP embryos and 3 WT embryos from the same mating were investigated. Despite the examination of more than 30 sections from each individual mouse heart, no specific GFP expression was detected. However, given the well described problems with non-specific autofluorescence in the heart (Van de les *et al.*, 1995), one explanation could be that such specific expression as there is could be masked by the background signal. An alternative approach was to examine GFP expression by flow cytometry, as proved successful for investigation of the dermis (section 5.1.2.1).

5.2.2 Flow cytometric analysis of the heart

Hearts from 3 mTert-GFP mice and 3 WT 3 day old littermates were used. Single cell suspensions were prepared from the neonatal hearts by enzyme dissociation according to Method section 2.13.1. The cell samples were analysed for viable cells (those that did not take up 7-AAD), that were lineage-ve and GFP+ve. A plot of one representative flow cytometric analysis is shown in figure 5.18. The number of viable, lineage-ve GFP+ve cells was $0.08 \pm 0.02\%$ of the cells recovered by enzymatic digestion of the hearts; a percentage which was smaller than that of the dermal cells which ranged from 0.17%-0.49% (figure 5.11- figure 5.13). A figure of $0.08 \pm 0.02\%$ is comparable to other reports for candidate cardiac stem cells isolated by other methods as summarised in Chapter 1 figure 1.2. These other reports also indicated that the numbers of candidate cardiac stem cells increased following injury. In order to determine whether a similar population could be identified in the heart following injury, cryo-infarct was investigated.

Figure 5.18: Flow cytometric analysis of the neonatal heart of the mTert-GFP mouse for viable GFP+ve cells that are non-haematopoietic



Representative flow cytometric analysis of the neonatal heart for GFP+ve cells. Gating was set according to WT hearts (*i*) of matching neonatal age and sex to the mTert-GFP hearts (*ii*). Only cells negative for lineage cocktail were analysed to exclude any blood derived cells. Viability was determined using Pi. The number of viable GFP+ve, lineage negative cells is shown in the gating (A) as a percentage of the entire cardiac population sorted; for the mTert-GFP population this was 0.08%.

5.2.3 Investigation of GFP+ve cells of the myocardium in response to cryo-infarct

Cryo-injury by trans-diaphragm cryoprobe application, which was cooled by liquid nitrogen (Method section 2.9), provides a highly reproducible model of anterior MI; the damaged myocardium undergoes modest adverse remodelling which is reported to be representative of infarcts encountered in clinical practice (Bos *et al.*, 2005). This model of cardiac injury was chosen as it may induce cardiac remodelling through stem cell activity and allowed investigation of a well defined area of injury surrounded by healthy myocardium. It was important to establish a reproducible injury and be able to investigate GFP+ve cells over a cryo-injury induced time course. Therefore a number of variables were considered as follows.

5.2.3.1 Size of probe and placing of injury

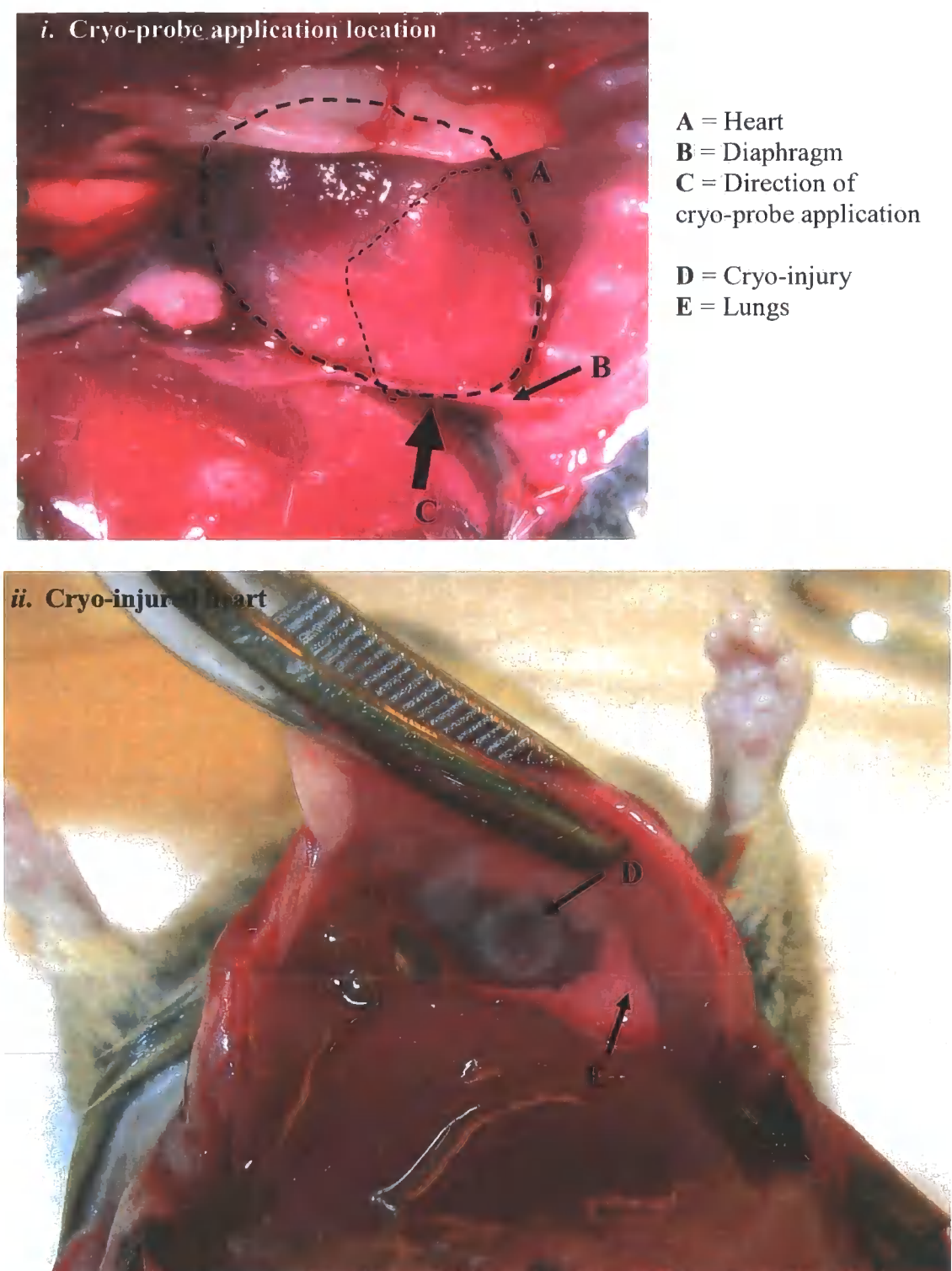
Legend 5.19i shows the internal organs in-situ; the contact between the diaphragm and heart made possible application of the cryo-probe across the diaphragm by intra-abdominal entry. The injury size was dependent upon the size of the probe. A number of probe sizes ranging from 1mm to 8mm were tested (data not shown); a 2 mm was small enough to pass through the abdominal incision but large enough to cause a notable injury which was well defined as shown in figure 5.19ii. It was possible to visualise the heart and lungs during insertion of the probe into the abdominal cavity, however this line of vision was blocked during probe application to the heart therefore alignment of the probe with the line of the sternum was essential; reproducible injury was confirmed by a pilot study of 3 WT mice. The injury was, on every occasion, close to the apex of the heart.

5.2.3.2 Cryo-probe application time

A 20s application of the cryoprobe (methods section 2.9) produced a reproducible injury as was confirmed by a pilot study on 3 WT mice. The cryo-injury was clearly apparent on the surface of the myocardium; this injury is shown in figure 5.19ii.

Previous descriptions using similar cryoprobes also described the option of using two 10s applications allowing the probe to be re-cooled for the second application. However, this was not suitable in creating a reproducible, defined injury as was determined by a pilot study on 2 WT mice.

Figure 5.19: Cryo-injury of heart as a model of cardiac infarct



The adult mouse heart in-situ after cryo-probe application. *i.* Ventral view of chest cavity illustrating the position of probe application (C) and *ii.* demonstration of the physical damage to the heart after application across the diaphragm. The nitrogen dipped probe was applied to the heart (A) for 20 seconds, via intra-abdominal incision, across the diaphragm (B) made possible due to the close contact between the two. The site of cryo-probe application (D) was immediately starved of oxygen as shown by the white coloration. The injury site shown is representative of 5 tested mice, 0.5 days after application.

A double application resulted in two overlapping injuries due to not being able to visualise the first injury during the second probe application (data not shown).

5.2.3.3 Diaphragm damage

In all the mice there was injury to the diaphragm. However, the injury was not lethal; there were no apparent breathing difficulties in treated mice, when evaluated after surgery, nor were there any effects upon the myocardial injury. The diaphragm was intact on all mice, observed on post-mortem examination.

5.2.3.4 Survival Rate

Cryo-injury was not lethal to treated mice, there were no fatalities in the pilot studies described above, which consisted of a total of 5 mice, and in the experimental study, described below, which consisted of 24 mice. All mice were monitored daily for cage activity, breathing rate and general health which were within acceptable levels. No mouse was sacrificed early due to complications post-surgery; this indicated that although the damage to the heart was severe the cryo-injury was representative of a recoverable myocardial infarction.

5.2.3.5 Cardiac cryo-injury

The application of the cryo-probe caused damage to the myocardium as was apparent from the initial white pigmentation to the application site as demonstrated in figure 5.19. In order to sample the myocardium at a time point when the majority of the remodelling occurs and when the stem cell population may be activated or recruited to the injury site, it was important to determine the time course for the repair of the tissue. The appearance of the injury was monitored over the 2 week experiment.

5.2.3.6 Time course of the appearance of the cryo-injury site

24 mice received induced cryo-injury and allowed a varying number of days recovery before sacrifice. Two groups were set up, the first a pilot study consisting of 2 WT mice sacrificed 24hrs post injury and 2 WT mice sacrificed at 3 days post infarct to monitor early recovery and ensure animal survival. There were 20 experimental mice consisting of 5 mTert-GFP mice with 5 WT mice sampled at 8 days post infarct as well as 5 mTert-GFP mice with 5 WT mice sampled at 14 days post infarct; time points where the infarct appeared to be undergoing a significant change.

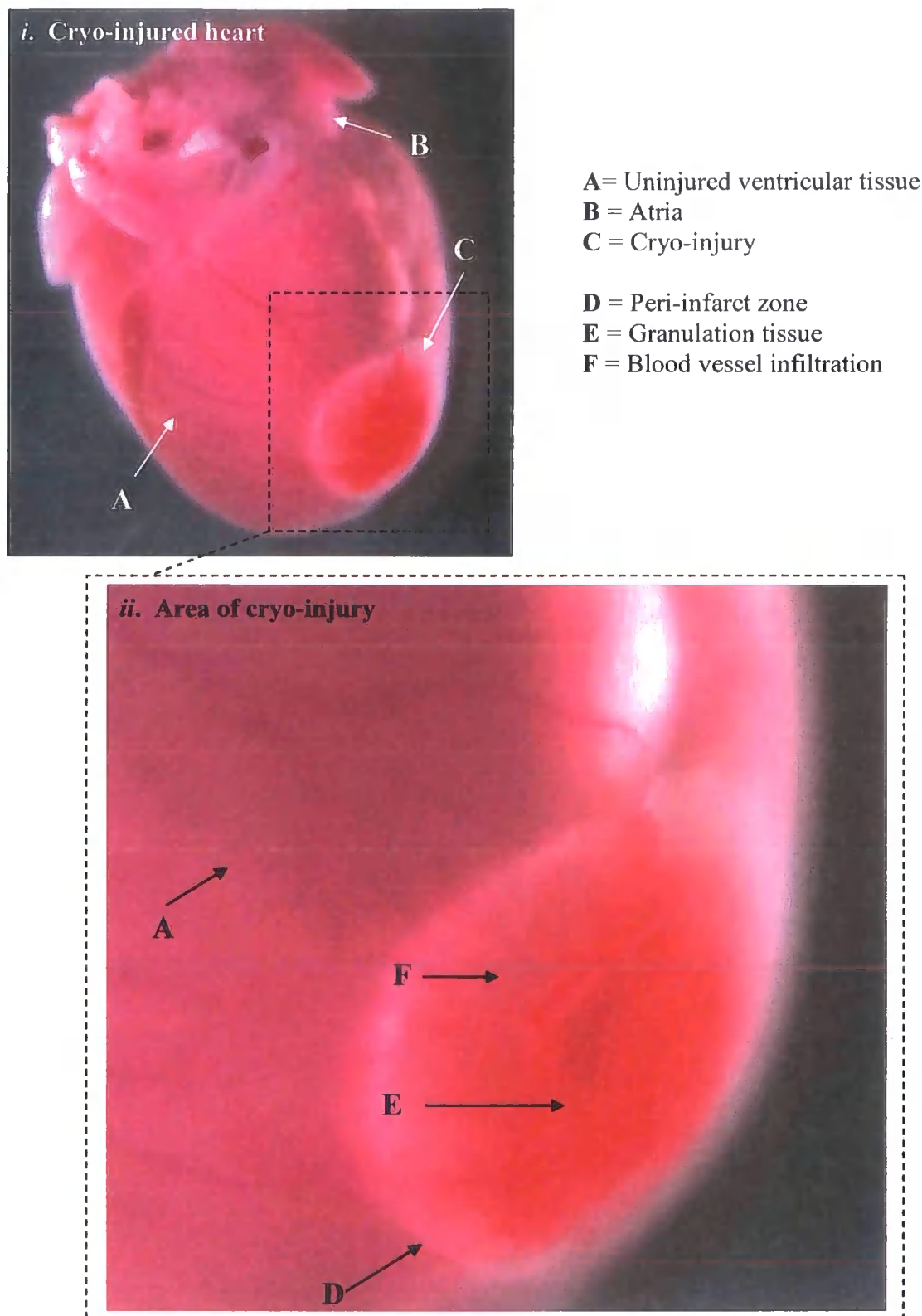
The hearts of the 2 WT mice analysed 24 hrs after injury demonstrated consistent inflammation at the injury with evidence of tissue granulation as shown in figure 5.20. At 3 days post-infarct, a degree of inflammation remained present and necrosis was apparent as shown in figure 5.21.

The first 10 experimental mice (5 mTert-GFP mice and 5 WT mice) were sacrificed 8 days post-infarct; a time point where inflammation was no longer apparent and necrosis was limited; the myocardial tissue appeared thinned as the blood within the ventricular chamber could be visualised as demonstrated in figure 5.22 This was indicative of a degree of remodelling and may have represented the initial increase in GFP+ve cells; as cells move to the infarct to aid tissue repair.

The second time point was one week later at 14 days post-infarct. The myocardial cell wall appeared extremely thinned at this time point but with normal tissue pigmentation. As shown in figure 5.23 the wall is so thinned it appeared transparent; the ventricular chamber could be visualised through the infarct tissue. Legend 5.24 shows sections through the day 14 cryo-injured heart at the infarct site demonstrating full depth tissue damage.

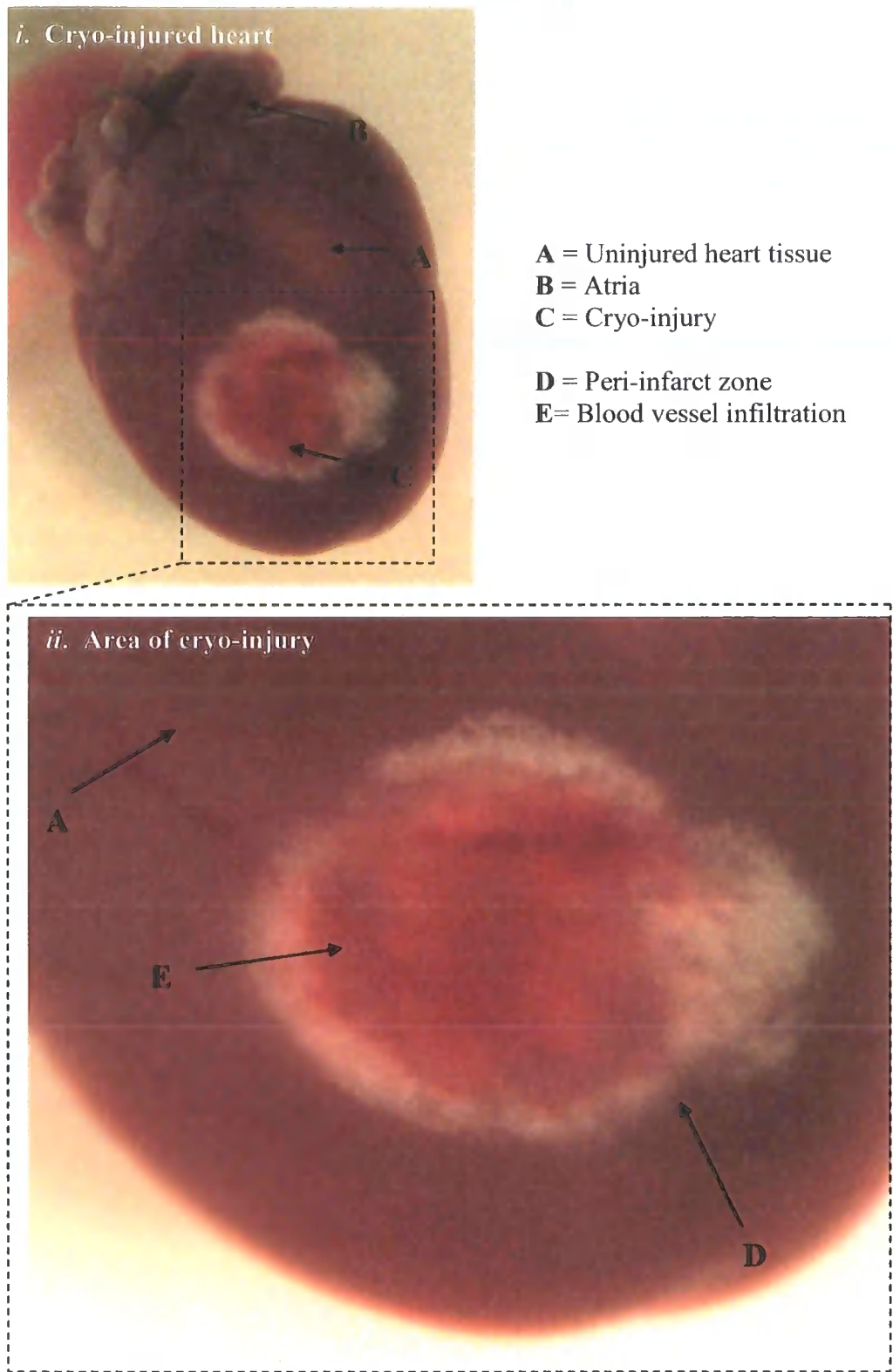
The day 8 and day 14 hearts were analysed by immunohistochemistry and immunofluorescence.

Figure 5.20: Excised cryo-injured heart 24 hrs post-infarct



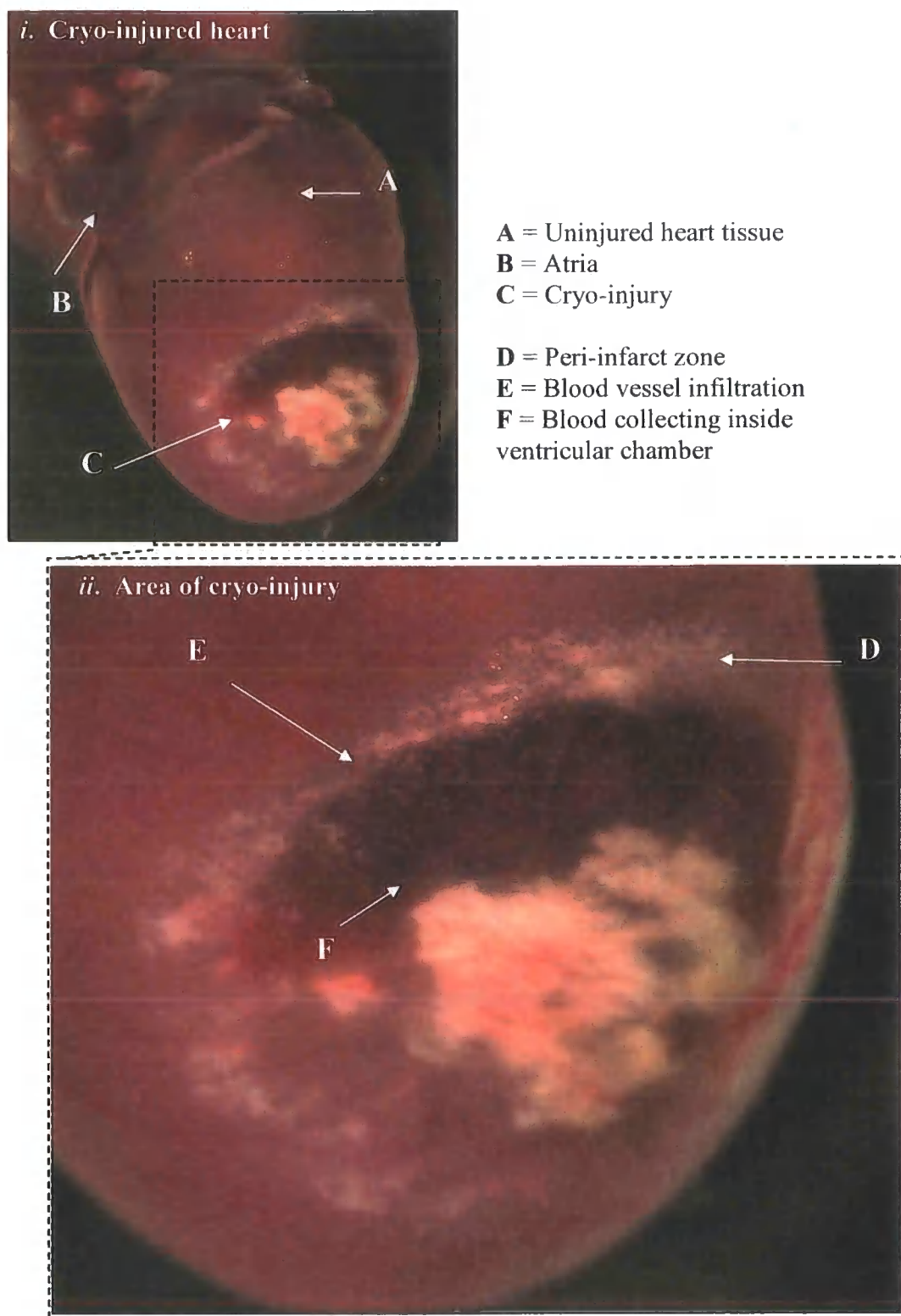
Excised mouse heart 24 hrs post-infarct (*i*) showing cryo-injury (*ii*). The area of cryo-injury (C) showed evidence of granulation (E), capillary infiltration (F) and inflammation as indicated by its raised appearance. The peri-infarct zone (D) was apparent and well defined. This photograph is representative of 2 mice; the heart was removed 24hrs post-infarct and photographed in PBS.

Figure 5.21: Excised cryo-injured heart 3 days post-infarct



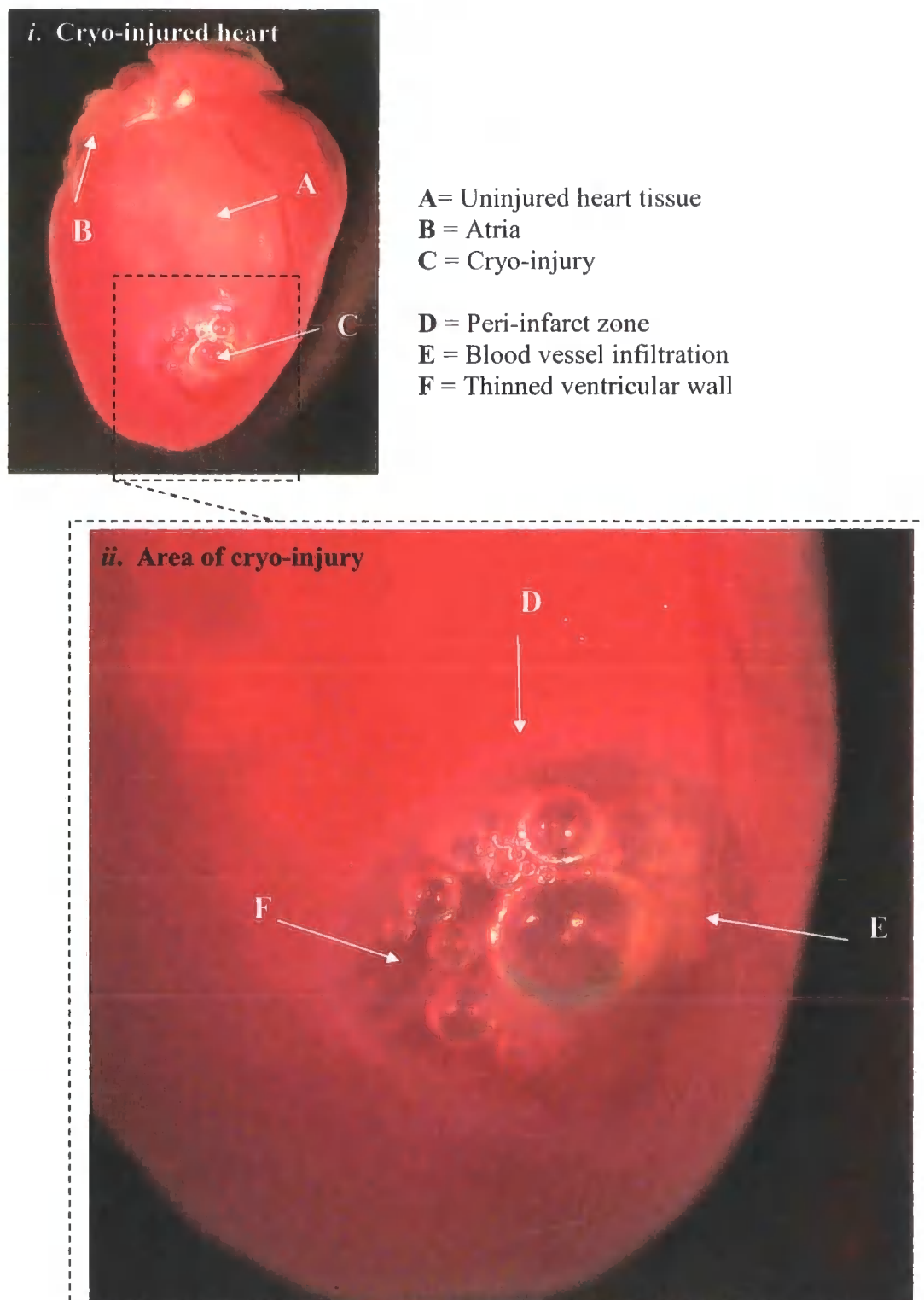
Excised mouse heart 3 days post-infarct (*i*) showing cryo-injury (*ii*). Granulation was not apparent however there remained a degree of inflammation and blood on the surface of the heart as well as capillary infiltration (E). The peri-infarct zone was less well defined (D). This photograph is representative of 2 mice, the heart was removed 3 days post-infarct and photographed in PBS.

Figure 5.22: Excised cryo-injured heart 8 days post-infarct



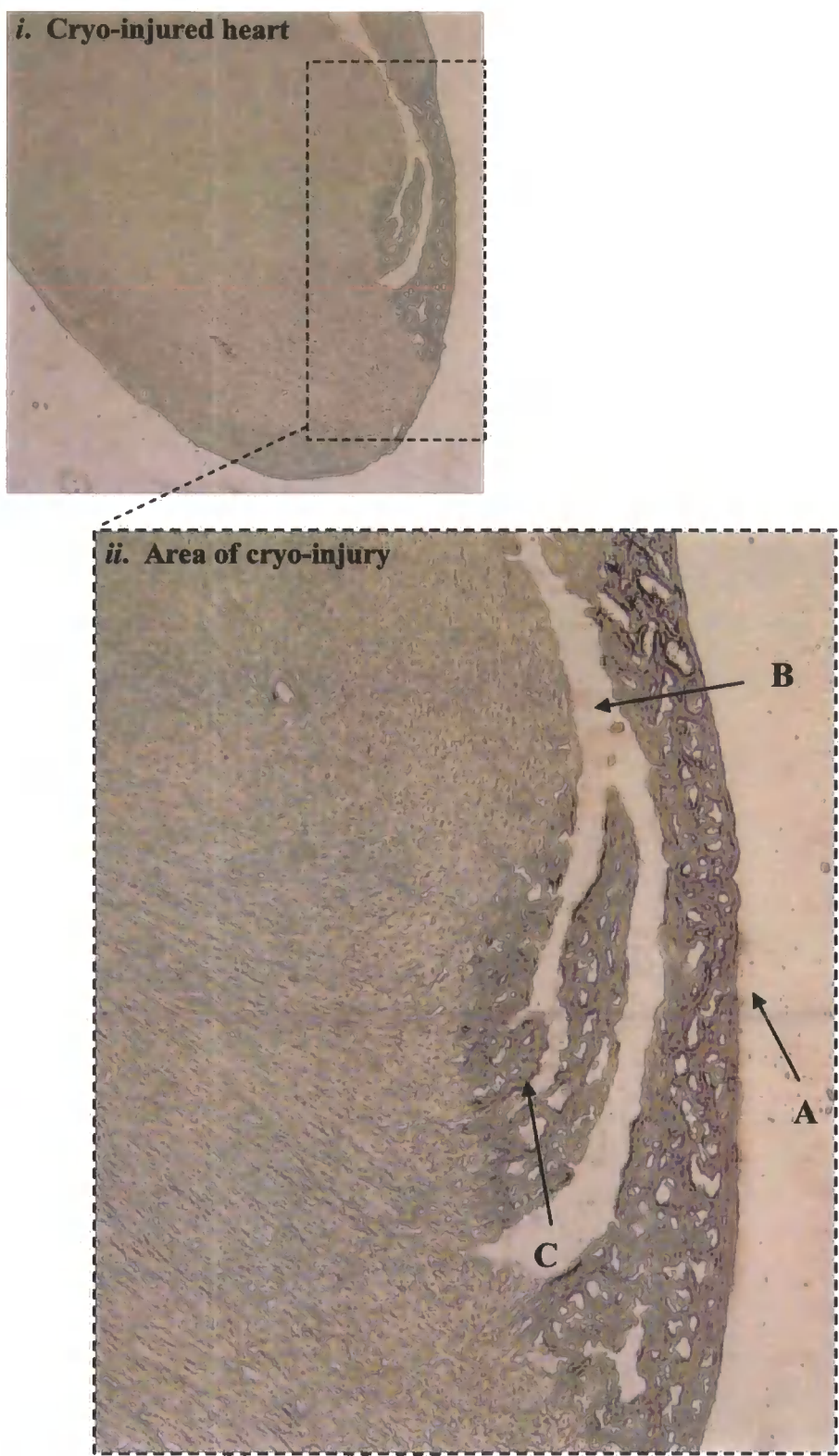
Excised mouse heart 8 days post-infarct (*i*) showing cryo-injury (*ii*). Granulation was not apparent however there remained a degree of inflammation. The ventricle wall at the site of injury is thin and the ventricular blood can be seen collecting here (F); capillary infiltration remains (E). The peri-infarct zone is less well defined (D). This photograph is representative of 10 mice (five mTert-GFP and five WT) the heart was removed 8 days post-infarct and photographed in PBS.

Figure 5.23: Excised cryo-injured heart 14 days post-infarct



Excised mouse heart 14 days post-infarct (*i*) showing cryo-injury (*ii*). The ventricular wall at the site of necrosis was extremely thinned; bubbles collected in the ventricle, on removal of the heart, which could be seen through the myocardium (F). Capillary infiltration remained (E) with the peri-infarct zone indistinguishable from normal tissue (A). It is noted that this mouse had normal levels of activity in the cage and appeared healthy.

Figure 5.24: Section of a 14 day cryo-infarct demonstrating typical depth of tissue damage



Sectioned mouse heart, 14 days post-infarct; a selected section of the cryo-injured tissue demonstrating full depth tissue damage. This representative section shows the inner most part of the infarct; the necrotic tissue penetrated the myocardium (A) through to the ventricle (B) and tissue adjacent to the initial contact site (C). This photograph is representative of 5 mice, the heart removed 14hrs post-infarct.

5.2.3.7 GFP antibody labelling of the cryo-injured heart

Following cryo-injury, each heart from the day 8 cryo-injury time point; 5 mTert-GFP mice and 5 WT littermates, and day 14 time point; 5 mTert-GFP mice and 5 WT littermates, were sectioned. GFP+ve cells were identified by immunohistochemical antibody labelling on both WT and mTert-GFP hearts. No GFP+ve cells were identified in the hearts from mice sacrificed 8 days after cryo-injury (data not shown).

GFP+ve cells were consistently identified in the mTert-GFP hearts 14 days after cryo-injury. One (figure 5.25) to two (figure 5.26) GFP+ve cells were identified in approximately every other 10µm section visualised; cells were associated with the cryo-injury area of the heart in, or closely located with, the epicardium. This was the case for each of the 5 mTert-GFP hearts where in excess of 50 sections from each heart were sampled.

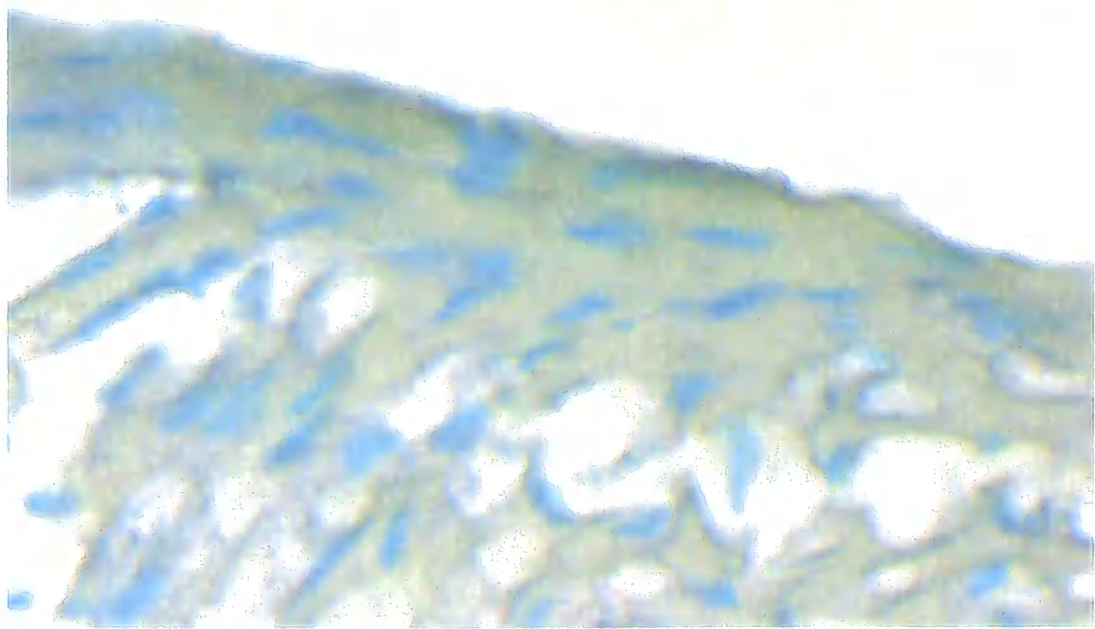
On occasion there appeared two cells within one section; these cells were located within close proximity of one another in the epicardium or within the myocardium, as demonstrated in figure 5.27. There were no GFP+ve cells identified in the WT heart sections, 8 days or 14 days after cryo-injury, as demonstrated in a representative section in figure 5.25.

To confirm the presence of cells that were identified as GFP+ve by immunohistochemical antibody labelling as well as to determine if the cells were of haematopoietic or endothelial lineage, the sections from the day 14 cryo-injury hearts were dual labelled for anti-GFP and anti-CD45 immunofluorescence. Representative GFP+ve cells are shown in figure 5.28. The cells were located in the epicardium, and correlated to nuclear Pi labelling and were CD45-ve.

In summary, figure 5.26 and figure 5.27 demonstrate GFP+ve cells that by immunofluorescence, in figure 5.28, were CD45-ve. These cells were associated with the epicardium around the infarct zone; in no instance were cells identified within the cryo-injured tissue. All labelled cells were clearly distinct from the surrounding GFP-ve cells. The frequency of such cells were low at one-two per section and only observed in the 14 day post-injury hearts and not detectable in the day 8 samples.

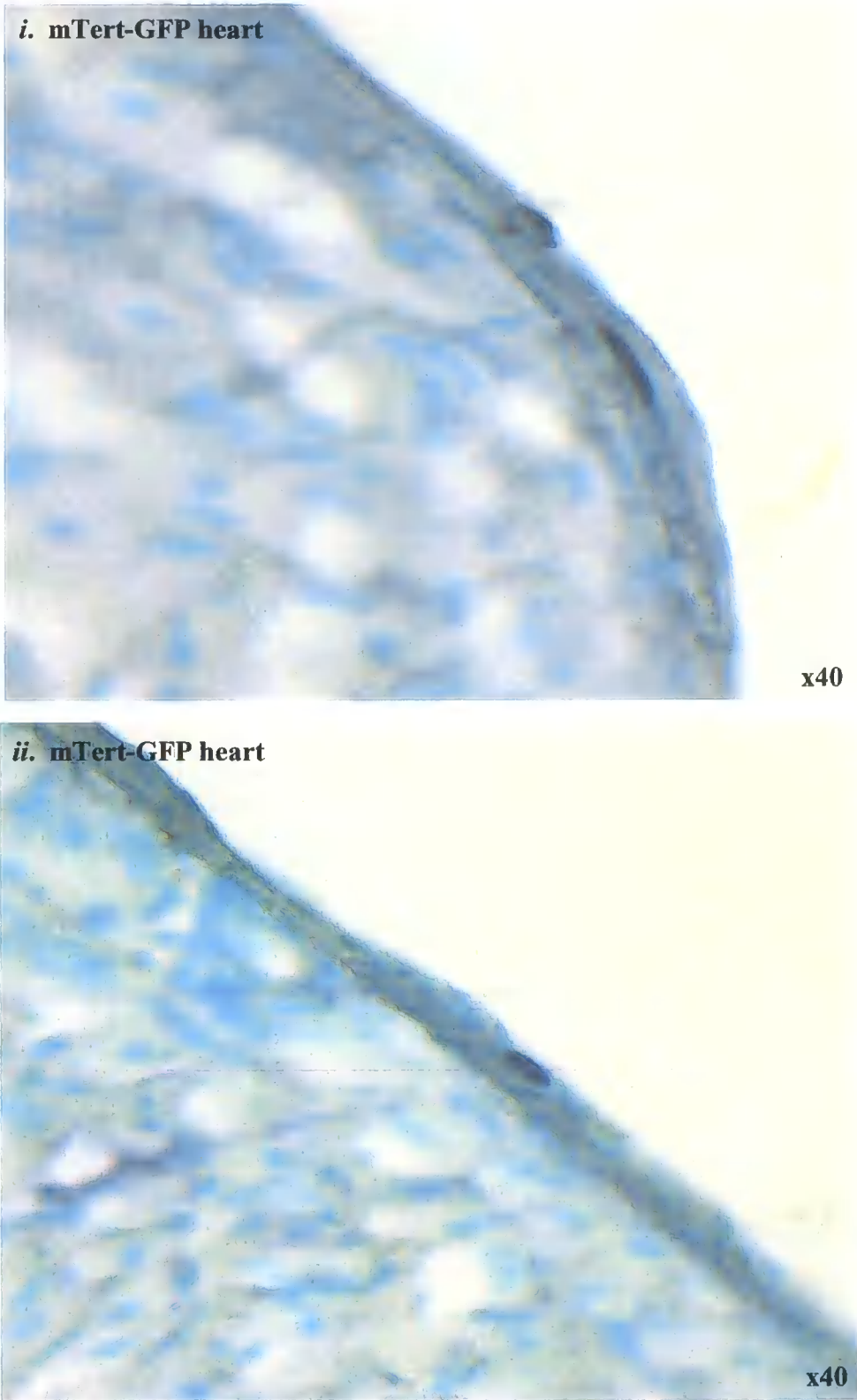
Figure 5.25: Immunohistochemical staining for GFP cells in 14 day cryo-injured myocardium of the WT mouse

WT heart



Immunohistochemistry on WT adult heart, 14 days after cryo-injury, for anti-GFP labelling. The area of myocardium shown correlates to the epicardium close to the cryo-injury zone where GFP+ve cells were identified in the mTert-GFP cryo-injured hearts. The WT hearts were removed from the mouse 14 days post-infarct; anti-GFP was detected using VIP (purple) and counter stained with methyl green (blue). This photograph is representative of 5 WT hearts with 50 sections analysed per heart, image shown at x40 magnification.

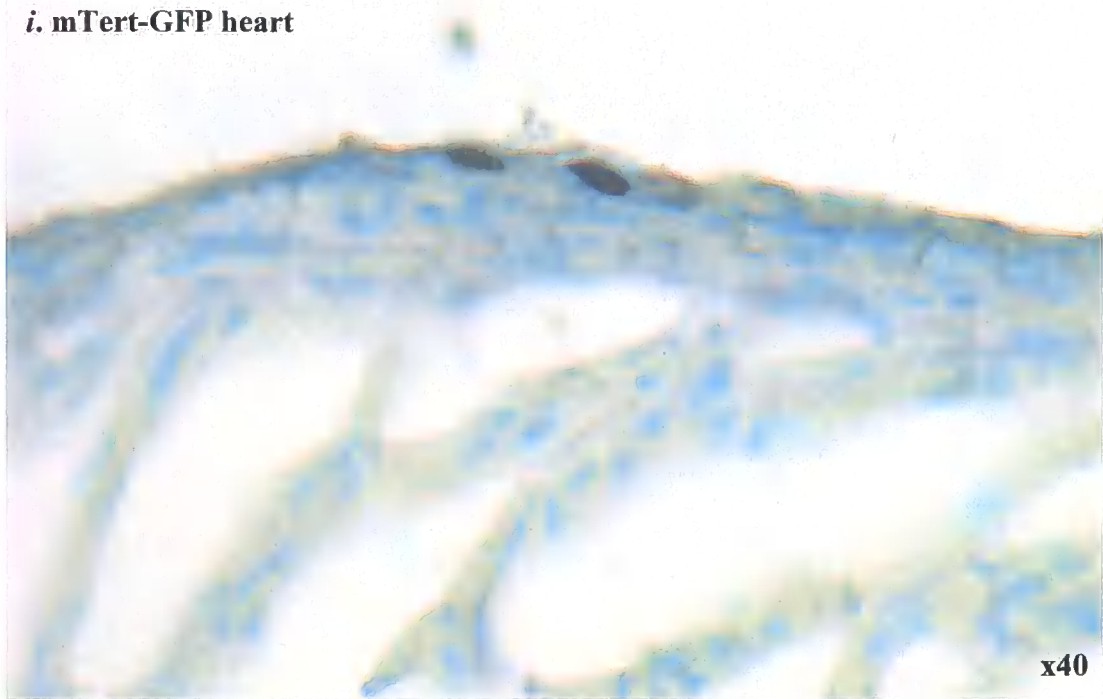
Figure 5.26: Immunohistochemical labelling for GFP cells in 14 day cryo-injured heart of the mTert-GFP mouse



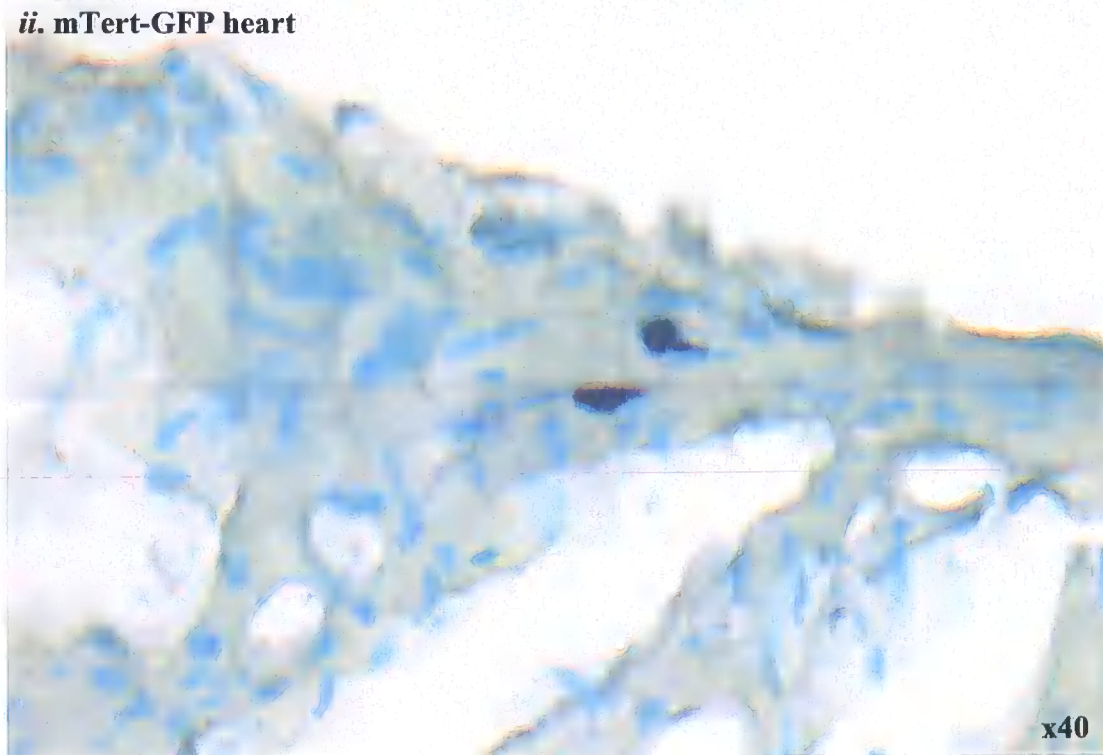
Anti-GFP antibody labelling detected by VIP (purple), counterstained with methyl green, from two separate hearts. 14 days after infarct, of the mTert-GFP mouse. The area of myocardium photographed is the epicardium close to the site of infarct showing representative GFP+ve cells.

Figure 5.27: Immunohistochemical labelling for GFP cells in the 14 day cryo-injured heart of the mTert-GFP mouse

***i.* mTert-GFP heart**

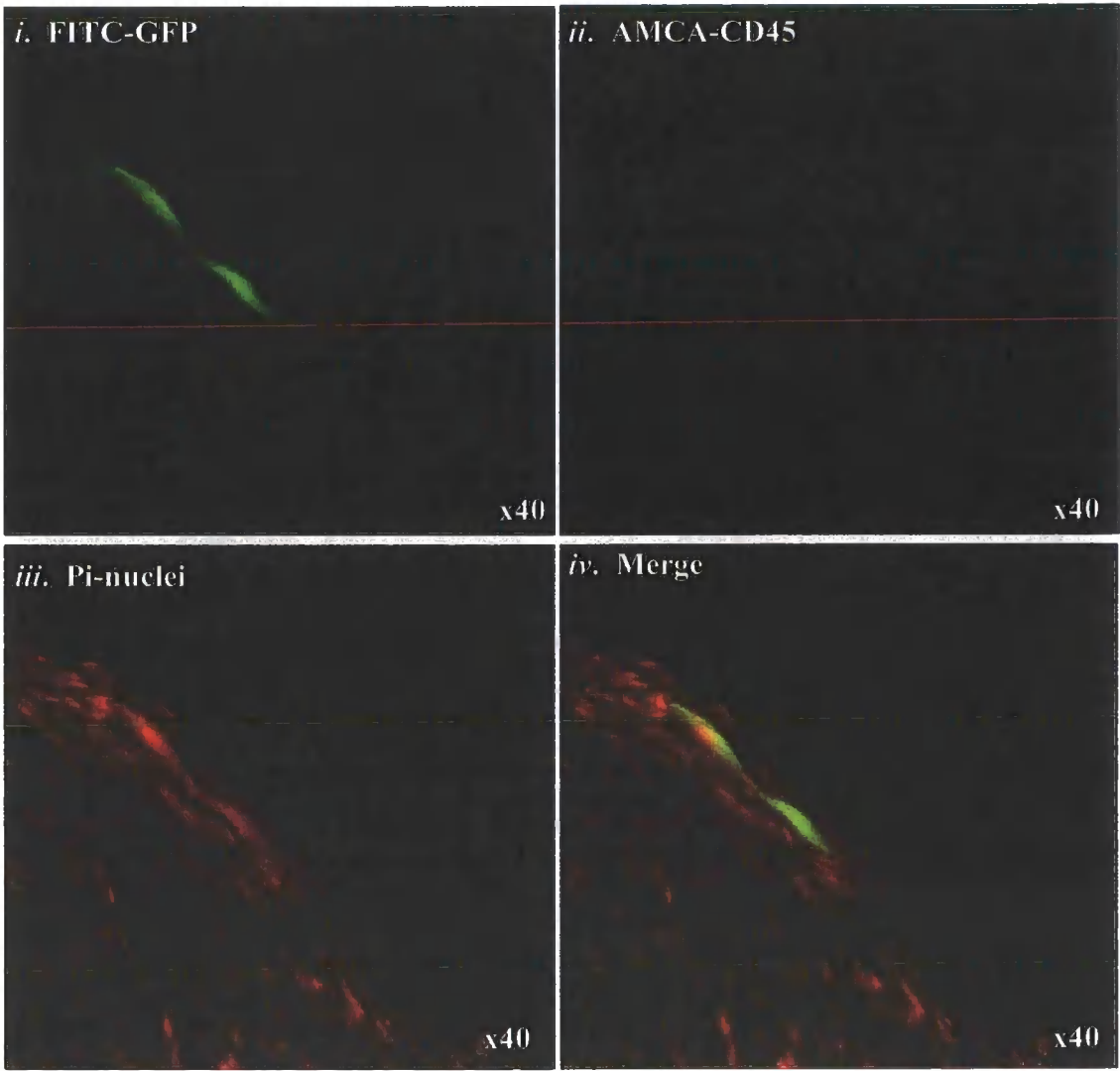


***ii.* mTert-GFP heart**

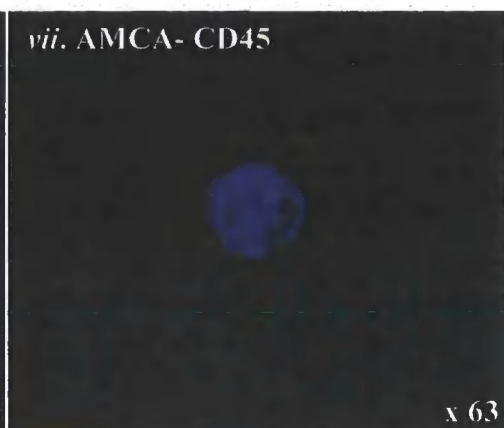
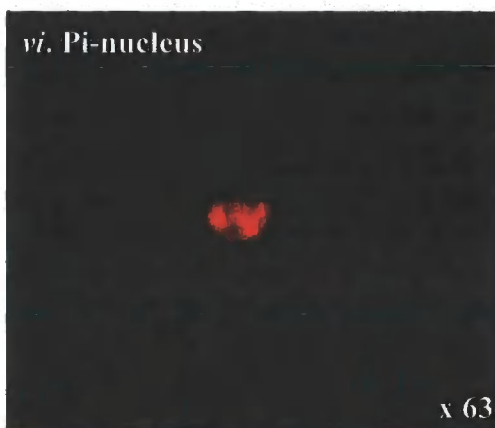
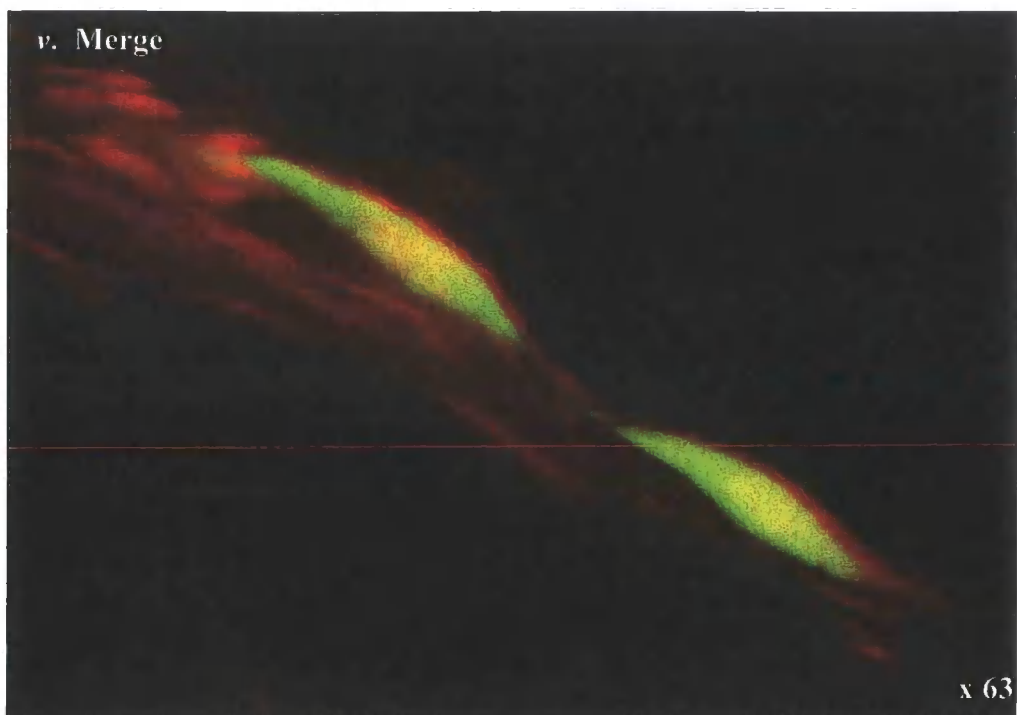


Anti-GFP antibody labelling detected by VIP, counterstained with methyl green, on two separate hearts, 14 days after infarct, of the mTert-GFP mouse. The area of myocardium photographed is the epicardium close to the site of infarct, showing two GFP+ve cells. Cells were commonly located in the epicardium (*i.*) and on rare occasions the cells appeared in the myocardium associated with the epicardium (*ii.*)

Figure 5.28: Immunofluorescent labelling for GFP cells in the 14 day cryo-injured heart of the mTert-GFP mouse



Immunofluorescence labelling for anti-GFP in the heart of the mTert-GFP mouse, 14 days after cryo-injury, with anti-CD45 co-labelling. The area of the myocardium, close to the cryo-injury, is shown where two GFP+ve cells (*i*) similar to those cells seen with immunohistochemistry (as shown in figure 5.27), were identified. These cells were CD45-ve as indicated by absence of AMCA fluorescence (*ii*). A higher magnification merge is shown over page.



The higher magnification merge (v) shows the anti-GFP antibody labelling clearly in the epicardium associating with Pi+ve nuclei labelling.

Figures vi-viii show a CD45+ve haematopoietic cell from the blood of the mTert-GFP mouse to demonstrate that the antibody could detect CD45 expression.

5.3 Chapter 5 Discussion

The mTert-GFP mouse was used to determine if there was a population of dermal follicular cells that expressed Tert, which have stem cell properties. This model was also examined to see if these GFP +ve cells could also be identified in the heart during health and disease.

In the first instance the mTert-GFP mouse was used to determine if there was a population of GFP expressing cell types in the dermis. Work described in Chapter 3 indicated that there was expression of Tert transcripts in the follicular dermis, but that this RT-PCR approach could not provide an indication of the numbers of cells expressing this gene product *in vivo*. Histological analysis of the mTert-GFP mouse demonstrated expression of the reporter gene in approximately 1 in 10 of the follicles examined. Where expression was observed within a follicle, Tert was found in bulge region, DS and DP. In no cases was expression exclusive one of these three compartments.

This data appears different that of Sarin *et al.*, (2005), who used immunofluorescence to directly detect mTert in mouse hair follicles. In this study, mTert RNA was detectable in the bulge region, as demonstrated by co-expression with BrdU labelled cells, and the outer root sheath of the follicle, but no expression was detected in the DP. Furthermore, expression was not restricted to a sub-population of follicles, but was common to all structures examined. There are at least reasons for these differences. The first is that with the mTert-GFP transgenic mouse there were multiple copies of the mTert-GFP transgene, making GFP easier to detect. Sarin did note that their own data might reflect an inability to detect all the Tert expression, as they failed to detect Tert in follicles known to express it, such as the DP. Secondly, Sarin was looking at the back skin and not the vibrissae follicles. In this study, vibrissae were chosen here as they are allowed clear distinction of the DP and DS from surrounding hair follicle structures, however, the hair cycle pattern between these two types of follicle can be different (Lavker *et al.*, 1991). The follicles of the vibrissae may have been in different cycles to the back skin follicles as investigated by Sarin. Indeed, this study had no data suggesting that GFP expression in the hair follicle followed the hair cycle.

The DP may have been activated in response to whisker loss, with the formation of new hair fibres (Reynolds and Jahoda 1991). During wound healing, the DS is particularly

active as DS cells are capable of regenerating the DP and of fibroblastic epidermal regeneration (Reynolds and Jahoda 2001). This may then account for the GFP expression in these compartments in some, but not all, follicles.

In an attempt to capture follicles that were inducing hair growth, the embryonic vibrissae were investigated. There was no detectable GFP expression in the developing vibrissa follicles of E14.5 embryos. The cells of the follicle, at this stage of development, have been reported to be actively involved in the formation of the follicle plugs and epidermal down growth (Davidson and Hardy 1952) which suggests these cells undergo significant proliferation, suggesting telomere length would need to be maintained, as well as differentiation to give rise to the adult hair follicle. However these cells may have been committed and therefore not require Tert activity. In addition, Human MSC have been reported to have no detectable telomerase even though these cells remain capable of differentiation into adipocytes, chondrocytes and osteoblasts (Zimmermann *et al.*, 2003). Telomerase activity in haematopoietic cells is associated with self renewal potential when telomerase activity was assayed in HSC in different stages of differentiation including lineage-committed progenitors and mature myeloid and lymphoid cells. The frequency of telomerase-expressing cells appeared to correlate with the frequency of cells with self-renewal potential (Morrison *et al.*, 1996).

If these stem cells are quiescent in the embryonic vibrissa at this embryonic age, where subsequent follicle formation results from differentiation and division of progenitor cells, then the actively dividing cells would not require telomere length maintenance if they are differentiating down a committed cell lineage, therefore not involved in self renewal. These cells would not be identified as GFP⁺ with the mTert-GFP mouse as they would not be maintaining their telomere length as has been described with the MSC and HSC above. The mTert-GFP mouse model may therefore indicate stem cells involved in self-renewal, which require longer telomeres. If this were the case, then in a highly active tissue the number of cells involved in self-renewal would be limited, as the stem cells have already produced cells that are more differentiated and lineage committed and these cells then divide to give rise to the specialised follicle components. Once the tissue has reached its proliferative capacity, the stem cells are more involved in self renewal and entering senescence. In addition, Tert has demonstrated a role in the skin that is independent of telomerase and is involved with hair growth (Sarin *et al.*,

2005) therefore it may be detectable when the hair is actively growing and not during embryonic follicle formation.

GFP expression was investigated in the neonatal back skin to attempt to identify cycling follicles which would be involved in stem cell mobilisation and new hair growth (Flores *et al.*, 2005; Choi *et al.*, 2008). A number of GFP+ve cells were identified in the follicular dermis; these cells were CD45-ve and CD34-ve indicating they are not derived from the haematopoietic lineage (Holyoake and Alcom 1994; Trowbridge and Thomas 1994).

GFP+ve cells were associated with two areas of the dermis; the first was the dermis surrounding the follicular end bulb and the second was the inter-follicular dermis where cells were located higher up the follicle, nearer the bulge region. The anti-GFP labelling of cells located in the dermis, associated with the end bulb as demonstrated in figure 5.9, did not correlate with the region of the DP structure in the end bulb as would be seen in a mature anagen hair follicle. There was not co-labelling of anti-GFP with the dense nuclei of the discrete hair follicle components. However, their consistent appearance in the vicinity of the end bulb suggests that their association with this structure is related to the EB components.

Using the staging as described by Paus *et al.*, the follicles photographed show different stages of developmental growth as would be expected in neonatal skin, where the hair is emerging through the skin for the first time. The staging of the follicles may correlate the GFP+ve cells with specific developing dermal compartments. There are 8 stages of hair follicle development from stage 0; an accumulation of nuclei termed the pre-germ stage, through to stage 8; a maximal length, mature anagen hair (Paus *et al.*, 1999). 10% of hair follicles are in stage 8 by day 3 post partum (p.p.), 35% in stage 8 by day 5 p.p. and 100% at stage 8 by day 9 p.p.. The skin isolated here was from 5 day old neonates, however, as Paus suggests, the hair follicles would be in a variety of stages with only 35% at full anagen. The follicles, shown here in association with GFP+ve cells, are of three different stages; stages 3-6 which are normally associated with the majority of hair follicles in neonates aged 2-4 days respectively; this may indicate why limited numbers of GFP+ve cells were identified in the 5 day old neonatal dermis by immunofluorescence which is also supportive of the concept of the stem cells to be entering senescence after self-renewal involved with earlier stages.

The first representative follicle, as demonstrated by figure 5.9, was stage 4 which normally correlate to follicles in neonates aged 3 days old. This type of follicle is a solid, elongated column of epithelial cells, consisting of multiple layers of keratinocytes concentrically arranged around the follicular axis; the hair peg is enlarged with a concave proximal end where dermal fibroblasts form the rounded, oval DP which is partially embedded in the concave end of the hair plug where the hair matrix is enclosing the DP by 50% (Paus *et al.*, 1999). The GFP+ve labelling, as shown in figure 5.9, was directly below the follicle associated with the region of either the remaining exposed DP or the hair matrix.

Figure 5.8 shows a follicle at stage 5 which normally correlate to follicles in neonates aged 3-4 days old. This is the advanced hair cone stage or bulbous peg, has elongation of the inner root sheath and an enlarged future bulge region, the DP is enclosed by the hair matrix and the hair canal has started to develop (Paus *et al.*, 1999). The GFP+ve labelling associated with follicles of this stage, as shown in figure 5.8, were situated in the developing future bulge region.

Figures 5.6 and 5.10 both show follicles at stage 6 which normally correlate to follicles in neonates aged 4 days old. This is the hair formation stage; the hair follicle end bulb is located in the subcutaneous layer of the skin where the DP is thicker and more elongated. The hair follicle is at a 40° angle to the epidermis with the inner root sheath extended to contain the hair shaft (Paus *et al.*, 1999). Most notable at this stage is the elongation of the hair shaft; the GFP+ve cells associated with these stages were deeper in the dermis most likely due to the movement of the follicle into the subcutaneous layer as the inner root sheath extends.

In summary, the GFP+ve cells associated with early stage follicles were located with the region of the developing DP. When the GFP+ve cells were associated with the later stage follicles, they were located in the area of the developing bulge region. This suggests that GFP expression was associated with DP development and in bulge region development or maintenance.

FACS analysis allowed isolation of the dermal-derived GFP+ve cells from a range of neonatal ages associated with i) initial hair appearance (day 2 neonates) ii) appearance of secondary hair follicle formation (day 3 neonates) and iii) with hairy skin (day 5 neonates). There was a consistent GFP+ve population present in the dermis which was

relatively low; the percentage of cells isolated did not reflect a proliferative population of cells; if this was the case the number of GFP+ve cells would be expected to be higher. The percentage of GFP+ve cells isolated, that were haematopoietic lineage-ve, were similar for the day 2 and day 5 neonates at 0.17% and 0.18% respectively with a higher percentage of 0.49% for the day 3 neonatal dermis which may correlate with the time of secondary follicle formation (Davidson and Harvey 1952).

When the mTert-GFP mouse was being initially investigated it was noted that the majority of spermatogonial stem cells lining the basement membrane and elongating spermatids in the innermost region of the tubule did not express GFP, suggesting that the quiescent cells were not identified with this mouse model (Breault *et al.*, 2008). This in turn, suggests that the percentage of dermal cells labelled here was consistent with the observation of Breault i.e. a population of cells re-entering quiescence.

Recently, Crigler *et al.*, reported the presence of a mesenchymal population resident in neonatal murine dermis which could be repeatedly isolated by a sequence of differential centrifugation and selective culture conditions. These cells had potential to develop an epidermis *in vitro*; in monolayer culture the cells had long-term survival capabilities in restricted serum and an inducible capacity to produce multiple cell lineages, both epithelial and mesenchymal, depending on culture conditions (Crigler *et al.*, 2007). The group identified two sub-populations in the dermis which they assigned as fraction D and E; these cells made up 0.4% and 0.7% of the dermis respectively with about 45% of these cells being CD34+ve; therefore 0.22% fraction D and 0.39% fraction E were CD34-ve, both of which are comparable percentages with the dermal fractions isolated by Tert-associated GFP expression. These cells had low labelling for keratin 15, associated with the bulge region, with less than 10% of fraction E labelling for c-kit which has also been associated with the bulge region. When these fractions were mixed with a crude epidermal population of interfollicular basal cells, which did not survive in culture when alone; fraction E formed viable monolayers in culture where fraction D did not. This is suggestive of fraction E containing epidermal precursors (Crigler *et al.*, 2007). When fraction D was implanted s.c. (sub-cutaneous) in the skin of immune-deficient mice, they formed a vascularised fibrotic mass, previously identified as precursors to the formation of follicular buds and then pegs (Zheng *et al.*, 2005). Fraction E, which expressed the bulge marker keratin 17, integrated with the host muscle on s.c. injection into the skin, as described above. Both fractions gave rise to

fusiform structures, reminiscent of disorganized muscle, which stained positive for smooth muscle actin and desmin. Interestingly, the GFP+ve cells isolated from the mTert-GFP mice did not adhere or aggregate in culture when in isolation in both hanging drop, suspension and adherent culture which is similar to the fractions isolated by Crigler, potentially indicating an overlap of cell populations. The two fractions identified by Crigler may correlate with the two different locations of the GFP+ve cells in the dermis i.e. fraction D with the end bulb and fraction E with the bulge region.

The lineage-ve dermal cells were cultured a week and two weeks, using 3 day old neonatal dermis; these cultures therefore contained GFP+ve and GFP-ve cells on seeding. The percentage of GFP+ve cells in freshly isolated day 3 neonatal skin was 0.49% which dropped to 0.30% after 1 week culture and furthermore to 0.13% after 2 weeks. It was not possible to determine if the cells identified as GFP+ve before culture were the same cells after 1 week and 2 week culture, however, these percentages were within with the range previously identified with freshly isolated dermis. If there were a percentage of cells in culture that were stem cell-like in their proliferative properties, as indicated by pulse chase experiments in chapter 3, the number of these cells would be small and would give rise to a number of more differentiated progeny. Interestingly, as demonstrated by figure 3.6 in chapter 3, there were population of DP and DS cells which constituted 0.4% and 1.0% of the original population put into culture, respectively, that demonstrated the most cell divisions. It would be interesting to ascertain if these cells from the DP and DS were comparable to the GFP+ve cells isolated from the 1 week and 2 week dermal cultures.

The GFP+ve and the GFP-ve cells did not adhere well or divide in adherent culture when they were separated from one another. When cultured together, with lineage+ve cells removed, the cells had fibroblastic appearance in adherent culture and increased in confluency indicative of cell division. This suggests the cells assigned GFP+ve status require cell-to-cell contact and communication with the GFP-ve cells necessary for adherence and propagation of the dermal population; a property observed with the maintenance of a number of pluripotent stem cells. There are a number of cells that require a feeder layer in order to settle and proliferate including mouse embryonic fibroblasts (MEF) for human embryonic stem cells (hESC) (reviewed by Skottman and Hovatta 2006) and, for example, umbilical cord blood derived MSC as a feeder layer

for umbilical cord derived committed haematopoietic progenitor cells (Jang *et al.*, 2006).

RT-PCR analysis of the isolated populations demonstrated all the detectable Tert expression in the GFP+ve cells; the *in vitro* culture results therefore indicate that the dermal cells expressing Tert required cell contact with the Tert+ve cells in order for the population as a whole to proliferate. The GFP+ve cells also contained all the detectable expression of the stem cell associated genes investigated i.e. Oct4, Nanog and Sox2 which are expressed by pluripotent embryonic stem cells. Q-PCR confirmed that the Nanog, Oct4 and Sox2 expression was only detectable in the GFP+ve dermal cells; expression of which was maintained even after 2 weeks culture suggestive of the maintenance of a stem-cell like population identifiable by Tert expression. These genes have not previously been associated with the dermis and their presence here in the Tert+ve dermal fraction may indicate their stem cell abilities and differentiation potential.

The majority of the cardiomyocyte-associated genes were not detectable in the dermis. Of the cardiomyocyte inductive genes these included Nkx2.5 and GATA4, as was undetectable in the DP and DS populations (Chapter 3, figure 3.12). Mef2c was not detectable in the GFP+ve, GFP-ve or unsorted cells' suggesting that previous Mef2c detection was attributed to the DP and DS. Tbx5, which was previously undetected in the DP and DS primary cells, was enriched in the GFP-ve population suggesting the cells responsible for this expression are derived from the interfollicular dermis. Of the cardiomyocyte functional genes, tropomyosin was expressed in both GFP fractions as was detected in the DP and DS cells. α -MHC, cardiac actin and titin were not detectable in either GFP+ve or GFP-ve fractions; these genes were undetectable in cultured DP and DS (Chapter 3, figure 3.13). The dermis had detectable expression of troponin I and tropoelastin in the GFP-ve fractions; elastin highly likely to be associated with the elasticity of the skin which is well described (Mithieux and Weiss 2005).

The general presence or absence of genes in the freshly isolated cells correlated with the 1 week and 2 week populations indicating although the cells in culture alter their expression levels of Tert there remains a consistent population of cells expressing a fraction of the genes investigated suggesting these cells as a population are maintained in culture.

The heart is now considered to contain a population of cardiac stem cells, although the markers used for the identification of these cells remains somewhat controversial. The identification of these cells has previously required a combination of cell surface markers and demonstration of functional capabilities. However, there is no consensus on the surface markers to identify a definitive single cardiac stem cell and the molecular mechanisms regulating their growth. Expression of Tert may allow the identification of a population of cells enriched for cardiac stem cells.

Flow cytometric analysis of the Tert+ve cells of the heart identified a very low percentage of cells, 0.08%, a percentage consistent with previous reported numbers. A recent investigation isolated cells by a single-cell clonogenic technique to analyse proliferative clonal cell populations from the heart (Tateishi *et al.*, 2007). They set up 9541 single cells of which 11 produced clones within 7 days; however only 3 grew in serum-free media. These 3 clones had significantly elevated telomerase activity and formed spherical clusters; interestingly these cells expressed Nanog and Sox2. The clonal cells constituted 0.03% of the cardiac cells which is similar to the percentage of cells identified by GFP expression here. In addition, Tateishi also produced an mTert-GFP mouse and FACS analysed Tert+ve cells. They identified the number of cells Tert+ve to be $0.9\% \pm 0.2\%$. Tateishi demonstrated the percentage of cells sca-1-ve (a component of the lineage cocktail used here to identify lineage negative cells) which was also Tert+ve to be 0.17%. The Tert+ve cells as shown in figure 5.18, constituted 0.08% of the lineage-ve cardiac cells. Considering a number of other markers were also used to identify lineage-ve cells in this study, which were not included in the work of Tateishi, the population identified here may overlap with the cells identified by Tateishi *et al.*, being in that 0.17%. Tateishi commented that within this 0.17% of cells there were cells which were CD45+ve and CD45-ve; a surface marker included in the lineage cocktail used here. Tateishi reported sca-1 expression in the majority of intrinsic cardiac stem cells in the adult heart which have the characteristics of ES-like and mesenchymal-like cells, and that sca-1 expression may play a role in cardiac stem cell maintenance and function. The lineage cocktail used here excluded sca-1+ve cells from the population, therefore, because the number of Tert+ve, lineage-ve cells identified in the heart was so low and to not exclude the possibility of sca-1 being an essential factor in the cardiac stem cells, the regenerative heart was investigated by histological analysis.

A cryo-induced injury is a representative model of a myocardial infarction (Van den Bos *et al.*, 2005). The injury to the myocardium was consistent with previous reports of cryo-induced myocardial infarctions with extensive areas of coagulation necrosis with haemorrhage at the centre of the infarct as observed in figure 5.20 and 5.21. There was dense inflammatory infiltrate as observed in fissure 5.20 with granulation tissue (Van den Bos *et al.*, 2005). Figure 5.24 showed apparent complete loss of cardiomyocytes of normal morphology in the infarct area as reported by Leferovich (Leferovich *et al.*, 2001) with the appearance of cardiomyocyte remnants (Vandervelde *et al.*, 2006).

GFP+ve cells, as indicated by immunohistochemistry and confirmed by immunofluorescence, were only detectable at day 14. These cells appeared morphologically distinct from the cardiomyocytes; they had a small, rounded appearance. GFP+ve cells were not observed in the hearts 8 days after infarct, but were present at day 14. At that stage the inflammatory cell infiltration is significantly reduced compared to earlier time points; there is reduced macrophage and T-lymphocyte density at the infarct area (Vandervelde *et al.*, 2006) which is overtaken by regeneration with the appearance of cells with stem cell properties as the scar is produced and a degree of cardiomyocyte infiltration.

The GFP+ve cells were mostly associated with the epicardium (figures 5.26); in cases when the cells were not in the epicardium they were very closely associated with it (figure 5.27) suggesting the GFP+ve cells may be related to the epicardium and its stem cells.

The epicardium is the outermost cardiac epithelial layer that covers the surface of the adult vertebrate heart; it is a single-layered flat mesothelium connected to the myocardium and is in contact with the fluid of the pericardial cavity (reviewed by Wessels and Perez-Pomares 2004). Between the myocardium and the epicardium lies the subepicardium, where mesenchymal cells that are epicardium-derived can be found. In the mouse at E9.5, there are three cell types in the heart: the cardiomyocytes, the endocardial epithelium and the subendocardial mesenchyme which at this stage is acellular; at this point of development a new layer of epithelial cells starts to populate the myocardial surface of the heart. These cells are derived from the endocardial epithelium and they generate the subepicardium as they form the epicardial sheet. Therefore the developing epicardium is often considered to be an extra-cardiac cell population as is the case with the cardiac neural crest cells (Wessels and Perez-Pomares

2004). A subset of these epicardial precursor cells also migrate into the myocardium and subsequently differentiate (demonstrated *in vitro* as well as *in vivo*) into a variety of cell types, including coronary endothelium, coronary smooth muscle cells, and blood progenitors, as well as being capable of differentiating into cardiomyocytes (reviewed by Wessels and Perez-Pomares 2004). There is also evidence that these cells are precursors to the cardiac fibroblasts (Gittenberger-de Groot *et al.*, 1998) however their role during postnatal life has not been elucidated. A number of these cells also remain in an undifferentiated state, raising the question of whether these cells may be a cardiac stem cell population. It has been proposed that these cells remain in position as an embryonic fibroblast population with a role in normal development and specifically in the formation of the fibrous cardiac skeleton. Under pathological conditions, these cells could be involved in the development of abundant fibroelastic tissue that cannot be explained simply as ischemic fibrous scar tissue (Gittenberger-de Groot *et al.*, 1998). It has been hypothesised that adult human epicardial cells could recapitulate part of their embryonic program when transplanted into diseased myocardium where they are capable of modifying the surrounding myocardium; epicardial cells transplanted into ischemic murine myocardium preserved cardiac function and attenuated ventricular remodelling (Winter *et al.*, 2007) indicating they may play a role in the infarcted heart.

In summary, there were populations of GFP+ve cells in the dermis, which correlate to Tert-expressing cells, as well as in the heart. Both cell types appear to be indicative of stem cell-like populations of cells which are limited in their number. The mTert-GFP mouse model was investigated in its ability to be a better model for the isolation of dermal derived cells with differentiation potential and it will be interesting to further assess the cells isolated here in comparison to the manually dissected DP and DS as proposed in Chapter 4. For the DP, DS or the GFP+ve population from the dermis to differentiate to cardiomyocyte-like cells and be used therapeutically, they would most likely need to express a gene profile similar to that of the cardiac stem cell population. Therefore, using the mTert-GFP mouse as a tool to isolate a stem cell population from the heart, although speculative, may allow more understanding of this specialised cell population and subsequently determine the best route of differentiation of the dermal cells, as well as provide a better understanding, or potential marker, of a cardiac stem cell population.

6 Discussion

The end bulb, representative of the DP and DS cells combined, demonstrated spontaneous synchronised contractions *in vitro*, suggestive of cardiomyocyte differentiation. The DP and DS, after co-culture *in vitro* with embryonic cardiomyocytes, demonstrated differentiation towards a cardiomyocyte lineage but the levels of gene expression were very modest. The results were suggestive of the presence of a small population of cells in dermis which may have high potency for differentiation and stem cell activity.

Cells of the DP and DS demonstrated a number of stem cell properties as described in chapter 3. *In vitro* both cell populations maintained their morphology, proliferative rate and characteristic gene expression over a number of passages. The presence of multipotent cells in the interfollicular dermis has previously been demonstrated in the work of Jahoda; the DP and DS were shown to be capable of differentiation towards adipocytic and osteocytic lineages (Jahoda *et al.*, 2003A). In addition, ongoing studies are investigating the potential of the DP and DS primary cells to populate the embryo with blastocyst injections (personal communication with Prof. Jahoda). The bulge region of the hair follicle has also demonstrated to give rise to all the epithelial cell types of the lower follicle, the epidermis during wound healing as well as cell types from lineages unrelated to the hair follicle such as Schwann cells and neurons (reviewed by Cotsarelis 2006). Other tissues have also demonstrated multipotency for example the bone marrow MSC which have demonstrated differentiation potential to osteogenic, adipogenic, chondrogenic and myogenic lineages and potentially neural cells also (reviewed by Jackson *et al.*, 2007). Therefore, it is not surprising that if the dermal cells represent a population of cells with stem cell properties, as other tissue have, that they would be able to give rise to a number of lineages. In addition, a number of these cell types have also demonstrated cardiomyocytic differentiation potential as discussed in Chapter 1, such as MSC (for example Toma *et al.*, 2002) and HSC (for example Kajstura *et al.*, 2005).

Although a number of stem cell types demonstrate *in vitro* and *in vivo* differentiation to cardiomyocytes, there is little evidence that exogenous stem cells contribute to the heart. A recent study demonstrated that after transplantation of GFP+ve bone marrow cells into a c-kit mutant mouse; these cells were subsequently found to reside in the

bone marrow as expected. After induction of myocardial infarction, there was a dramatic increase in the number of c-kit⁺ve cells in the heart of which the majority were GFP⁺ve. Although this argues that bone marrow-derived cells have the capacity to home to the heart, where they express c-kit, the study does not determine whether these bone marrow-derived cells typically reside in the normal heart or whether they were recruited only in response to injury (Fazel *et al.*, 2006). In addition, in sex mismatched cardiac transplants in humans, the female hearts in male hosts had a significant number of Y chromosome-positive myocytes and coronary vessels (Quaini *et al.*, 2002) suggesting male cells colonized the female heart after transplantation; cells of both donor and recipient origin were found to express c-kit, as well as sca-1, however the possibility of fusion was not entirely investigated which may indicate these cells grafted but did not differentiate to cardiomyocytes. *In vitro* animal experiments, whereby cells are introduced to the heart by injection directly into the MI heart or into a blood vessel after MI, have demonstrated the presence of cells in the myocardium that are donor derived as discussed throughout Chapter 1. These grafted cells have demonstrated cardiomyocyte properties including gene expression changes, gap junctions with native cardiomyocytes and contractions however not all of these studies have investigated fusion events with native cardiomyocytes. A number of clinical trials cite functional improvement in patients receiving donor cells. However, the degree of functional improvement is very modest, 3–5% significant improvement in ejection fraction versus controls is typically the range reported (Assmus *et al.*, 2006; Lunde *et al.*, 2006; Schachinger *et al.*, 2006). In addition, this range is not proportional to the number of cells administered, which is on average approximately 1×10^6 cells, in relation to the number of cells in the heart. It raises the question of whether the functional improvement is as a result of donor cell integration and differentiation or whether the mere presence of the cells induced a paracrine effect irrespective of donor cell type or grafting efficiency. In these clinical trials, when there was functional improvement, the control for the transplanted cell is normally PBS/saline i.e. the vehicle for the donor cells. Should the control be a cell type for example fibroblasts or a population of the donor cells that have been irradiated, rendering them unable divide, then the functional improvement, if any, may then be able to be attributed to the donor cell type. In addition, receptors for granulocyte colony-stimulating factor (G-CSF), a hematopoietic cytokine which induces the mobilization of hematopoietic stem cells and endothelial progenitor cells from bone marrow into the peripheral blood circulation, have been

identified on cardiomyocytes. G-CSF has been shown to prevent left ventricular remodelling and dysfunction after acute MI as well as induce angiogenesis (Takano *et al.*, 2006). Therefore functional improvement could be as a result of the cardio-protective action of G-CSF on the receptors of the viable cardiomyocytes after MI and not cellular differentiation of donor cells.

The evidence of cardiomyocyte differentiation potential of the dermal follicular cells suggests the presence of stem cells in the DP and DS population. One potential reason is that these are cells that remain in the hair follicle after embryogenesis. The DP and DS play a role in hair follicle morphogenesis and wound healing (Jahoda *et al.*, 2001A; Jahoda *et al.*, 2001B). As has been suggested by Jahoda, the dermal cells are considered to be embryonic type cells which are retained in an adult system rather than specialised adult stem cells. The embryonic-like properties of the hair follicle dermal cells derive from the fact that they segregate from intrafollicular dermis relatively early on in follicle development at which point they assume characteristic morphological and molecular phenotypes distinct from the interfollicular dermis (Jahoda *et al.*, 2002). There are suggestions that stem cells from other tissues may be cells left from embryogenesis, including cells from the heart. A number of studies into cardiac stem cells have identified putative stem cells that express a number of genes associated with embryogenesis including *Isl1* (Cai *et al.*, 2003), *GATA4*, *Nkx2.5* and *Mef2* (Beltrami *et al.*, 2003).

There are no reported cases of skin spontaneously differentiating to cardiomyocytes therefore the ability of the hair follicle DP and DS to demonstrate differentiation to a cardiomyocytic lineage is most likely physiologically irrelevant to the skin and the follicular dermis.

The heart has been reported to contain a population of endogenous stem cells, identified by a variety of marker combinations not always consistent from one group to another. These markers include *c-kit*, *sca-1*, *Abcg2*, *Isl1* as well as a number of functional tests including cardiosphere formation and side population properties including Hoechst dye efflux, these are discussed individually in Chapter 1. In addition, a number of these cell surface markers have been identified in cells collecting in niches in the myocardium. There is evidence the heart has degree of cellular maintenance, as demonstrated by the presence of a small number of cycling myocardial cells (Soonpaa and Field 1998; Kajstura *et al.*, 1998; Beltrami *et al.*, 2001). However, the role of the stem cell in the

heart is still not entirely understood. There is little evidence of these cells, in response to injury, contributing to myocardial repair and people remain to die of MI and heart disease indicating a putative cardiac stem cell population is not able to cope with cardiac insult of this magnitude. Understanding potential cardiac stem cells that may be functional in MI, or being able to identify prospective stem cells that can be recruited or activated to respond to MI, would further out understanding of the heart and lead to new avenues of treatment.

The mTert-GFP mouse is a prospective candidate for identification of proliferating stem cell populations by telomerase and, in tracking them thorough homeostasis and in response to injury, could be used to elucidate the role and potential for the putative cardiac stem cell as well as stem cells form a number of tissues. It is proposed as a model to be used in parallel with, or as an alternative to, complex cell surface antigen detection. This study describes the isolation of distinct dermal and cardiac-derived cell populations using the mTert-GFP mouse model.

There is evidence this mouse model identifies, by GFP expression, cells with stem-cell associated functional properties. Published analysis of the mTert-GFP mouse has shown that GFP+ve cells were enriched among bone-marrow derived HSC; telomerase expressing GFP+ve cells have also demonstrated long-term, serial, multi-lineage bone marrow reconstitution (Breault *et al.*, 2008). In addition, when the cells identified in the intestinal crypts are isolated and injected into blastocysts, they are found to give rise to the intestine of the embryo suggesting that the cells identified by Tert were stem cells of the intestine (personal communication). This study describes Tert+ve cells isolated from the dermis which contain all the detectable Oct4, Nanog and Sox2 expression. Tert+ve cells were also identified in the cryo-injury, concentrated close to the resultant infarct.

Tert, expressed in stem cells and in progenitor cells, serves to maintain telomere function through the de novo addition of telomere repeats to chromosome ends. However, Tert has also demonstrated a role, independent of the telomerase RNA component, in the mouse skin epithelium where, when over-expressed, it caused rapid transition of hairs from telogen to anagen. Tert over-expression promoted this transition by causing proliferation of multipotent stem cells in the hair follicle bulge region. This new function was reported to operate through a mechanism independent of its activity in synthesizing telomere repeats, but instead by promoting proliferation of resting

multipotent stem cells in the hair follicle bulge region (Sarin et al., 2005). It is therefore a marker for functional stem cells as well as having a role in proliferating cells, making it a potential marker for stem cell investigation in many tissues including the skin and heart.

6.1 Future Experiments

There are a number of experiments that would not only build upon the results described here but would provide new avenues of investigation for cells of both dermal and cardiac lineage.

The GFP+ve dermal cells would be a candidate for differentiation experiments. Investigating the cardiomyocytic potential of the GFP+ve cells in comparison to the DP and DS would be useful in determining if the dermal follicular cells are stem cell-like in their potency. The potential of the GFP+ve cells to other lineages, as has been described with dermal cells, to determine if these cells are multipotent. GFP+ve cells were identified in the heart although at very low levels. FACS analysis of these cells, namely into their expression of sca-1, c-kit, isl1 and abcg2 would allow them to be compared to previously identified potential cardiac stem cell populations.

Labelling the GFP+ve cells as well as DP and DS cells would allow them to be tracked in a number of *in vivo* experiments. One option would be to cross the mTert-GFP mouse with a Zin40 mouse; GFP+ve cells from any tissue of this mouse, once injected into a WT mouse, could be identified by lacZ expression. An alternative would be to produce a new mTERT-GFP mouse model with a tamoxifen inducible cre-lox system. On administration of tamoxifen the cells expressing Tert, as well as their progeny, would be identifiable by β -galactosidase expression.

Using these transgenic mice, a number of tracking experiments would be possible. For the skin, injecting the GFP+ve cells from the dermis into wounds and non-hairy skin to determine if they have proliferative properties, demonstrate multipotent differentiation and are inductive. Tamoxifen could be administered by injection to the skin at the time points investigated here, namely embryonic, neonatal and adult ages, where the hair follicle is developing. The dermis would be sampled after varying periods of time (pulse chase) to determine which structures the Tert+ve cells give rise to. Tamoxifen could be administered to the skin shortly after injury and the skin allowed a period of time to heal to determine if the Tert+ve cells identified here contribute to wound

healing in a similar manner to bulge cells. Plucking of the hairs would induce new hair growth, a different mechanism to wound healing, where tracking Tert+ve cells by cre-recombinase expression throughout the formation of new hair growth would indicate if these cells are involved in hair morphogenesis in a similar manner to the DP and DS. Monitoring the Tert+ve cells through normal hair cycling by administering tamoxifen to the back skin and allowing the cells a longer period of time before sampling sections of the skin may indicate changes in the cells that coordinate with the cycling events.

If the GFP+ve cells are pluripotent as their gene expression profile suggests then they should be capable of giving rise to all of the cells of the body. GFP+ve cells isolated from a Zin40/mTert-GFP mouse could be injected into the blastocyst and the resultant embryos investigated for lacZ expression. If the GFP+ve cells are pluripotent they should give rise to cells of the three germ layers. In comparison, it would also be interesting to determine if embryos could be produced from injection of labelled DP and DS cells into the blastocyst. GFP+ve cells from the heart and skin could be injected to determine if they give rise to the heart and skin, respectively, of the embryo in a similar manner to the intestinal stem cells.

Tracking of the cells identified as GFP+ve in the cryo-injury model would help our understanding of their role in injury as well as the resting heart. If the GFP+ve cells could be labelled as describe above i.e. with tamoxifen inducible cre-recombinase then these cells and more importantly their progeny could be tracked in the heart. Tert+ve cells labelled during early neonatal life when the heart has a level of proliferation; these cells could be tracked out to the adult heart to determine if they are responsible for the increase in the heart in transition from neonatal to adult age, as well as if these cells eventually congregate in niches. Tert+ve cells labelled in the neonate and the adult could be tracked for their response to injury to determine if these cells are responsible for remodelling of the injury site and if they correlate to the cells identified in the epicardium by GPF expression as demonstrated in chapter 5. Cells could be labelled after injury; between day 8 and day14 after cryo-injury, time points demonstrated here, to determine if these cells are homing, to or originate, from the injury site.

In summary, the cells of the dermal merit further investigation. They have demonstrated a number of stem-cell associated properties as well as modest differentiation potential to a cardiomyocytic lineage. The mTert-GFP is an exciting mouse model for the potential identification of stem cells, as isolated by a functional marker. There is

conflicting evidence for the presence of a cardiac stem cell population; the mTert-GFP mouse provides an alternative technique for their study.

Appendix

1 Abbreviations

ACE	angiotensin-converting enzyme
AMCA	7-amino-4-methylcoumarin-3-acetic acid
ANF	atrial natriuretic factor
ASTAMI	Autologous Stem Cell Transplantation in Acute Myocardial Infarction
BM	bone marrow
BOOST	Bone marrow transfer to enhance ST-elevation infarct regeneration
BrdU	bromodeoxyuridine
CFSE	Carboxyfluorescein Succinimidyl Ester
DAPI	4', 6-diamidino-2-phenylindole
dATP	deoxyadenosine triphosphate
dCTP	deoxycytidine triphosphate
DEPC	diethyl pyrocarbonate
dGTP	deoxyguanosine triphosphate
DMSO	dimethyl sulfoxide
dNTP	deoxyribonucleotide triphosphate
DP	dermal papilla
DS	dermal sheath
DTT	1,4-dithiothreitol
dTTP	deoxythymidine triphosphate
E e.g. E9	embryonic age e.g. 9 days old embryo
EB	embryoid body
EC cell	embryonic carcinoma cell
EG cell	embryonic germ cell
eNCSC	epidermal neural crest cells
EPU	epidermal proliferative unit
ES cell	embryonic stem cell
FACS	fluorescence activated cell sorter
FBS	foetal bovine serum
FHF	first heart field
FSC	forward scatter
G-CSF	granulocyte colony-stimulating factor
GMEM	glasgows minimal essential media
HBSS	hank's balanced salt solution
hESC	human embryonic stem cell
HIF-1 α	hypoxia-inducible factor 1alpha
HSC	haematopoietic stem cell
HSP-90 α	heat shock protein 90alpha
Isl1	Islet1
K-15	keratin 15
KO	knock out
L-15	leibovitz-15 media

LIF	leukemia inhibitory factor
MEF	mouse embryonic fibroblasts
MEM	minimal essential Media
MGB	minor groove binder
MHC	myosin heavy chain
MI	myocardial infarction
min	minutes
MLC	myosin light chain
MLC1A	myosin light chain 1A: atrial form
MLC1V	myosin light chain 1V: ventricular form
MSC	mesenchymal stem cell
p.p.	post partum
PAP	phthalamidoperoxycaproic acid
PBS	phosphate buffered saline
PBS-T100	PBS-tritonX-100 buffer
PCR	polymerase chain reaction
PI	Propidium Iodide
Q-PCR	quantitative polymerase chain reaction
RBC	red blood cell
REPAIR-AMI	Reinfusion of Enriched Progenitor Cells and Infarct Remodelling in Acute Myocardial Infarction
RQ	relative quantitation
RT	reverse transcriptase
RT-PCR	reverse transcriptase polymerase chain reaction
s	seconds
s.c.	subcutaneous
SHF	second heart field
SKP	skin-derived precursors
SP	side population
SSC	side scatter
STEMI	ST-Elevation acute Myocardial Infarction
Streptavidin-AMCA	streptavidin-7-amino-4-methylcoumarin-3-acetic acid
Sv40	simian virus 40
TERC	telomerase RNA component
TERT	telomerase reverse transcriptase
TOPCARE-CHD	Transplantation Of Progenitor Cells And Recovery of left ventricular function in patients with Chronic ischemic Heart Disease
TRAP	Telomeric Repeat Amplification Protocol
TVP	Trypsin, Versene, Phosphate
WT	wild type
xg	G force
α -MHC	alpha myosin heavy chain

2 Chemicals and Reagents

0.1% gelatin (Sigma) for coating flasks: Gelatin is provided as a 10% solution in PBS. It is diluted 1 in 10, in PBS, for use. 5ml is applied to the flask for 5 min to coat the culture flask. Excess gelatin is removed from the flask and cells immediately added in culture media.

4% (w/v) paraformaldehyde: paraformaldehyde is weighed out and slowly added to PBS in fume hood with constant agitation. Solution is maintained at 60°C until paraformaldehyde is dissolved and solution is transparent.

Agarose (Sigma): Analytical Grade. Gelling point (1.5%) 36-39°C, Melting point (1.5%) 87-89°C.

Collagenase (Worthington): Type 1, A dialyzed, lyophilized powder. Greater than 125 units/mg dry weight where one Unit releases one micromole of L-leucine equivalents from collagen in 5 hours at 37°C, pH 7.5

DEPC water: water treated with 0.1% DEPC; an inhibitor of RNases, Solution was incubated for 12 hours at 37°C then autoclaved to remove any trace of DEPC

Dispase (Sigma): cell culture tested, ~4 unit/mg solid, where 1 unit will hydrolyze casein to produce colour equivalent to 1.0µmole (181µg) of tyrosine per min at pH 7.5 at 37°C

dNTP's (Invitrogen): 2.5mM stock of dATP, dTTP, dCTP and dGTP neutralized to pH 8.0 with NaOH, and supplied in purified water

Ethidium bromide (Sigma): powder diluted in water to 10mg/ml for use. Solution is stored in the dark in a double sealed container

Goat serum (Vector): Vecastain ABC Goat IgG kit, PK-4005, used at a 3 in 10 dilution (by drops).

H₂O₂ (Sigma): provided as a 30% solution in PBS; solution is diluted further for use

LIF (Sigma): mouse, expressed in *Escherichia coli*, 10 µg/ml, buffered aqueous solution, cell culture tested, supplied as a solution in PBS, pH 7.4 with 0.02% (v/v) Tween 20.

3 Buffers

HBSS (Sigma): HBSS Modified, with phenol red, without calcium, without magnesium, liquid.

PBS (Sigma): One tablet dissolved in 200mL of deionized water yields 0.01 M phosphate buffer, 0.0027 M potassium chloride and 0.137 M sodium chloride, pH 7.4, at 25 °C and autoclaved before use.

PBS-T100: (0.025% (v/v) triton X-100 (Sigma) in PBS

TAE buffer: 50xTAE stock solution is diluted to a 1XTAE solution for use. 50xTAE: 242 g Tris base in 750ml water; add 57.1 ml glacial acid, 100ml of 0.5 M EDTA (pH 8.0) and volume adjusted to 1l with water.

TVP: - 1mM Na₂-EDTA (Sigma), 1% (v/v) chick serum, 2.5% trypsin (Sigma) (Sigma) in PBS

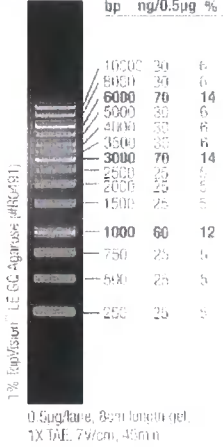
4 Kits

Ambion totally RNA kit: Phenol chloroform, premixed with Isoamyl alcohol, molecular biological grade, Purity >99%: Sodium Acetate 3.0M solution, pH 4.5: Acid Phenol Chloroform: agarose gel load buffer

CellTrace CFSE Cell Proliferation Kit C34554 (Invitrogen): Each vial contained 50µg of lyophilized powder. DMSO supplied separate; high quality 0.5ml

DNA-free kit: DNase-1 enzyme (2units/µl), 10x DNaseI Buffer (100mM Tris-HCl, 25mM MgCl₂, 5mM CaCl₂), DNase inactivation reagent

Gel loading ladder (Fermentas): 1kb loading ladder #SM1163, O'GeneRuler™, ready-to-use, 0.5ug/lane provides the following ladder:



High Capacity cDNA Reverse Transcription Kit (Applied Biosystems): 10xRT buffer, 25xdNTP Mix 100mM, 10xRT random primers, MultiScribe reverse transcriptase (50U/μl), RNase inhibitor, Nuclease free water.

Streptavidin/Biotin Blocking Kit SP-2001 (Vector): Biotin 4 drops/ml of primary antibody. Streptavidin 4 drops/ml of the diluted normal blocking serum.

Superscript II RNase H- Reverse Transcriptase Kit” (Invitrogen): Oligo(dT) primer 5pmoles/μl (polyT primer, 500μg/ml): 5xFirst strand buffer (250mM Tris-HCl, pH 8.3 at room temperature) 375mM KCl: 15mM MgCl₂: 0.1M DTT: Reverse transcriptase 200 units/μl of SuperScript™ II RT where 1 unit incorporates 1 nmole of dTTP into acid-precipitable material in 10 min.at 37°C using oligo(dT)primer as a template-primer.

Taq DNA polymerase, recombinant kit (Invitrogen): 10X Taq buffer (500mM KCL, 100mM tris-HCL pH9, 1% (v/v) triton X-100): 50mM MgCl₂: Taq polymerase 5 Units/μl in 20% glycerol where 1 unit incorporates 10 nmol of deoxyribonucleotide in 30 minutes at 74°C.

TaqMan Fast Universal PCR Master Mix (2x) (Applied Biosystems): PCR Master Mix (2x), Nuclease free water.

TaqMan gene expression assay mix (20x) (Applied Biosystems): contains 18μM forward primer, 18μM reverse primer and 18μM TaqMan probe specific to gene of interest

Vectastain ABC kit (Vector): ABC solution: 2 drops A (Avidin) then 2 drops B (Biotinylated Horseradish Peroxidase) in 5ml PBS, mix immediately then 30 mins incubation.

Vector VIP Substrate Kit for peroxidise SK-4600 (Vector): 3 drops reagent 1, 3 drops reagent 2, 3 drops reagent 3, 3 drops H₂O₂ in 5ml PBS mixed well

5 Cell lines and culture media

10% GMEM: GMEM with additives and 10% (v/v) FBS

10% L-15: L-15 with additives and 10% (v/v) FBS

10% MEM: MEM with additives and 10% (v/v) FBS

CGR8 ES cell line: Depositor: Dr A Smith, AFRC Centre for Genome Research, Edinburgh, UK (Originator)

GMEM (Sigma): Sterile filtered, Endotoxin tested, cell culture tested, Supplement with 0.292 g/L L-glutamine and Tryptose phosphate broth solution (T 8159) at 100 ml/L of medium used with the following additives: at a final concentration: 0.1mM non-essential amino acids (Sigma), 2mM Glutamine (Sigma) and 0.05mM 2-Mercaptoethanol (Sigma)

L-15 (Sigma): Sterile filtered, with L-glutamine, endotoxin tested, was always used with the following additives: 0.5µg/ml amphotericin B (Sigma), 20mM glutamine (Sigma), 50µg/ml gentamycin (Sigma)

MEM (Sigma): Sterile filtered, endotoxin tested with earles salts, L-glutamine and NaHCO₃. MEM was always used with the following additives: 0.5µg/ml amphotericin B (Sigma), 20mM glutamine (Sigma), 50µg/ml gentamycin (Sigma)

6 Primer Design

ncbi software online: (<http://www.ncbi.nlm.nih.gov/>)

6.1 RT-PCR Primer Sequences

Alpha-myosin heavy chain: Rat forward sequence: TGT GAA AAG ATT AAC CGG AGT. Rat reverse sequence: TCT GAC TTG CGG AGG TAT CG. Anneal at 53°C. 93bp product size. Mouse forward sequence: CCA CTG TGG TGC CTC GTT C. Mouse reverse sequence: GCG TCC GTC ATT CTG TCA CTC. Anneal at 51°C. 89bp product size.

Atrial myosin light chain 1 (MLC1A): Rat forward sequence: ACC CAA GCC TGA AGA GAT GA. Rat reverse sequence: ACT GTG CCG TTG CTT TCT TT. Anneal at 45°C. 150bp product size Mouse forward sequence: CGG ATA GAA GGC GGG AGC TC. Mouse reverse sequence: AGC CTT CAG TGA CCC TTT GCC C. Anneal at 64.1°C. 325bp product size.

Cardiac alpha-actin: Rat forward sequence: TAT CAC CAA CTG GGA CGA CA. Rat reverse sequence: AAC AAT GCC TGT GGT TCT CC. Anneal at 55°C. 232bp product

size. Mouse forward sequence: TGA AGC CCA GAG CAA GCG AGG. Mouse reverse sequence: CTG TCG CCA TCT CGT TCT CA. Anneal at 61.6°C. 521bp product size.

c-myc: Mouse forward sequence: GAC ACA GCC ACG ACG ATG C. Mouse reverse sequence: GTC GTC AGG ATC GCA GAT. Anneal at 66.5°C. 378bp product size.

GAPDH: Rat/Mouse forward sequence: ATG GCC CTA CAT GGC CTC CAA GG. Rat/Mouse reverse sequence: AGG CCC CTC CTG TTG TTA TTG G. Anneal at 58°C. 155bp product size (mouse), 184bp product size (rat).

GATA binding protein 4: Rat forward sequence: GTG CTG CTT CTG GAG CCA CC. Rat reverse sequence: GTG GGG AGA GCT TCA GAG CC. Anneal at 61°C. 1037bp and 629bp product size. Mouse forward sequence: CCG CTG CAG CTG GAA CCA CC. Mouse reverse sequence: GTG GGG ACA GCT TCA GAG CAG. Anneal at 53°C. 1040bp product size.

Lymphoid Enhancer-Binding Factor (LEF1): Rat forward sequence: CTG TTT TTA TTA GCC GAT TAG TGG G. Rat reverse sequence: GCT CAG CAC GTT AAC TCA AAC TGG. Anneal at 59.2°C. 190bp product size.

Mef2c: Rat forward sequence: CAA AGA GGA AAT TCG GAC TG. Rat reverse sequence: CCC AGT GAG CTG ACA GGG. Anneal at 55°C. 828bp product size. Mouse forward sequence: CGA AGA GGA AAT TTG GAT TG. Mouse reverse sequence: CCC AGT GTG CTG ACA GGA. Anneal at 51°C. 423bp product size.

Nanog: Mouse forward sequence: CGT TCA TCT TCC TGA GGA. Mouse reverse sequence: TCC AGA CGC GTT CAT CAG. Anneal at 53.8°C. 305bp product size.

Nexin: Rat forward sequence: GGG ATC TTG CCA AGG TGA TGC. Rat reverse sequence: CCT GTG GTA CAC GGT GTA TGG. Anneal at 60°C. 622bp product size.

Nkx2.5: Rat forward sequence: GCG CCG AGA GGC GAC GAC. Rat reverse sequence: GTA GGC GTT GAG ACC CAG G. Anneal at 57°C. 309bp product size. Mouse forward sequence: GCG CCG AGA GAC CAC GCG. Mouse reverse sequence: ATA GGC ATT GAG ACC CAC GC. Anneal at 58°C. 349bp product size.

Oct4: Mouse forward sequence: TGT GCC GAC CGC CCC AAT. Mouse reverse sequence: GGG AAT ACT CAA TAC TTG. Anneal at 45.7°C. 532bp product size.

Sca-1: Rat forward sequence: GCT ACA ATT GCT TGG GGA. Rat reverse sequence: TGC AAA GAT CTC TGG TGC. Anneal at 50°C. 232bp product size Mouse forward sequence: CTC TGA GGA TGG ACA CTT CT. Mouse reverse sequence: GGTCTG CAG GAG GAC TGA GC. Anneal at 61.5°C. 398bp product size.

Sox2: Mouse forward sequence: TGCCGT TGC TCC AGC CGT T. Mouse reverse sequence: CGC CTT CAT GGT ATG GTC CCG. Anneal at 67.3°C. 370bp product size.

Tbx5: Rat forward sequence: TAC ACA GGA TGT CTC GGA TG. Rat reverse sequence: CAG TCT GAG GCC CGC ATT GC. Anneal at 55°C. 689bp product size. Mouse forward sequence: GCG CCT TTA CGT GCA CCC GG. Mouse reverse sequence: CCG AGC GAT AGA AGG TGT CT. Anneal at 58.3°C. 670bp product size.

TERT: Rat/Mouse forward sequence: ACC CAG GAT GTA CTTTGTTAAG. Rat/Mouse reverse sequence: AGC AAA CAG CTT GTT CTCCATG. Anneal at 57.8°C. 465bp product size.

Titin: Rat forward sequence: TTA TCA GTG CTG TAG AAC. Rat reverse sequence: GTT TTT GTT CTT GTT TAG TA. Anneal at 45°C. 326bp product size. Mouse forward sequence: TGA CAC TGG CGC ATA CAC CTG T. Mouse reverse sequence: AGC ACT GCC GGC ATC ATT GGT. Anneal at 73.7°C. 327bp product size.

Tropoelastin: Rat forward sequence: AAA ACC CCC GAA GCC CTA. Rat reverse sequence: ACA TTC TCC ACC AAG CAG TA. Anneal at 51°C. 156bp (elastin), 774bp and 156bp (tropoelastin) product sizes. Mouse forward sequence: CCA AGT CGG AGC TGG CAT CG. Mouse reverse sequence: AGG AAT GCC ACC AAC ACC TG. Anneal at 62.2°C. 651bp product size.

Tropomyosin: Rat forward sequence: AGT GAT CTG GAG CGT GCG. Rat reverse sequence: TGC ACC TTT CTC TTC TAAGT. Anneal at 53°C. 263bp product size. Mouse forward sequence: AGC GAC CTG GAA CGT GCA. Mouse reverse sequence: GCC ACT TTC TCT TCT AAG T. Anneal at 49°C. 262bp product size

Troponin I: Rat forward sequence: GCT TCA GGA CCT ATG CCG. Rat reverse sequence: TCG GCC TTC CAT TCC ACT. Anneal at 51°C. 336bp product size Mouse

forward sequence: GCT TCA GGA CTT ATG CCG A. Mouse reverse sequence: CGG CCT TCC ATG CCA CTC. Anneal at 53°C. 335bp product size

Ventricular myosin light chain 1 (MLC1V): Forward sequence: AAT CCT ACC CAG GCA GAG GT. Reverse sequence: AAC CAT AAC AGT TCC GTT GC. Anneal at 55°C. 195bp product size

Versican: Rat forward sequence: GAC TAT GGC TGG CAC AA. Rat reverse sequence: GTC CTT TGG TAT GCA GA. Anneal at 53.1°C. 575bp product size.

6.2 Q-PCR probes and primer sets

Alpha tropomyosin 1: Mm00600378_m1

Cardiac muscle alpha myosin heavy chain (a-MHC): Mm00440354_m1

Ly6a (sca-1): Mm00726565_s1

mTERT: Mm01352136_m1

Nanog: Mm02384862_g1

Oct4: Mm00658129_gH

Sox2: Mm00488369_s1

T-box 5 (tbx5): Mm00803521_m1

7 Antibodies and Fluorochromes

7.1 Immunohistochemistry

DAPI (Vector): Vectasheld Mounting Media with DAPI, 1.5ug/ml, excitation 360nm, emission 460nm)

Primary CD34 antibody (Abcam, ab8158): monoclonal Rat anti-mouse CD34 in 0.02% sodium azide (w/v) in PBS, 0.1mg/ml used at a 1 in 50 dilution

Primary CD45 antibody (Abcam, ab25386): monoclonal Rat anti-mouse CD45 in 100mM borate buffered saline, 0.5mg/ml used at a 1 in 200 dilution

Primary GFP antibody (Abcam, ab6556): polyclonal Rabbit anti-GFP, 25% (v/v) Glycerol, 50mM Tris-HCl, 0.1% (w/v) sodium azide, 0.5mg/ml used at 1 in 6000 dilution.

Secondary antibody (Abcam ab6720): polyclonal Goat anti-rabbit biotin, 0.02M potassium phosphate, 0.15M NaCl, 0.01% (w/v) sodium azide, 2mg/ml used at a 1 in 200 dilution

Secondary antibody (Abcam, 7086): polyclonal goat anti-rabbit FITC, excitation 495nm emission 528nm, 1mg/ml used at a 1 in 150 dilution

Secondary antibody (Abcam, ab6835): biotinylated monoclonal Chicken anti-rat in 0.01M Na phosphate, 0.25M NaCl, pH7.7, 0.05% (w/v) sodium azide, 0.01% (v/v) Thimerisol, 15mg/ml BSA, 1mg/ml used at a 1 in 200 dilution

Streptavidin-AMCA(Vector): 10mM HEPES, 0.15M NaCL, pH7.5, 0.08 (w/v) sodium azide, excitation 345-355nm emission 448-454nm, 1mg/ml used at a 1 in 50 dilution

7.2 Flow cytometry

Flow cytometric analysis on a FACS Aria fluorescence activated cell sorter (FACS) (Becton Dickinson) by The Centre for Life flow cytometry unit (University of Newcastle)

7-AAD (BD Pharmingen): detected in the far red range of the spectrum at 650 nm using a long-pass filter.

Mouse lineage antibody cocktail (BD Pharmingen): APC conjugated in BSA and 0.09% (w/v) Sodium Azide. APC fluorochrome is excited at 595-647 nm, and its emission is collected in a detector for fluorescence wavelengths at 640-680nm.

8 Equipment

Cryostat: Leica CM3050 Research cryostat

Dissection Microscope: Nikon

Electrophoresis Tank (CBS Scientific): CBS Scientific MGU 202T

Gas tight culture tank for low oxygen (Billups-rothernberg): Modular incubator chamber

Haemocytometer (Sigma): Bright-Line Hemacytometer. Cells counted within 5x5 grid and population cell count calculated by equation: $\text{cell count} \times 3.2 \times 10^3$

Incubator: Shell Lab, CO₂ incubator

Light microscope for phase microscopy: Olympus ckx41 0.2 lens 10x eyepiece

Power pack (Consort): Electrophoresis power supply Consort E844 440-400mA

Rocker (Stuart): mini-gyro rocker SSM3

Rocking incubator : Labnet 211DS

Spectrophotometer (GenQuest): Cecil CE2301

References

- Abraham MR, Henrikson CA, Tung L, Chang MG, Aon M, Xue T, et al. Antiarrhythmic engineering of skeletal myoblasts for cardiac transplantation (2005). *Circulation Research* 97: 159–167.
- Adhikari BB, Wang K. Interplay of Troponin- and Myosin-Based Pathways of Calcium Activation in Skeletal and Cardiac Muscle: The Use of W7 as an Inhibitor of Thin Filament Activation (2004). *Biophysical Journal* 86: 359–370
- Alison MR, Poulsom R, Jeffery R, Dhillon AP, Quaglia A, Jacob J, Novelli M, Prentice G, Williamson J, Wright NA. Hepatocytes from non-hepatic adult stem cells (2000). *Nature* 406: 257.
- Altschul S, Madden T, Schaffer AA, Zhang J, Zhang Z, Miller W, and Lipman DJ. Gapped BLAST and PSI-BLAST: a new generation of protein database search programs (1997). *Nucleic Acids Res.* 25: 3389-3402.
- Amado LC, Saliaris AP, Schuleri KH, St John M, Xie JS, Cattaneo S, Durand DJ, Fitton T, Kuang JQ, Stewart G, Lehrke S, Baumgartner WW, Martin BJ, Heldman AW, Hare JMC. Cardiac repair with intramyocardial injection of allogeneic mesenchymal stem cells after myocardial infarction (2005). *PNAS* 102: 11474-11479.
- Amoh Y, Li L, Katsuoka K, Penman S, Hoffman RM. Multipotent nestin-positive, keratin-negative hair follicle bulge stem cells can form neurons (2005). *Proc Natl Acad Sci USA* 102: 5530-5534
- Annabi B, Lee YT, Turcotte S, Naud E, Desrosiers RR, Champagne M, Eliopoulos N, Galipeau J, Béliveau R. Hypoxia promotes murine bone-marrow-derived stromal cell migration and tube formation (2003). *Stem Cells* 21: 337-347
- Angelini P and Markwald RR. Stem Cell Treatment of the Heart: A Review of Its Current Status on the Brink of Clinical Experimentation (2005). *Texas Heart Institute Journal* 32: 479–488
- (A). Anversa P, Kajstura J, Leri A and Bolli R. Life and Death of Cardiac Stem Cells: A Paradigm Shift in Cardiac Biology (2006). *Circulation* 113: 1451-1463
- (B). Anversa P, Leri A, Kajstura J. Cardiac regeneration (2006). *Jour Am Coll Cardio.* 47: 1769-1776
- Arnold MA, Kim Y, Czubryt MP, Phan D, McAnally J, Qi X, Shelton JM, Richardson JA, Bassel-Duby R, Olson EN. MEF2C Transcription Factor Controls Chondrocyte Hypertrophy and Bone Development (2007). *Dev Cell* 12: 377-389

Armstrong L, Lako M, Lincoln J, Cairns PM, Hole N. mTert expression correlates with telomerase activity during the differentiation of murine embryonic stem cells (2000). *Mechanisms of Development* 1-2: 109-16.

Asakura A, Seale P, Girgis-Gabardo A, Rudnicki MA. Myogenic specification of side population cells in skeletal muscle (2002). *J Cell Biol* 159: 123-134

Assmus B, Honold J, Schachinger V, Britten MB, Fischer-Rasokat U, Lehmann R, et al. Transcoronary transplantation of progenitor cells after myocardial infarction (2006). *New England Journal of Medicine* 355: 1222–1232.

Baharvand H, Piryaei A, Rohani R, Taei A, Heidari MH, Hosseini A. Ultrastructural comparison of developing mouse embryonic stem cell- and *in vivo*- derived cardiomyocytes (2006). *Cell Biology International* 1-8.

Baker DEC, Harrison NJ, Maltby E, Smith K, Moore HD, Shaw PJ, Heath PR, Holden H, Andrews PW. Adaptation to culture of human embryonic stem cells and oncogenesis *in vivo* (2007). *Nature Biotechnology* 25: 207-215.

Balsam LB, Wagers AJ, Christensen JL, Kofidis T, Weissman IL, Robbins RC. Haematopoietic stem cells adopt mature haematopoietic fates in ischemic myocardium (2004). *Nature* 668–673.

Barile L, Messina E, Giacomello A, Marbán E. Endogenous Cardiac Stem Cells Progress in Cardiovascular Diseases (2007). *Progress in Cardiovascular Disease* 50: 31-48

Bassukas ID, Aria A, Schell H, Hornstein OP. Growth and cell kinetics of human hair papilla cells *in vitro*. An autoradiographic and flow cytometric study (1991). *Cell Proliferation* 24: 367-374.

Beeres SL, Atsma DE, van der Laarse A, Pijnappels DA, van Tuyn J, Fibbe WE, de Vries AA, Ypey DL, van der Wall EE, Schalij MJ. Human adult bone marrow mesenchymal stem cells repair experimental conduction block in rat cardiomyocyte cultures. (2005). *Journal of the American College of Cardiology* 46: 1943-1952

Beltrami AP, Urbanek K, Kajstura J, Yan SM, Finato N, Bussani R, Nadal-Ginard B, Silvestri F, Leri A, Beltrami CA, and Anversa P. Evidence that human cardiac myocytes divide after myocardial infarction (2001). *New England Journal of Medicine* 344: 1750–1757

Beltrami AP, Barlucchi L, Torella D, Baker M, Limana F, Chimenti S, Kasahara H, Rota M, Musso E, Urbanek K, Leri A, Kajstura J, Nadal-Ginard B. Adult Cardiac Stem Cells Are Multipotent and Support Myocardial Regeneration (2003). *Cell* 114: 763–776

Benson DA, Karsch-Mizrachi I, Lipman DJ, Ostell J, Rapp BA, Wheeler DL. GenBank (2000). *Nucl. Acids Res.* 28: 15-18

Bertani N, Malaesta P, Volpi G, Sonogo P, Perris R. Neurogenic potential of human mesenchymal stem cells revisited: analysis by immunostaining, time-lapse video and microarray (2005). *Journal of Cell Science* 118: 3925-3936.

Blanpain C and Fuchs E. Epidermal Stem Cells of the Skin (2006). *Annu Rev Cell Dev Biol.* 22: 339–373.

Boheler K Czyz J, Tweedie D, Yang H, Anisimov SV, Wobus AM. Differentiation of Pluripotent Embryonic Stem Cells Into Cardiomyocytes (2002). *Circ Res.* 91: 189-201

Boyle AJ, Schulman SP, Hare JM. Stem Cell Therapy for Cardiac Repair: Ready for the Next Step (2006). *Circulation* 114: 339-352

Brand T. Heart development: molecular insights into cardiac specification and early morphogenesis (2003). *Developmental Biology* 25:1–19

Breault DT, Min IM, Carlone DL, Farilla LG, Ambruzs DM, Henderson DE, Algra S, Montgomery RK, Wager AJ, Hole H. Generation of mTert-GFP Mice as a Model to Identify and Study Tissue Progenitor Cells (2008). *PNAS* 105:10420-10425

Brown CO, Chi X, Garcia-Gras E, Shirai M, Feng X, Schwartz RJ. The Cardiac Determination Factor, Nkx2-5, Is Activated by Mutual Cofactors GATA-4 and Smad1/4 via a Novel Upstream Enhancer (2004). *The Journal of Biological Chemistry* 279: 10659–10669

Buckingham M, Meilhac S, Zaffran S. Building the Mammalian Heart From Two Sources of Myocardial Cells (2005). *Nature Reviews-Genetics* 6: 826-835

Byrne B, Kessler PD. Human Mesenchymal Stem Cells Differentiate to a Cardiomyocyte Phenotype in the Adult Murine Heart (2003). *Basic Appl Myol* 13: 15-22

Cai CL, Liang X., Shi Y, Chu PH, Pfaff SL, Chen J, Evans S. Isl1 identifies a cardiac progenitor population that proliferates prior to differentiation and contributes a majority of cells to the heart (2003). *Developmental Cell* 5: 877–889.

Capers C. Multinucleation of Skeletal Muscle in vitro (1960). *J. Biophys Biochem* 7: 559-579

Cerni C. Telomeres, telomerase, and myc. An update (2000). *Mutation Research* 462: 31-47.

Chen S, Fang WW, Ye F, Liu YH, Qian J, Shan SJ, Zhang JJ, Chunhua RZ, Liao LM, Lin S, Sun JP. Effect on left ventricular function of intracoronary transplantation of autologous bone marrow mesenchymal stem cell in patients with acute myocardial infarction (2004). *American Journal of Cardiology* 94: 92–95.

Cheng W, Reiss K, Kajstura J, Kowal K, Quaini F, Anversa P. Downregulation of the IGF-1 system parallels the attenuation in the proliferative capacity of rat ventricular myocytes during postnatal development (1995). *Lab Invest* 72: 646–655.

Chien KR, and Olson EN. Converging pathways and principles in heart development and disease (2002). *Cell* 110: 153–162

Choi J, Southworth LK, Sarin KY, Venteicher AS, Ma W, Chang W, Cheung P, Jun S, Artandi MK, Shah N, Kim SK, Artandi SE. TERT Promotes Epithelial Proliferation through Transcriptional Control of a Myc and Wnt-Related Developmental Program (2008). *PLoS Genetics* 4: 124-138

Christoffels VM, Habets PE, Franco D, Campione M, de Jong F, Lamers WH, Bao ZZ, Palmer S, Biben C, Harvey RP, Moorman AF. Chamber formation and morphogenesis in the developing mammalian heart (2000). *Dev Biol* 223: 266-278

Christoforou N and Gearhart JD. Stem Cells and Their Potential in Cell-Based Cardiac Therapies Progress in Cardiovascular Diseases (2007). *Progress in Cardiovascular Disease* 49: 396-413

Chui HC, Chan CH, Chen JS, Jee SH. Human hair follicle dermal papilla cell, dermal sheath cell and interstitial dermal fibroblast characteristics (1996). *Journal of the Formosan Medical Association* 95: 667-674

Clubb FJ and Bishop SP. Formation of binucleated myocardial cells in the neonatal rat: an index for growth hypertrophy (1984). *Lab Invest* 50:571–577

Collins CA. Satellite cell self-renewal. (2006). *Current Opinion in Pharmacology* 6: 301-306

Condorelli G, Borello U, De Angelis L, Latronico M, Sirabella D, Coletta M, Galli R, Balconi G, Follenzi A, Frati G, Cusella De Angelis MG, Gioglio L, Amuchastegui S, Adorini L, Naldini L, Vescovi A, Dejana E, Cossu G. Cardiomyocytes induce endothelial cells to trans-differentiate into cardiac muscle: implications for myocardium regeneration (2001). *Proc atl Acad Sci USA* 98: 10733-10738

Coppen SR, Kaba RA, Halliday D, Dupont E, Skepper JN, Elneil S, Severs NJ. Comparison of connexin expression patterns in the developing mouse heart and human foetal heart (2003). *Mol Cell Biochem* 242: 121-127

Cotsarelis G, Sun T, Lavker RM. Label-Retaining Cells Reside in the Bulge Area of Pilosebaceous Unit: Implications for Follicular Stem Cells, Hair Cycle, and Skin Carcinogenesis (1990). *Cell* 61: 1329-1337

Cotsarelis G. Epithelial Stem Cells: A Folliculocentric View (2006). *Journal of Investigative Dermatology* 126: 1459–1468

Crigler L, Kazhanie A, Yoon T, Zakhari J, Anders J, Taylor B, Virador VM. Isolation of a mesenchymal cell population from murine dermis that contains progenitors of multiple cell lineages (2007). *FASEB J.* 21:2050–2063

Dai W, Field LJ, Rubart M, Reuter S, Hale SL, Zweigerdt R, Graichen RE, Kay GL, Jyrala AJ, Colman A, Davidson BP, Pera M, Kloner RA. Survival and maturation of human embryonic stem cell-derived cardiomyocytes in rat hearts (2007). *J Mol Cell Cardiol.* 43: 504-516

DasGupta R, Fuchs E. Multiple roles for activated LEF/TCF transcription complexes during hair follicle development and differentiation (1999). *Development* 126: 4557-4568.

Dawn B, Stein AB, Urbanek K, Rota M, Whang B, Rastaldo R, Torella D, Tang X, Rezazadeh A, Kajstura J, Leri A, Hunt G, Varma J, Prabhu SD, Anversa P, Bolli R. Cardiac stem cells delivered intravascularly traverse the vessel barrier, regenerate infarcted myocardium, and improve cardiac function (2005). *PNAS* 102: 3766–3771

Davidson P and Hardy M. The Development of mouse vibrissae in vivo and in vitro (1952). *J Anat* 86: 342-56

Deepak S. Making or Breaking the Heart: From Lineage Determination to Morphogenesis (2006). *Cell* 126: 1037-1048

Di Lisi R, Millino C, Calabria E, Altruda F, Schiaffino S, Ausoni S. Combinatorial cis-acting elements control tissue-specific activation of the cardiac troponin I gene in vitro and in vivo (1998). *J Biol Chem* 273: 25371-25380

Discorde MT, Prost S, Nandrot E, Kirszenbaum M. Spatial and temporal mapping of c-kit and its ligand, stem cell factor expression during human embryonic haemopoiesis (1999). *British Journal of Haematology* 107: 247-253

Dodou E, Verzi MP, Anderson JP, Xu SM, Black BL. Mef2c is a direct transcriptional target of ISL1 and GATA factors in the anterior heart field during mouse embryonic development (2004). *Development* 131: 3931–3942.

Dowell JD, Rubart M, Pasumarthi KB, Soonpaa MH, Field LJ. Myocyte and myogenic stem cell transplantation in the heart (2003). *Cardiovascular Research* 58:336-350

Eglitis MA and Mezey E. Hematopoietic cells differentiate into both microglia and macroglia in the brains of adult mice (1997). *PNAS* 94: 4080–4085.

Eisenberg LM, Moreno R, Markwald RR. Multiple stem cell populations contribute to the formation of the myocardium. (2005). *Ann NY Acad Sci* 1047: 38-49.

Erokhina IL, Rumyantsev PP. Ultrastructure of DNA-synthesizing and mitotically dividing myocytes in sinoatrial node of mouse embryonal heart (1986). *J Mol Cell Cardiol.* 18: 1219–1231.

Fazel S, Cimini M, Chen L, Li S, Angoulvant D, Fedak P, Verma S, Weisel RD, Keating A, Li R. Cardioprotective c-kit⁺ cells are from the bone marrow and regulate the myocardial balance of angiogenic cytokines (2006). *The Journal of Clinical Investigation* Volume 116: 1865-77

Fernandes KJL, McKenzie I, Mill P, Smith K, Akhavan M, Barnabe-Heider F, Biernaskie J, Junek A, Kobayashi NR, Toma JG, Kaplan DR, Labosky PA, Rafuse V, Hui C, Miller F. A dermal niche for multipotent adult skin-derived precursor cells (2004). *Nature Cell Biology* 6: 1082-1093.

Fijnvandraat AC, van Ginneken AC, Schumacher CA, Boheler KR, Lekanne Deprez RH, Christoffels VM, Moorman AF. Cardiomyocytes purified from differentiated embryonic stem cells exhibit characteristics of early chamber myocardium (2003). *Journal of Molecular and Cellular Cardiology* 35: 1461–1472

Fijnvandraat AC, Lekanne Deprez RH, Christoffels VM, Ruijter JM, Moorman AF. TBX5 overexpression stimulates differentiation of chamber myocardium in P19Cl6 embryonic carcinoma cells (2003). *Journal of Muscle Research and Cell Motility* 24: 211-218

Fina L, Molgaard HV, Robertson D, Bradley NJ, Monaghan P, Delia D, Sutherland R, Baker MA, and Greaves MF. Expression of the CD34 Gene in Vascular Endothelial Cells (1990). *Blood* 75: 2417-2426

Fink C, Ergun S, Kralisch D, Remmers U, Weil J, Eschenhagen T. Chronic stretch of engineered heart tissue induces hypertrophy and functional improvement (2000). *FASEB* 14: 669-679

Flores I, Cayuela ML, Blasco MA. Effects of Telomerase and Telomere Length on Epidermal Stem Cell Behavior (2005). *Science* 309: 1253-1256

Florini JR, Magri KA, Ewton DZ, Jamesn PL, Grindstaff K, Rotweinn PS. Spontaneous Differentiation of Skeletal Myoblasts Is Dependent upon Autocrine Secretion of Insulin-like Growth Factor-11 (1991). *The Journal of Biological Chemistry* 266: 15917-15923

Frangogiannis NG, Smith CW, Entman ML. The inflammatory response in myocardial infarction (2002). *Cardiovascular Research* 53: 31-47

Fuchs S, Satler LF, Kornowski R, Okubagzi P, Weisz G, Baffour R, et al. Catheter-based autologous bone marrow myocardial injection in nooption nooption patients with advanced coronary artery disease: a feasibility study (2003). *J Am Coll Cardiol* 41: 1721–1724.

Fukuhara S, Tomita S, Yamashiro S, Morisaki T, Yutani C, Kitamura S, Nakatani T. Direct cell-cell interaction of cardiomyocytes is key for bone marrow stromal cells to go into cardiac lineage in vitro (2003). *J Thorac Cardiovasc Surg* 125:1470-1480

Gawronska-Kozak B, Manuel JA, Prpic V. Ear Mesenchymal Stem Cells (EMSC).Can Differentiate Into Spontaneously Contracting Muscle Cells (2007). *Journal of Cellular Biochemistry* 102: 122–135

Gharzi A, Reynolds AJ, Jahoda CA. Plasticity of hair follicle dermal cells in wound healing and induction (2003). 12: 126-136

Ghostine S, Carrion C, Souza LCG, Richard P, Bruneval P, Vilquin J-T, Pouzet B, Schwartz K, Menasche P, Hagege AA. Long-term efficacy of myoblast transplantation on regional structure and function after myocardial infarction (2002). *Circulation* 106: 131-136

Gibson AJ, Karasinski J, Relvas J, Moss J, Sherratt TG, Strong PN, Watt DJ. Dermal fibroblasts convey to a myogenic lineage in mdx mouse muscle (1995). *Journal of Cell Science* 108: 207-214.

Ginzinger DG. Gene quantification using real-time quantitative PCR: An emerging technology hits the mainstream (2002). *Experimental Hematology* 30: 503–512

Gittenberger-de Groot AC, Mark-Paul F.M. Peeters V, Mentink MMT, Gourdie RG and Poelmann RE. Epicardium-Derived Cells Contribute a Novel Population to the Myocardial Wall and the Atrioventricular Cushions (1998). *Circ. Res.* 82: 1043-1052

Gojo S, Gojo N, Takeda Y, Mori T, Abe H, Kyo S, Hata J, Umezawa A. In vivo cardiovascularogenesis by direct injection of isolated adult mesenchymal stem cells (2003). *Exp Cell Res.* 288: 51–59.

Goodell MA, Brose K, Paradis G, Conner AS, Mulligan RC. Isolation and functional properties of murine hematopoietic stem cells that are replicating in vivo (1996). *J. Exp. Med.* 183: 1797–1806.

Goodell MA, Rosenzweig M, Kim H, Marks DF, DeMaria M, Paradis G, Grupp SA, Sieff CA, Mulligan RC, Johnson RP. Dye efflux studies suggest that hematopoietic stem cells expressing low or undetectable levels of CD34 antigen exist in multiple species (1997). *Nat. Med.* 3: 1337–1345.

Haddad F, Bodell PW, Qin AX, Giger JM, Baldwin KM. Role of Antisense RNA in Coordinating Cardiac Myosin Heavy Chain Gene Switching (2003). *The Journal of Biological Sciences* 278: 37132–37138,

Hagege AA, Carrion C, Menasche P, Vilquin JT, Duboc D, Marolleau J-P, Desnos M, Bruneval P. Viability and differentiation of autologous skeletal myoblast grafts in ischaemic cardiomyopathy (2003). *Lancet* 361: 491– 492.

Hahn WC, Counter CM, Lundberg AS, Beijersbergen RL, Brooks MW, Weinberg RA Creation of human tumour cells with defined genetic elements (1999). *Nature* 400: 464-468.

Hardy MH. The secret life of the hair follicle (1992). *Trends in genetics*. 2: 55-61

Harris SJ, Jahoda CAB. A correlation between versican and neurolament expression patterns during the development and adult cycling of rat vibrissa follicles (2001). *Mechanisms of Development* 101: 227-231.

Hata H, Matsumiya G, Miyagawa S, Kondoh H, Kawaguchi N, Matsuura N, Shimizu T, Okano T, Matsuda H, Sawa Y. Grafted skeletal myoblast sheets attenuate myocardial remodeling in pacing-induced canine heart failure model (2006). *J Thorac Cardiovasc Surg* 132: 918- 924

Hatcher CJ, Goldstein MM, Mah CSW, Delia S, Basson CT. Identification and Localization of TBX5 Transcription Factor During Human Cardiac Morphogenesis (2000). *Developmental dynamics* 219: 90-95

Hattan N, Kawaguchib H, Andoc K, Kuwabaraa E, Fujitad J, Muratad M, Suematsub M, Moria H, Fukudad K. Purified cardiomyocytes from bone marrow mesenchymal stem cells produce stable intracardiac grafts in mice (2005). *Cardiovascular Research* 65: 334

Hay, E.D. Collagen and other matrix glycoproteins in embryogenesis. In *Cell Biology of Extracellular Matrix* (1991). *Acta Anatomica* 154: 419–462.

Heo J, Lee J, Chu I, Takahama Y, Thorgeirsson SS. Spontaneous differentiation of mouse embryonic stem cells in vitro: Characterization by global gene expression profiles (2005). *Biochemical and Biophysical Research Communications* 332: 1061-1069

Herreros J, Prósper F, Perez A, Gavira JJ, Garcia-Velloso MJ, Barba J, Sánchez PL, Cañizo C, Rábago G, Martí-Climent JM, Hernández M, López-Holgado N, González-Santos JM, Martín-Luengo C, Alegria E. Autologous intramyocardial injection of cultured skeletal muscle– derived stem cells in patients with non-acute myocardial infarction. (2003). *Eur Heart J* 24: 2012- 2020

Hildreth V, Webb S, Bradshaw L, Brown NA, Anderson RH, Henderson DJ. Cells migrating from the neural crest contribute to the innervations of the venous pole of the heart (2008). *Journal of Anatomy* 212: 1-11.

Hill LE, Mehegan JP, Butters CA, Tobacman LS. Analysis of troponin-tropomyosin binding to actin. Troponin does not promote interactions between tropomyosin molecules (1992). *J Biol Chem.* 267: 16106-16113

Hiroi Y, Kudoh S, Monzen K, Ikeda Y, Yazaki Y, Nagai R, Komuro T. Tbx5 associates with Nkx2-5 and synergistically promotes cardiomyocyte differentiation (2001). *Nature Genetics* 28: 276-280.

Hiyama E and Hiyama K. Telomere and telomerase in stem cells (2007). *British Journal of Cancer* 96:1020-1024

Holyoake TL, Alcorn MJ. CD34 + Positive Haemopoietic Cells: Biology and clinical Applications (1994). *Blood Reviews* 8: 113-124

Hoogduijn MJ, Gorjup E, Genever PG. Comparative Characterization of Hair Follicle Dermal Stem Cells and Bone Marrow Mesenchymal Stem Cells (2006). *Stem Cells and Development* 15: 49-60.

Horne KA and Jahoda CAB. Restoration of hair growth by surgical implantation of follicular dermal sheath (1992). *Development* 116: 563-571

Hosenpud JD. Immunosuppression in cardiac transplantation (2005). *N Engl J Med* 352: 2749-2750

Itabashia Y, Miyoshia S, Yuasaa S, Fujitaa J, Shimizub T, Okanob T, Fukudaa K, Ogawaa S. Analysis of the electrophysiological properties and arrhythmias in directly contacted skeletal and cardiac muscle cell sheets (2005). *Cardiovascular Research* 67: 561 – 570

Ito M, Liu Y, Yang Z, Nguyen J, Liang F, Morris RJ et al. Stem cells in the hair follicle bulge contribute to wound healing but not to homeostasis of the epidermis (2005). *Nat Med* 11: 1351–1354

Jackson KA, Majka SM, Wang H, Pocius J, Hartley CJ, Majesky MW, et al. Regeneration of ischemic cardiac muscle and vascular endothelium by adult stem cells (2001). *J Clin Invest* 107: 1395–402

Jackson L, Jones DR, Scotting P, Sottile V. Adult mesenchymal stem cells: differentiation potential and therapeutic applications (2007). *J Postgrad Med* 53 :121-7

Jahoda CA, Oliver RF. The growth of vibrissa dermal papilla cells in vitro (1981). *British Journal of Dermatology* 105: 623-627.

Jahoda CA, Oliver RF. Vibrissa dermal papilla cell aggregative behaviour in vivo and in vitro (1984). *Journal of Embryology and Experimental Morphology* 79: 211-224.

A).Jahoda CAB and Reynolds AJ. Hair follicle dermal sheath cells: unsung participants in wound healing (2001). *Lancet* 358: 1445-48

B).Jahoda CAB, Oliver RF, Reynolds AJ, Forrester JC, Gillespie JW, Cserhalmi-Friedman PB, Christiano AM, Horne KA. Trans-species hair growth induction by human hair follicle dermal papillae (2001). *Exp Dermatol* 10: 229-237.

A). Jahoda CAB, Whitehouse CJ, Reynolds AJ, Hole N. Hair follicle dermal cells differentiate into adipogenic and osteogenic lineages (2003). *Experimental Dermatology* 12: 849-859.

B). Jahoda Colin A B . Cell Movement in the Hair Follicle Dermis – More Than a Two-Way Street? (2003). *Journal of Investigative Dermatology* 121: ix-xi

Jaiswal R K, Jaiswal N, Bruder S P, Mbalaviele G, Marshak D R, PittengerMF. Adult human mesenchymal stem cell differentiation to the osteogenic or adipogenic lineage is regulated by mitogen-activated protein kinase (2000). *J Biol Chem* 275: 9645-9652.

Jang YK. Jung DH, Jung MH, Kim DH, Yoo KH, Sung WK, Koo HH. Oh W. Yang YS. Yang S. Mesenchymal stem cells feeder layer from human umbilical cord blood for ex vivo expanded growth and proliferation of hematopoietic progenitor cells (2006). *Ann hematol* 85: 212-225

Janssens S, Dubois C, Bogaert J, Theunissen K, Deroose C, Desmet W, et al. Autologous bone marrow-derived stem-cell transfer in patients with ST-segment elevation myocardial infarction: double-blind, randomised controlled trial (2006). *Lancet* 367: 113-21.

Jensen UB., Lowell S and Watt FM. The spatial relationship between stem cells and their progeny in the basal layer of human epidermis: a new view based on whole-mount labelling and lineage analysis (1999). *Development* 12: 62409-2418.

Jones WK, Grupp IL, Doetschman T, Grupp G, Osinska H, Hewett TE, Boivin G, Gulick J, Ng WA, Robbins J. Ablation of the murine alpha myosin heavy chain gene leads to dosage effects and functional deficits in the heart (1996). *Journal of Clinical Investigation* 98: 1906-1917

Kajstura J, Leri A, Finato N, Di Loretto C, Beltrami CA, and Anversa P. Myocyte proliferation in end-stage cardiac failure in humans (1998). *PNAS* 95: 8801-8805

Kajstura J, Rota M, Whang B, Cascapera S, Hosoda T, Bearzi C, et al. Bone marrow cells differentiate in cardiac cell lineages after infarction independently of cell fusion (2005). *Circ Res* 96: 127-37.

Kajstura J, Zhang X, Reiss K, Szoke E, Li P, Lagrasta C, Cheng W, Darzynkiewicz Z, Olivetti G, Anversa P. Myocyte cellular hyperplasia and myocyte cellular hypertrophy contribute to chronic ventricular remodeling in coronary artery narrowing-induced cardiomyopathy in rats (1994). *Circ Res.* 74: 383–400.

Karamboulas C, Dakubo GD, Liu J, De Repentigny Y, Yutzey K, Wallace VA, Kothary R, Skerjanc IS. Disruption of MEF2 activity in cardiomyoblasts inhibits cardiomyogenesis (2006). *Journal of Cell Science* 119: 4315-4321

Kaufman MH. *The Atlas of Mouse Development* (1992). Academic Press,.

Kern S, Eichler H, Stoeve J, Kluter H, Bieback K. Comparative Analysis of Mesenchymal Stem Cells from Bone Marrow, Umbilical Cord Blood or Adipose Tissue (2006). *Stem Cells* 24: 1294-1301.

Kim M, Turnquist H, Jackson J, Sgagias M, Yan Y, Gong M, Dean M, Sharp J, Cowan K. The multidrug resistance transporter ABCG2 (breast cancer resistance protein 1) effluxes Hoechst 33342 and is overexpressed in hematopoietic stem cells (2002). *Clin. Cancer Res.* 8: 22–28.

Kobayashi K, Rochat A, and Barrandon Y, Segregation of keratinocyte colony-forming cells in the bulge of the rat vibrissa (1993). *PNAS* 90: 7391–7395

Kolodziejczyk SM, Wang L, Balazsi K, DeRepentigny Y, Kothary R, Megeney LA. MEF2 is upregulated during cardiac hypertrophy and is required for normal post-natal growth of the myocardium (1999). *Current Biology* 9: 1203–1206

Kolossov E, Lu Z, Drobinskaya I, Gassanov N, Duan Y, Sauer H, Manzke O, Bloch W, Bohlen H, Hescheler J, Fleischmann BK. Identification and characterization of embryonic stem cell-derived pacemaker and atrial cardiomyocytes (2005). *FASEB.* 6: 577-579.

Kolossov E, Bostani T, Roell W, Breitbach M, Pillekamp F, Nygren JM, Sasse P, Rubenchik O, Fries JW, Wenzel D, Geisen C, Xia Y, Lu Z, Duan Y, Kettenhofen R, Jovinge S, Bloch W, Bohlen H, Welz A, Hescheler J, Jacobsen SE, Fleischmann BK. Engraftment of engineered ES cell-derived cardiomyocytes but not BM cells restores contractile function to the infarcted myocardium (2006). *Journal of Experimental Medicine* 203: 2315-2327

Kolossov E, Bostani T, Roell W, Breitbach M, Pillekamp F, Nygren JM, Sasse P, Rubenchik O, Fries JW, Wenzel D, Geisen C, Xia Y, Lu Z, Duan Y, Kettenhofen R, Jovinge S, Bloch W, Bohlen H, Welz A, Hescheler J, Jacobsen SE, Fleischmann BK. Engraftment of engineered ES cell-derived cardiomyocytes but not BM cells restores contractile function to the infarcted myocardium (2006). *The journal of experimental medicine* 203: 2315-27

Kuhn H, Pfitzer P, Stoepel K. DNA content and DNA synthesis in the myocardium of rats after induced renal hypertension (1974). *Cardiovasc Res.* 8: 86–91.

Laflamme M, Gold, J., Xu, C., Hassanipour, M., Rosler, E., Police, S., Muskheli, V., and Murry, C. Formation of human myocardium in the rat heart from human embryonic stem cells (2005). *American Journal of Pathology* 167: 663-71.

Lako M, Armstrong L, Cairns PM, Harris S, Hole N, Jahoda CAB. Hair follicle dermal cells repopulate the mouse haematopoietic system (2002). *Journal of Cell Science* 115: 3967-3974.

Langton AK, Herrick SE, Headon DJ. An Extended Epidermal Response Heals Cutaneous Wounds in the Absence of a Hair Follicle Stem Cell Contribution (2008). *Journal of Investigative Dermatology* 128: 1311–1318;

Laugwitz KL, Moretti A, Lam J, Gruber P, Chen Y, Woodard S, Lin LZ, Cai CL, Lu MM, Reth M, Platoshyn O, Yuan JX, Evans S, Chien KR. Postnatal isl1+ cardioblasts enter fully differentiated cardiomyocyte lineages (2005). *Nature* 433:647–653

Lavjer RM, Costarelis G, Wei Z, Sun T. Stem Cells of Pelage, Vibrissae, and Eyelash Follicles: The Hair Cycle and Tumor Formation (1991). *The Molecular and Structural Biology of Hair* 642: 214-224

Leferovich J, Bedelbaeva K, Samulewicz S, Zhang X, Zwas D, Lankford EB, Heber-Katz E. Heart regeneration in adult MRL mice (2001). *PNAS* 98: 9830–9835

Leri A, Kajstura J, Anversa P Cardiac stem cells and mechanisms of myocardial regeneration (2005). *Physiological Reviews* 85: 1373-416.

Leobon B, Garcin I, Menasche P, Vilquin JT, Audinat E, Charpak S. Myoblasts transplanted into rat infarcted myocardium are functionally isolated from their host (2003). *PNAS* 100: 7808–11.

A). Li F, Wang X, Capasso JM, Gerdes AM. Rapid transition of cardiac myocytes from hyperplasia to hypertrophy during postnatal development (1996). *J Mol Cell Cardiol.* 28: 1737–1746.

B). Li RK, Mickle DA, Weisel RD, Zhang J, Mohabeer MK. In vivo survival and function of transplanted rat cardiomyocytes (1996). *Circ Res.* 78(2): 283-8

A). Li W, Li Y, Guan S, Fan J, Cheng C, Bright A, Chinn C, Chen C, Woodley DT. Extracellular heat shock protein-90a: linking hypoxia to skin cell motility and wound healing (2007). *The EMBO Journal* 26: 1221–1233

B). Li X, Yu X, Lin Q, Deng C, Shan Z, Yang M, Lin S. Bone marrow mesenchymal stem cells differentiate into functional cardiac phenotypes by cardiac microenvironment (2007). *J Mol Cell Cardiol.* 42: 295-303.

- Liadaki K, Kho AT, Sanoudou D, Schienda J, Flint A, Beggs AH, Kohane IS, Kunkel LM. Side population cells isolated from different tissues share transcriptome signatures and express tissue-specific markers (2005). *Experimental Cell Research* 303: 360-74
- Lin Q, Schwarz J, Bucana C, Olson EN. Control of mouse cardiac morphogenesis and myogenesis by transcriptional factor MEF2C (1997). *Science* 276: 1404-1407
- Lin H. The Stem Cell Niche Theory: Lessons from flies (2002). *Nature Reviews Genetics* 3: 931-940
- Liu J, Whitehouse CJ, Harris SJ, Crawford H, Yung S, Zhang X, Lako M, Hole N, Jahoda CAB. Hair Follicle Dermal Cells Support Undifferentiated Expansion of Murine and Human Embryonic Stem Cells (2008). In press
- Lopez AD, Mathers CD, Ezzati M, Jamison DT, Murray CJ. Global and regional burden of disease and risk factors 2001: systematic analysis of population health data. (2006). *Lancet* 367: 1747–1757.
- Lunde K, Solheim S, Aakhus S, Arnesen H, Abdelnoor M, Egeland T, Endresen K, Ilebekk A, Mangschau A, Fjeld JG, Smith HJ, Taraldsrud E, Grøgaard HK, Bjørnerheim R, Brekke M, Müller C, Hopp E, Ragnarsson A, Brinchmann JE, Forfang K. Intracoronary injection of mononuclear bone marrow cells in acute myocardial infarction (2006). *N Engl J Med* 355: 1199–209.
- Lunde K, Solheim S, Aakhus S, Arnesen H, Abdelnoor M, Forfang K. Autologous stem cell transplantation in acute myocardial infarction: The ASTAMI randomized controlled trial. Intracoronary transplantation of autologous mononuclear bone marrow cells, study design and safety aspects (2005). *Scand Cardiovasc J* 39: 150–158.
- Lyons I, Parsons LM, Hartley L, Li R, Andrews JE, Robb L, Harvey RP. Myogenic and morphogenetic defects in the heart tubes of murine embryos lacking the homeo box gene *Nkx2-5* (1995). *Genes and development* 9: 1654-1666
- Lyons AB. Analysing cell division in vivo and in vitro using flowcytometric measurement of CFSE dye dilution (2000). *Journal of Immunological Methods* 243: 147-154.
- MacDonald DJ, Luo J, Saito T, Duong M, Bernier PL, Chiu RC, Shum-Tim D. Persistence of marrow stromal cells implanted into acutely infarcted myocardium: Observations in a xenotransplant model (2005). *The Journal of Thoracic and Cardiovascular Surgery* 130: 1114-21
- Machida N, Brisse N, Sreenan C, Bishop SP. Inhibition of cardiac myocyte division in c-myc transgenic mice (1997). *J Mol Cell Cardiol.* 29: 1895–1902.
- MacLellan WR and Schneider M.D. Genetic dissection of cardiac growth control pathway (2000). *Annu. Rev. Physiol.* 62: 289–319.

Makino S, Fukuda K, Miyoshi S, Konishi F, Kodama H, Pan J, Sano M, Takahashi T, Hori S, Abe H, Hata J, Umezawa A, Ogawa S. Cardiomyocytes can be generated from marrow stromal cells in vitro (1999). *Clin. Invest.* 103: 697–705

Maltsev VA, Wobus AM, Rohwedel J, Bader M, Hescheler J. Cardiomyocytes Differentiated In Vitro From Embryonic Stem Cells Developmentally Express Cardiac-Specific Genes and Ionic Currents (1994). *Circ Res.* 75: 233-244

Maltsev V, Rohwedel J, Hescheler J, Wobus AM. Embryonic stem cells differentiate in vitro into cardiomyocytes representing sinus nodal, atrial and ventricular cell types (1993). *Mechanisms of Development* 44: 41-50

Marino TA, Haldar S, Williamson EC, Beaverson K, Walter RA, Marino DR, Beatty C, Lipson KE. Proliferating cell nuclear antigen in developing and adult rat cardiac muscle cells (1991). *Circ Res* 69: 1353–1360.

Martin CM, Meeson AP, Robertson SM, Hawke TJ, Richardson JA, Bates S, Goetsch SC, Gallardo TD, Garry DJ. Persistent expression of the ATP-binding cassette transporter, Abcg2, identifies cardiac SP cells in the developing and adult heart (2004). *Developmental Biology* 265: 262–275

Mather JP and Roberts PE. *Introduction to Cell and Tissue Culture: Theory and Technique* (1998). Plenum Press.

A).Matsuura K, Nagai T, Nishigaki N, Oyama T, Nishi J, Wada H, Sano M, Toko H, Akazawa H, Sato T, Nakaya H, Kasanuki H, Komuro I. Adult Cardiac Sca-1-positive Cells Differentiate into Beating Cardiomyocytes (2004). *The Journal of Biological Chemistry* 12: 11384–11391

B).Matsuzaki Y, Kinjo K, Mulligan RC, Okano H. Unexpectedly efficient homing capacity of purified murine hematopoietic stem cells (2004). *Immunity* 20: 87–93.

McElwee KJ, Kissling S, Wenzel E, Huth A, Hoffmann R. Cultured peribulbar dermal sheath cells can induce hair follicle development and contribute to the dermal sheath and dermal papilla (2003). *J Invest Dermatol* 121:1267–1275.

McKee JA, Banik SS, Boyer MJ, Hamad NM, Lawson JH, Niklason LE, Counter CM. Human arteries engineered in vitro (2003). *EMBO Reports* 4: 633-658.

McMichael BK, Kotadiya P, Singh T, Holliday LS, Lee BS. Tropomyosin isoforms localize to distinct microfilament populations in osteoclasts (2006). *Bone* 39: 694–705.

Meeson MAP, Robertson SM, Hawke TJ, Richardson JA, Bates S, Goetsch SC, Gallardo TD, Garry DJ. Persistent expression of the ATP-binding cassette transporter, Abcg2, identifies cardiac SP cells in the developing and adult heart (2004). *Dev Biol.* 265: 262-275

Menasché P, Hagege AA, Vilquin JT, Desnos M, Abergel E, Pouzet B, Bel A, Sarateanu S, Scorsin M, Schwartz K, Bruneval P, Benbunan M, Marolleau JP, Duboc D. Autologous skeletal myoblast transplantation for severe postinfarction left ventricular dysfunction (2003). *J Am Coll Cardiol*. 41: 1078-84

Menasche P. Skeletal myoblast for cell therapy (2005). *Coron Artery Dis* 16: 105–10.

Menasche P: Skeletal myoblast transplantation for cardiac repair (2004). *Expert Rev Cardiovasc Ther* 2: 21-28,

Merrill B, Gat U, DasGupta R, Fuchs E. Tcf3 and Lef1 regulate lineage differentiation of multipotent stem cells in skin (2001). *Genes and Development* 12: 1688-1705.

Messenger AG, Senior HJ, Bleehen SS. The in vitro properties of dermal papilla cell lines established from human hair follicles (1986). *British Journal of Dermatology* 114: 425-430.

Messina E, De Angelis L, Frati G, Morrone S, Chimenti S, Fiordaliso F, Salio M, Battaglia M, Latronico MV, Coletta M, Vivarelli E, Frati L, Cossu G, Giacomello A. Isolation and Expansion of Adult Cardiac Stem Cells From Human and Murine Heart (2004). *Circ. Res.* 95: 911-921

Meyer GP, Wollert KC, Lotz J, Steffens J, Lippolt P, Fichtner S, Hecker H, Schaefer A, Arseniev L, Hertenstein B, Ganser A, Drexler H. Intracoronary bone marrow cell transfer after myocardial infarction: eighteen months' follow-up data from the randomized, controlled BOOST (BOne marrOw transfer to enhance ST-elevation infarct regeneration).trial (2006). *Circulation* 113: 1287–94.

Min JY, Yang Y, Converso KL, Liu L, Huang Q, Morgan JP, Xiao YF. Transplantation of embryonic stem cells improves cardiac function in postinfarcted rats (2002). *J Appl Physiol* 92: 288-296,

Minamino T and Kourembanas S. Mechanisms of telomerase induction during vascular smooth muscle cell proliferation (2001). *Circ Res.* 89: 237-43

Mithieux SM and Weiss AS. Elastin (2005). *Advances in protein chemistry* 70: 437-61

Molkentin JD, Lin Q, Duncan SA, Olson EN. Requirement of the transcription factor GATA4 for heart tube formation and ventral morphogenesis (1997). *Genes Dev* 11: 1061-1072.

Molkentin JD, Markham BE. Myocyte-specific enhancer-binding factor (Mef-2) regulates alpha-cardiac myosin heavy chain gene expression in vitro and in vivo (1993). *Journal of Biol Chem* 268: 19512-19520.

Moore KA and Lemischka IR. Stem Cells and Their Niches (2006). *Science* 311:1880-1885

Moretti A, Caron L, Nakano A, Lam JT, Bernshausen A, Chen Y, Qyang Y, Bu L, Sasaki M, Martin-Puig S, Sun Y, Evans SM, Laugwitz KL, Chien KR. Multipotent Embryonic Isl1+ Progenitor Cells Lead to Cardiac, Smooth Muscle, and Endothelial Cell Diversification (2006). *Cell* 127: 1151–1165,

Morimoto T, Hasegawa K, Kaburagi S, Kakita T, Wada H, Yanazume T, Sasayama S. Phosphorylation of GATA-4 Is Involved in α_1 -Adrenergic Agonist-responsive Transcription of the Endothelin-1 Gene in Cardiac Myocytes (2000). *J Biol Chem.* 275: 13721-13726

Morin S, Charron F, Robitaille L, Nemer M. GATA-dependent recruitment of MEF2 proteins to target promoters (2000). *EMBO* 19: 2046-2055

Morris RJ, Potten CS. Highly persistent label-retaining cells in the hair follicles of mice and their fate following induction of anagen (1999). *J Invest Dermatol* 112: 470–475.

Morrison SJ, Prowse KR, Ho P, Weissman IL. Telomerase Activity in Hematopoietic Cells Is Associated with Self-Renewal Potential (1996). *Immunity* 5: 207–216

Moscoso I, Centeno A, López E, Rodriguez-Barbosa JI, Santamarina I, Filgueira P, Sánchez MJ, Domínguez-Perles R, Peñuelas-Rivas G, Domenech N. Differentiation "in vitro" of primary and immortalized porcine mesenchymal stem cells into cardiomyocytes for cell transplantation (2005). *Transplant Proc* 37: 481-482

Mouquet F, Pfister O, Jain M, Oikonomopoulos A, Ngoy S, Summer R, Fine A, Liao R. Restoration of cardiac progenitor cells after myocardial infarction by self-proliferation and selective homing of bone marrow-derived stem cells (2005). *Circ Res.* 97: 1090-1092.

Moussavi-Harami F, Duwayri Y, Martin JA, Moussavi-Harami F, Buckwalter JA. Oxygen effects on senescence in chondrocytes and mesenchymal stem cells: consequences for tissue engineering (2004). *Iowa Orthop J.* 24: 15-20

Muller-Borer BJ, Cascio WE, Anderson PA, Snowwaert JN, Frye JR, Desai N, Esch GL, Brackham JA, Bagnell CR, Coleman WB, Grisham JW, Malouf NN. Adult-Derived Liver Stem Cells Acquire a Cardiomyocyte Structural and Functional Phenotype ex Vivo (2004). *American Journal of Pathology*, 165: 135-45

Murry CE, Soonpaa MH, Reinecke H, Nakajima H, Nakajima HO, Rubart M, Pasumarthi KB, Virag JJ, Bartelmez SH, Poppa V, Bradford G, Dowell JD, Williams DA, Field LJ. Haematopoietic stem cells do not transdifferentiate into cardiac myocytes in myocardial infarcts (2004). *Nature.* 428: 664–668.

Murry CE, Wiseman RW, Schwartz SM, Hauschka SD. Skeletal myoblast transplantation for repair of myocardial necrosis (1996). *J Clin Invest.* 98: 2512–2523.

Murtuza B, Suzuki K, Bou-Gharios G, Beauchamp JR, Smolenski RT, Partridge TA, Yacoub MH. Transplantation of skeletal myoblasts secreting an IL- 1 inhibitor modulates adverse remodeling in infarcted murine myocardium (2004). PNAS 101: 4216–21.

Nag AC, Lee ML. Breakdown and rebuilding of myofibrils in cultured adult cardiac muscle cells (1997).39: 907-912.

Nakagawa M, Hamaoka K, Hattori T, Sawada T. Postnatal DNA synthesis in hearts of mice: autoradiographic and cytofluorometric investigations (1988). Cardiovasc Res. 22: 575–583.

Nussbaum, J Minami E, Laflamme MA, Virag JA, Ware CB, Masino A, Muskheli V, Pabon L, Reinecke H, Murry CE. Transplantation of undifferentiated murine embryonic stem cells in the heart: teratoma formation and immune response (2007). FASEB J. 2: 1345–1357.

Nygren JM, Jovinge S, Breitbach M, Sawen P, Roll W, Hescheler J, et al. Bone marrow-derived hematopoietic cells generate cardiomyocytes at a low frequency through cell fusion, but not transdifferentiation. Nat Med 2004; 10:494–501.

Nussbaum J, Minami E, Laflamme MA, Virag JA, Ware CB, Masino A, Muskheli V, Pabon L, Reinecke H, Murry CE. Bone marrow-derived hematopoietic cells generate cardiomyocytes at a low frequency through cell fusion, but not transdifferentiation (2004). Nat Med. 10: 494–501.

Odorico JS, Kaufman DS, Thomson JA. Multilineage Differentiation from Human Embryonic Stem Cell Lines Stem Cells (2001).Stem Cells 19: 193-204

Ogawa M, LaRue AC, Drake CJ. Hematopoietic origin of fibroblasts/myofibroblasts: Its pathophysiologic implications (2006). Blood 108: 2893-2896

Oh H, Bradfute SB, Gallardo TD, Nakamura T, Gaussin V, Mishina Y, Pocius J, Michael LH, Behringer RR, Garry DJ, Entman ML, Schneider MD. Cardiac progenitor cells from adult myocardium: Homing, differentiation, and fusion after infarction (2003). PNAS 100: 12313–12318

Oka T, Xu J, Molkentin JD. Re-employment of developmental transcription factors in adult heart disease (2007). Seminars in Cell & Developmental Biology 18: 117–131

A).Orlic D, Kajstura J, Chimenti S, Jakoniuk I, Anderson SM, Li B, Pickel J, McKay R, Nadal-Ginard B, Bodine DM, Leri A, Anversa P. Bone marrow cells regenerate infarcted myocardium (2001). Nature 410: 701–705.

B).Orlic D, Kajstura J, Chimenti S, Limana F, Jakoniuk I, Quaini F, Nadal-Ginard B, Bodine DM, Leri A, Anversa P. Mobilized bone marrow cells repair the infarcted heart, improving function and survival (2001). PNAS 98: 10344–10349.

Osawa M, Hanada K, Hamada H, Nakauchi H. Long-term lymphohematopoietic reconstitution by a single CD34-low/negative hematopoietic stem cell (1996). *Science* 273: 242-245

Oshima H, Rochat A, Kedzia C, Kobayashi K, Barrandon Y. Morphogenesis and Renewal of Hair Follicles from Adult Multipotent Stem Cells (2001). *Cell* 104: 233-245

Ott, H., Matthiesen, T., Brechtken, J., Grindle, S., Goh, S., elson, W., and Taylor, D. The adult human heart as a source for stem cells: repair strategies with embryonic-like progenitor cells (2007). *Nature Clinical Practice Cardiovascular Medicine* 4: S27-39.

Oyamada Y, Komatsu K, Kimura H, Mori M, Oyamada M. Differential Regulation of Gap Junction Protein (Connexin). Genes during Cardiomyocytic Differentiation of Mouse Embryonic Stem Cells in Vitro (1996). *Experimental Cell* 229: 318-326

Pagani FD, DerSimonian H, Zawadzka A, Wetzel K, Edge AS, Jacoby DB, Dinsmore JH, Wright S, Aretz TH, Eisen HJ, Aaronson KD. Autologous skeletal myoblasts transplanted to ischemia- damaged myocardium in humans. Histological analysis of cell survival and differentiation (2003). *J Am Coll Cardiol* 41: 879- 888

Parf G, Thomson JA Nanog and transcriptional networks in embryonic stem cell pluripotency (2007). *Cell Res.* 17: 42-9.

Paus R. Principles of hair cycle control (1998). *The Journal of dermatology* 25: 793-802

Park JH, Park BH, Kim HK, Park TS, Baek HS. Hypoxia decreases Runx2/Cbfa1 expression in human osteoblast-like cells (2000). *Molecular Cell Endocrinology* 192: 197-203.

Petersen BE, Bowen WC, Patrene KD, Mars WM, Sullivan AK, Murase N, Boggs SS, Greenberger JS, Goff JP. Bone marrow as a potential source of hepatic oval cells (1999). *Science* 284: 1168-1170.

Pfister O, Mouquet F, Jain M, Summer R, Helmes M, Fine A, Colucci WS, Liao R. CD31₊ but Not CD31₋ Cardiac Side Population Cells Exhibit Functional Cardiomyogenic Differentiation (2005). *Liao Circ Res.* 97: 52-61

Plotnikov EY, Khryapenkova TG, Vasileva AK, Marey MV, Galkina SI, Isaev NK, Sheval EV, Polyakov VY, Sukhikh GT, Zorov DB. Cell-to-cell cross-talk between mesenchymal stem cells and cardiomyocytes in coculture. (2007). *J Cell Mol Med.*

Polak JM, Bishop AE. Stem Cells and Tissue Engineering: Past, Present, and Future (2006). *Annals of the New York Academy of Sciences* 1068: 352-366.

Potten C, and Lajtha L. Stem cells versus stem lines (1982). *Annals of the New York Academy of Sciences* 397: 49-61.

Potten C, and Loeffler M. Stem cells: attributes, cycles, spirals, pitfalls and uncertainties. Lessons from and for the crypt (1990). *Development* 10: 1001-20.

Potter AM, Potter CW. Transformation of human cells by SV40 virus (1975). *Br J Cancer*. 31:348-54

Prelle K, Zink N, Wolf E. Pluripotent stem cells-model of embryonic development, tool for gene targeting, and basis of cell therapy (2002). *Anatomia Histologia Embryologia*. 31: 169-86

Prost-Squarcioni C. Histology of skin and hair follicle (2006). *Medicine Sciences (Paris)* 22: 131-7

Pye D, Watt DJ. Dermal fibroblasts participate in the formation of new muscle fibres when implanted into regenerating normal mouse muscle (2001). *Journal of Anatomy* 198: 163-173.

Quaini F, Urbanek K, Beltrami AP, Finato N, Beltrami CA, Nadal-Ginard B, Kajstura J, Leri A, Anversa P. Chimerism of the transplanted heart (2002). *N Engl J Med*. 346:5-15.

Qu-Petersen Z, Deasy B, Jankowski R, Ikezawa M, Cummins J, Pruchnic R, Mytinger J, Cao B, Gates C, Wernig A, Huard J. Identification of a novel population of muscle stem cells in mice: potential for muscle regeneration (2002). *J. Cell Biol*. 157: 851-864

Reddy KL, Wohlwill A, Dzitoeva S, Lin MH, Holbrook S, Storti RV. The *Drosophila* PAR domain protein 1 (Pdp1) gene encodes multiple differentially expressed mRNAs and proteins through the use of multiple enhancers and promoters (2000). *Dev Biol* 224: 401-414

Reinecke H, MacDonald GH, Hauschka SD, et al: Electromechanical coupling between skeletal and cardiac muscle. Implications for infarct repair (2000). *J Cell Biol* 149: 731-740,

Reinecke H, Minami E, Poppa V, Murry CE. Evidence for fusion between cardiac and skeletal muscle cells (2004). *Circ Res* 94: e56-60.

Reinecke H, Poppa V, Murry CE, et al: Skeletal muscle stem cells do not transdifferentiate into cardiomyocytes after cardiac grafting (2002). *J Mol Cell Cardiol* 34: 241-249

Reiss K, Kajstura J, Capasso JM, Marino TA, Anversa P. Impairment of myocyte contractility following coronary artery narrowing is associated with activation of the myocyte IGF1 autocrine system, enhanced expression of late growth related genes, DNA synthesis, and myocyte nuclear mitotic division in rats (1993). *Exp Cell Res*. 207 :348 – 360

Ren H, Cao Y, Zhao Q, Li J, Zhou C, Liao L, Jia M, Zhao Q, Cai H, Han ZC, Yang R, Chen G, Zhao RC. Proliferation and differentiation of bone marrow stromal cells under hypoxic conditions (2006). *Biochemical and Biophysical Research Communications* 347: 12–21.

Reynolds AJ. In vivo and in Vitro Studies of Isolated and Interacting Dermal and Epidermal Components of the Integument (1989). PhD Thesis

Reynolds AJ and Jahoda CA. Hair follicle stem cells? A distinct germinative epidermal cell population is activated in vitro by the presence of hair dermal papilla cells (1991). *J Cell Sci* 99: 373–85

Richardson GD, Arnott EC, Whitehouse CJ, Lawrence CM, Reynolds AJ, Hole N, Jahoda CA. Plasticity of rodent and human hair follicle dermal cells: implications for cell therapy and tissue engineering (2005). *Journal of Investigative Dermatology* 10: 180–183

Romani N, Ebner S, Tripp CH, Flacher V, Koch F, Stoitzner P. Epidermal Langerhans cells—Changing views on their function *in vivo* (2006). *Immunology Letters* 106: 119–125
Rubin H. Cell aging in vivo and in vitro (1997). *Mechanisms of Ageing and Development* 98: 1–35.

Rufaut NW, Goldthorpe NT, Wildermoth JE, Wallace OA. Myogenic Differentiation of Dermal Papilla Cells From Bovine Skin (2006). *Journal of Cellular* 209: 959–966

Rumyantsev PP, Marakjan VO. Reactive synthesis of DNA and mitotic division in atrial heart muscle cells following ventricle infarction (1968). *Experientia* 24: 1234–1235.

Rumyantsev PP. DNA synthesis in atrial myocytes of rats with aortic stenosis (1983). *Adv Myocardiol.* 4: 147–162.

Sadoshima J, Jahn L, Takahashi T, Kulik TJ, Izumo S. Molecular characterization of the stretch-induced adaptation of cultured cardiac cells. An in vitro model of load-induced cardiac hypertrophy (1992). *The Journal of Biological Chemistry* 267: 10551–10560

Salvatori G, Lattanzi L, Coletta M, Aguanno S, Vivarelli E, Kelly R, Ferrari G, Harris AJ. Myogenic conversion of mammalian fibroblasts induced by differentiating muscle cells (1995). *Journal of Cell Science* 108: 2733–2739.

Sarin KY, Cheung P, Gilson D, Lee E, Tennen RI, Wang E, Artandi MK, Oro AE, Artandi SE. Conditional telomerase induction causes proliferation of hair follicle stem cells (2005). *Nature* 436: 1048–1052

Sasaki R, Morishita T, Yamagata S. Mitosis of heart muscle cells in normal rats (1968). *Tohoku J Exp Med.* 96: 405–411

Schachinger V, Erbs S, Elsasser A, Haberbosch W, Hambrecht R, Holschermann H, et al. Improved clinical outcome after intracoronary administration of bone-marrow-derived progenitor cells in acute myocardial infarction: final 1-year results of the REPAIR-AMI trial (2006). *Eur Heart J* 27: 2775–83.

Scharenberg CW, Harkey MA, Torok-Storb B. The ABCG2 transporter is an efficient Hoechst 33342 efflux pump and is preferentially expressed by immature human hematopoietic progenitors (2002). *Blood* 99: 507– 512.

Schofield R. The relationship between the spleen colony-forming cell and the haemopoietic stem cell (1978). *Blood Cells* 4: 7-25

Sepulveda JL, Belaguli N, Nigam V, Chen CY, Nemer M, Schwartz RJ. GATA-4 and Nkx-2.5 Coactivate Nkx-2 DNA Binding Targets: Role for Regulating Early Cardiac Gene Expression (1998). *Molecular and Cellular Biology* 18: 3405–3415

Serakinci N, Graakjaer J, Kolvraa S. Telomere stability and telomerase in mesenchymal stem cells (2008). *Biochimie* 90: 33-40.

Short B, Brouard N, Occhiodoro-Scott T, Ramakrishnan A, Simmons PJ. Mesenchymal stem cells (2003). *Archives of Medical Research* 34: 565-571

Sieber-Blum M, Grim M, Hu YF, Szeder V. Pluripotent neural crest stem cells in the adult hair follicle (2004). *Dev Dyn*. 231: 258-69

Sieck GC, Regnier MJ. .Plasticity and energetic demands of contraction in skeletal and cardiac muscle (2001). *Appl Physiol*. 90: 1158-64.

Siegl-Cachedenier I, Flores I, Klatt P, Blasco MA. Telomerase reverses epidermal hair follicle stem cell defects and loss of long-term survival associated with critically short telomeres (2007). *The Journal of Cell Biology* 179: 277–290

Siminiak T, Kalawski R, Fiszer D, Jerzykowska O, Rzeźniczak J, Rozwadowska N, Kurpisz M. Autologous skeletal myoblast transplantation for the treatment of postinfarction myocardial injury: phase I clinical study with 12 months of follow-up (2004). *Am Heart J* 148: 531-537

Sinauer Gilbert S. A companion to developmental biology 8th edition. Associates.

Singla DK, Hacker TA, Ma L, Douglas PS, Sullivan R, Lyons GE, Kamp TJ. Transplantation of embryonic stem cells into the infarcted mouse heart: formation of multiple cell types (2006). *J Mol Cell Cardiol* 40: 195- 200

Skerjanc IS, Petropoulos H, Ridgeway AG, Wilton S. Myocyte Enhancer Factor 2C and Nkx2–5 Up-regulate Each Other's Expression and Initiate Cardiomyogenesis in P19 Cells (1998). *The Journal of biological Chemistry* 273: 34904–34910

Skottman H and Outi H. Culture conditions for human embryonic stem cells (2006). *Reproduction* 132: 691–698

Smith RR, Barile L, Cho HC, Leppo MK, Hare JM, Messina E, et al. Regenerative potential of cardiosphere-derived cells expanded from percutaneous endomyocardial biopsy specimens (2007). *Circulation* 115: 896–908.

Smits PC, van Geuns RJ, Poldermans D, Bountiukos M, Onderwater EE, Lee CH, Maat AP, Serruys PW. Catheter-based intramyocardial injection of autologous skeletal myoblasts as a primary treatment of ischemic heart failure: clinical experience with six-month follow-up (2003). *J AM Coll Cardiol* 17: 2063-2069

Sonada T, Asada Y, Kurata S, Takayasu S. The mRNA for Protease Nexin-1 is Expressed in Human Dermal Papilla Cells and its Level is Affected by Androgen (1999). *Journal of Investigative Dermatology* 113: 308-313.

Soonpaa MH, Koh GY, Klug MG, Field LJ. Formation of nascent intercalated disks between grafted fetal cardiomyocytes and host myocardium (1994). *Science*. 264: 98-101

Soonpaa MH, Kim KK, Pajak L, Franklin M, Field LJ. Cardiomyocyte DNA synthesis and binucleation during murine development (1996). *Am J Physiol*. 271: H2183–H2189.

Soonpaa MH and Field LJ. Survey of Studies Examining Mammalian Cardiomyocyte DNA Synthesis (1998). *Circ. Res.* 83: 15-26

Srivastava D and Olson EN. A genetic blueprint for cardiac development (2000). *Nature* 407: 221-226

Srivastava D. Making or Breaking the Heart: From Lineage Determination to Morphogenesis (2006). *Cell* 126: 1037-1048.

Stamm C, Westphal B, Kleine HD, Petzsch M, Kittner C, Klinge H, et al. Autologous bone-marrow stem-cell transplantation for myocardial regeneration (2003). *Lancet* 361: 45-46.

Steinbrech DS, Mehrara BJ, Saadeh PB, Chin G, Dudziak ME, Gerrets RP, Gitted GK, Longaker MT. Hypoxia regulates VEGF expression and cellular proliferation by osteoblasts in vitro (1999). *Plastic Reconstructive Surgery* 104: 738-47.

Studer L, Csete M, Lee SH, Kabbani N, Walikonis J, Wold B, McKay R.. Enhanced proliferation, survival, and dopaminergic differentiation of CNS precursors in lowered oxygen (2000). *J. Neurosci.* 20: 7377–7383

Sun Y, Weber KT. Infarct scar: a dynamic tissue (2000). *Cardiovascular Research* 46: 250-256

- Suva D, Garavaglia G, Menetrey J, Chapuis B, Hoffmeyer P, Bernheim L, Kindler VJ. Non-hematopoietic human bone marrow contains long-lasting, pluripotential mesenchymal stem cells (2004). *Cell Physiol.* 198: 110-118
- Takahashi K and Yamanaka S. Induction of Pluripotent Stem Cells from Mouse Embryonic and Adult Fibroblast Cultures by Defined Factors (2006). *Cell* 126: 663–676
- Takano H, Qin Y, Hasegawa H, Ueda K, Niitsuma Y, Ohtsuka M, Komuro I. Effects of G-CSF on left ventricular remodeling and heart failure after acute myocardial infarction (2006). *J Mol Med* 84: 185–193
- Takeda N. Cardiomyopathy: molecular and immunological aspects (review).(2003). *Int J Mol Med* 11: 13-16.
- Takeuchi M, Takeuchi K, Kohara A, Satoh M, Shioda S, Ozawa Y, Ohtani A, Morita K, Hirano T, Terai M, Umezawa A, Mizusawa H. Chromosomal instability in human mesenchymal stem cells immortalized with human papilloma virus E6, E7, and hTERT genes (2007). *In Vitro Cell.Dev.Biol. Animal* 43: 129–138
- Takeuchi JK, Mileikovskaia M, Koshiba-Takeuchi K, Heidt AB, Mori AD, Arruda EP, Gertsenstein M, Georges R, Davidson L, Mo R, Hui CC, Henkelman RM, Nemer M, Black BL, Nagy A, Bruneau BG. Tbx20 dose-dependently regulates transcription factor networks required for mouse heart and motoneuron development (2005). *Development* 132: 2463–2474.
- Tateishi K, Ashihara E, Takehara N, Nomura T, Honsho S, Nakagami T, Morikawa S, Takahashi T, Ueyama T, Matsubara H, Oh H. Clonally amplified cardiac stem cells are regulated by Sca-1 signaling for efficient cardiovascular regeneration (2007). *Journal of Cell Science* 120: 1791-1800
- Taylor DA, Atkins BZ, Hungspreugs P, Jones TR, Reedy MC, Hutcheson KA, Glower DD, Kraus WE. Regenerating functional myocardium: improved performance after skeletal myoblast transplantation (1998). *Nat Med.* 4: 929–933.
- Taylor G, Lehrer MS, Jensen PJ, Sun TT, Lavker RM. Involvement of follicular stem cells in forming not only the follicle but also the epidermis (2000). *Cell* 102: 451–61.
- Theise ND, Nimmakayalu M, Gardner R, Illei PB, Morgan G, Teperman L, Henegariu O, Krause DS. Liver from bone marrow in humans (2000). *Hepatology* 32: 11–16
- Theise ND, Badve S, Saxena R, Henegariu O, Sell S, Crawford JM, Krause DS. Derivation of hepatocytes from bone marrow cells in mice after radiation-induced myeloablation (2000). *Hepatology* 31: 235–240

Toko H, Zhu W, Takimoto E, Shiojima I, Hiroi Y, Zou Y, Oka T, Akazawa H, Mizukami M, Sakamoto M, Terasaki F, Kitaura Y, Takano H, Nagai T, Nagai R, Komuro I. Csx/Nkx2-5 Is Required for Homeostasis and Survival of Cardiac Myocytes in the Adult Heart (2002). *The Journal of Biological Chemistry* 277: 24735–24743

Toma C, Pittenger MF, Cahill KS, Byrne BJ, Kessler PD. Human mesenchymal stem cells differentiate to a cardiomyocyte phenotype in the adult murine heart (2002). *Circulation* 105: 93–98.

Tomita Y, Matsumura K, Wakamatsu Y, Matsuzaki Y, Shibuya I, Kawaguchi H, Ieda M, Kanakubo S, Shimazaki T, Ogawa S, Osumi N, Okano H, Fukuda K. Cardiac neural crest cells contribute to the dormant multipotent stem cell in the mammalian heart (2005). *The Journal of Cell Biology* 170: 1135–1146

Toraason M, Luken ME, Breitenstein M, Krueger JA, Biagini RE. Comparative Toxicity of Allylamine and Acrolein in Cultured Myocytes and Fibroblasts from Neonatal Rat Heart (1988). *Toxicology* 56: 107-117

Torrente Y, Tremblay JP, Pisati F, Belicchi M, Rossi B, Sironi M, Fortunato F, El Fahime M, D'Angelo MG, Caron NJ, Constantin G, Paulin D, Scarlato G, Bresolin N. Intraarterial injection of muscle-derived CD34(+).Sca-1(+).stem cells restores dystrophin in mdx mice. (2001). *J. Cell Biol.* 152: 335–348

Trempus CS, Morris RJ, Bortner CD, Cotsarelis G, Faircloth RS, Reece JM, Tennant RW. Enrichment for Living Murine Keratinocytes from the Hair Follicle Bulge with the Cell Surface Marker CD34 (2003). *Invest Dermatol* 120: 501-511

Trowbridge IS, Thomas ML. CD45: an emerging role as a protein tyrosine phosphatase required for lymphocyte activation and development (1994). *Annu. Rev. Immunol* 12: 85-116

Tuncay OC, Ho D, Barker MK. Oxygen tension regulates osteoblast function. (1994). *American Journal of orthodontics and dentofacial orthopedics* 105: 457-63.

Urbanek K, Torella D, Sheikh F, De Angelis A, Nurzynska D, Silvestri F, Beltrami CA, Bussani R, Beltrami AP, Quaini F, Bolli R, Leri A, Kajstura J, Anversa P. Myocardial regeneration by activation of multipotent cardiac stem cells in ischemic heart failure (2005). *PNAS* 102: 8692–8697

Urbani S, Caporale R, Lombardini L, Bosi A, Saccardi R. Use of CFDA-SE for evaluating the in vitro proliferation pattern of human mesenchymal stem cells (2006). *Cytotherapy* 8: 243-253

Van de Lest CH, Versteeg EM, Veerkamp JH, Van Kuppevelt TH. Elimination of autofluorescence in immunofluorescence microscopy with digital image processing (1995). *Journal of histochemistry and cytochemistry* 43: 727-730,

Van den Bos EJ, Mees BM, de Waard MC, de Crom R, Duncker DJ. A novel model of cryoinjury-induced myocardial infarction in the mouse: a comparison with coronary artery ligation (2005). *Am J Physiol Heart Circ Physiol* 289: H1291-H1300,

Vandervelde S, van Amerongen MJ, Tio RA, Petersen AH, van Luyn MJ, Harmsen MC. Increased inflammatory response and neovascularization in reperfused vs. non-reperfused murine myocardial infarction (2006). *Cardiovasc Pathol.* 15: 83-90.

Van Vranken BE, Romanska HM, Polak JM, Rippon HJ, Shannon JM, Bishop AE. Coculture of Embryonic Stem Cells with Pulmonary Mesenchyme: A Microenvironment That Promotes Differentiation of Pulmonary Epithelium (2005). *Tissue Engineering* 11: 1177-1187

Vozzi C, Dupont E, Coppen SR, Yeh HI, Severs NJ. Chamber-related differences in connexin expression in the human heart (1999). *J Mol Cell Cardiol* 31: 991–1003

Wachtlova M, Mares V, Ostadal B. DNA synthesis in the ventricular myocardium of young rats exposed to intermittent high altitude (IHA).hypoxia: an autoradiographic study. *Virchows (1977).Arch B Cell Pathol.* 24: 335–342.

Wang J, Xie LY, Allan S, Beach D, Hannon GJ. Myc activates telomerase (1998). *Genes Dev.* 12: 1769-1774

Wang T, Zhengyun Xu, Wenhui Jiang, Aiqun Ma. Cell-to-cell contact induces mesenchymal stem cell to differentiate into cardiomyocyte and smooth muscle cell (2006). *International Journal of Cardiology* 109: 74 – 81

Warren SM, Steinbrech DS Mehrara BJ, Saadeh PB, Greewald JA, Spector JA, Bouletreau PJ, Longaker MT. Hypoxia regulates osteoblast gene expression (2001). *Journal of Surgical Research* 99: 147-55.

Wei H, Ondrej Juhasz, Jinliang Li, Yelena S. Tarasova, Kenneth R. Boheler JEmbryonic stem cells and cardiomyocyte differentiation:phenotypic and molecular analyses (2005). *Cell. Mol. Med.* 9: 804-817

Weissman IL, Anderson DJ, Gage F. Stem and progenitor cells: origins, phenotypes, lineage commitments, and transdifferentiations. (2001). *Annu Rev Cell Dev Biol* 17: 387–403

Wessels A, Vermeulen JL, Virág S, Kálmán F, Lamers WH, Moorman AF.Spatial distribution of tissue-specific antigens in the developing human heart and skeletal muscle. II. An immunohistochemical analysis of myosin heavy chain isoform expression patterns in the embryonic heart (1991). *Anat Rec.* 229: 355-68

Wessels A, Pérez-Pomares JM. The Epicardium and Epicardially Derived Cells (EPDCs).as Cardiac Stem Cells (2004). *Anat Rec A Discov Mol Cell Evol Biol.* 276: 43-57

Winter EM, Grauss RW, Hogers B, van Tuyn J, van der Geest R, Lie-Venema H, Steijn RV, Maas S, DeRuiter MC, deVries AA, Steendijk P, Doevendans PA, van der Laarse A, Poelmann RE, Schalij MJ, Atsma DE, Gittenberger-de Groot AC. Preservation of Left Ventricular Function and Attenuation of Remodeling After Transplantation of Human Epicardium-Derived Cells Into the Infarcted Mouse Heart (2007). *Circulation* 116: 917-927

Wollert KC and Drexler H. Cell-based therapy for heart failure (2006). *Curr Opin Cardiol* 21: 234-9

Xiang M, Yang T. A study of Nexin 1 of skin and hair follicle during postnatal development period of rat (1998). *Zhongguo Yi Xue Ke Xue Yuan Xue Bao* 20: 127-32.

Xu M, Wani M, Dai YS, Wang J, Yan M, Ayub A, Ashraf MDifferentiation of bone marrow stromal cells into the cardiac phenotype requires intercellular communication with myocytes (2004). *Circulation* 110: 2658-65.

Yao S and Weber KT. Infarct scar: a dynamic tissue (2000). *Cardiovascular Research* 46: 250-256

Yasuda M, Miyachi Y, Ishikawa O, Takahashi K. Spatial expressions of fibronectin and integrins by human and rodent dermal fibroblasts (2006). *British Journal of Dermatology* 155: 522-531

Yasuyuki Y, Li L Katsuoka K, Penman S, Hoffman RM. Multipotent nestin-positive, keratin-negative hair-follicle bulge stem cells can form neurons. (2005). *PNAS* 102: 5530-5534

Yokomuro H, Li RK, Mickle DA, Weisel RD, Verma S, Yau TM. Transplantation of cryopreserved cardiomyocytes (2001). *J Thorac Cardiovasc Surg* 121:98-107

Yoon YS, Park JS, Tkebuchava T, Luedeman C, Losordo DW. Unexpected Severe Calcification After Transplantation of Bone Marrow Cells in Acute Myocardial Infarction (2004). *Circulation* 109:3154-3157

Yoon J, Shim WJ, Ro YM, Lim DS. Transdifferentiation of mesenchymal stem cells into cardiomyocytes by direct cell-to-cell contact with neonatal cardiomyocyte but not adult cardiomyocytes (2005). *Ann Hematol* 84: 715-721

Young RD. Morphological and ultrastructural aspects of the dermal papilla during the growth cycle of the vibrissal follicle in the rat (1980). *Journal of Anatomy* 131: 355-365

Yu D, Yang T, Sonoda T, Gaffney K Jensen P, Dooley T, Ledbetter S, Freedberg I, Lavker R, Sun T. Message of nexin 1, a serine protease inhibitor, is accumulated in the follicular papilla during anagen of the hair cycle (1995). *Journal of Cell Science* 108: 3867-3874.

Zammit PS, Kelly RG, Franco D, Brown N, Moorman AF, Buckingham ME. Suppression of atrial myosin gene expression occurs independently in the left and right ventricles of the developing mouse heart (2000). *Dev Dyn.* 217: 75-85.

Zheng Y, Du X, Wang W, Boucher M, Parimoo S, Stenn K. Organogenesis From Dissociated Cells: Generation of Mature Cycling Hair Follicles From Skin-Derived Cell (2005). *J Invest Dermatol* 124: 867-876,

Zhou YF, Bosch-Marce M, Okuyama H, Krishnamachary B, Kimura H, Zhang L, Huso DL, Semenza GL. Spontaneous Transformation of Cultured Mouse Bone Marrow-Derived Stromal Cells (2006). *Cancer Res* 66: 10849-10854

Zhu W, Chen J, Cong X, Hu S, Chen X. Hypoxia and Serum Deprivation-Induced Apoptosis in Mesenchymal Stem Cells (2006). *Stem Cells* 24: 416-425

Zimmermann S, Voss M, Kaiser S, Kapp U, Waller CF, Martens UM. Lack of telomerase activity in human mesenchymal stem cells (2003). *Leukemia* 17: 1146-1149

